# DESIGN AND SYNTHESIS OF NOVEL PRODRUGS TO MODULATE GABA RECEPTORS IN CANCER

## HUI ZHANG

**Thesis submitted in partial fulfilment of the requirements of Edinburgh Napier University for the degree of Doctor of Philosophy**

**March 2017**

<u>Declaration</u>

It is hereby declared that this thesis and the research work upon which it is based were conducted by the author, Hui Zhang.

Hui Zhang

# Abstract of Thesis

GABA (gamma-amino butanoic acid) is the main inhibitory neurotransmitter in the mammalian central nervous system. GABA has been found to play an inhibitory role in some cancers, including colon carcinoma, cholangiocarcinoma, and lung adenocarcinoma.

Growing evidence shows that GABAB receptors are involved in tumour development. The expression level of GABAB receptors was found to be upregulated in some human tumours, including the pancreas, and cancer cell lines, suggesting that GABAB receptors may be potential targets for cancer therapy and diagnosis.

In this research programme, several diverse series of potential anticancer prodrugs of GABA and GABA receptor-targeting agents have been rationally designed and synthesised for selective activation in the tumour microenvironment.

In one approach, a series of oligopeptide conjugate prodrugs have been synthesised as protease-activatable substrates for either the extracellular matrix metalloproteinase MMP-9 or the lysosomal endoprotease legumain; each of which are overexpressed in the tumour environment and are effectors of tumour growth and metastasis. Specifically, a novel fluorogenic, oligopeptide FRET substrate prodrug of legumain HZ101 (Rho-Pro-Ala-Asn~GABA-spacer-AQ) has been characterised and shown to have theranostic potential. Proof of principle has been demonstrated using recombinant human legumain for which HZ101 is an efficient substrate and is latently quenched until cleaved. HPLC methods have been developed to monitor prodrug activation.

In another approach, cyclic prodrugs of the GABA-B receptor agonist baclofen have been designed to be activated in the acidic environment of solid tumours to exert antitumour effects through modulation of the receptor response.

During the oligopeptide synthetic work, novel, coloured, anthraquinone-based reagents have been designed and evaluated as new chemical tools for amine detection and monitoring in solid phase peptide synthesis (SPPS); characterisation by spectroscopic and HPLC methods have demonstrated their advantages over existing methods and their potential applications for use on solid supported resins.

# Contents

# Acknowledgements

Undertaking this PhD has been a truly life-changing experience for me and it would not have been possible to do without the support and guidance that I received from my supervisor Dr David Mincher. I am also very grateful to Dr Agnes Turnbull and Dr Amy Poole who were always so helpful and provide me with their assistance throughout my dissertation.

I would like to thank all of my friends in Edinburgh with whom I have shared so many excellent times over the last four years. In particular, I would like to thank Maria Gauci for her friendship and the warmth.

Finally, I would also like to say a heartfelt thank you to my Mum and Dad for always believing in me and encouraging me to follow my dreams.

# Preface

Results from this research programme have been reported in part in the following publication:

Zhang H, Poole A, Darlison MG, Turnbull A, Mincher DJ. (2013). Protease-Activated Prodrug Modulation of GABA receptors in Cancer. *Proceedings of the APS Pharm Sci 2013 Conference: The Science of Medicines*, Heriot-Watt University, Edinburgh UK 2nd – 4th September 2013 (Abstract No. 203)

## Graphical Abstract Concept Diagrams

### Chapter 1: MMP-9 Activated Prodrugs

Chapter 1 presents the results and discussion of a series of novel oligopeptide Matrix Metalloproteinase (MMP)-9 substrates for prodrug therapy, designed to be activated by overexpressed MMP-9 in the tumour microenvironment.
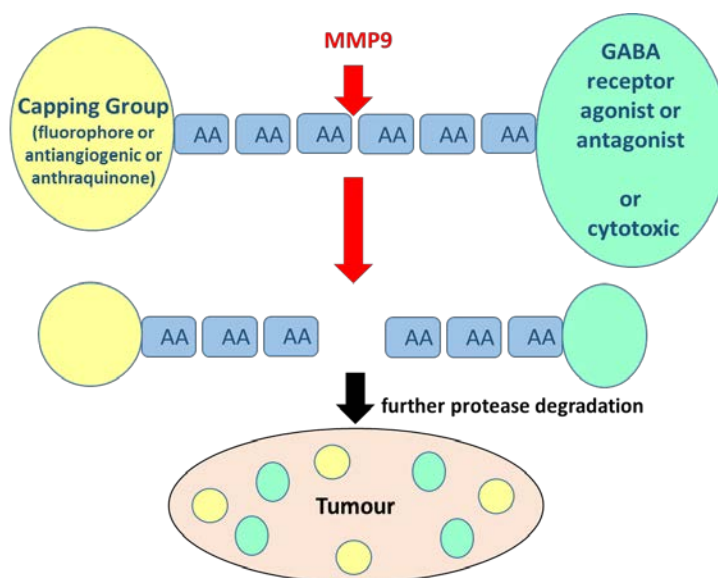


**Figure 1.** Design strategy and concept for MMP-9 activated prodrugs

**Figure 1** illustrates the general concept for the design of the MMP-9 targeted prodrugs, where an MMP-9 cleavable peptide is amide linked at its carboxy

terminus to either a GABA$_B$ receptor agonist or antagonist or cytotoxic agent; the amino terminus is protected by either a capping group, fluorophore (for diagnostic purpose) or antiangiogenic agent. Activation of the prodrug at the MMP-9 specific cleavage site ('hotspot'), followed by further degradation by ubiquitous aminopeptidase should result in release of the active agents in the tumour microenvironment, which may then enter into tumour cells and lead to cell death.

## Chapter 2: Baclofen Based Prodrugs

Chapter 2 describes the synthesis and preliminary evaluation of new cancer chemotherapeutic prodrugs targeted to the GABA$_B$ receptor with the potential to increase therapeutic index.
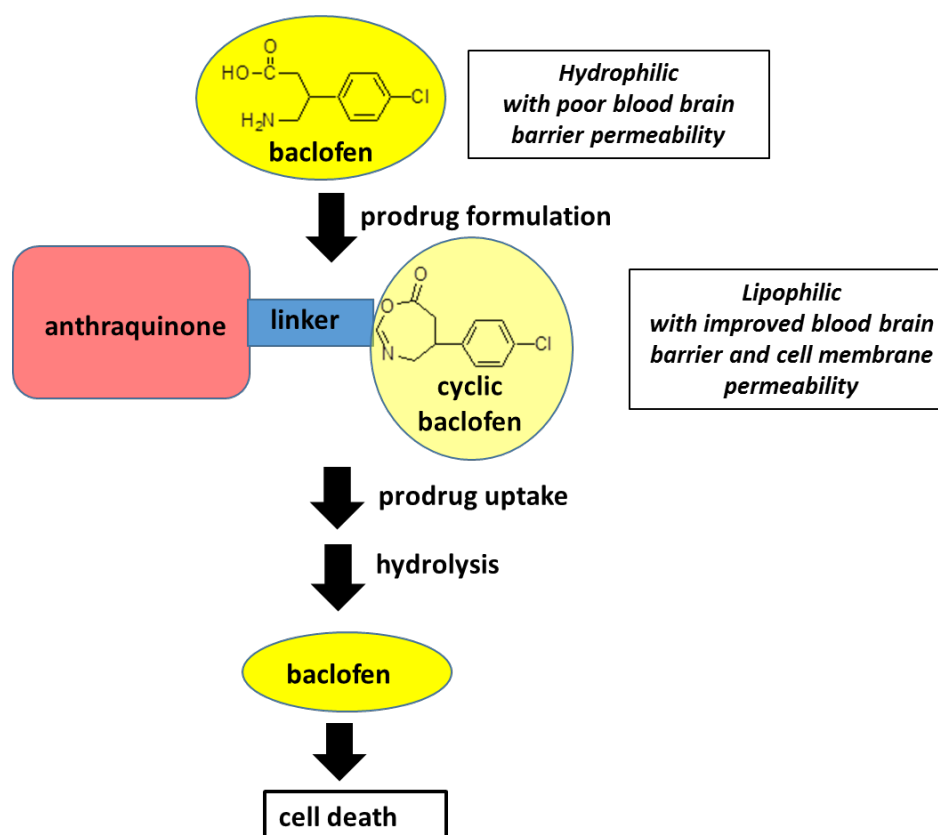


**Figure 2.** Design strategy and concept for cyclic baclofen based prodrugs

Figure 2 outlines the rationale for the synthesis of a series of compounds where the GABA$_B$ receptor agonist baclofen was converted into a lipophilic cyclic

prodrug form in order to enhance cell membrane and blood brain barrier permeability for potential brain tumour therapy.

## Chapter 3: Design of legumain activated GABA prodrugs

This chapter focuses on the synthesis of a legumain targeted prodrug and presents the results of in vitro metabolism studies by HPLC and fluorescence spectroscopic methods.
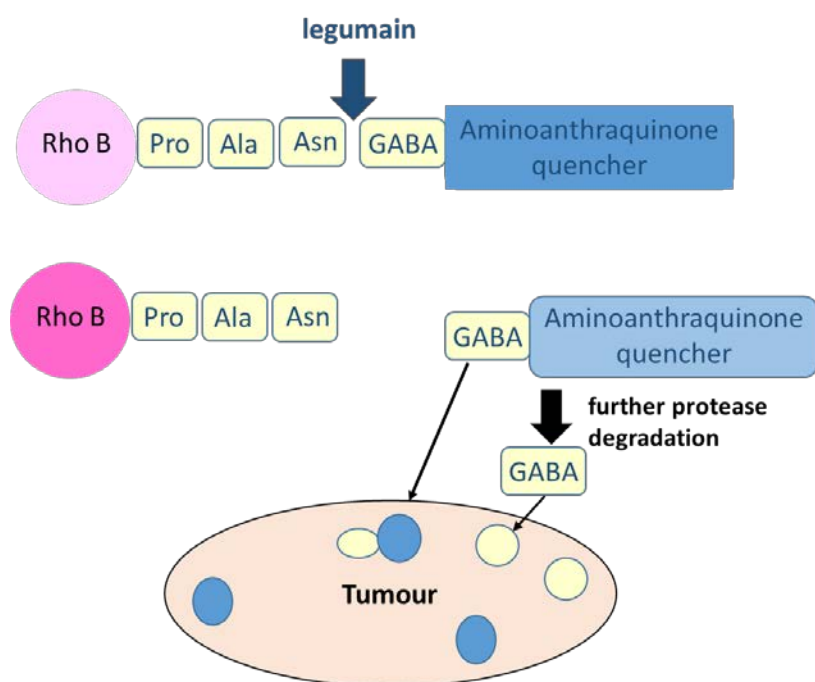


**Figure 3** Design strategy for legumain activated prodrugs

Figure 3 illustrates the general design strategy and activation concept for legumain targeted fluorogenic prodrugs/probes.   The prodrug has been designed   to exploit the proteolytic activity of overexpressed legumain, a lysosomal endoprotease with strict specificity for Asn at the P1 position of peptide substrates. On activation by legumain, the latently fluorogenic prodrug releases a fluorogenic tripeptide and a GABA-containing aminoanthraquinone fragment, designed to be further cleaved by aminopeptidases to release the ligand GABA which may then enter into tumour cells and lead to cell death or

modulate GABA receptors to induce an antitumour effect.

## Chapter 4: New colour reagents for SPPS

In the course of this research programme, synthetic peptide chemistry methods were used considerably (as reported in chapter 1 to 3). Due to inherent difficulties in monitoring peptide coupling reactions by published available methods, novel methods were explored. Chapter 4 describes how new colour test reagents were developed for the amine detection and monitoring of reaction steps in solid phase peptide synthesis (SPPS). Three new colour reagents (blue, red, and purple) were synthesized that gave a rapid colour change to resin beads at room temperature with both sterically hindered primary and secondary amines. Examples of their application are described.



**AQ-Ahx-OPFP (HZ22)**
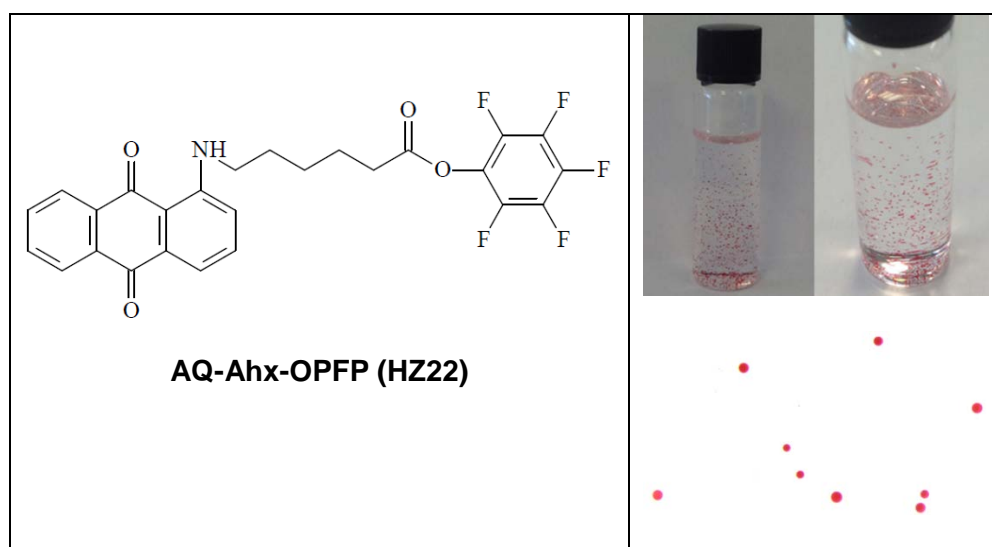
**Figure 4.** An example reagent for amine detection and resin bead colouration
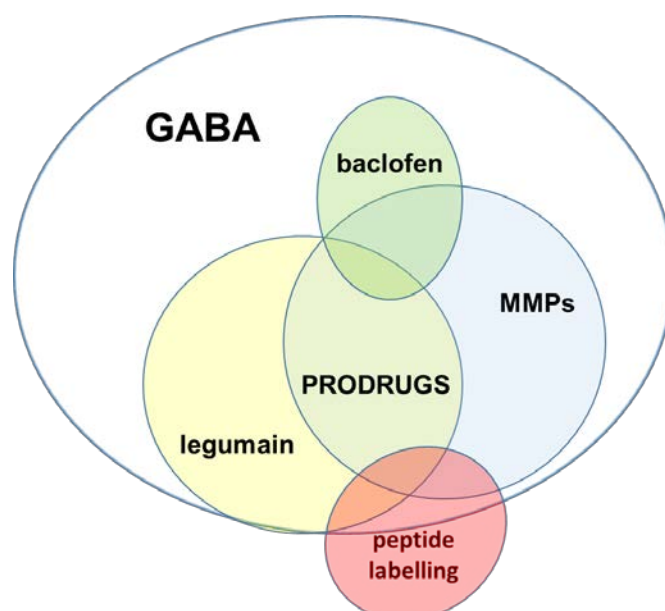
**Graphical Summary of Research Undertaken**

Venn diagram representation of the *Areas of Research* presented in this thesis showing the fundamental relationships between them. The common theme running through all chapters is **GABA** (gamma aminobutanoic acid). This natural ligand may be a pro- or anti-tumour effector. Protease activated prodrugs of GABA are targeted either to MMP-9 or legumain endoproteases that are overexpressed in the tumour microenvironment. Prodrugs of the $GABA_B$ receptor agonist baclofen (which has antitumor properties) are designed to be either oligopeptide prodrugs activated by MMPs or cyclic, hydrophobic prodrugs activated by a pH-dependent mechanism in tumours. Peptide labelling with novel reagents developed for N-terminus capping in SPPS methodology spans the areas of endoprotease mediated GABA prodrug activation.

# Abbreviations

| | |
|---|---|
| Ala | Alanine |
| AQ | Anthraquinone |
| BBB | Blood brain barrier |
| cAMP | Cyclic adenosine monophosphate |
| DCC | N,N-Dicyclohexylcarbodiimide |
| DCU | Dicyclohexylurea |
| DIPEA | N,N-Diisopropylethylamine |
| DMAP | 4-Dimethylaminopyridine |
| DMSO | Dimethysulphoxide |
| DMF | N,N-Dimethylformamide |
| EDTA | Ethylene diamine tetraacetic acid |
| GABA | Gamma-amino butyric acid |
| GAD | Glutamate decarboxylase |
| MeOH | Methanol |
| MMPs | Matrix metalloproteinases |
| NU:UB | Napier University: University of Bradford |
| PBS | Phosphate buffered saline |
| PFP | Pentafluorophenol |
| Pro | Proline |
| RT | Room temperature |
| SPPS | Solid phase peptide synthesis |
| TLC | Thin layer chromatography |
| UV | Ultraviolet |

# Nomenclature

The compounds synthesised here are relatively large molecules. To facilitate communication through the thesis, the compounds were described in their simplest format. The chemical structure (**Example A**) below represents one of the synthesised MMP-9 activated prodrugs (**HZ16**).

**Example A:**



Podophyllotoxin-Succinyl-Pro-Ala-Gly-Leu-Ala-Ala-Piperazinyl-AQ
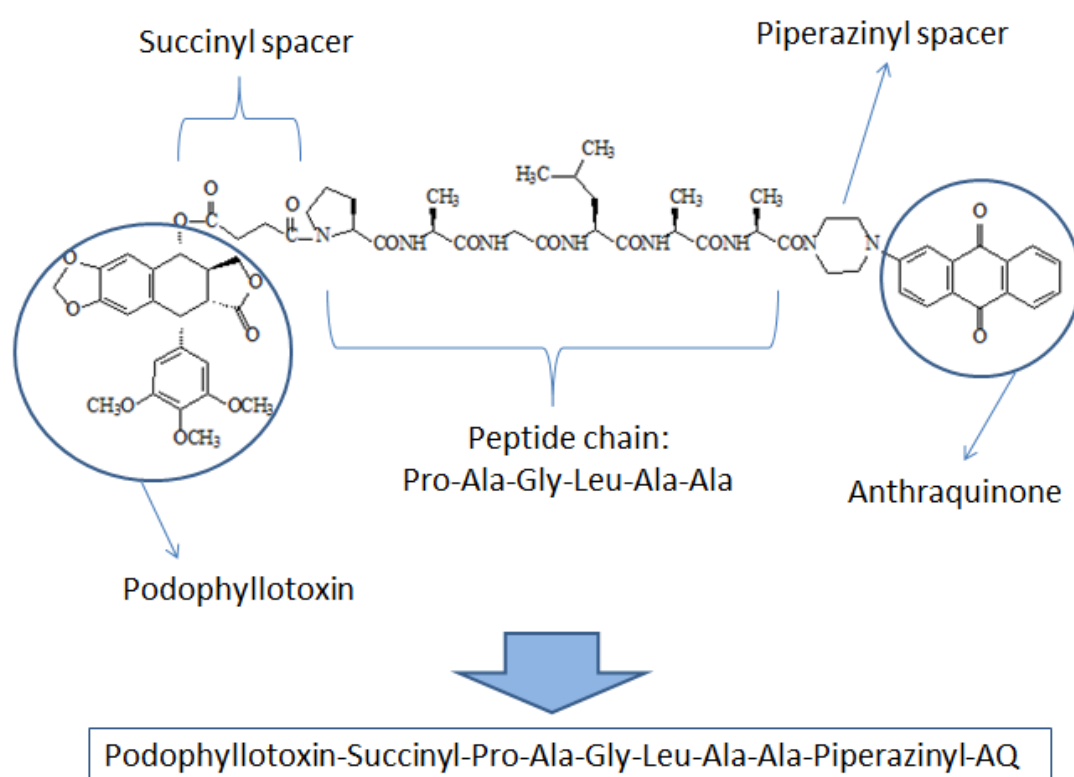
The hexapeptide chain in the middle is described conventionally using 3-letter codes as Pro-Ala-Gly-Leu-Ala-Ala to allow easy recognition of the amino acids present in the prodrug. The spacer groups have been abbreviated to succinyl and piperazinyl. The short term 'AQ' is used in this thesis to represent the most commonly used anthraquinone group. Podophyllotoxin is the active agent of the prodrug. Eventually, the synthesised prodrug has the short name in the context described as: Podophyllotoxin-Succinyl-Pro-Ala-Gly-Leu-Ala-Ala-Piperazinyl-AQ

(HZ16). HZ16 is the descriptor and number wherein HZ is the code name for newly synthesised compounds.

**Example B:**
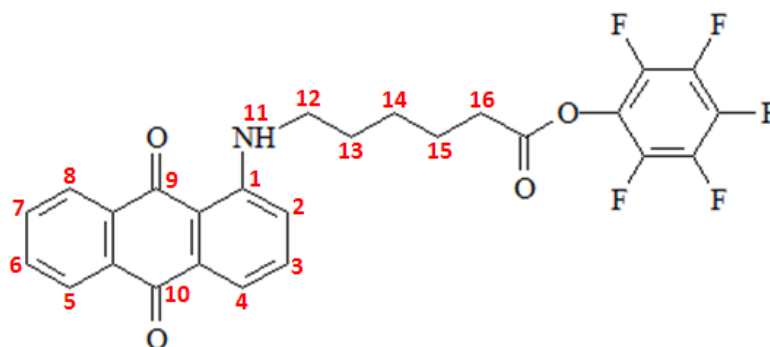


Numbering of anthraquinone conjugate

A numbering system of anthraquinone conjugates were used here. This will particularly support the NMR spectral analysis. The **Example B** (AQ-Ahx-OPFP **HZ22**) is one of the synthesised compounds from Chapter 4. The numbers in red indicate the positions of atoms or groups of atoms allocated to the reported nmr signals of the HZ22 chemical structure.

# Chapter 1. MMP-9 Activated Prodrugs

## 1.1 Abstract

One aspect of this project aims to design, synthesize and evaluate MMP-9 activated prodrugs that target GABA receptors (with GABA modulators) and further incorporating either an antiangiogenic and/or cytotoxic agent. The objective will be to find out whether tumour-selective targeting the MMP-9 increases the anticancer activity (a synergistic effect) and reduces the general toxicity compared to using the cytotoxic/antiangiogenic agent alone.

## 1.2 Hypothesis

The specificity of the human matrix metalloproteinase, MMP-9 (overexpressed in ovarian and colon cancer) for key amino acid residues in the P1- P1´ positions can be exploited to activate synthetic oligopeptide prodrug substrates in the tumour microenvironment selectively, with concomitant improvement in therapeutic index.

It is proposed that MMP-mediated prodrug activation can be exploited to deliver GABA (free ligand) and/or GABA receptor-targeting agents to modulate tumour response to cytotoxic and/or vascular disrupting agents.

**1.3 Introduction**

**1.3.1 MMPs in Tumour and Neurodegenerative Disease**

Matrix metalloproteinases (MMPs) are detected to be over expressed in a variety of tumour types. For instance, small cell lung cancer was detected with high levels of MMP-3, MMP-11 and MMP-14. High expression of MMP-11 has been demonstrated in breast cancer. Patients with prostate cancer have high MMP-2 level. It was also found that MMP-2 and MMP-9 levels were increased in gastric cancer. These findings suggest that MMPs have potential to be used as the markers for cancer diagnosis (Zucker *et al*. 1999). The role of MMPs in tumour growth, invasion and metastasis was proposed mainly by preclinical animal studies (Vihinen and Kähäri, 2002). It is now widely believed that the activity of MMPs facilitates the tumour progression through the extracellular matrix (ECM) in two aspects: First, MMPs are responsible for degrading the ECM and basement membrane, consequently malignant cells can move through blood vessel walls and connective tissues and resulting in cancer metastases (Ray and Stetler-Stevenson 1994). Second, MMPs stimulate the secretion or activation of ECM growth factors, such as vascular endothelial growth factor (VEGF), basic fibroblast growth factor (bFGF) and insulin-like growth factor. The multiple roles of MMPs in cancer progression are illustrated in **Figure 1.**
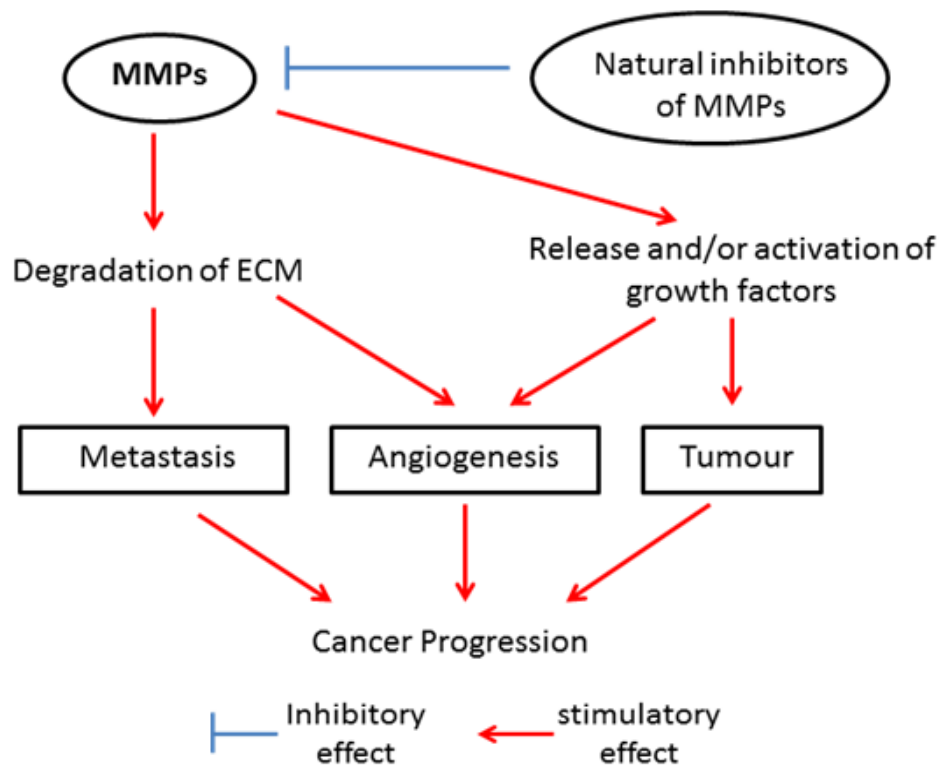
**Figure 1.** The role of MMPs in cancer progression
(Adapted from Klein *et al.* 2004)

Based on extensive literature, MMP-2 and MMP-9 are the most discussed MMPs in relation to cancer (for reviews, see Gialeli, Theocharis and Karamanos, 2011; Hidalgo and Eckhardt, 2001).

Moreover, MMP activities are linked to the pathogenesis of acute and chronic neurodegenerative disorders (Rosenberg, 2009). The level of MMPs, especially MMP-9 was detected to be elevated in patients with Alzheimer's disease, epilepsy, dementia, and Parkinson's disease (Ethell and Ethell, 2007; Mizoguchi, Yamada and Nabeshima, 2011; Yong *et al.,* 1998). It is believed that MMPs can increase the permeability of the blood-brain barrier and eventually cause white matter damage, brain edema, haemorrhage, ischemia and stroke (Candelario-Jalil *et al.,* 2011). Recent studies revealed that MMPs are also involved in the degradation of amyloid β-proteins in Alzheimer's disease and dopaminergic neurons in Parkinson's disease (Yong *et al.,* 2001; Mizoguchi,

Yamada and Nabeshima, 2011). To sum up, MMPs are promising targets for the treatment of cancer and neurodegenerative disease because of their involvement in disease initiation and progression.

### 1.3.1.1 MMPs activation and regulation

MMPs are a family of zinc-dependent endopeptidases that are capable of degrading a variety of Extracellular Matrix (ECM) components and involved in remodeling of many tissues and organs. The MMPs were first described in 1962 as the enzymes with proteolytic action for dissolution of the tadpole tail (Tallant *et al.*, 2010). Now there are more than 20 enzymes classified as MMPs. MMPs were found to be over-expressed in a variety of tumours and play a pivotal role in tumor growth, invasion, metastasis and angiogenesis (Curran and Murray, 2000). The general structure of MMPs consists of five domains: a signal peptide domain, a propeptide domain containing a cysteine switch, a catalytic domain, a hinge region, and a hemopexin-like domain at the C terminus (showed in figure 2) (Nagase and Woessner, 1999). Most MMPs are produced as inactive enzymes (zymogens) with a propeptide domain that must be removed for the enzyme activation. The propeptide domain contains a cysteine residue which interacts with the catalytic zinc atom and prevents the binding and cleavage of the substrate. The proteolytic cleavage of propeptide domain triggers a conformational change and exposes the catalytic site to the substrate (Murphy and Knäuper, 1997).
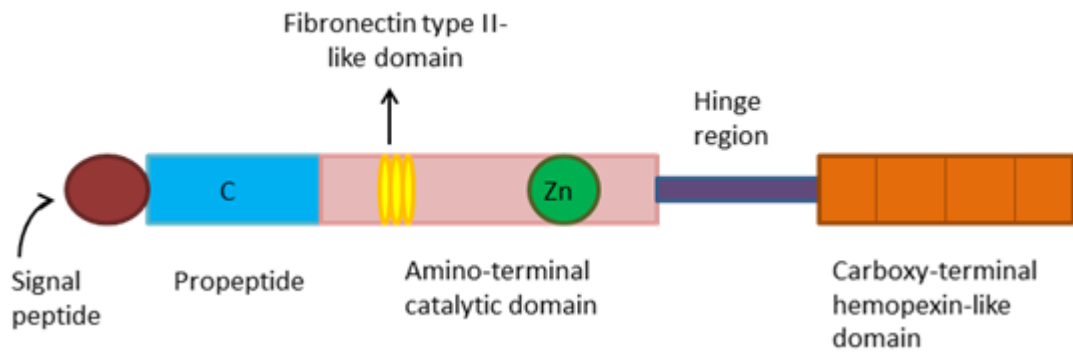
**Figure 2.** The general domain structure of matrix metalloproteinases (MMPs), MMP2 and MMP-9 are gelatinases which contain a fibronectin type II domain inserted into the catalytic domain
(Adapted from Murphy and Nagase, 2008)

The MMPs activity is closely regulated by gene expression and proenzyme activators. Most of the time, the level of MMPs produced is very low. The expression of MMPs can be induced by a variety of growth factor, cytokines, hormones and oncogenes in respond to normal tissue remodelling, wound healing, inflammation and cancer (Clark *et al.,* 2009).

### 1.3.1.2 MMPs inhibitors

The MMPs activity can be inhibited by non-specific endogenous inhibitors which include α1-antiprotease and α2-macroglobulin, and by specific tissue inhibitors of the metalloproteinases (TIMPs) (Woessner, 1991; Cao, 2001). The family of TIMPs is composed of TIMP-1, TIMP-2, TIMP-3, and TIMP-4. A variety of cell types produce the TIMPs (Bonomi, 2002). The TIMPs contain a chelating group which binds to the active zinc atom of MMPs resulting in the formation of a non-covalent complex. TIMPs are able to inhibit the proteolytic activity of all MMPs and many pro-MMPs (Clark *et al.,* 2009; Brew and Nagase, 2010). The design of MMPs inhibitors represents an important approach of MMPs targeting anticancer drugs (Hinnen *et al.,* 2001).

A number of synthesised MMPs inhibitors have been shown to be effective in the treatment of cancer. The peptidomimetic and nonpeptidic MMP inhibitors are most studied in clinical trials (Hidalgo and Eckhardt, 2001). The peptidomimetic inhibitors were synthesised to mimic the structure of collagen and irreversibly bind at the active site of MMPs. The most common clinical used zinc-binding group of inhibitors is hydroxamate (Konstantinopoulos et al., 2008). Batimastat is the first peptidomimetic inhibitor used in cancer patients. The beneficial aspects of Batimastat include mild toxic side effects, prolonged half-life up to 3-4 weeks and well tolerated in patients. However, this drug has poor orally bioavailability and needed to be intraperitoneally or intrapleurally administered. Marimastat is a low molecular weight analogue of Batimastat that has improved solubility. Marimastat has now been withdrawn due to the poor performance in clinical trials (Sparano et al., 2004). Furthermore, both Batimastat and Marimastat have nonselective binding to MMPs (Rasmussen and McCann, 1997).

One major problem of peptidomimetic inhibitors is the lack of specificity for MMPs. In order to overcome this problem, a series of nonpeptidic inhibitors have been developed based on the differential three-dimensional conformations of the MMPs active zinc sites. Prinomastat (AG3340), BAY 12-9566 and BMS-275291 were synthesised as specific inhibitors of MMP-2, 3 and 9. The antitumour activity of these drugs has been demonstrated in preclinical models (Gatto et al., 1999; Giavazzi and Taraboletti, 2001). These agents then underwent clinical trials for cancer therapy. However, the trials of prinomastat, BAY 12-9566 and BMS-275291 had been stopped at phase III because of negative findings and did not improve the outcome of chemotherapy (Bissett et al., 2005; Giavazzi and Taraboletti, 2001; Leigh et al., 2004)

The tetracycline derivatives have also been found to inhibit both the activity and

production of MMPs. The tetracycline analogues, Doxycycline and Col-3 both inhibit the secretion of activity of MMP-2 and MMP-9. Bisphosphonates are prevalently used in patients with breast cancer and multiple myeloma. The drug also has inhibitory effects on MMPs activity (Hidalgo and Eckhardt, 2001).

**1.3.1.3 The substrate preference of MMP-9**

The proteolysis domain structure of MMP-9 gives it well-defined substrate preference. The catalytic sites of MMPs are determined by X-ray crystallography and NMR spectroscopy, and are assigned to mainly six subunits (subsites or pockets): S1, S2, S3 and S1', S2', S3'. Correspondingly, the functional residues (individual amino acid side-chains) of an MMP substrate interacting with these pockets are designated as P1, P2, P3 and P1', P2', P3' positions (Gupta and Patil, 2012). The structure relationship between MMPs and their substrates is shown in **Figure 3**. The amide (peptide) bond between the P1 and P1' position of the MMP peptide substrate is called the scissile bond or cleavage 'hot spot'.

The substrate selectivity of MMP-9 has been investigated. It becomes clear that the deep S1' pocket prefers a large hydrophobic residue, such as leucine (Leu), in the P1' position of MMP-9 substrates (Gupta and Patil, 2012). Proline (Pro) is the most optimizing binding residue in the P3 position. This is because proline has a cambered structure which fits well in the S3 pocket of MMP-9. However, other MMPs with the same substrate preference in P3 positions are very common, such as MMP-7 and MMP-13. For the P2 position, an amino acid with long side chain is favoured for MMP-9, such as arginine (Arg). Although Arg was also found at P2 in substrates for MMP-13, the frequency was much lower than MMP-9 (Kridel *et al.* 2001). Besides, aspartic acid (Asp) was also reported to be prevalent in the P2' position of natural MMP-9 substrates, whereas MMP-2 prefers glutamic acid (Glu) (Chen *et al.* 2003). It has been revealed that glycine

(Gly) most often occupies the P1 position of MMP-2 and MMP-9 substrates (Lauer-Fields *et al.* 2003). The binding of serine (Ser) and threonine (Thr) to the S2' pocket of MMP-9 also showed high frequency (Kridel *et al.,* 2001).

The MEROPS data base was searched for information on preferred peptide sequence of MMP-9. Based on 367 cleavages, for example, Gly was in the P1 position most times (120). Previous work from this laboratory had indicated that long, straight chain hydrocarbon residues of the non-proteinogenic amino acids norvaline and norleucine were favoured in the P1´ position (Mincher *et al.*, 2006; Mincher *et al.*, 2008). The rest of the amino acids of peptide substrate for design and synthesis of MMP-9 activated prodrugs in this study were chosen here by most common occurrences in reported cleavages (Rawlings, Barrett and Bateman, 2012) and illustrated in **Figure 3**.
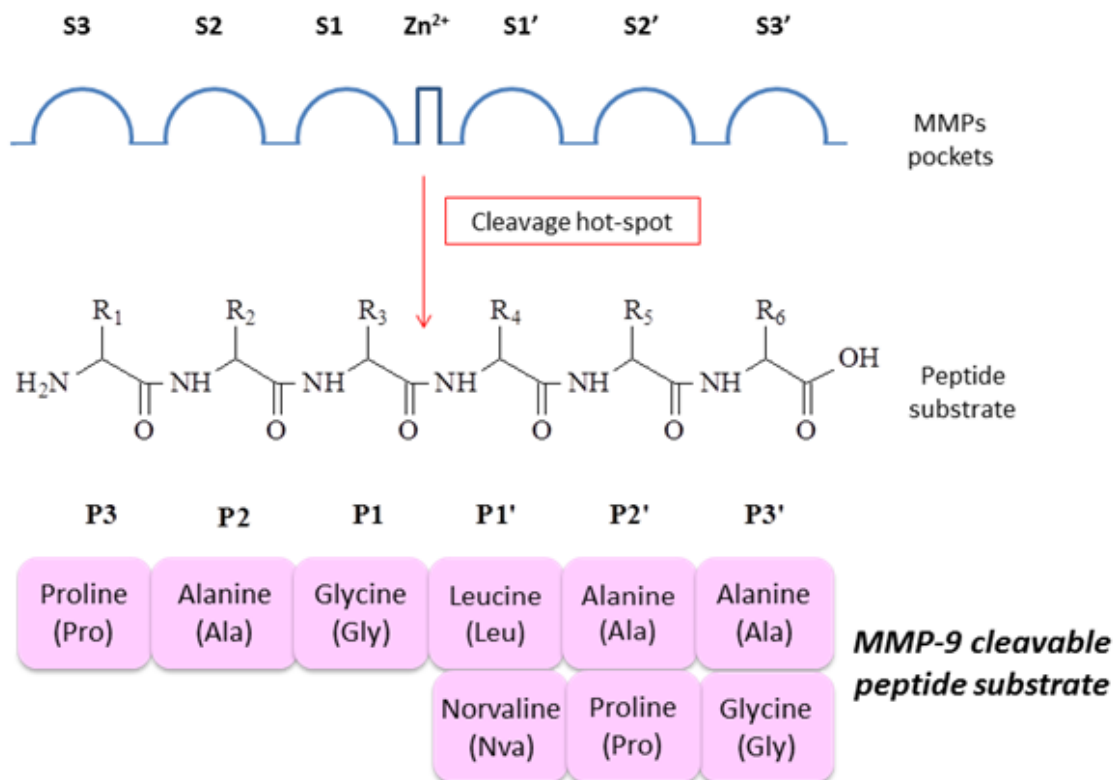


**Figure 3.** MMPs proteolysis pockets and MMP-9 substrate specificity

### 1.3.2 GABA and its receptors

GABA (gamma-amino butyric acid) is the main inhibitory neurotransmitter in the mammalian central nervous system (CNS). The catalytic enzyme, glutamate decarboxylase (GAD), is involved as the major effector in the biosynthesis of GABA from glutamate (Barker *et al.,* 1998).

GABA acts on two distinct types of receptors, $GABA_A$ and $GABA_B$. $GABA_A$ receptor is a ligand-gated chloride ion channel with a fast synaptic inhibition effect (Jacob *et al.,* 2008), while $GABA_B$ receptor is a G-protein coupled receptor with slower synaptic inhibitory transmission. They are both important therapeutic targets for the clinical treatment of psychiatric and neurological disease (Watanabe *et al.,* 2002).

It is also found that GABA and its receptors exist in many peripheral organs, for instance, liver, pancreas, intestine, kidney, prostate and ovary (Watanabe *et al.,* 2006). This fact indicates that GABA has more functions than being a neurotransmitter. Many studies suggested that GABA plays a regulatory role in cell proliferation and migration, which leads to the consideration of the involvement of GABA in tumour cell proliferation (Szczaurska *et al.,* 2003).

### 1.3.2.1 Regulatory role of GABA in Tumour

The GABA content and its synthesizing enzyme (GAD) activity were reported to be increased in certain cancer types such as prostate, gastric, colon, ovarian, glioma, and breast cancers (Young and Bordey, 2009).

In 2003, Azuma *et al.* reported that GABA promotes prostate cancer metastasis by increasing MMP production in cancer cells via the $GABA_B$ receptor pathway. Also, GABA showed a stimulatory effect on pancreatic cancer with upregulated the π subunit of the $GABA_A$ receptor (Takehara *et al.,* 2007).

In contrast, GABA was found to play an inhibitory role in colon carcinoma

(Joseph *et al.*, 2002; Ortega, 2003), cholangiocarcinoma (Fava *et al.,* 2005), and lung adenocarcinoma (Schuller *et al.,* 2008b). At this point, it is evident that the connections between GABA and cancer are not well understood and this adds to the motivation behind this research project.

**1.3.2.2 GABA$_A$ receptors in Tumour**

The GABA$_A$ receptor is a ligand-gated ion channel which selectively conducts chloride anions (Cl$^-$) through its pore. GABA$_A$ receptors can be found in all organisms that have a nervous system (Campagna-Slater and Weaver, 2007). In humans, the structure of GABA$_A$ receptor consists of varying combinations of α, β, γ, π, θ, ε, δ, and ρ protein subunits (**Figure 4**). Five subunits can combine in different ways to form GABA$_A$ receptors. Different combinations of these subunits may result in distinct pharmacological properties (Olsen and Sieghart, 2009). The minimal requirement to build a GABA$_A$ receptor pentamer is the inclusion of both α and β subunits (Connolly *et al.*, 1996). When endogenous ligand GABA binds to the GABA$_A$ receptor complex, the protein receptor changes conformation that cause opening the pore to allow Cl$^-$ pass through the membrane. Consequently, agonists activate the GABA$_A$ receptor resulting in increased Cl$^-$ conductance. Muscimol is one of selective agonists for the GABA$_A$ receptor that binds to the same site as GABA, as opposed to drug benzodiazepine which binds to a separate regulatory site. For antagonists, though they have no effect on their own, compete with GABA for binding and thereby inhibit its action, resulting in decreased Cl$^-$ conductance (Frølund *et al.,* 2002)
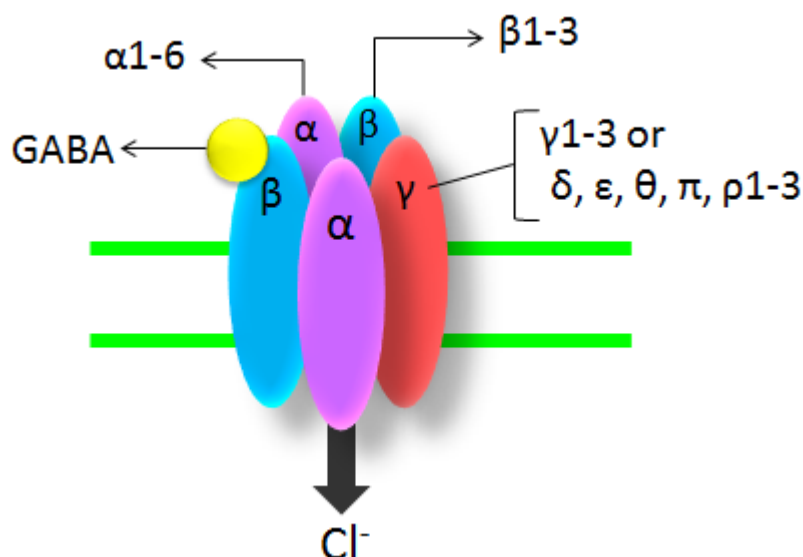
**Figure 4**. Structure of GABA$_A$ receptor
(Adapted from Jacob *at al.* 2008)

A number of reports suggested a relationship between GABA$_A$ receptors and oncogenesis. Considering brain tumours, the expression of GABA$_A$ receptors was upregulated in human glioma cells (Synowitz *et al.,* 2001), but glioblastoma had downregulated GABA$_A$ receptor expression (Aronica *et al.,* 2007). The decreased level of GABA$_A$ α3 subunit and increased level of GABA$_A$ β3 subunit were detected in human hepatocelluar carcinoma (Liu *et al.,* 2008; Minuk *et al.,* 2007). The π subunit of GABA$_A$ receptor was upregulated in pancreatic and breast cancers (Johnson and Haun, 2005). In addition, patients with prostate cancer have upregulated expression of GABA and GABA$_A$ receptor (Abdul, *et al.,* 2008).

The stimulatory action of propofol, a well-known anaesthetic agent and a GABA$_A$ receptor agonist, on colon tumours inhibited the cancer cell invasion and expression of MMP-2 and MMP-9 (Miao *et al.,* 2010). Additionally, the GABA$_A$ receptor antagonist picrotoxin inhibited prostate cancer cell proliferation (Ippolito *et al.,* 2006).

### 1.3.2.3 GABA<sub>B</sub> receptors in Tumour

The heterodimer structure (**Figure 5)** of the $GABA_B$ receptor is composed of two subunits $GABA_{B1}$ and $GABA_{B2}$. The extracellular domain (ECD) of $GABA_{B1}$ is capable of binding GABA, agonist and antagonist, whereas the ECD of $GABA_{B2}$ does not bind any ligands (Kaupmann *et al.,* 1998). The transmembrane domain of $GABA_{B2}$ can bind to certain modulators. The Intracellular domain of $GABA_{B2}$ coupled to G-protein and regulates the activities of the $Ca^{2+}$ channel, $K^+$ channel and Adenylyl Cyclase (AC). Both subunits are required for normal $GABA_B$ receptor function *in vivo* (Filip and Frankowska, 2008).
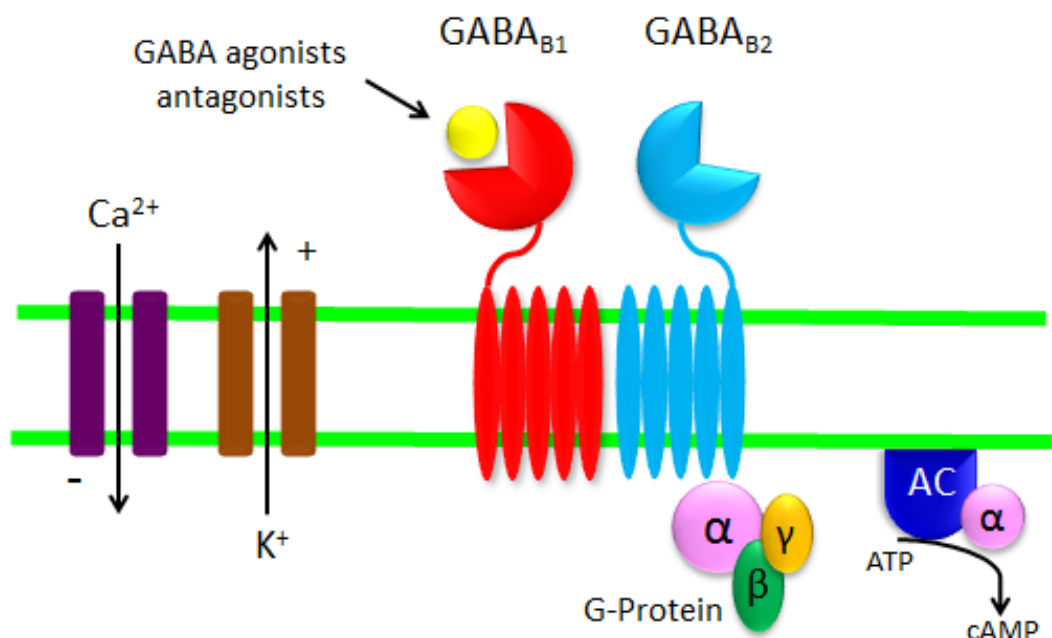


**Figure 5.** The schematic structure of GABA<sub>B</sub> receptors
(Adapted from Jiang *et al.* 2012)

Growing evidence showed that $GABA_B$ receptors are involved in tumour development. The expression level of $GABA_B$ receptors was found to be upregulated in human colon cancer cell lines (Thaker *et al.,* 2005), thyroid tumours (Roberts *et al.,* 2009), breast cancer (Jiang *et al.,* 2012) and hepatocellular carcinoma cell lines (Wang *et al.,* 2008). Furthermore, Zhu *et al.* (2004) revealed that in human gastric cancers, not only $GABA_B$ receptors were

overexpressed, but also the localization of GABA$_B$ receptors in gastric cancer cells is different from normal cells. They found that the majority of GABA$_B$ receptors were localized on the gastric cancer cell surface other than in the cytoplasm which is the main location site of GABA$_B$ receptors in normal cells. These facts suggest that GABA$_B$ receptors may be potential targets for cancer therapy and diagnosis.

The GABA$_B$ receptor agonist baclofen significantly attenuated the malignancy of human pancreatic (Schuller *et al.,* 2008a), lung (Schuller *et al.,* 2008b), liver (Wang *et al.,* 2008), breast, colon, and gastric tumours (Jiang *et al.,* 2012). The activation of GABA$_B$ receptors has an inhibitory effect on most of human tumour types except prostate cancer (Abdul *et al.,* 2008).


### 1.3.3 Tumour activated prodrugs

The majority of anticancer drugs are anti-proliferative agents that are able to kill rapidly dividing tumours cells. However, these drugs affect normal proliferating cells such as hair follicles, bone marrow, lymphatic cells and red blood cells (Denny, 2001).The poor selectivity of these chemotherapy drugs could cause lethal damage of normal cells and making them not suitable for long term use. Hence, improving the target ability and selectivity of anticancer drugs is a major challenge. The tumour activated prodrugs (TAPs) strategy in anticancer chemotherapy represents a promising approach. TAPs are relatively non-toxic and the active pharmacologic agents can be selectively released in tumour cells (Rautio *et al.,* 2008). The general design of TAPs is depicted in **Figure 6**. TAPs may consist of four components: 1) an active drug that exhibits the pharmacologic effect. 2) a chemical linker which links the active drug to the rest part of TAPs. 3) a peptide spacer that can be cleaved by tumour specific enzymes, or a polymer spacer 4) a targeting moiety that is responsible for

specific delivery to tumour cells. Many antigens and enzymes have been proven to be over expressed in tumour cells and are commonly used targets for TAPs (Mahato *et al.,* 2011).
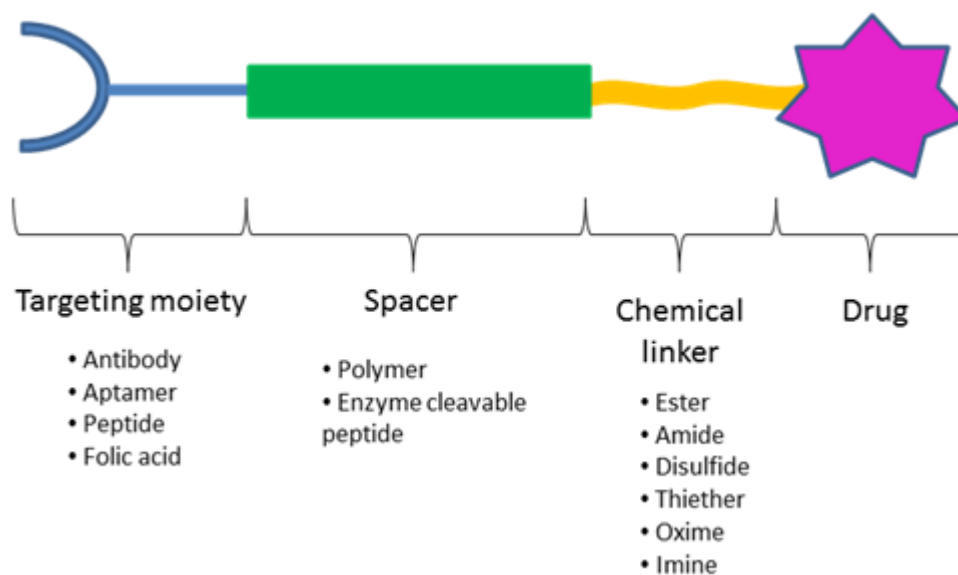


**Figure 6**. General design of a tumour activated prodrug
(Adapted from Mahato *et al.,* 2011).

**1.4   Results and discussion**

**1.4.1 The design strategy of MMP-9 activated prodrugs**

In this study, the general proposed design of MMP-9 activated prodrugs is composed of three main parts **(Figure 7)**: an MMP-9 cleavable peptide linker in the middle of the prodrug, one side of the peptide linker is attached with a ligand of GABA, either a GABA agonist or antagonist that targets GABA receptors, the other side of the cleavable oligopeptide linker can be an antiangiogenic/cytotoxic agent (for therapeutic purpose) or a fluorescent label such as a fluorescein-derived agent (for diagnostic purpose).
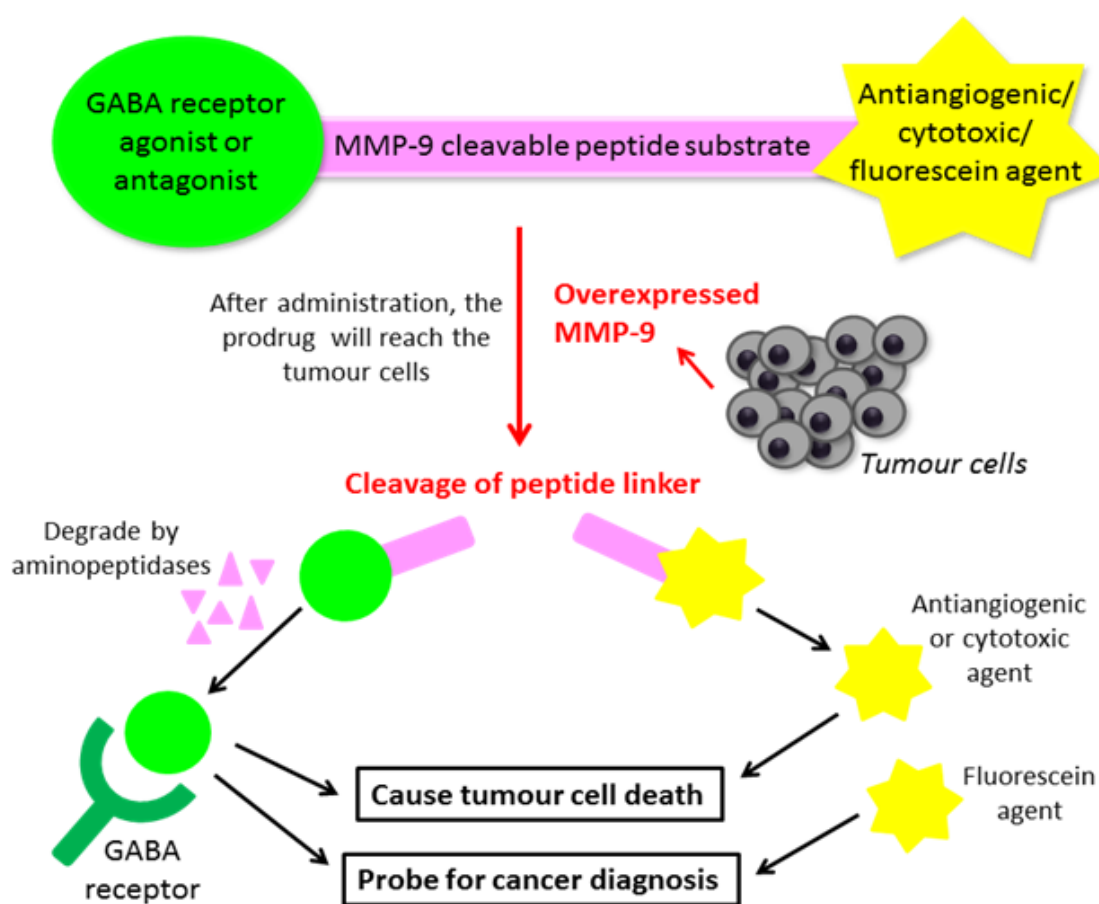


**Figure 7.** General concept of MMP-9 activated prodrug design

Once the prodrug has been administered and reached the tumour, because tumour cells have over expressed MMP-9, the prodrug will be cleaved extracellularly at the MMP-9 specific peptide cleavage site or 'hotspot'. After that,

the remaining amino acids that are still attached to the active agent will be degraded by aminopeptidases, which are ubiquitous in almost all cell types. This will cause the release of the active drugs to the tumour cells.

The MMP-9 activated prodrug will remain inactive until the peptide linker is cleaved by MMP-9. The presence of high levels of MMP-9 in tumours but not in normal tissues increases the prodrug selectivity (Lim *et al.* 2010)

Based on the previous work of this lab, a prototype, latently fluorescent oligopeptide conjugate of a cytotoxic topoisomerase inhibitor, EV1-FITC was a good proof-of-principle example of MMP-9 activated prodrugs. The prodrug was able to target multiple myeloma and release fluorescence by MMP-9 activation (Van Valckenborgh *et al.* 2005).

### 1.4.2 Synthesis of Model compounds

The active drug propranolol was first considered in this study. Propranolol is a well-known non-selective beta-blocker (or $GABA_B$ receptor antagonist) and has been introduced as a novel drug for the treatment of haemangiomas, which are the most common tumours of infants (Zimmermann *et al.* 2010). Several recent papers reported the Inhibitory efficacy of propranolol on MMP-9 secretion (Annabi *et al.* 2001) and the anti-angiogenic property in tumours (Lamy *et al.* 2010; Pasquier *et al.* 2011).

Before using the active drug propranolol for the synthesis of designed MMP9 activated prodrugs, a model compound (NU: UB 491), which serves as a mimic of the structure of propranolol was used first. The compound NU:UB 491 used in this study had been previously synthesised, in two steps, from the reaction of 1-chloroanthraquinone with 1,3-diamino-2-propanol in DMSO, following methods described by Katzhendler *et al.* (1989), to give the (aminoalkyl)aminoanthraquinone intermediate. This was further reacted with

di-*tert*-butyl dicarbonate (Boc$_2$)O, in order to protect the primary amino group, ensuring that only the secondary alcohol was available for reaction.

The model compound NU: UB 491 and propranolol both have hydroxyl (-OH) and amine (-NH) functional group which are important sites for chemical reactions, including acting as potential positions for attachment of peptide linkers in the intended prodrug substrates here **(Figure 8)**.
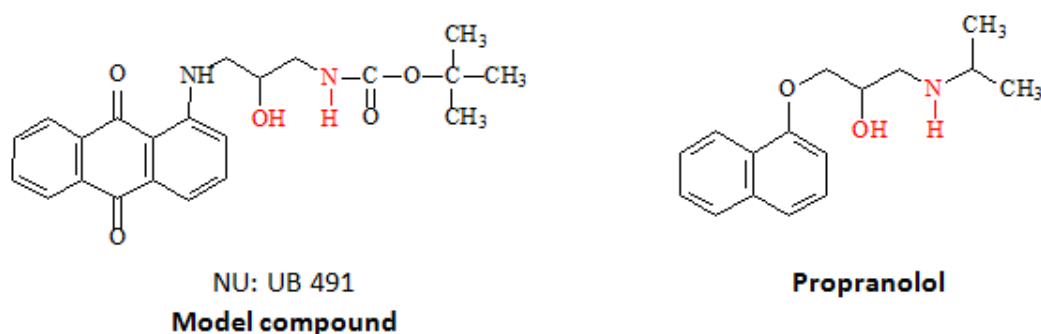


**Figure 8.** Chemical structures of NU:UB 491 and propranolol

In order to find conditions for selective reactions on the NH or OH functional group of propranolol, the model compound was used as a starting material for the synthesis of HZ26, HZ27 and HZ28. Moreover, the model compound is red which makes it easier for monitoring the synthesis of derivatives and easier to establish good chromatographic purification methods ahead of using the colourless and more expensive propranolol.

### 1.4.2.1 Synthesis of Fmoc-Ala-[Boc-Spacer]-AQ (HZ26)

The N-Fmoc protected β-Alanine amino acid (Fmoc-β-Ala-OH) (intended linker) was reacted with the model compound, NU: UB 491 using DCC and DMAP as ester coupling reagents (El-Faham and Albericio, 2011) in dichloromethane (solvent) **(Scheme 1)**. The mixture was stirred and monitored by thin-layer

chromatography on silica plates (TLC test). The reaction was completed in 1 hour. The precipitated byproduct DCU was filtered off. The crude product was purified by solvent extraction and silica gel column chromatography using the eluting solvent dichloromethane-ethyl acetate (7:1). The pure product (HZ26) was triturated by the addition of diethyl ether and the resulting red solid was collected. Fmoc-Ala-[Boc-Spacer]-AQ (HZ26) was characterized by NMR spectroscopy. The $^1$H spectrum showed a signal for a 9-proton singlet at 1.45 ppm confirming the Boc group. All of the anthraquinone protons were successfully assigned; a doublet at 7.15 was assigned to H-2, H-3 and H-4 gave a triplet at 7.4ppm, H-6 and H-7 were found between 7.5 and 7.63 ppm, H-5 and H-8 appeared as a triplet at 8.22 ppm and 8.3 ppm respectively.



NU: UB 491                           Fmoc-β-Ala-OH

(a)
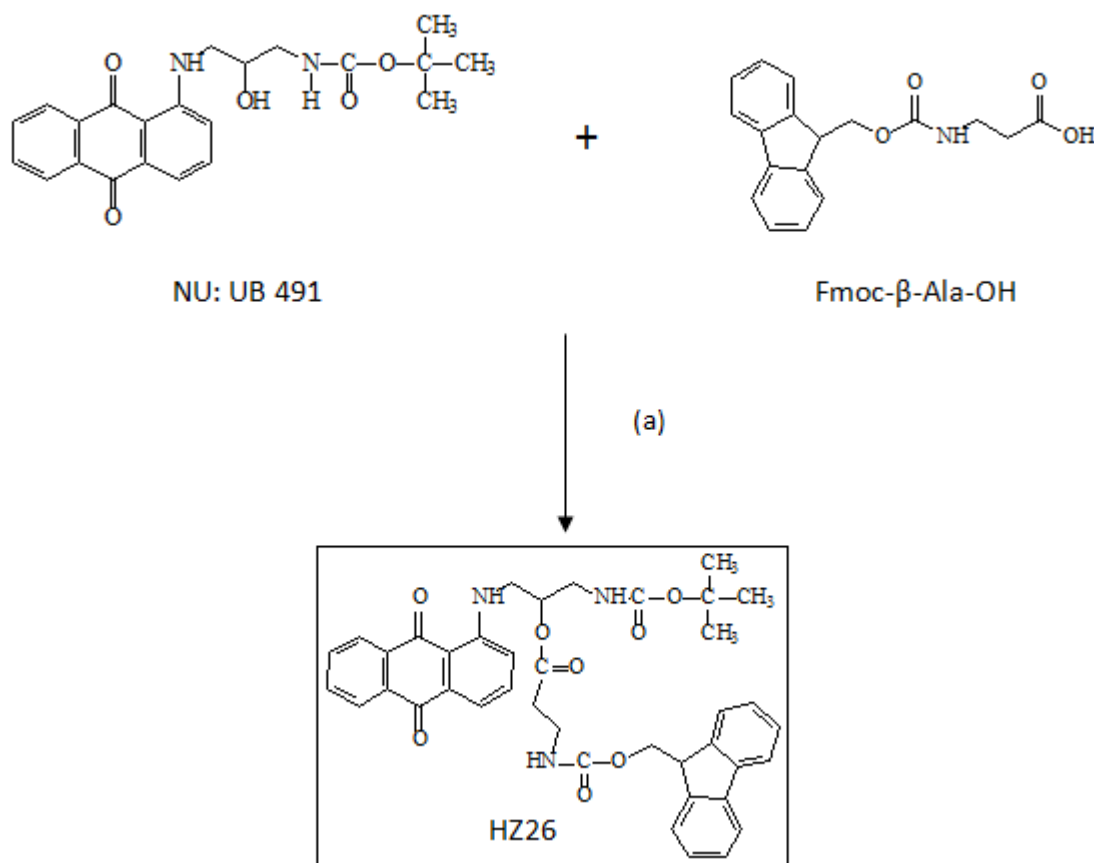
HZ26

Reagents and Conditions: (a) DCC & DMAP In dichloromethane

**Scheme 1.** Outline of HZ26 chemical synthesis

**1.4.2.2 Synthesis of H-Ala-Spacer-AQ TFA salt (HZ27)**

The Boc protecting group of Fmoc-Ala-[Boc-Spacer]-AQ (HZ26) was removed by TFA (Montalbetti and Falque, 2005) in solution after 10 minutes of reaction **(Scheme 2)**. According to TLC test, the product was pure and ready to collect. The solution was then evaporated to a small volume and diethyl ether was added to precipitate the solid product. H-Ala-Spacer-AQ TFA salt (HZ27) was characterized by NMR spectroscopy.
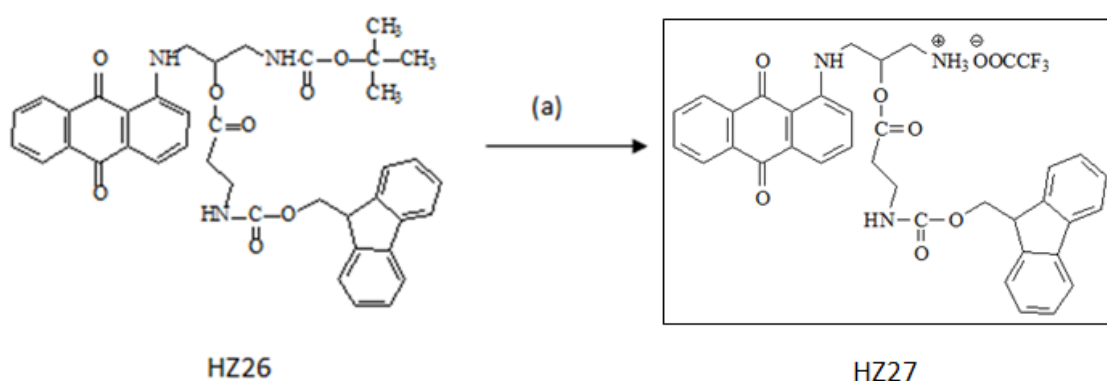


Reagents and Conditions: (a) TFA

**Scheme 2.** Outline of HZ27 synthesis

**1.4.2.3 Synthesis of H-Ala-[Boc-Spacer]-AQ (HZ28)**

Fmoc-Ala-[Boc-Spacer]-AQ (HZ26) was Fmoc deprotected by 2% piperidine in DMF **(Scheme 3)**. The reaction was completed in 30 min by checking the TLC. The amount of piperidine used in this reaction was much less than usual literature precedent which is 20% in DMF (Montalbetti and Falque, 2005). The crude compound was purified by extraction and column chromatography using chloroform-methanol (8:1) solvent system. The pure product was collected by precipitation in diethyl ether. The chemical structure of H-Ala-[Boc-Spacer]-AQ (HZ28) was confirmed by NMR spectroscopy.
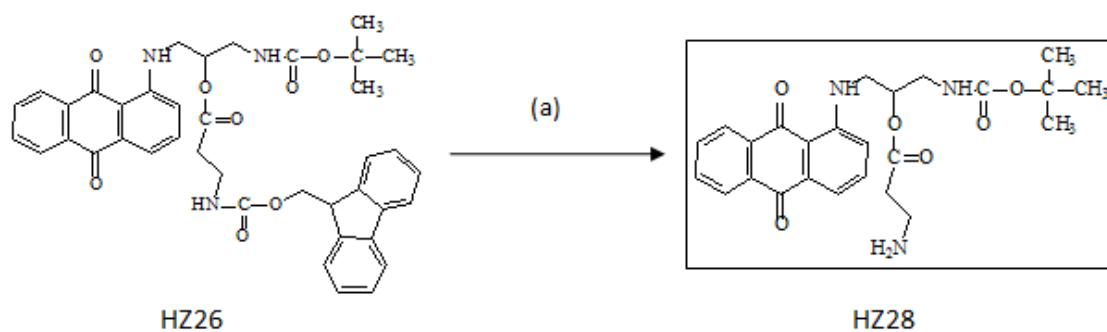
Reagents and Conditions: (a) 2% piperidine in DMF

**Scheme 3.** Outline of HZ28 synthesis

### 1.4.2.4 Synthesis of Fmoc-Ala-Propranolol (HZ29)

Using some of the knowledge gained from selective reaction on functional groups in the model compound (above), derivatisation of the antiangiogenic GABA$_B$ antagonist propranolol was attempted. The design strategy was to introduce an amino acid (β-alanine) as the first residue for peptide synthesis, by selective reaction on the amino group (NH) of the drug. The success of this reaction would depend on the intrinsic greater reactivity of the amino group over hydroxyl. If reaction occurs at the hydroxyl group then an ester would be formed. Propranolol hydrochloride (its OH and NH functions unprotected) was reacted with Fmoc-β-Ala-OH, using standard coupling reagents TBTU, HOBt, and DIPEA (Montalbetti and Falque, 2005). The mixture was suspended in DMF at RT overnight **(Scheme 4)**. All reagents and product are colourless in solution and on TLC plates. In order to confirm which spot on the TLC plate is the product, a de-Fmoc mini test using piperidine (20%) in dichloromethane was performed. After 2 hours reaction, a TLC was checked under the UV light and found that one of the spots on product lane moved down to the bottom line, which indicates that spot is the product HZ29. The crude product was extracted with dichloromethane/water, dichloromethane/aqueous citric acid (to remove propranolol free base) and dichloromethane/aqueous sodium bicarbonate (to

remove excess Fmoc-β-Ala-OH). Further purification was done by column chromatography using eluting system dichloromethane-ethyl acetate (1:1). The pure product fractions were combined, filtered and evaporated to dryness. The white solid Fmoc-Ala-Propranolol (HZ29) was collected under vacuum.
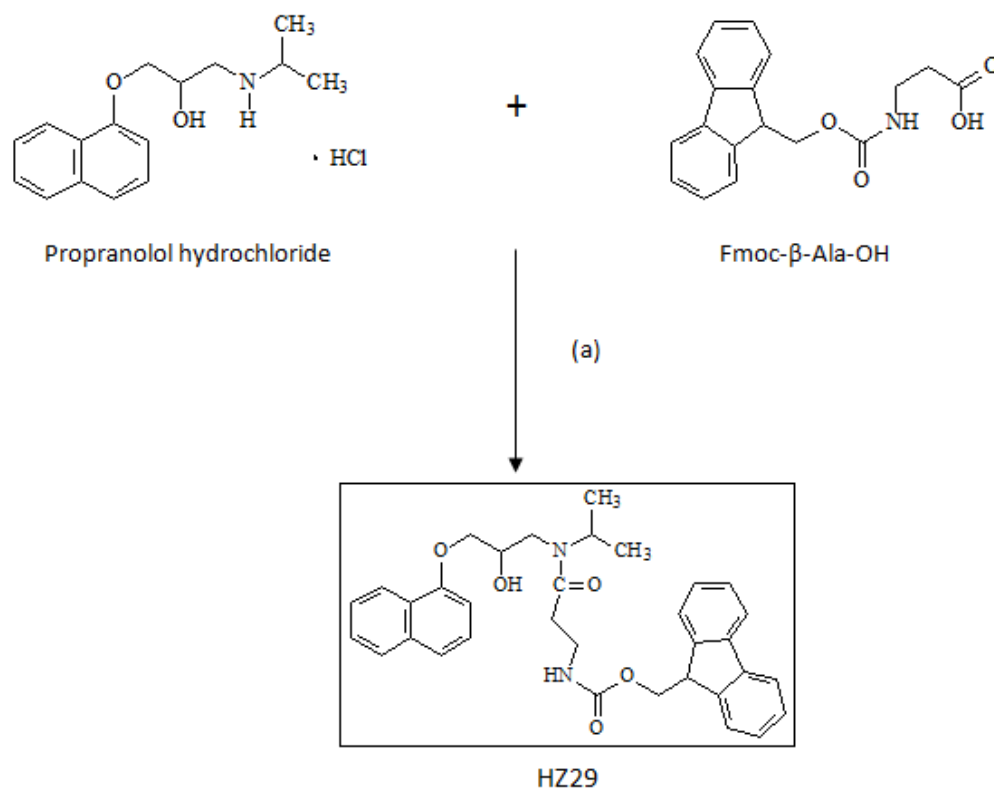


Reagents and Conditions: (a) TBTU, HOBt, DIPEA in DMF
**Scheme 4.** Outline of HZ29 synthesis

The structure of Fmoc-Ala-Propranolol (HZ29) was confirmed by is ^{1}H NMR spectrum. The signals between 7.28 and 7.58 were assigned to the aromatic protons of the Fmoc protecting group. The propranolol protons were fully assigned; H-2 at 6.9 ppm, H-3 and H-4 gave a multiplet at 7.6-7.7 ppm, H-5, H-6, H-7 and H-8 gave a multiplet between 7.7 and 7.9 ppm. The signals at 1.2-1.45 ppm reflected the protons of the two methyl group.

### 1.4.3 Synthesis of Prodrug 1: Fmoc-Pro-Ala-Gly-Leu-Ala-Ala-Propranolol (HZ32)

After the work on model compound derivatives, a series of MMP-9 activated prodrugs targeting GABA receptors were synthesised. The design strategy of prodrug 1 was to use a MMP-9 cleavable peptide substrate (Pro-Ala-Gly-Leu-Ala-Ala) as a linker. One side of the peptide linker is attached to propranolol which is both an antiangiogenic agent and a $GABA_B$ receptor antagonist. The other side of the linker is an Fmoc protecting or so called 'capping' group.

The synthetic process for prodrug 1 was started with the N-terminal Fmoc-protected hexapeptide linker, Fmoc-Pro-Ala-Gly-Leu-Ala-Ala-OH (HZ31) which was synthesised by a solid phase peptide synthesis (SPPS) method. SPPS is the process by which peptide synthesis can be carried out on solid support, was first developed by Bruce Merrifield and earned him the Nobel Prize in 1984. SPPS has many advantages over traditional synthesis such as all reagents can be simply washed away each step, overall quicker time for synthesis, convenient work-up and the synthetic intermediates do not have to be isolated (Montalbetti & Virginie 2005). By contrast, in solution phase peptide synthesis, all peptide intermediates requires isolation and the synthesis cycles are very labour intensive. In this study, five steps were involved in the SPPS: (1) Resin swelling (2) Amino acid deprotection (3) Colour test to detect the presence or absence of free amino groups during the synthesis process (4) Peptide coupling (5) Hexapeptide-resin cleavage.

### 1.4.3.1 Resin swelling

Fmoc-Ala-Wang resin **(Figure 9)** was shaken at RT, 750 rpm for 1.5 hour in 10ml dichloromethane using an orbital shaker to maximize its surface area for peptide

coupling. Dichloromethane was drained off and resin was washed by DMF 3 times (2 mins each time) for the next step.
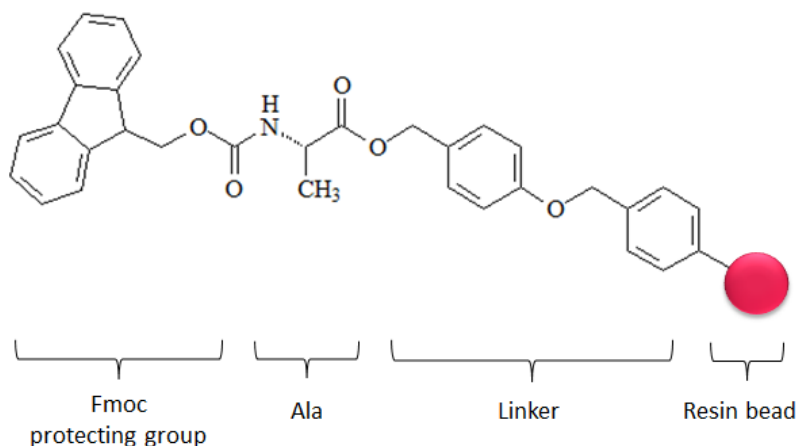


**Figure 9.** Fmoc-Ala-Wang Resin

### 1.4.3.2 Deprotection of Fmoc protecting group

The Fmoc protected group of the amino acid must be removed before growing the peptide. This was achieved by the addition of 20% (v/v) piperidine in DMF to the SPPS vessel and shaken for 15 mins. The deprotection step was repeated for 3 times. The reagents were drained off and the resin was washed by DMF 3 times (2 mins each time). The chemical mechanism of Fmoc deprotection by piperizine is showed in **Scheme 5.**
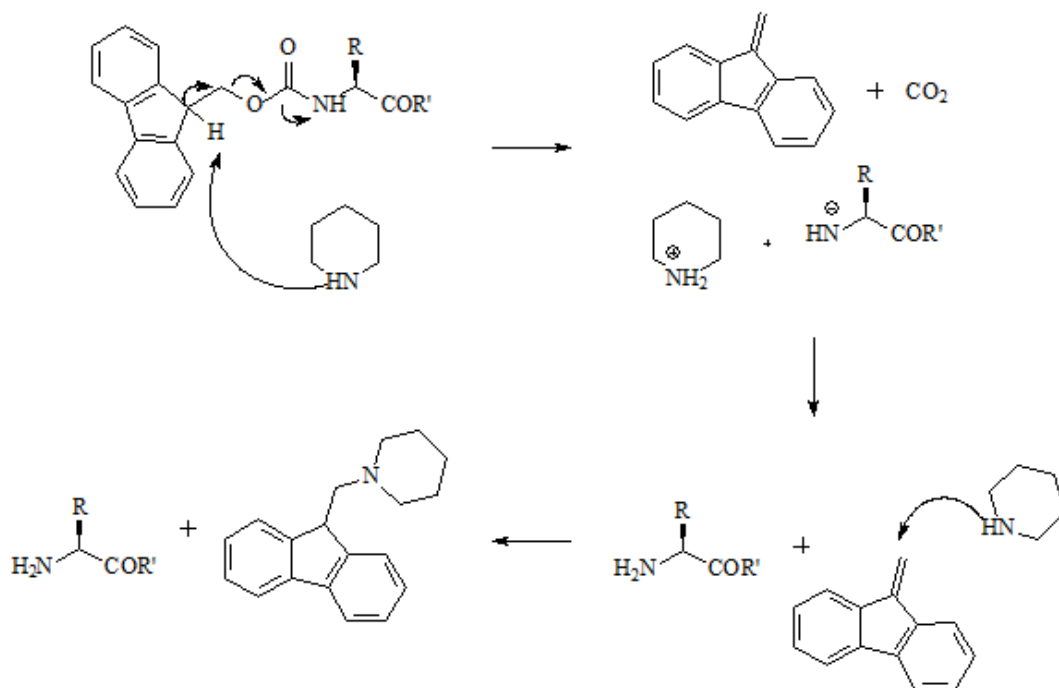
**Scheme 5.** Proposed mechanism of Fmoc deprotection by piperidine
(Adapted from Okada 2001)

### 1.4.3.3 Colour Test

In this study, an in-house Colour test **(Figure 10)** was performed to replace the
Kaiser test (which often gives poor results with Wang resin and requires toxic
reagents). [Refer also to the topic of Chapter 4].
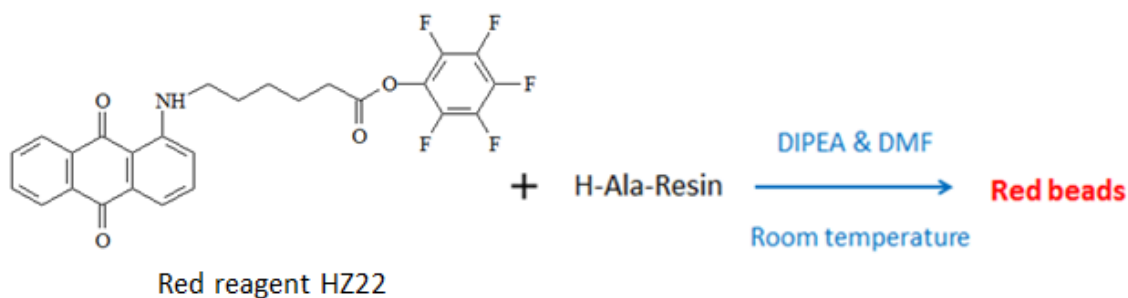


**Figure 10**. The reaction mechanism of HZ22 colour test.

About 1 mg of the colour test reagent AQ-Ahx-OPFP (HZ22) compound, 2 drops
of DMF and 1 drop of DIPEA were added to a sample bottle to give a red solution.
A small number of resin beads were then transferred to the vial. After 5 minutes,
a large amount of DMF was added to dilute the solution. This facilitated the

colour observation of the beads. All beads had turned into red from their original light yellow colour, which indicated that the deprotection has completed. For each stage of amino acid coupling or Fmoc deprotection, the colour test was performed. The synthesis of AQ-Ahx-OPFP (HZ22) compound is discussed in Chapter 4.

Compared to the Kaiser Test, this colour test is more sensitive and less toxic. For instance, one of the reagents for the Kaiser test is potassium cyanide which is highly toxic (Friedman 2004). Based on the experiments in our laboratory, the Kaiser test is not very effective for some amino acids, eg. Proline. Needless to say, the Kaiser test requires 80°C for the reaction while the colour test used in this study was done at RT. Hence, the colour test can be a promising technique for future SPPS.


### 1.4.3.4 Peptide coupling

At the peptide coupling stage, an Fmoc-protected amino acid containing its free carboxylic acid was reacted with the free amino group of the growing peptide-resin. Based on the formation of amide bond, the basic conditions and coupling agents included Fmoc-protected amino acid, TBTU, HOBt and DIPEA dissolved in DMF. The coupling solution was added to the SPPS vessel by two times, each time shaken for 40 min at RT. The colour test was performed to confirm the completion of peptide coupling.

The Fmoc-protected amino acid was deprotonated by DIPEA and nucleophilic substituted by TBTU which had two forms, uranium salt and guanidium in solution. The generated uranium ester intermediate was rapidly reacted with HOBt and leading to the production of the coupled peptide (**Scheme 6)**.
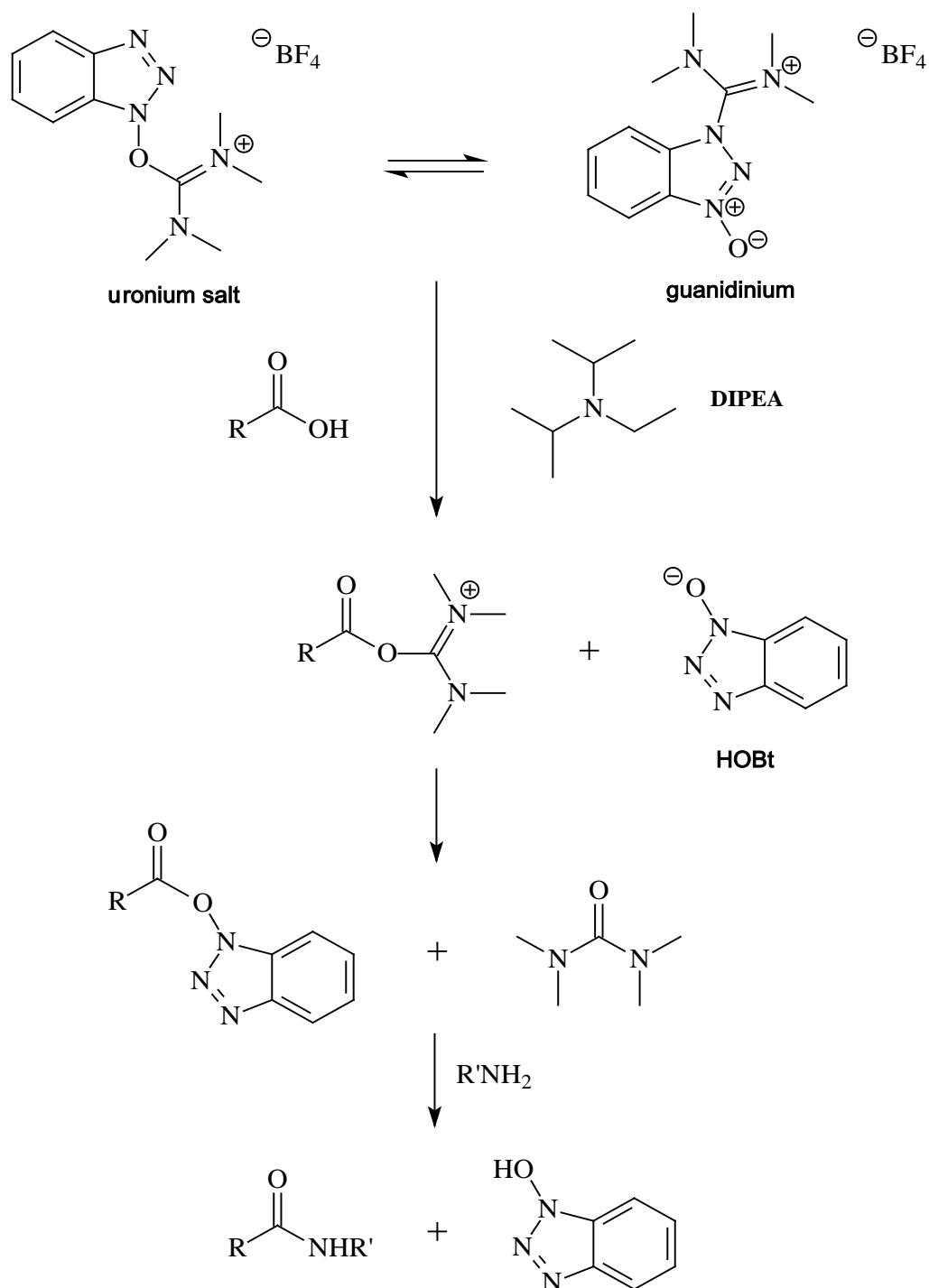
**Scheme 6**. Chemical mechanism of peptide coupling using reagents TBTU, HOBt and DIPEA

(Adapted from Carpino *et al.* 2001; Montalbetti & Virginie 2005)

### 1.4.3.5 Hexapeptide-resin cleavage

After the hexapeptide coupling, the Fmoc-protected hexapeptide needed to be removed from the resin. The Wang resin is known to be sensitive to acid and hence the attached hexapeptide was cleaved by the addition of 95% TFA and 5%

dichloromethane to the vessel for 2-3 min with shaking. The solution was drained into the flask and checked by TLC The procedure was repeated up to 10 times until there was no new spot on the TLC The resin was then washed with dichloromethane (2 times), methanol (2 times), and dichloromethane once. All filtrates were combined, evaporated to dryness and triturated in diethyl ether at 5 °C for 1 hour. The product was collected by filtration and dryness in a desiccator. **Figure 11** shows the overview of Fmoc-Pro-Ala-Gly-Leu-Ala-Ala-OH (HZ31) on solid phase peptide synthesis.
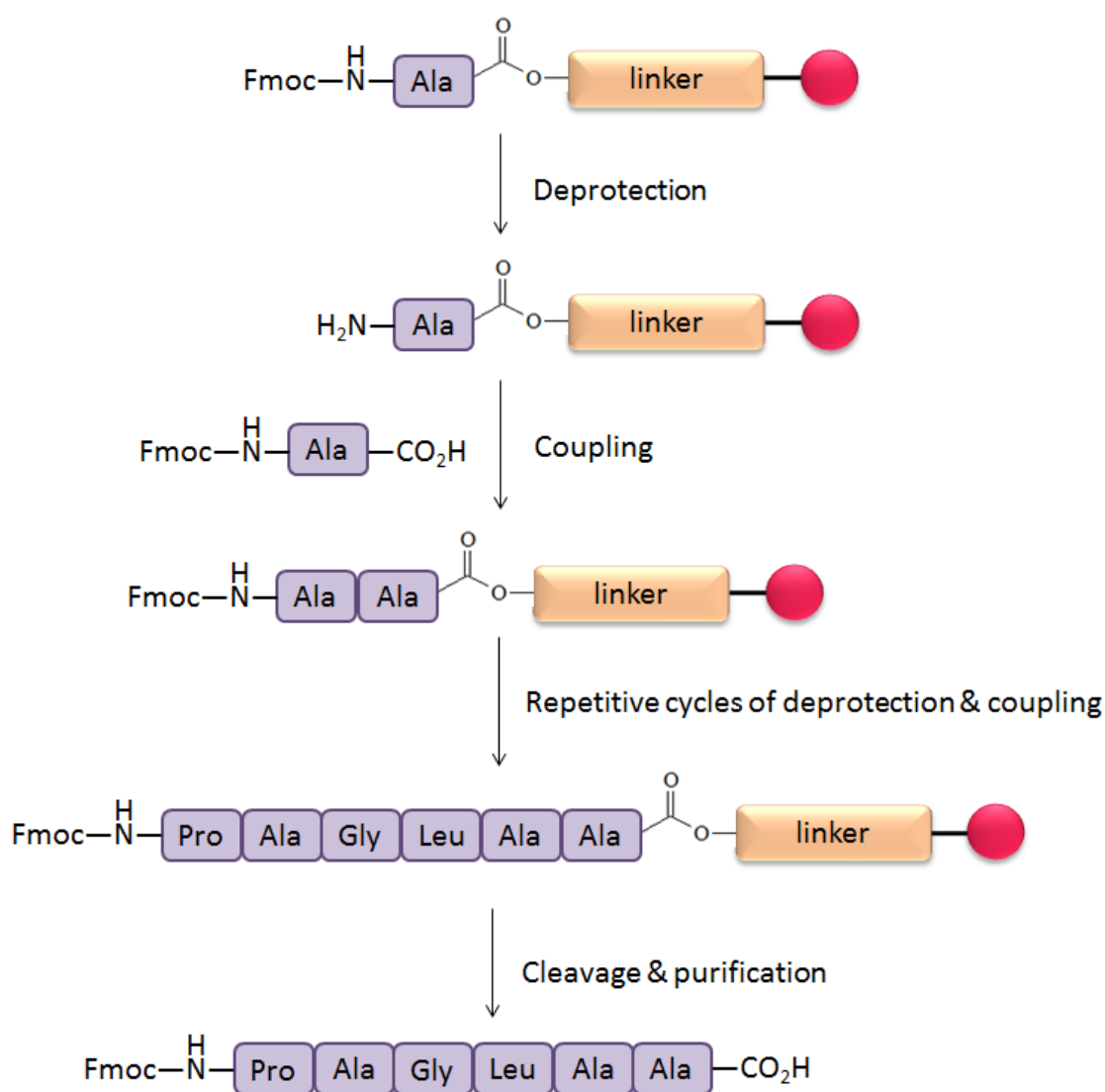


**Figure 11.** Solid phase peptide synthesis of Fmoc-Pro-Ala-Gly-Leu-Ala-Ala-OH (HZ31)

The prodrug 1 Fmoc-Pro-Ala-Gly-Leu-Ala-Ala-Propranolol (HZ32) was prepared from the reaction of propranolol hydrochloride and Fmoc-Pro-Ala-Gly-Leu-Ala-Ala-OH (HZ31) in DMF using TBTU, HOBt and DIPEA as the coupling agent. DIPEA was added to make the free base of propranolol hydrochloride (**Scheme 7**). Because the reaction between NH group and COOH group is faster than OH group and COOH group, a large amount of DMF was used to facilitate the NH group of propranolol to react with the COOH group of Fmoc-Pro-Ala-Gly-Leu-Ala-Ala-OH (HZ31).



HZ31
Fmoc-Pro-Ala-Gly-Leu-Ala-Ala-OH

Propranolol hydrochloride

(a)

Fmoc-Pro-Ala-Gly-Leu-Ala-Ala-Propranolol (HZ32)
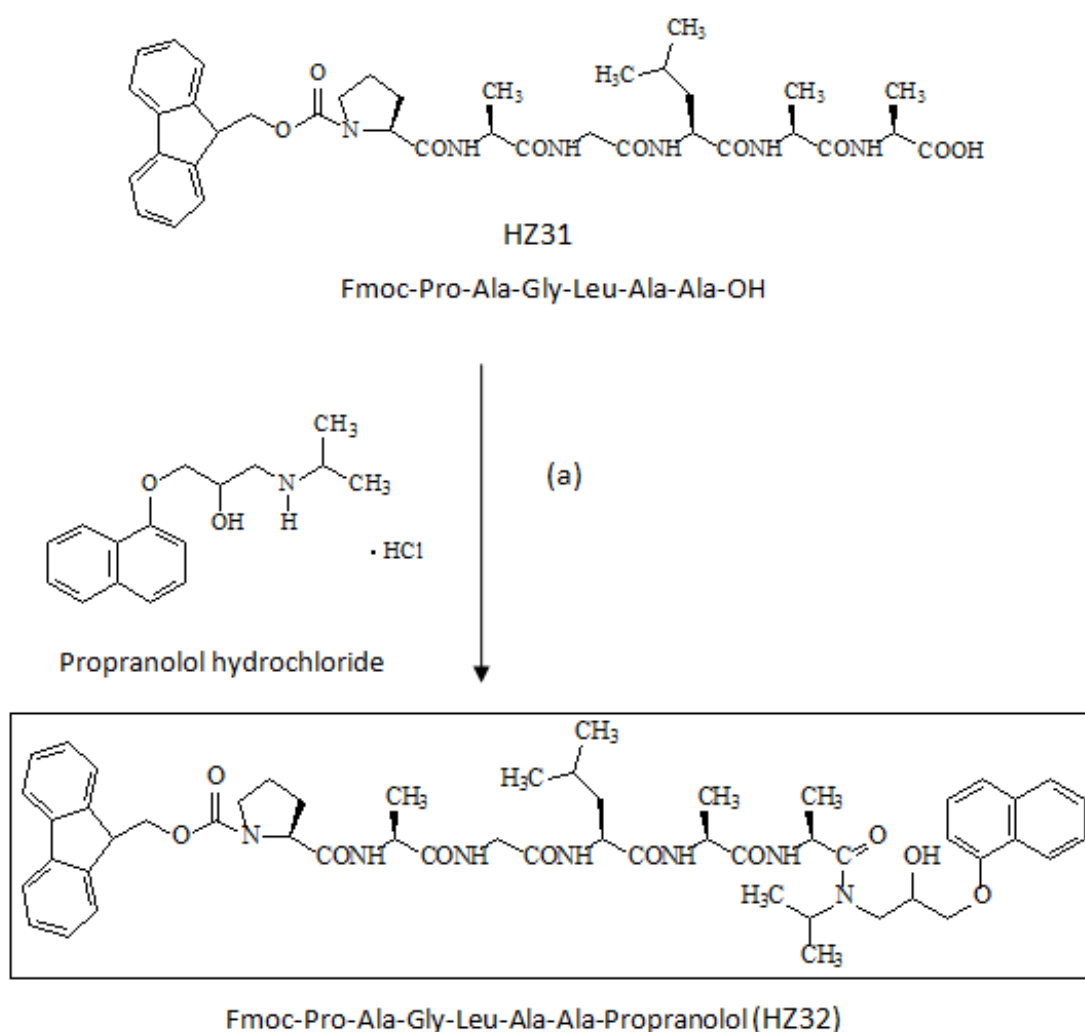
Reagents and Conditions: (a) TBTU, HOBt, DIPEA in DMF
**Scheme 7.** Outline of Prodrug 1 (HZ32) synthesis

The reaction was completed overnight at RT. The crude product was purified by extraction and silica gel column chromatography. The reaction solution was

extracted with water and dichloromethane. Multiple extractions were required to wash away impurities. For the first extraction, citric acid was added to the water layer to get rid of excess propranolol free base. Secondly, the excess Fmoc-Pro-Ala-Gly-Leu-Ala-Ala-OH (HZ31) was removed from the organic phase by shaking the organic extract with aqueous sodium bicarbonate. The weak acid HZ31 can react with sodium bicarbonate to form the sodium salt, carbon dioxide and water.

Because the starting material, reagents and crude product were colourless on TLC plate, a mini de-Fmoc colour test was performed to confirm the presence of the product (Prodrug 1). The product will have a free amine group which is able to be detected after the Fmoc deprotecting reaction. Piperidine 20% in DMF was added to the crude product sample solution. After 20 minutes, the solution was extracted with water and dichloromethane. The extract in organic layer was checked by TLC using the running solvent, dichloromethane and methanol 9:1. A few drops of 5% ninhydrin in ethanol were added on the TLC plate at the product lane. After 5min, there was a purple spot emerged which indicated the Fmoc free prodrug 1.

The eluting solvent system, dichloromethane-ethyl acetate-ethanol (9: 2: 1) was used during the column chromatography. The difficulty of this purification process was that the crude product solution was colourless. In this case, many fractions were collected and every fraction was about 2-3 ml in volume. All fractions were confirmed by TLC under UV light. The appropriate fractions were combined, filtered and evaporated to dryness. Diethyl ether was used to precipitate the pure white product. Due to the small amount of solid precipitate in ether, the final product was collected in centrifuge tubes.

Prodrug 1 compound (Fmoc-Pro-Ala-Gly-Leu-Ala-Ala-Propranolol) HZ32 was characterized by its electrospray mass spectrum which gave a signal at m/z 962

for (M+H)⁺ corresponding to a molecular mass of 961 **(Figure 12)**.
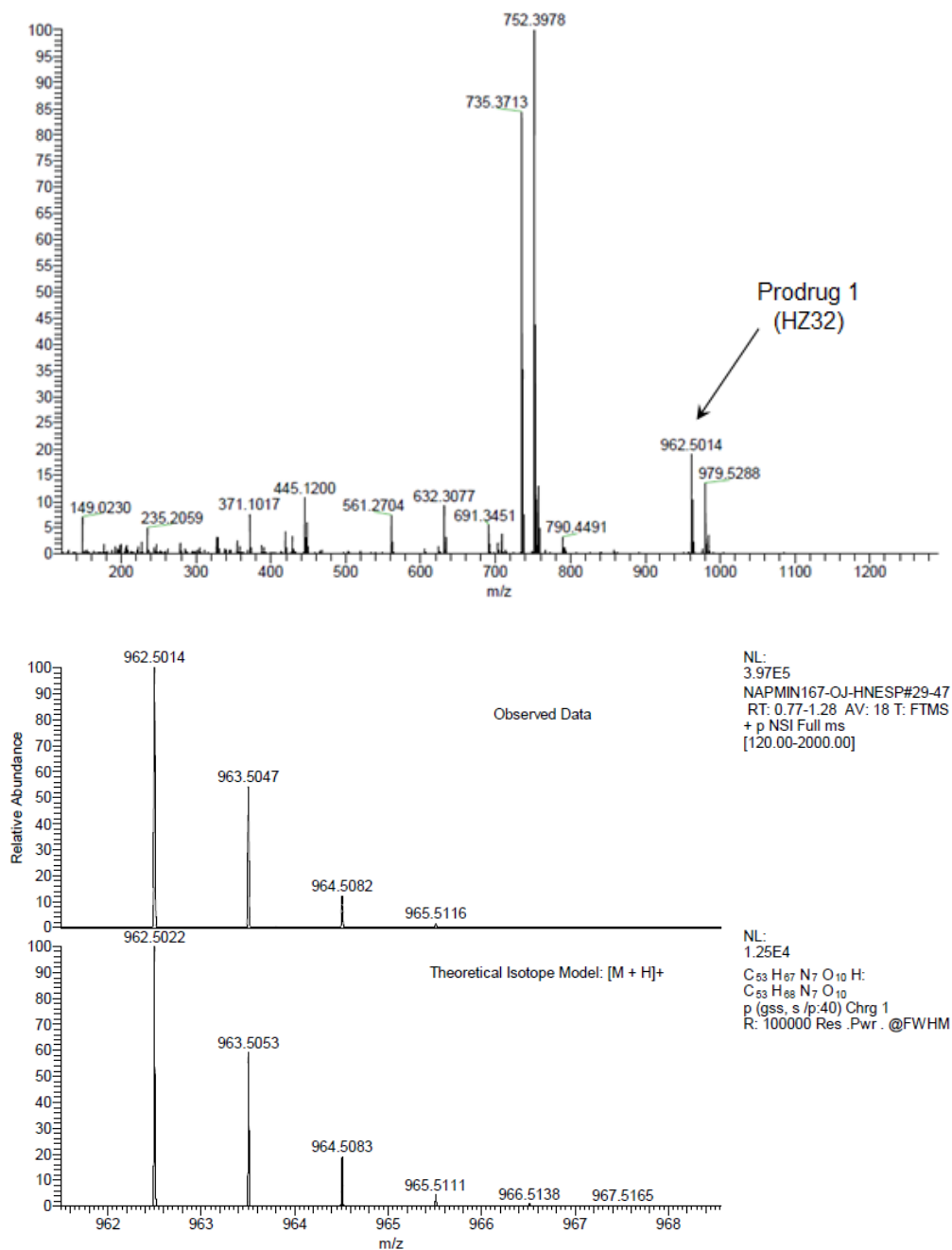


**Figure 12.** The ESI (+) Mass spectrum of Prodrug 1 (HZ32)

## 1.4.4 Synthesis of Prodrug 2:

**AQ-Spacer-Pro-Ala-Gly-Leu-Ala-Ala-Propranolol (HZ34)**

Prodrug 2 had the same MMP-9 cleavable hexapeptide chain in the middle and active drug propranolol on one side as prodrug 1. The only difference is that

Prodrug 2 has the capping group which is an anthraquinone derivative instead of Fmoc **(Scheme 8)**.

The N-Fmoc protected hexapeptide (Fmoc-Pro-Ala-Gly-Leu-Ala-Ala-OH) HZ31 was repeatedly synthesised by SPPS method for prodrug 2. However, this time instead of cleaving HZ31 off the resin, HZ31 was remained on the resin for the next step. The Fmoc group of HZ31 was removed by 20% piperidine in DMF to give an N-terminal free hexapeptide HZ32.

The free amino group of the resin bound hexapeptide was then capped with a cytotoxic aminoanthraquinone via a carbamate bond, by reaction with the activated anthraquinone derivative (HB8) using DIPEA in DMF.

HZ31 + Resin

Fmoc-Pro-Ala-Gly-Leu-Ala-Ala-RESIN

HB8

(a)
(b)
(c)

HZ33
Anthraquinone-spacer-Pro-Ala-Gly-Leu-Ala-Ala-OH

Propranolol hydrochloride

(C)

Anthraquinone-spacer-Pro-Ala-Gly-Leu-Ala-Ala-Propranolol (HZ34)

Reagents and Conditions: (a) 20% piperidine in DMF (b) DIPEA, in DMF (c) 87% TFA in dichloromethane (c) TBTU, HOBt, DIPEA in DMF

**Scheme 8.** Outline of Prodrug 2 (HZ34) synthesis

The compound HB8 used here had been previously synthesised from the

reaction of 1-[3-hydroxypropyl)amino]-anthraquinone with 4-nitrophenyl chloroformate (NPC) in dichloromethane and pyridine; activated NPC derivatives of alcohols readily react with amines to give carbamates, with the 4-nitrophenol by-product being easily washed out with DMF during the SPPS process after 2 hours of reaction. The anthraquinone-spacer-Pro-Ala-Gly-Leu-Ala-Ala-OH (HZ33) was cleaved off the resin by TFA in dichloromethane. The TLC test was performed and showed a major red product had formed. The product solution was evaporated to a small volume and added with diethyl ether to precipitate the pure red solid (HZ33).

The collected HZ33 was then reacted via its free carboxylic acid group with the free amino group of propranolol•HCl salt, followed by the addition of TBTU, HOBt, and DIPEA as the standard coupling reagents. The reaction mixture was suspended in DMF. The reaction was completed in 4 hours by checking the TLC. After solvent extraction and column chromatography using dichloromethane-methanol (9:1), the pure prodrug 2 (HZ34) was precipitated in diethyl ether to give a red solid product.

The prodrug 2 AQ-Space-Pro-Ala-Gly-Leu-Ala-Ala-Propranolol (HZ34) was characterized by mass spectroscopy. A signal at m/z 1069 for the mono-cation $(M+Na)^+$ confirmed the molecular mass of 1046 Daltons **(Figure 13)**.
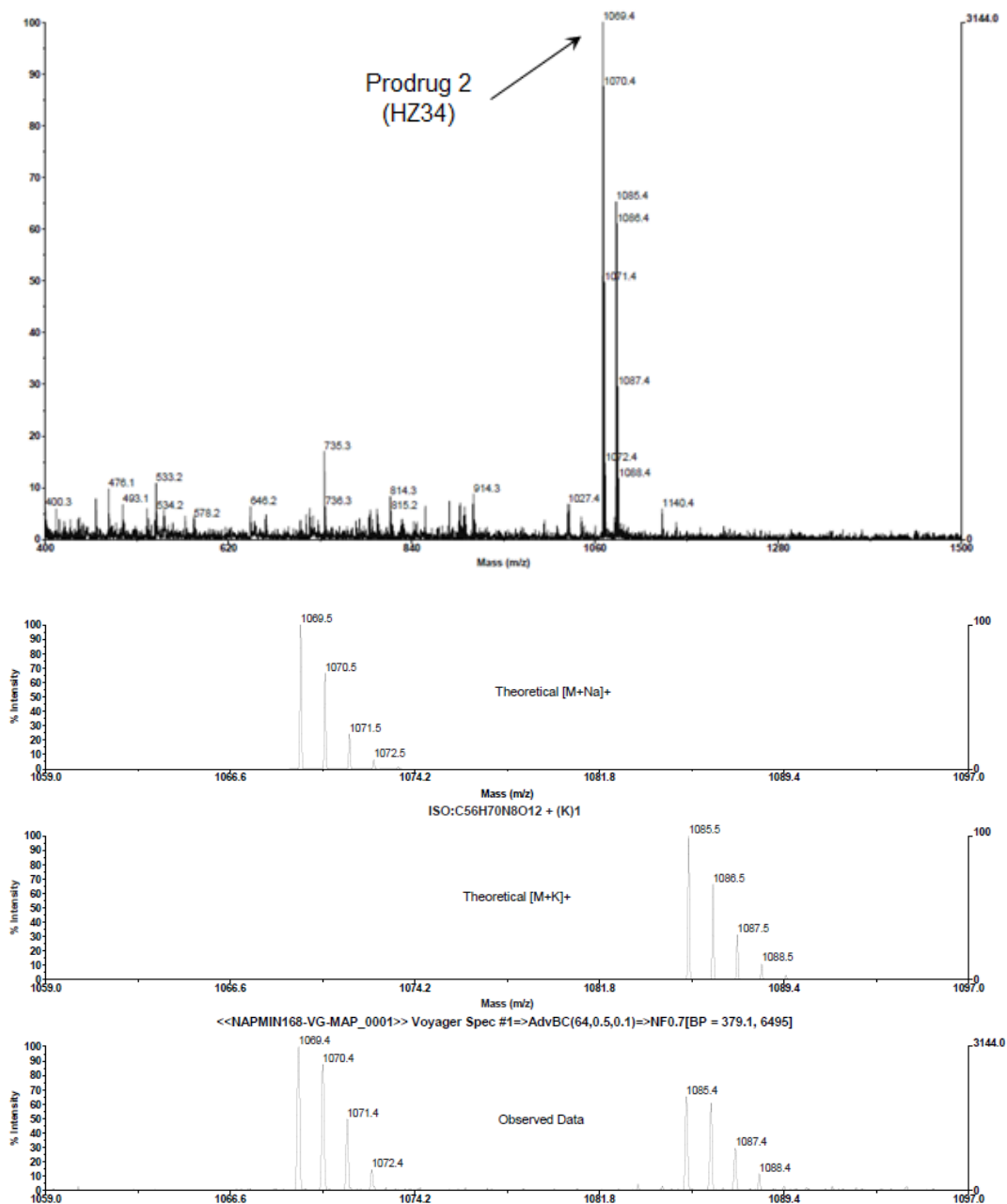
**Figure 13.** MALDI Mass spectrum of Prodrug 2 (HZ34)

### 1.4.5 Synthesis of Prodrug 3:

### FITC-Pro-Ala-Gly-Leu-Pro-GABA-[Propyl-spacer]-AQ (HZ43)

The middle part of the chemical structure of prodrug 3 (HZ43) contains a MMP-9 cleavable pentapeptide (Pro-Ala-Gly-Leu-Pro) and GABA. Fluorescein isothiocyanate isomer I (FITC) was attached to one side of the middle chain. The other side of the prodrug 3 was capped by the anthraquinone derivative

**(Scheme 9)**.

Prodrug 3 (HZ43) was designed to release GABA and fluorescein in tumour cells which have over-expressed MMP-9. The prodrug can be a diagnostic probe of MMP-9 activity, and also the released GABA into tumour cells will be able to evaluate the expression level of GABA receptors.
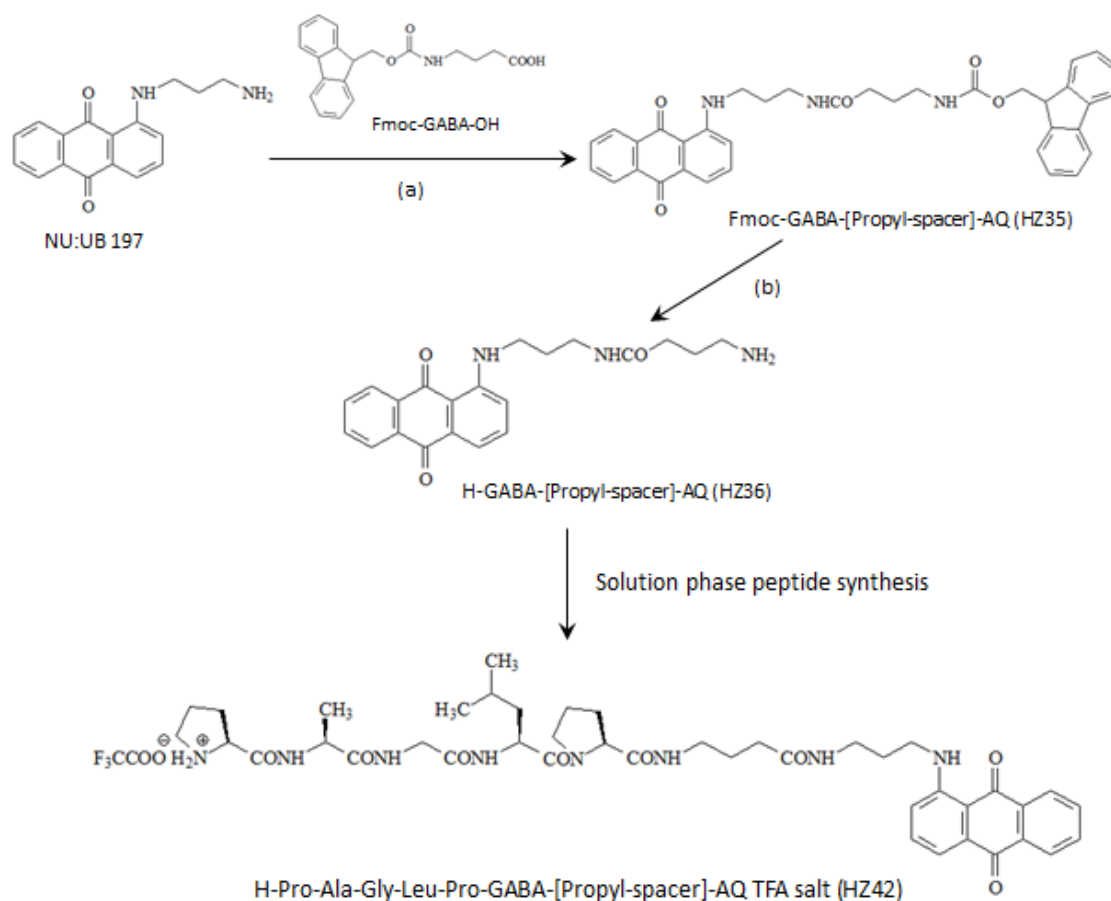
Fluorescein isothiocyanate
isomer I

FITC-Pro-Ala-Gly-Leu-Pro-GABA-[Propyl-spacer]-AQ (HZ43)
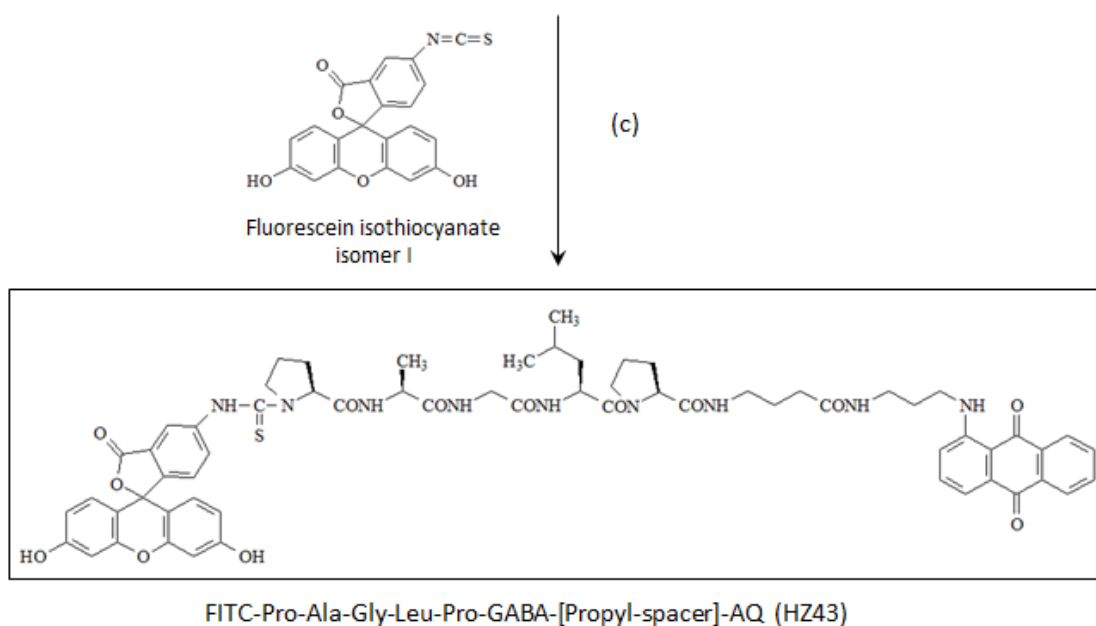
Reagents and Conditions: (a) TBTU, HOBt, DIPEA in DMF (b) 20% piperidine in DMF (c) DIPEA, in DMF

**Scheme 9.** Outline of Prodrug 3 (HZ43) synthesis

The synthesis of Prodrug 3 (FITC-Pro-Ala-Gly-Leu-Pro-GABA-[Propyl-spacer]-AQ) started with the reaction of NU: UB 197 and Fmoc-γ-aminobutyric acid (GABA). NU:UB 197 is an aminopropylamino anthraquinone derivative that has been used extensively in previous and current research within this laboratory. Where NU:UB can be described as an 'anthraquinone-spacer', coupling of NU:UB 197 to amino acids, to give spacer-linked anthraquinone-amino acid conjugates, afforded a series of compounds that were shown to be DNA binding, topoisomerase inhibitors (Pettersson, 2004; Turnbull, 2003; Young, 2006). These compounds had broad-spectrum activity in vitro at low micromolar concentrations in panels of human and animal tumour cell lines, including those of the NCI 60 cell line anticancer drug screen (https://dtp.cancer.gov/default.htm). Additionally, leading members of the 'NU:UB' series were active *in vivo* in experimental colon cancer (Mincher et al., 1999) and have been used at various times throughout this research programme, for example, in chapter 2, the propyl- spaced proline,

conjugate was incorporated into a cyclic baclofen prodrug. Here, GABA was coupled to NU:UB 197 to afford a novel spacer-linked anthraquinone-amino acid conjugate. Fmoc-γ-aminobutyric acid (GABA) was reacted with the free amino group of NU:UB 197 in DMF, using standard coupling reagents TBTU, HOBt, and DIPEA. The reaction was completed in 1 hour. The reaction solution was poured into water which contained a small amount of HCl. The red solid precipitate in the water was collected by filtration. The crude product was then purified by silica gel column chromatography, using the eluting solvent dichloromethane-methanol (9:1). The pure product (HZ35) was dried in an evaporating basin. Fmoc-GABA-[Propyl-spacer]-AQ (HZ35) was Fmoc deprotected for the further coupling reaction with amino acids, using 20% piperidine in DMF. After solvent extraction and evaporation, diethyl ether was added to precipitate the pure red solid product H-GABA-[Propyl-spacer]-AQ (HZ36).

The MMP-9 specific peptide linker, Pro-Ala-Gly-Leu-Pro was added to HZ36 by solution phase peptide synthesis which allowed large-scale and high yield production of peptide. The solution phase peptide synthesis involved coupling of N-Boc protected amino acids and Boc group removal reaction. The Coupling reagents are as the same as solid phase peptide synthesis, which are TBTU, HOBt, and DIPEA. Solvent extraction and column chromatography were required. TFA was used to remove the Boc protecting group.

Fluorescein isothiocyanate isomer I was coupled to Pro-Ala-Gly-Leu-Pro-GABA-spacer-Anthraquinone TFA salt (HZ42) in DMF by the addition of DIPEA to form the final product Prodrug 3. The reaction was completed overnight at RT. The reaction solution was poured into water to get orange solid precipitate. The crude product was purified by silica gel column chromatography using eluting solvent dichloromethane- methanol (6:1).

The nanoelectrospray negative ion mass spectrum (M-H)⁻ of prodrug 3
(FITC-Pro-Ala-Gly-Leu-Pro-GABA-[Propyl-spacer]-AQ) HZ43 had a strong
signal at m/z 1188 confirmed the molecular mass of 1189 **(Figure 14)**.
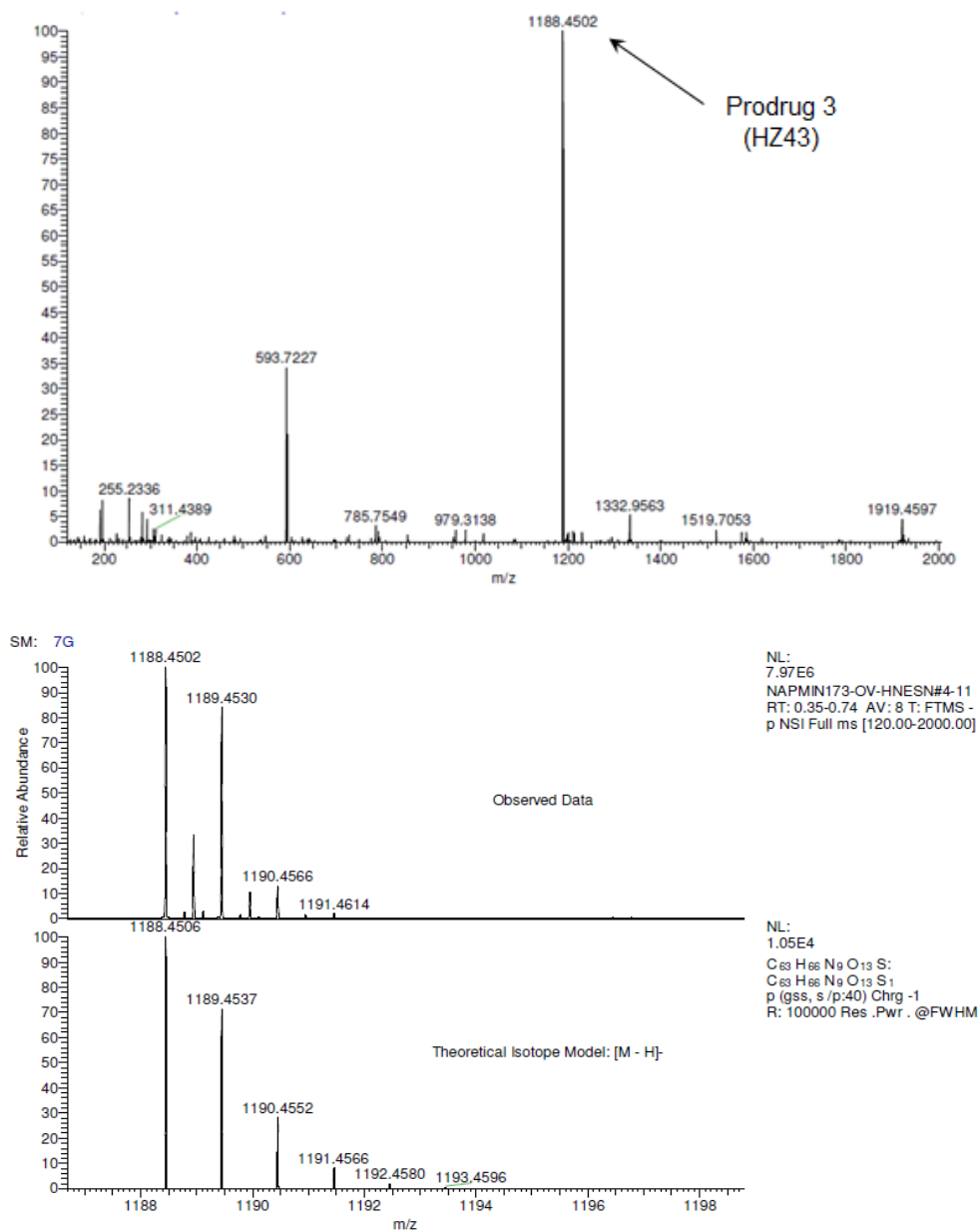


**Figure 14.** Mass spectrum of Prodrug 3 (HZ43)

## 1.4.6 Synthesis of Prodrug 4:

## AQ-[Propyl-spacer]-Pro-Ala-Gly-Leu-Ala-ethylpiperidine-3-carboxylate

## (HZ45)

The GABA receptor antagonist, (R)-ethylpiperidine-3-carboxylate (Zhang *et al.*

2007) was used as the active drug in Prodrug 4 synthesis. The anthraquinone-spacer-Pro-Ala-Gly-Leu-Ala-Ala-OH conjugate (HZ44) was linked to it to form Prodrug 4.

AQ-[Propyl-spacer]-Pro-Ala-Gly-Leu-Ala-OPFP (HZ44) was prepared from the overnight reaction of AQ-Spacer--Pro-Ala-Gly-Leu-Ala-Ala-OH HZ33 (from prodrug 2 synthesis) and pentafluorophenol in dichloromethane using DCC and DMAP as coupling reagents (**Scheme 10**).
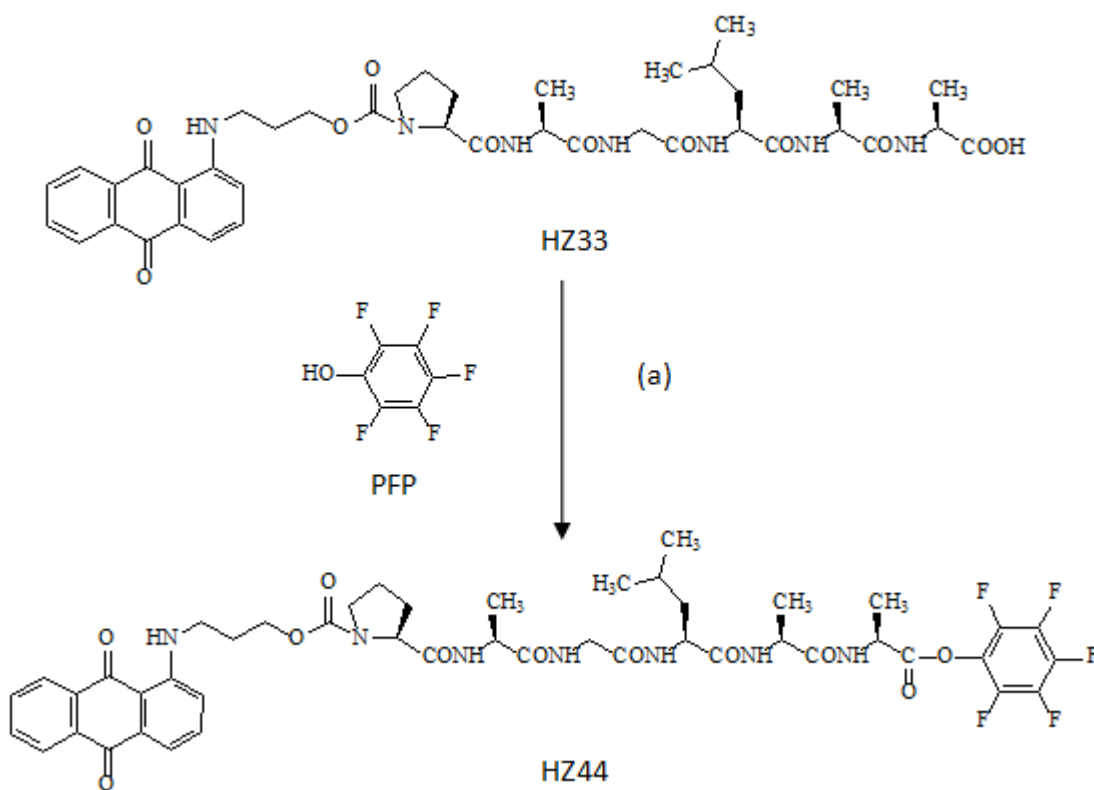


HZ33

PFP

(a)

HZ44

(R)-ethyl piperidine-3-carboxylate
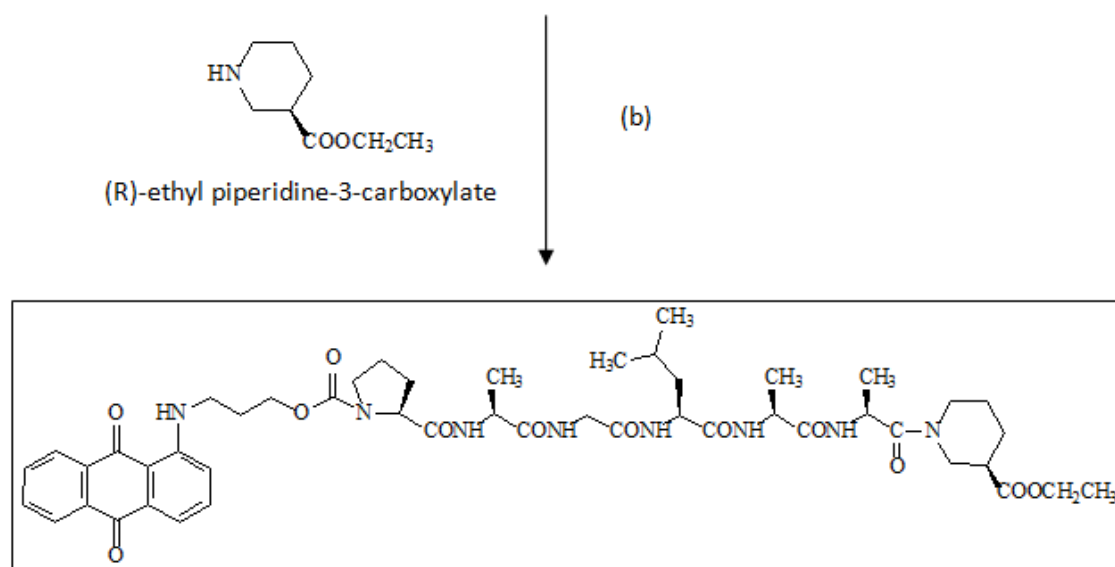
Anthraquinone-spacer- Pro-Ala-Gly-Leu-Ala-Ala-ethyl piperidine-3-carboxylate (HZ45)

Reagents and Conditions: (a) DCC & DMAP in Dichloromethane (b) DIPEA, in Dichloromethane

**Scheme 10.** Outline of Prodrug 4 (HZ45) synthesis

The carboxylic group of AQ-Spacer--Pro-Ala-Gly-Leu-Ala-Ala-OH (HZ33) was converted into a pentafluorophenolate active ester which will be more reactive for adding the active drug (R)-ethylpiperidine-3-carboxylate. The precipitated dicyclohexylurea (DCU) was filtered off. The crude product was kept in the dichloromethane for the next reaction without further purification. (R)-Ethylpiperidine-3-carboxylate and DIPEA was put into the solution. Solvent extraction and column chromatography were performed to give a pure red product, Prodrug 4 (AQ-[Propyl-spacer]-Pro-Ala-Gly-Leu-Ala-ethylpiperidine-3-carboxylate).

The final HZ45 compound, anthraquinone-spacer-Pro-Ala-Gly-Leu-Ala-Ala-ethylpiperidine-3-carboxylate (Prodrug 4) was characterized by its mass spectrum (M+Na)$^+$ and (M+K)$^+$ which showed signals at m/z 967 and 983, corresponding to a relative molecular mass of 944 Da **(Figure 15)**.
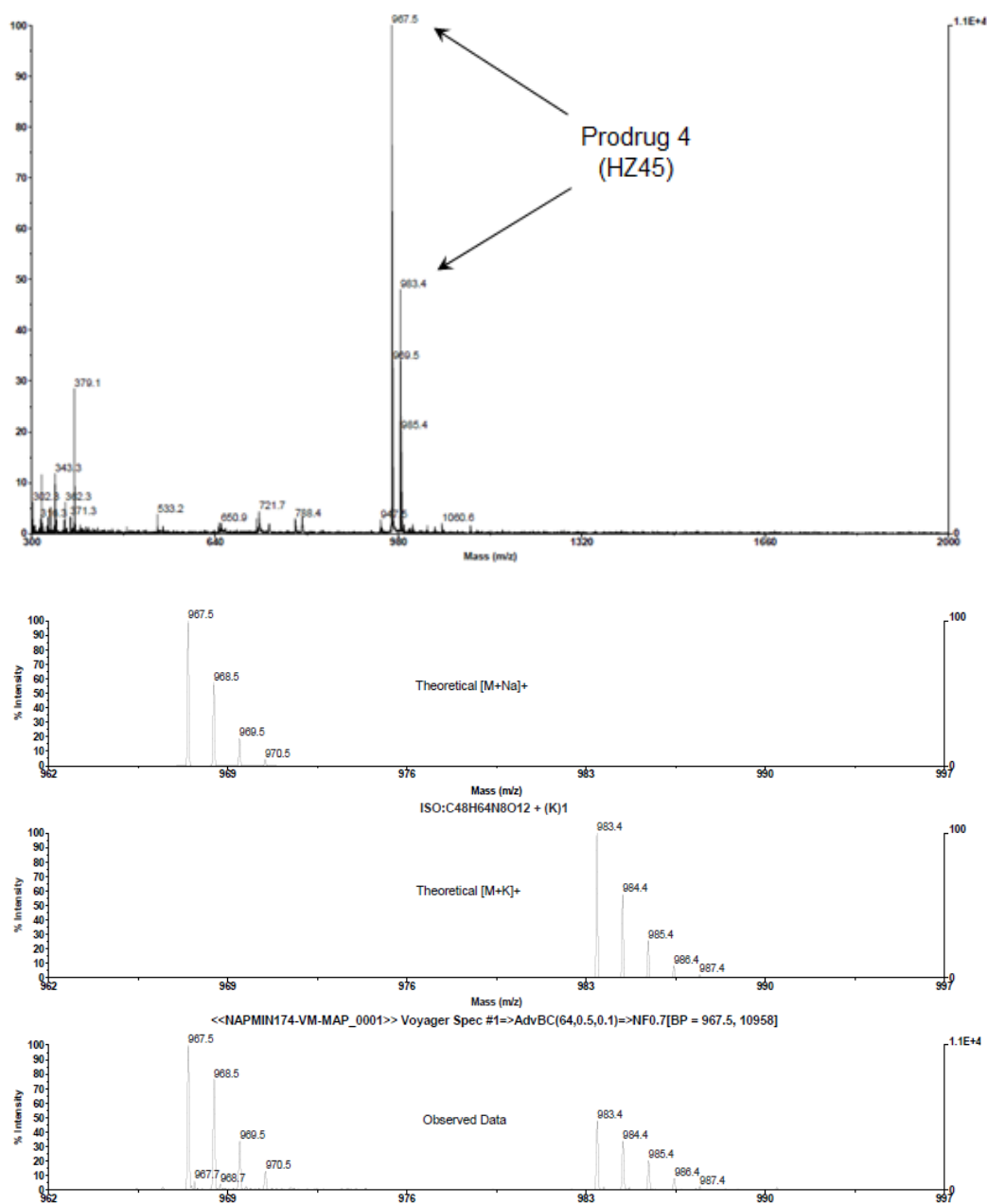
**Figure 15.** MALDI Mass spectrum of Prodrug 4 (HZ45)

### 1.4.7 Synthesis of Prodrug 5:

### Podophyllotoxin-Pro-Ala-Gly-Leu-Pro-GABA-[Propyl-spacer]-AQ (HZ 47)

The designed tumour activated Prodrug 5 (HZ47) consists of the cytotoxic drug podophyllotoxin (Canel *et al.* 2000), a MMP-9 cleavable pentapeptide (Pro-Ala-Gly-Leu-Pro), GABA, and a capping group (anthraquinone derivative). For the synthesis of prodrug 5 Podophyllotoxin-Pro-Ala-Gly-Leu-Pro-GABA-[Propyl-spacer]-AQ (HZ47),

H-Pro-Ala-Gly-Leu-Pro-GABA-[Propyl-spacer]-AQ TFA salt HZ42 (from Prodrug 3 synthesis) was reacted with succinic anhydride by the addition of DIPEA in DMF **(Scheme 11)**.



H-Pro-Ala-Gly-Leu-Pro-GABA-[Propyl-spacer]-AQ TFA salt (HZ42)

Succinic anhydride (a)

Succinyl-Pro-Ala-Gly-Leu-Pro-GABA-[Propyl-spacer]-AQ (HZ46)

Podophyllotoxin (b)

Podophyllotoxin-Pro-Ala-Gly-Leu-Pro-GABA-[Propyl-spacer]-AQ (HZ47)
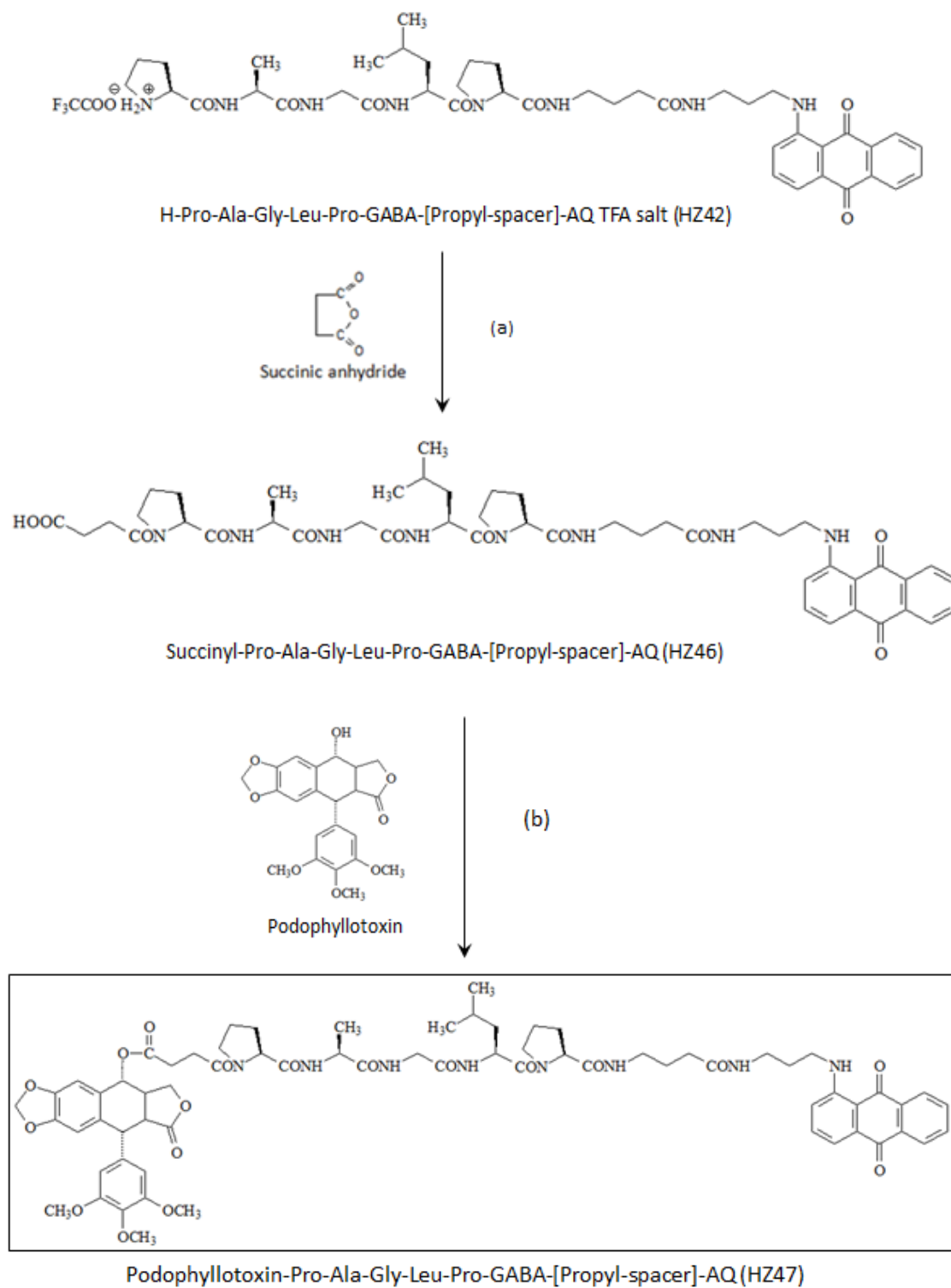
Reagents and Conditions: (a) DIPEA, in DMF (b) TEA & TBTU in DMF & Acetonitrile

**Scheme 11.** Outline of Prodrug 5 (HZ47) synthesis

The reaction was completed in 4 hours. The crude product was firstly isolated by partitioning between dichloromethane and water. During the process, the water phase was coloured purple. This is because H-Pro-Ala-Gly-Leu-Pro-GABA-[Propyl-spacer]-AQ TFA salt (HZ42) has relatively high solubility in water. The yield of HZ42 was low due to the loss during extraction. Further purification by column chromatography was performed using dichloromethane-methanol (4:1) eluting solvent. The pure HZ42 was collected in diethyl ether.

Podophyllotoxin was coupled to the H-Pro-Ala-Gly-Leu-Pro-GABA-[Propyl-spacer]-AQ TFA salt (HZ42) by using the reagents TEA and TBTU (Balalaie, Mahdidoust and Eshaghi-najafabadi, 2008) in a mixture solvent of DMF and acetonitrile. The reaction was completed in 3 hours by checking the TLC. Acetonitrile was evaporated off. The crude product in DMF was extracted with dichloromethane and water. Column chromatography was applied for further purification using the dichloromethane-methanol (9:1) eluting solvent. The final product Podophyllotoxin-Pro-Ala-Gly-Leu-Pro-GABA-[Propyl-spacer]-AQ (HZ47) was collected in an evaporating basin at RT.

In the mass spectrum **(Figure 16)** of prodrug 5 (HZ47), a signal at 1321 m/z was assigned to the ion $(M+Na)^+$ confirming the molecular mass of 1296 Da.
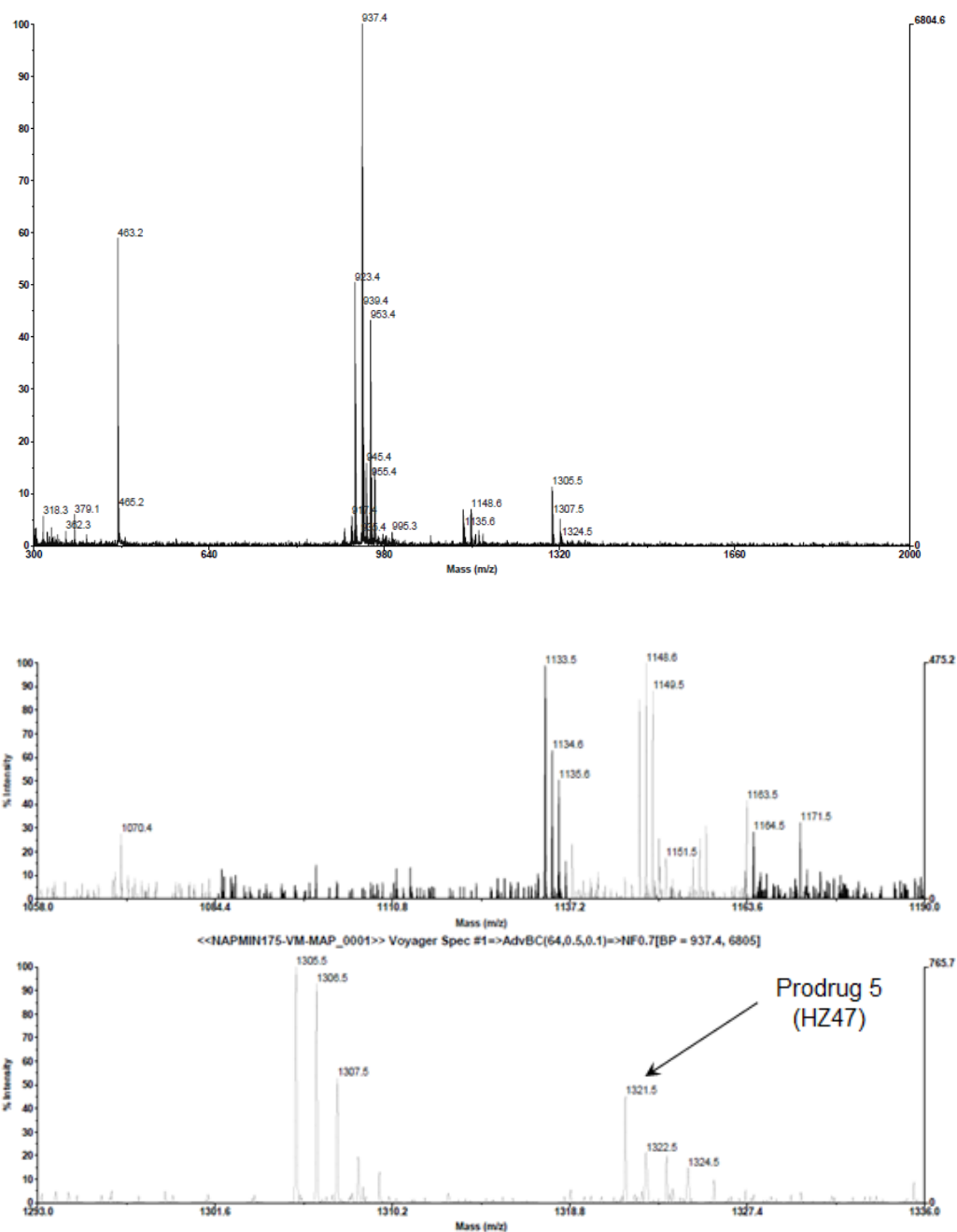
**Figure 16.** Mass spectrum of Prodrug 5 (HZ47)

## 1.4.8 Synthesis of Prodrug 6: AQ-Spacer-Pro-Ala-Gly-Nva-Pro-Baclofen (HZ54)

Prodrug 6 was designed to use active drug baclofen which is a GABA$_B$ agonist. The capping group anthraquinone derivative was attached to the MMP-9 specific pentapeptide (Pro-Ala-Gly-Nva-Pro). Baclofen was linked to the other side of the peptide chain. During the anticipated prodrug 6 metabolism, baclofen is expected to be released in the tumour cells which have over-expressed MMP-9

53

and targets the GABA$_B$ receptor.
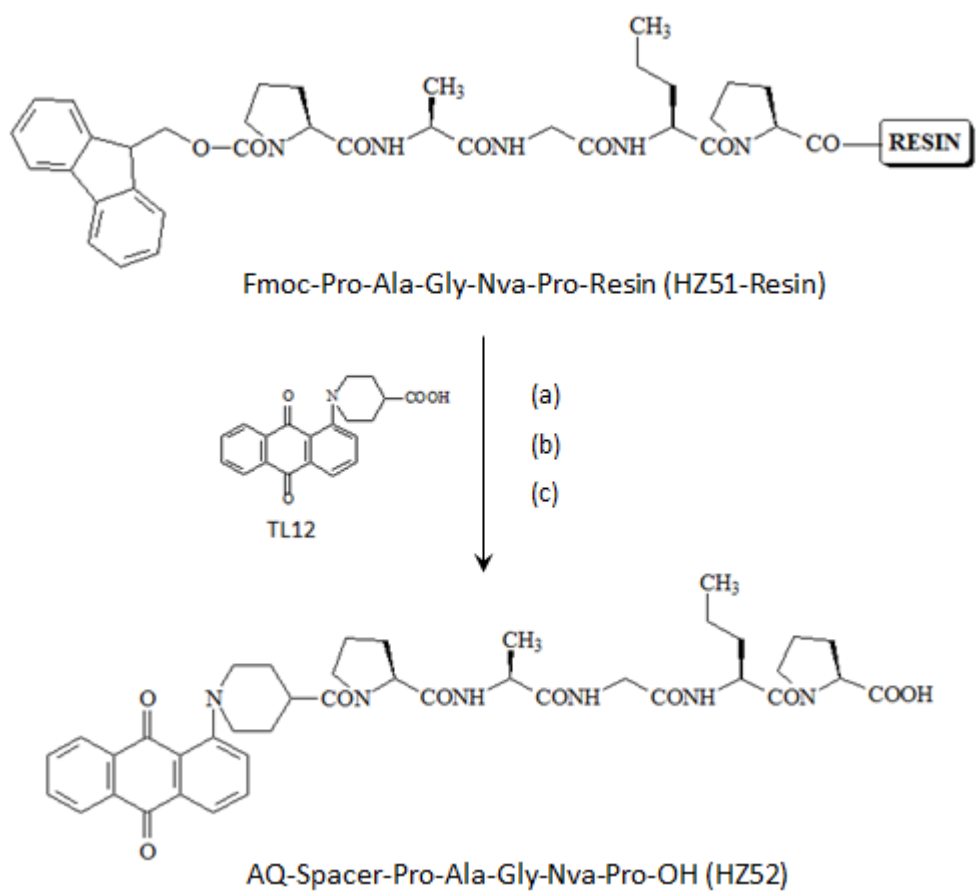


Fmoc-Pro-Ala-Gly-Nva-Pro-Resin (HZ51-Resin)



TL12

(a)
(b)
(c)



AQ-Spacer-Pro-Ala-Gly-Nva-Pro-OH (HZ52)

54

AQ-Spacer-Pro-Ala-Gly-Nva-Pro-OPFP (HZ53)



AQ-Spacer-Pro-Ala-Gly-Nva-Pro-Baclofen (HZ54)
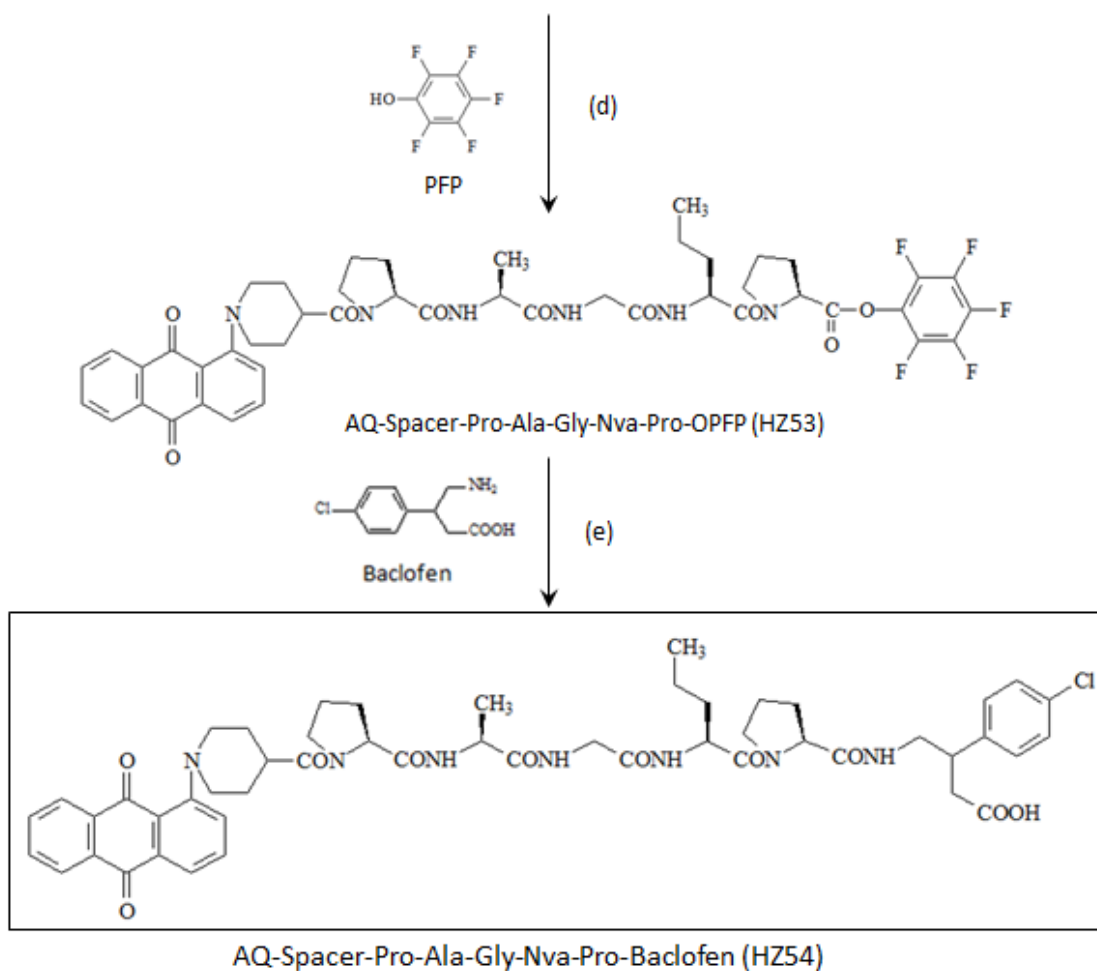
Reagents and Conditions: (a) 20% piperidine in DMF (b) TBTU, HOBt, DIPEA, in DMF (c) 5% TFA in dichloromethane (d) DCC & DMAP, in dichloromethane (e) DIPEA, in dichloromethane

**Scheme 12.** Outline of Prodrug 6 (HZ54) solid-phase synthesis

H-Pro-2ClTrt resin was used for building up the MMP 9 cleavable peptide linker Fmoc-Pro-Ala-Gly-Nva-Pro-Resin (HZ51) for Prodrug 6 (HZ54) based on the SPPS method **(Scheme 12)**. After completed synthesis of the pentapeptide Fmoc-Pro-Ala-Gly-Nva-Pro on resin, the Fmoc group was removed by 20% piperidine in DMF. The anthraquinone capping group (TL12) was coupled to the pentapeptide chain by TBTU, HOBt and DIPEA in DMF. The Anthraquinone-spacer-Pro-Ala-Gly-Nva-Pro-OH conjugate (HZ52) was cleaved off the resin using 5% TFA in dichloromethane. The red solid AQ-Spacer-Pro-Ala-Gly-Nva-Pro-OH (HZ52) was precipitated in diethyl ether

and collected for the reaction with PFP. DCC and DMAP were used as standard reagents for the addition of PFP to AQ-Spacer-Pro-Ala-Gly-Nva-Pro-OH (HZ52). The reaction mixture was suspended in dichloromethane. The reaction was very slow at RT. In order to push the reaction, the round bottomed flask was put on 40°C water bath. Due to the TLC test, there was still unreacted starting material AQ-Spacer-Pro-Ala-Gly-Nva-Pro-OH (HZ52) after 2 days. DCU was filtered off. Solvent extraction was done between chloroform and aqueous sodium bicarbonate (to remove unreacted HZ52).

The purity of pentapeptide Fmoc-Pro-Ala-Gly-Nva-Pro-OH (HZ51) was analysied by HPLC (**Figure 17**). A reverse phase column (Agilent Zorbax Extend C18, 5 µm, 4.6 mm x 50 mm) was used with gradients developed over a 15 min period as shown in **Table 1**.
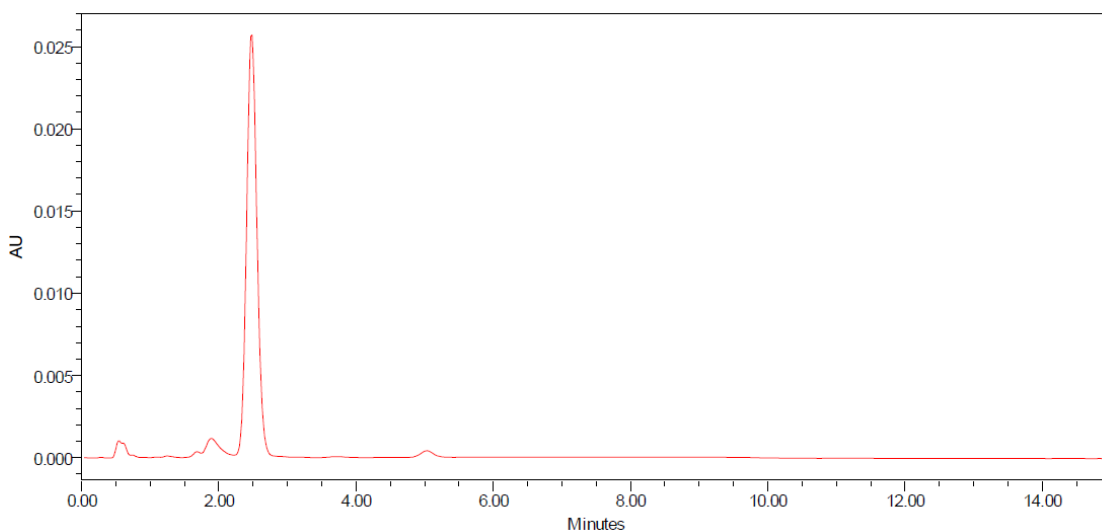


**Figure 17.** HPLC chromatogram of HZ51

| Time | Mobile Phase A (%) | Mobile Phase B (%) |
|:---:|:---:|:---:|
| 0 | 40 | 60 |
| 5 | 42 | 58 |
| 8 | 42 | 58 |
| 9 | 40 | 60 |
| 15 | 40 | 60 |

**Table 1.** HPLC gradient mobile phase composition

The HPLC result (**Figure 17**) above confirms that pentapeptide Fmoc-Pro-Ala-Gly-Nva-Pro-OH (HZ51) has high purity through the solid phase peptide synthesis.

The prodrug 6: AQ-Spacer-Pro-Ala-Gly-Nva-Pro-Baclofen (HZ54) was prepared by the reaction of AQ-Spacer-Pro-Ala-Gly-Nva-Pro-OPFP (HZ53) and baclofen using DIPEA in dichloromethane. Because the solubility of baclofen in dichloromethane is very low, the reaction mixture was stirred over 30 hours. DCU and unreacted baclofen were filtered off and the crude compound was purified by thick TLC plate using the running solvent dichloromethane-methanol (6:1).

Furthermore, the mass spectrum showed a signal at m/z 950 (M-H)⁻ corresponding to the molecular mass of 951 for prodrug 6: AQ-Spacer-Pro-Ala-Gly-Nva-Pro-Baclofen (HZ54) as shown in **Figure 18**.
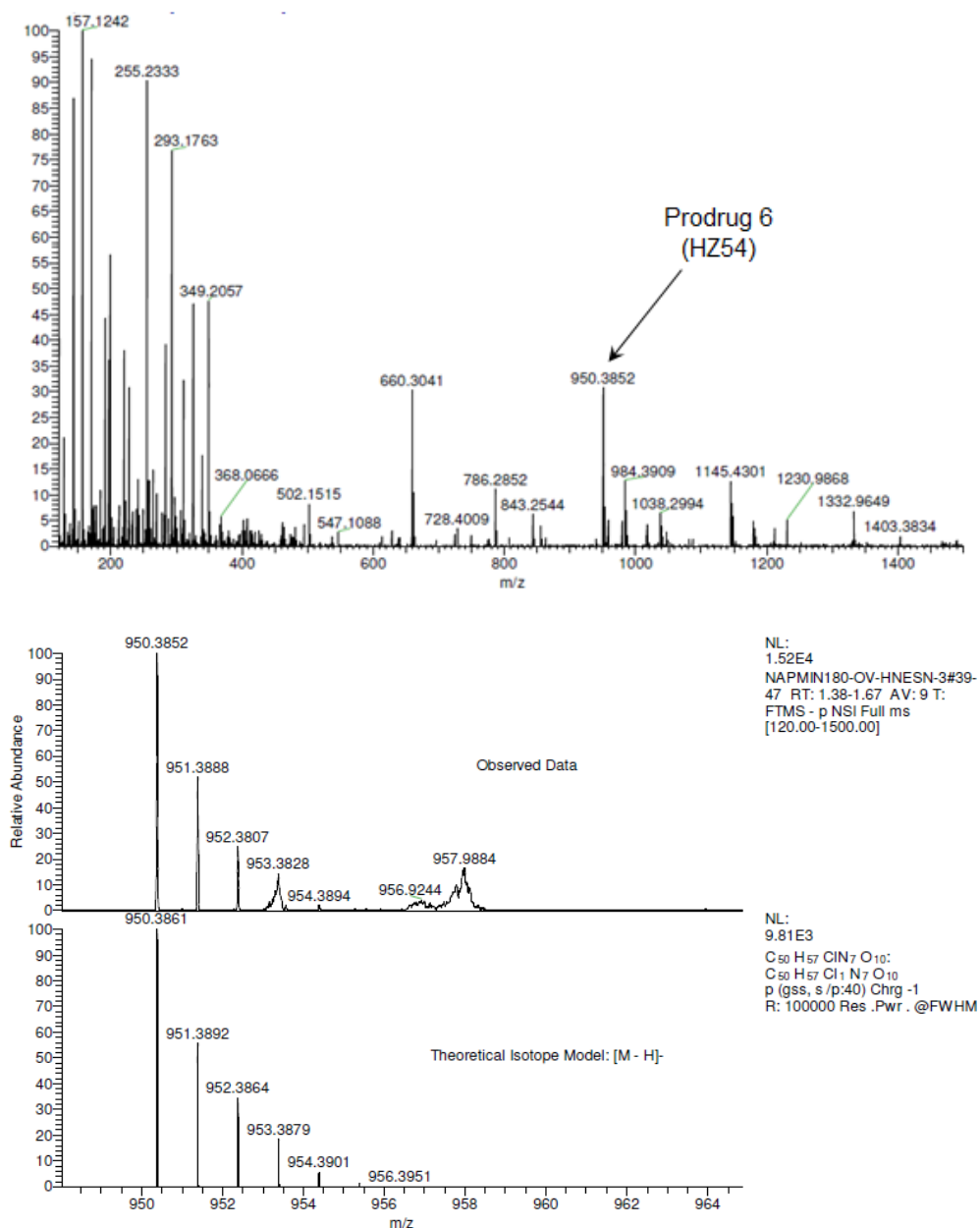
**Figure 18.** ESI (+) Mass spectrum of Prodrug 6 (HZ54)

## 1.4.9 Synthesis of Prodrug 7:

## 5(6)-Carboxyfluorescein-Pro-Ala-Gly-Leu-Pro-GABA-[Propyl-spacer]-AQ

## (HZ57)

Prodrug 7 (HZ57) has the same chemical structure as prodrug 3 (FITC-Pro-Ala-Gly-Leu-Pro-GABA-[Propyl-spacer]-AQ), except for using the different fluorescent group, 5(6)-carboxyfluorescein.

H-Pro-Ala-Gly-Leu-Pro-GABA-[Propyl-spacer]-AQ TFA salt (HZ42)

5(6)-Carboxyfluorescein

(a)

5(6)-Carboxyfluorescein-Pro-Ala-Gly-Leu-Pro-GABA-[Propyl-spacer]-AQ (HZ57)
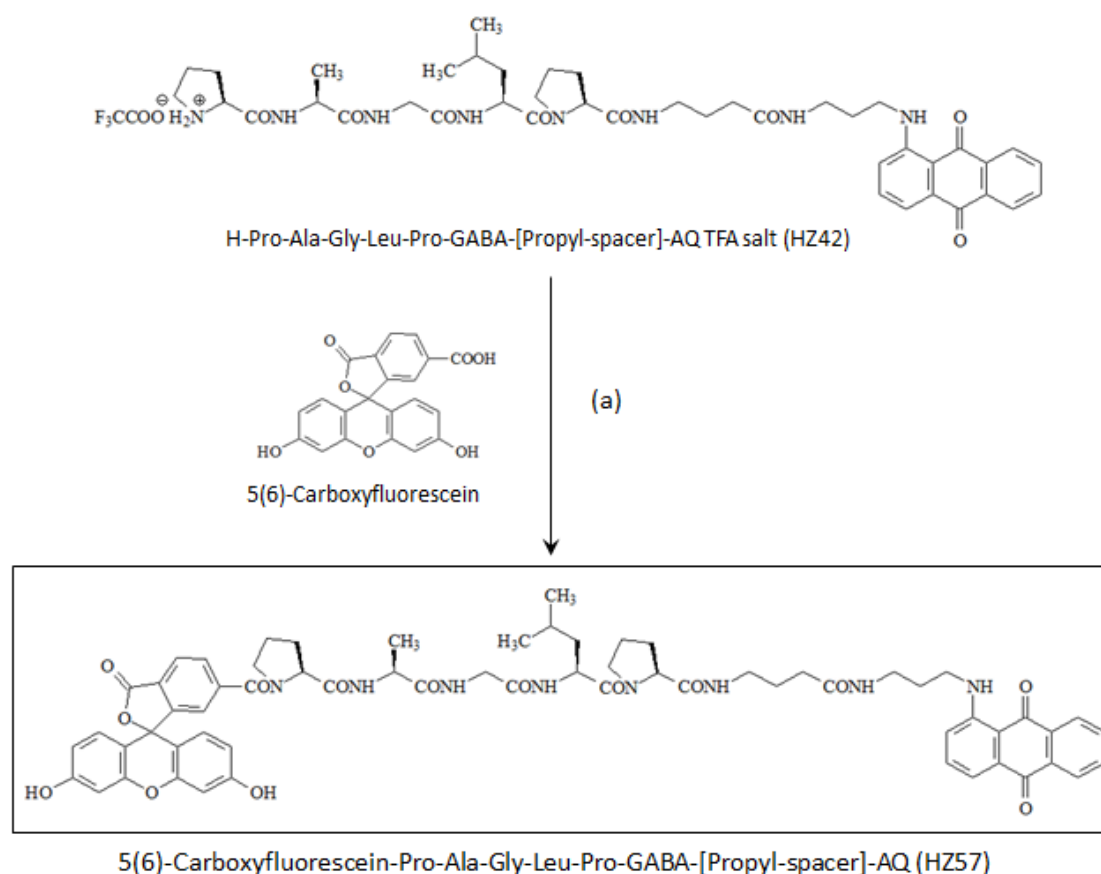
Reagents and Conditions: (a) ByBOP & DIPEA, in DMF

**Scheme 13.** Outline of Prodrug 7 (HZ57) synthesis

For the synthesis of prodrug 7 5(6)-Carboxyfluorescein-Pro-Ala-Gly-Leu-Pro-GABA-[Propyl-spacer]-AQ (HZ57), the fluorescein agent 5(6)-carboxyfluorescein was coupled to the compound of H-Pro-Ala-Gly-Leu-Pro-GABA-[Propyl-spacer]-AQ TFA salt (HZ42), using PyBOP and DIPEA in DMF for overnight reaction **(Scheme 13)**. The crude product was purified by extraction and silica gel column chromatography (dichloromethane-methanol 5:1). The appropriate fractions were combined, filtered to an evaporating basin and evaporated to dryness at RT.

The final product Prodrug 7: 5(6)-carboxyfluorescein-Pro-Ala-Gly-Leu-Pro-GABA-[Propyl-spacer]-AQ (HZ57) was characterized by its mass spectrum $(M+H)^+$ which has a strong signal at m/z 1159 corresponding to a molecular mass of 1158 **(Figure 19)**.
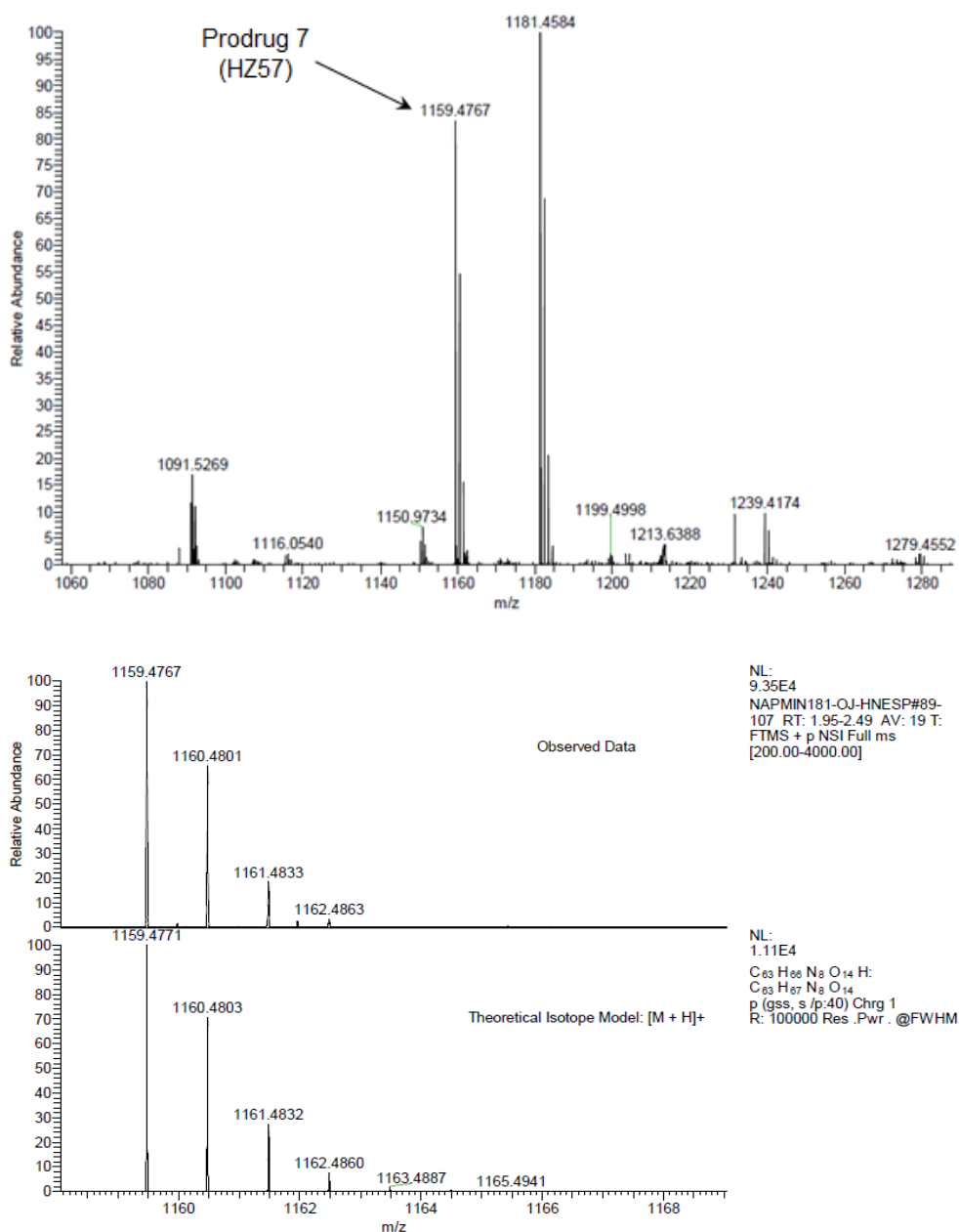
**Figure 19.** ESI (+) Mass spectrum of Prodrug 7 (HZ57)

## 1.4.10 Synthesis of Prodrug 8:

## Podophyllotoxin-Succinyl-Pro-Ala-Gly-Leu-Ala-Ala-Piperazinyl-AQ (HZ16)

### 1.4.10.1 Synthesis of Boc-Ala-Ala-Piperazinyl-AQ (HZ7)

The synthesis of prodrug 8 started with the synthesis of a 2-piperazinyl anthraquinone spacer compound, NU: UB 341, where NU:UB 341 was synthesised following a previously described method (Mincher, Turnbull and Kay, 2003), by nucleophilic displacement of chlorine from 2-chloroanthraquinone with

60

a large excess of piperazine hexahydrate in DMSO. Crude NU:UB 341 was isolated by precipitation and purified by column chromatography before reaction with a commercially available Boc protected dipeptide (Boc-Ala-Ala-OH) in DMF, using standard peptide coupling conditions, TBTU, HOBt and DIPEA. The reaction mixture was kept at RT overnight **(Scheme 14)**.
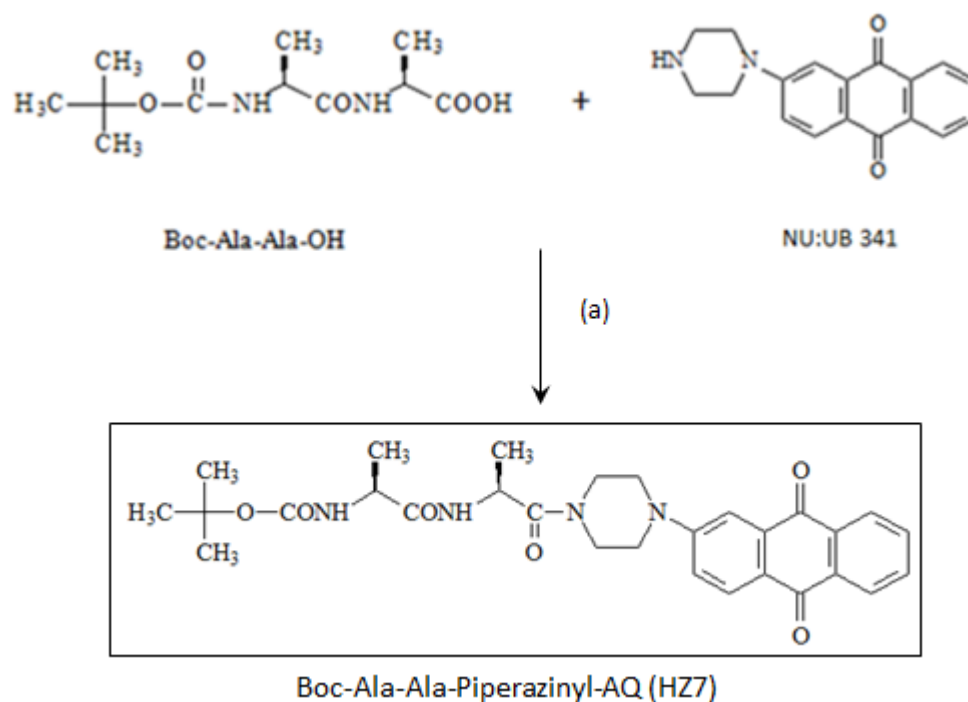


Reagents and conditions: TBTU, HOBt, DIPEA, dissolved in DMF, RT, overnight
**Scheme 14.** Synthesis of Boc-Ala-Ala-Piperazinyl-AQ (HZ7)

Once the reaction was completed by checking TLC (dichloromethane-methanol 9:1), the mixture solution was extracted using dichloromethane and water to remove DMF. The organic layer was dried (by the addition of anhydrous sulphate), filtered, evaporated to a small volume and the purified by column chromatography using the same solvent system as TLC test. The eluted solution was filtered to get rid of silica gel and then evaporated to dryness by using the rotational evaporating machine. The product remained in the round bottomed flask for the Boc-deprotection reaction. This procedure allowed two amino acids to be simultaneously incorporated by the use of a pre-formed dipeptide, ala-ala.

Single amino acid conjugates of the 2-piperazinyl anthraquinone spacer compound, NU:UB 341, have previously shown anticancer activity in vitro. For example, a isoleucine conjugate, NU:UB 234, had broad-spectrum activity in vitro at low micromolar concentrations in the NCI 60 cell line anticancer drug screen and was a dual topoisomerase I and II inhibitor (Mincher, Turnbull and Kay, 2001; Young, 2006). From previous studies on this class of compound, where amino acids are coupled to piperazinyl spacers through a tertiary amide bond, it would be expected that after metabolism of prodrug 8 (HZ 16) at the key gly~leu bond by endoprotease cleavage by MMP-9, further protease degradation should result in release of a potentially cytotoxic anthraquinone-piperazinyl-alanine conjugate, with no further metabolism to the spacer compound (NU: UB 341), as tertiary amides are generally considered to be resistant to enzymatic cleavage. Hence, prodrug 8 has been designed as a dual acting 'twin' prodrug containing both cytotoxic anthraquinone derived and tubulin binding, vascular disrupting podophyllotoxin active agents.

### 1.4.10.2 Synthesis of H-Ala-Ala-Piperazinyl-AQ TFA salt (HZ8)

The Boc group of Boc-Ala-Ala-Piperazinyl-AQ (HZ7) was removed by TFA treatment for the next amino acids coupling reaction. TFA was added to the round bottomed flask until the solid had completely dissolved **(Scheme 15)**.

Boc-Ala-Ala-Piperazinyl-AQ (HZ7)

(a)
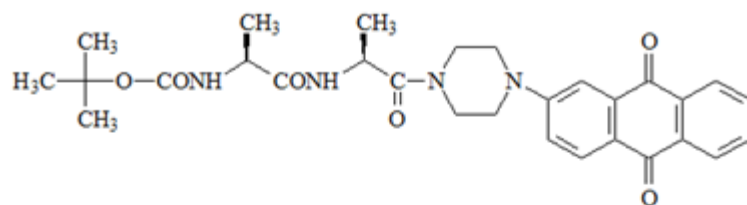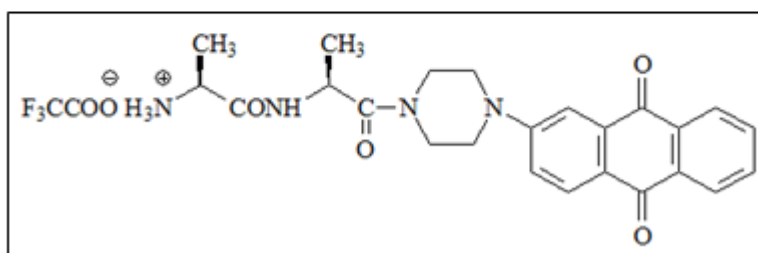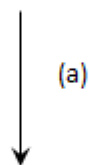
H-Ala-Ala-Piperazinyl-AQ TFA salt (HZ8)

Reagents and conditions: (a) TFA, RT, 1.15 hours

**Scheme 15.** Synthesis of H-Ala-Ala-Piperazinyl-AQ TFA salt (HZ8)

After 1.15 hours, the reaction had completed by checking TLC (chloroform-methanol 9:1). The solution was evaporated to dryness by using the rotary evaporator. Diethyl ether was added and the mixture was cooled at 5 °C for 1 hour. The precipitated compound was then filtered, dried and collected. The structure of H-Ala-Ala-Piperazinyl-AQ TFA salt (HZ8) was confirmed by is ^{1}H NMR spectrum. The signals between 1.27 and 1.35 were assigned to the methylene groups of the Ala-Ala dipeptide. The anthraquinone protons were fully assigned; H-3 at 7.35 ppm, H-1 and H-4 gave a 2-proton multiplet at 7.5 ppm, H-6 and H-7 was a multiplet at 7.9 ppm, H-5 and H-8 a multiplet between 8.08 and 8.2 ppm. The signals at 3.2-3.75 ppm reflected the protons of the piperazine spacer group.

### 1.4.10.3 Synthesis of Boc-Leu-Ala-Ala-Piperazinyl-AQ (HZ9)

The next step of the synthesis involved coupling leucine to the dipeptide chain of H-Ala-Ala-Piperazinyl-AQ TFA salt (HZ8). The synthesis of Boc-Leu-Ala-Ala-piperazinyl-AQ (HZ9) was carried out by initially dissolving HZ8 and Boc-Leu-OSu in DMF, followed by addition of DIPEA at RT for 3 hours **(Scheme 16)**.



H-Ala-Ala-Piperazinyl-AQ TFA salt (HZ8)

Boc-Leu-OSu

(a)

Boc-Leu-Ala-Ala-Piperazinyl-AQ (HZ9)
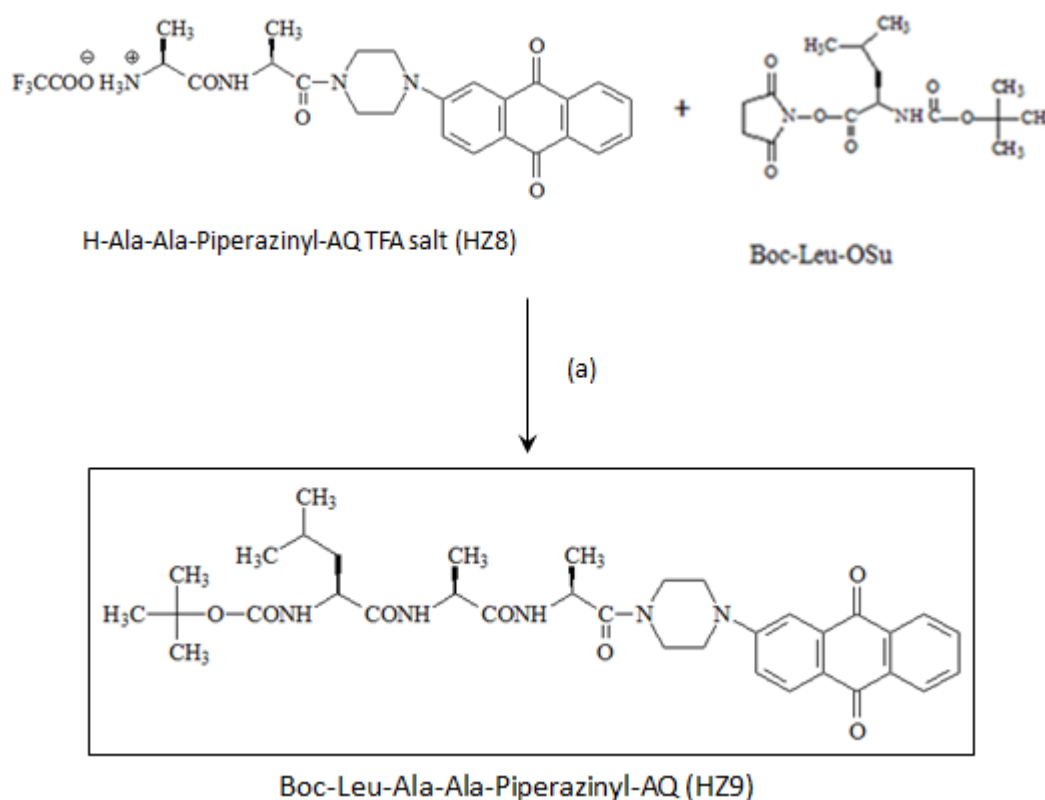
Reagents and conditions: (a) DIPEA, dissolved in DMF, RT, 3 hours

**Scheme 16**. Synthesis of Boc-Leu-Ala-Ala-Piperazinyl-AQ (HZ9)

After the completion of the reaction indicated by TLC test using dichloromethane-methanol 9:1 solvent system, the solution was evaporated to dryness.

### 1.4.10.4 Synthesis of H-Leu-Ala-Ala-Piperazinyl-AQ TFA salt (HZ10)

The Boc-Leu-Ala-Ala- piperazinyl-anthraquinone compound was de-protected

by the addition of the strong acid, TFA at RT for 1.5 hours **(Scheme 17)**.



Boc-Leu-Ala-Ala-Piperazinyl-AQ (HZ9)

(a)

H-Leu-Ala-Ala-Piperazinyl-AQ TFA salt (HZ10)
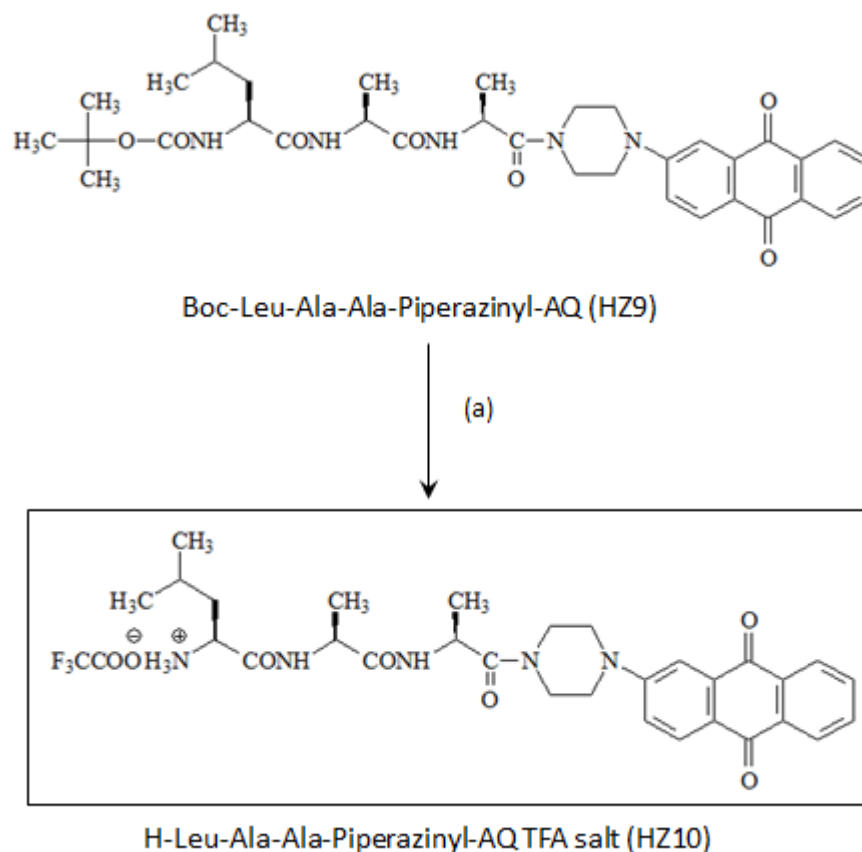
Reagents and conditions: (a) TFA, RT, 1.5 hours

**Scheme 17.** Synthesis of H-Leu-Ala-Ala-Piperazinyl-AQ TFA salt (HZ10)

The reaction was closely monitored by TLC (chloroform-methanol). Once the reaction was completed, the solution was evaporated to dryness and triturated in diethyl ether at 5°C for 1 hour. The mixture was then filtered, dried and collected.

**1.4.10.5 Synthesis of Boc-Ala-Gly-Leu-Ala-Ala-Piperazinyl-AQ (HZ11)**

The previous tripeptide conjugate was extended by the use of another preformed dipeptide fragment, alanylglycine. After the reaction, the compound had the intended MMP-9 cleavage site which is gly and leu occupied the P1 and P1' positions respectively. The Boc-protected pentapeptide anthraquinone conjugate was synthesised by dissolving the HZ10 and Boc-Ala-Gly-OSu in DMF, and the reaction mixture was added by DIPEA and reacted at RT overnight

**(Scheme 18).**



H-Leu-Ala-Ala-Piperazinyl-AQ TFA salt (HZ10)　　　+　　　Boc-Ala-Gly-OSu

(a)

Boc-Ala-Gly-Leu-Ala-Ala-Piperazinyl-AQ (HZ11)
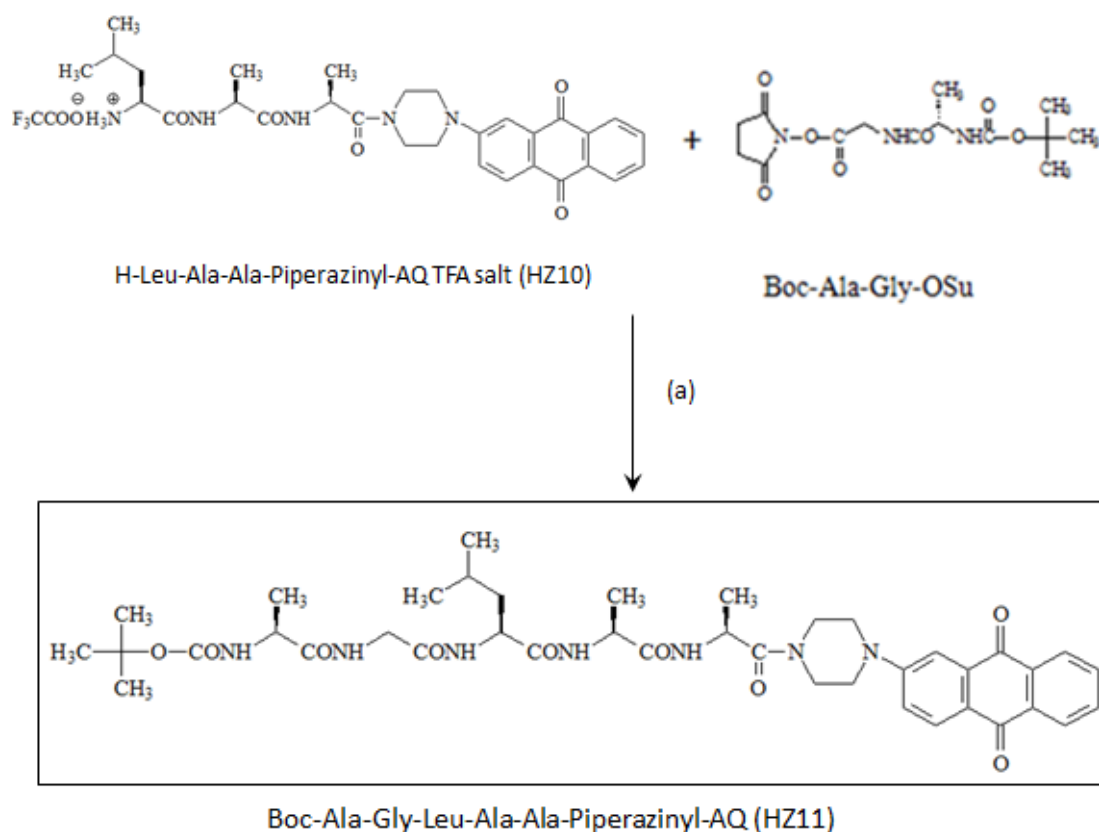
Reagents and conditions: (a) DIPEA, dissolved in DMF, RT, 25 hours

**Scheme 18.** Synthesis of Boc-Ala-Gly-Leu-Ala-Ala-Piperazinyl-AQ (HZ11)

The TLC (chloroform-methanol 10:1) result showed that the reaction was not complete after 20 hours. Another 0.5 equivalent of Boc-Ala-Gly-OSu and DIPEA were added to the solution and left at RT for a further 3 hours. The TLC (chloroform-methanol 9:1) showed that still have starting material on the product lane. Continued addition of a further 0.5 equivalent of Boc-Ala-Gly-OSu to the solution was made and reacted at RT for 2 hours. There was only one clean red spot on the TLC plate, which indicated that the reaction had fully completed. Extraction was performed by using chloroform and water, anhydrous sodium sulphate was then added to the organic solution to absorb water. The solution was filtered and evaporated to dryness. The dried product was continued for the next step of synthesis without purification by column chromatography to

maximize the yield.

## 1.4.10.6 Synthesis of H-Ala-Gly-Leu-Ala-Ala-Piperazinyl-AQ TFA salt (HZ12)

The Boc-protected pentapeptide anthraquinone compound was dissolved by the addition of TFA for the de-Boc reaction at RT for 2 hours **(Scheme 19)**.



Boc-Ala-Gly-Leu-Ala-Ala-Piperazinyl-AQ (HZ11)

(a)

H-Ala-Gly-Leu-Ala-Ala-Piperazinyl-AQ TFA salt (HZ12)
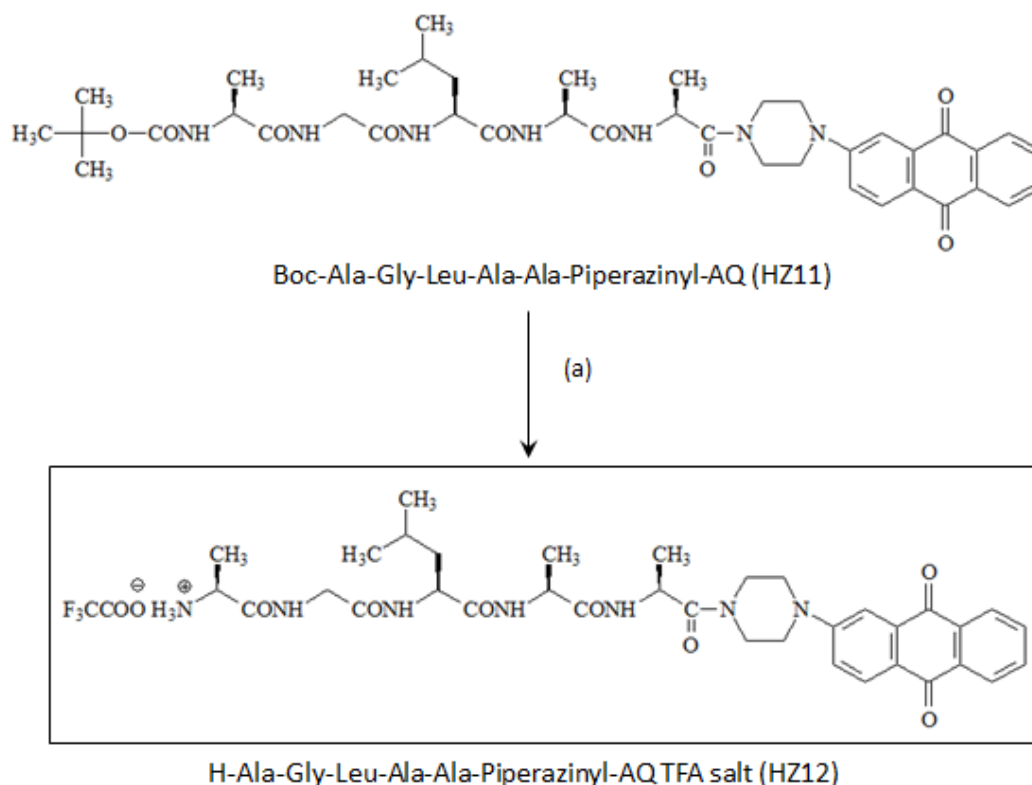
Reagents and conditions: (a) TFA, RT, 2 hours

**Scheme 19.** Synthesis of H-Ala-Gly-Leu-Ala-Ala-Piperazinyl-AQ TFA salt (HZ12)

The TLC result (dichloromethane-methanol 9:1) showed that the reaction has completed. The solution was evaporated using a rotary evaporator. A few drops of methanol were added to the solution to help evaporation. The dried product was added with diethyl ether at 5°C for 1 hour and the mixture was filtered and collected.

**1.4.10.7 Synthesis of Boc-Pro-Ala-Gly-Leu-Ala-Ala-Piperazinyl-AQ (HZ13)**

Finally, proline was added to form the target hexapeptide adduct which would place proline in the P3 position with respect to the cleavage site. The Boc-protected hexapeptide piperazinyl-anthraquinone compound was synthesised by using Boc-Pro-OH to react with D-Ala-Gly-Leu-Ala-Ala-anthraquinone in DMF at RT for 1 hour, followed by the addition of reagents TBTU, HOBt, and DIPEA to the solution **(Scheme 20)**.



H-Ala-Gly-Leu-Ala-Ala-Piperazinyl-AQ TFA salt (HZ12)

Boc-Pro-OH

(a)

Boc-Pro-Ala-Gly-Leu-Ala-Ala-Piperazinyl-AQ (HZ13)
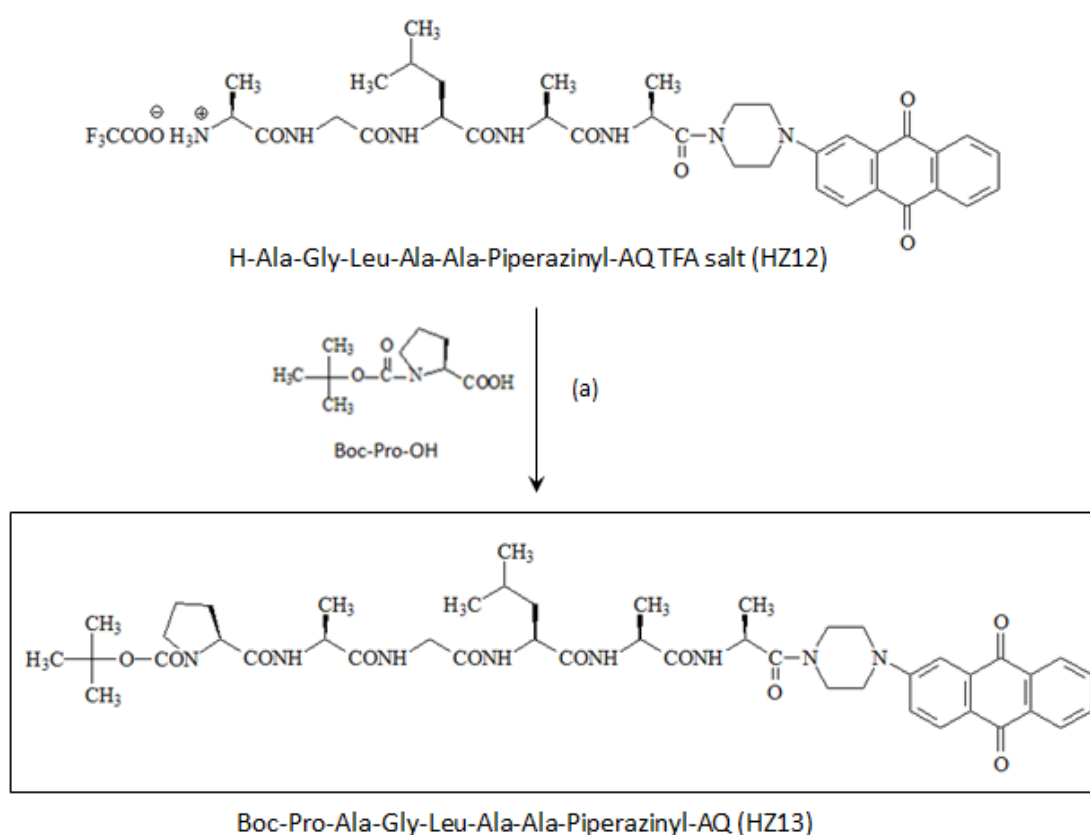
Reagents and conditions: (a) TBTU, HOBt, DIPEA, dissolved in DMF, RT, 1 hour

**Scheme 20.** Synthesis of Boc-Pro-Ala-Gly-Leu-Ala-Ala-Piperazinyl-AQ (HZ13)

Once the TLC test (dichloromethane-methanol 9:1) showed the appearance of the new red spot and the disappearance of starting material, HZ12 on the product lane, the reaction solution was evaporate to a small volume. Purification of the product was performed using column chromatography in the same solvent

system as TLC analysis. The eluted solution was filtered and evaporated to dryness in vacuum.

## 1.4.10.8 Synthesis of H-Pro-Ala-Gly-Leu-Ala-Ala-Piperazinyl-AQ TFA salt (HZ14)

Removal of the Boc group from Boc-protected hexapeptide piperazinyl-anthraquinone conjugate was carried out by dissolving the compound in TFA at RT for 2.5 hours **(Scheme 21)**.



Boc-Pro-Ala-Gly-Leu-Ala-Ala-Piperazinyl-AQ (HZ13)

(a)

H-Pro-Ala-Gly-Leu-Ala-Ala-Piperazinyl-AQ TFA salt (HZ14)
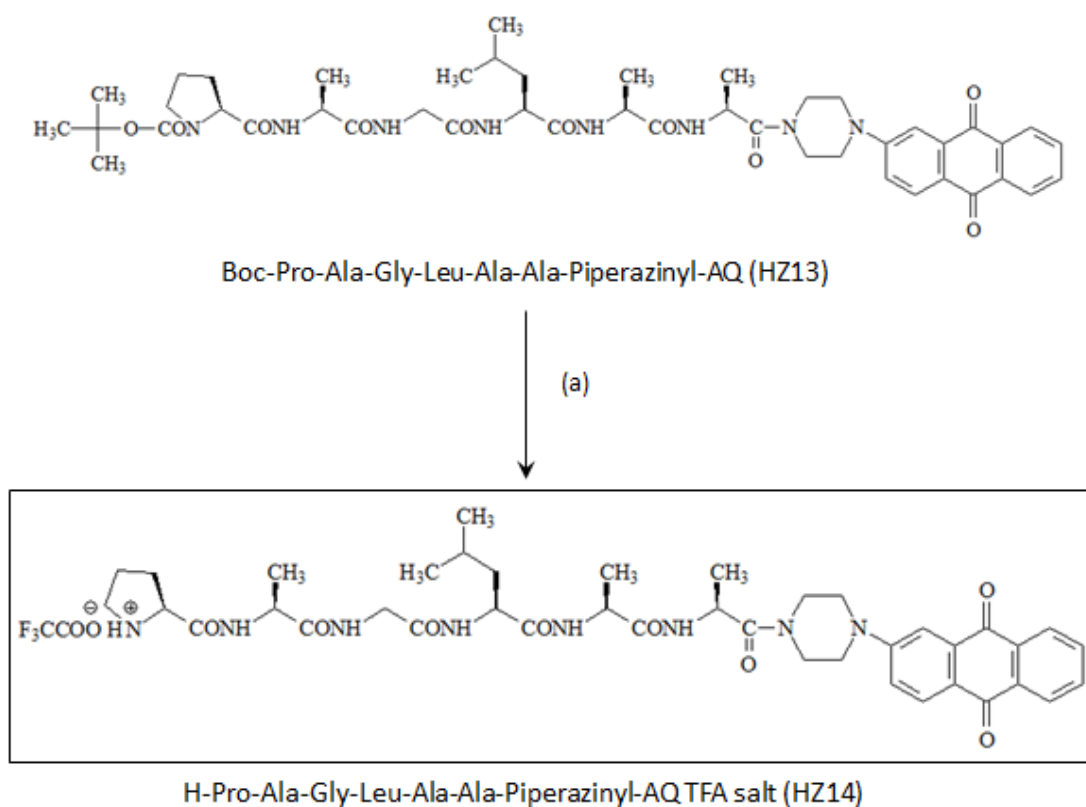
Reagents and conditions: (a) TFA, RT, 2.5 hours

**Scheme 21**. Synthesis of H-Pro-Ala-Gly-Leu-Ala-Ala-Piperazinyl-AQ TFA salt (HZ14)

Once the reaction was complete indicated by TLC using dichloromethane-methanol 9:1 solvent system, the solution was evaporated to dryness using a rotary evaporator. Addition of diethyl ether precipitated the product H-Pro-Ala-Gly-Leu-Ala-Ala-Piperazinyl-AQ TFA salt (HZ14). The solid

compound was dried in a desiccator and collected.

## 1.4.10.9 Synthesis of Succinyl-Pro-Ala-Gly-Leu-Ala-Ala-Piperazinyl-AQ (HZ15)

The starting material H-Pro-Ala-Gly-Leu-Ala-Ala-Piperazinyl-AQ TFA salt (HZ14) was reacted with succinic anhydride in DMF with adding the base DIPEA at RT **(Scheme 22)**.



H-Pro-Ala-Gly-Leu-Ala-Ala-Piperazinyl-AQ TFA salt (HZ14)

(a)

Succinyl-Pro-Ala-Gly-Leu-Ala-Ala-Piperazinyl-AQ (HZ15)
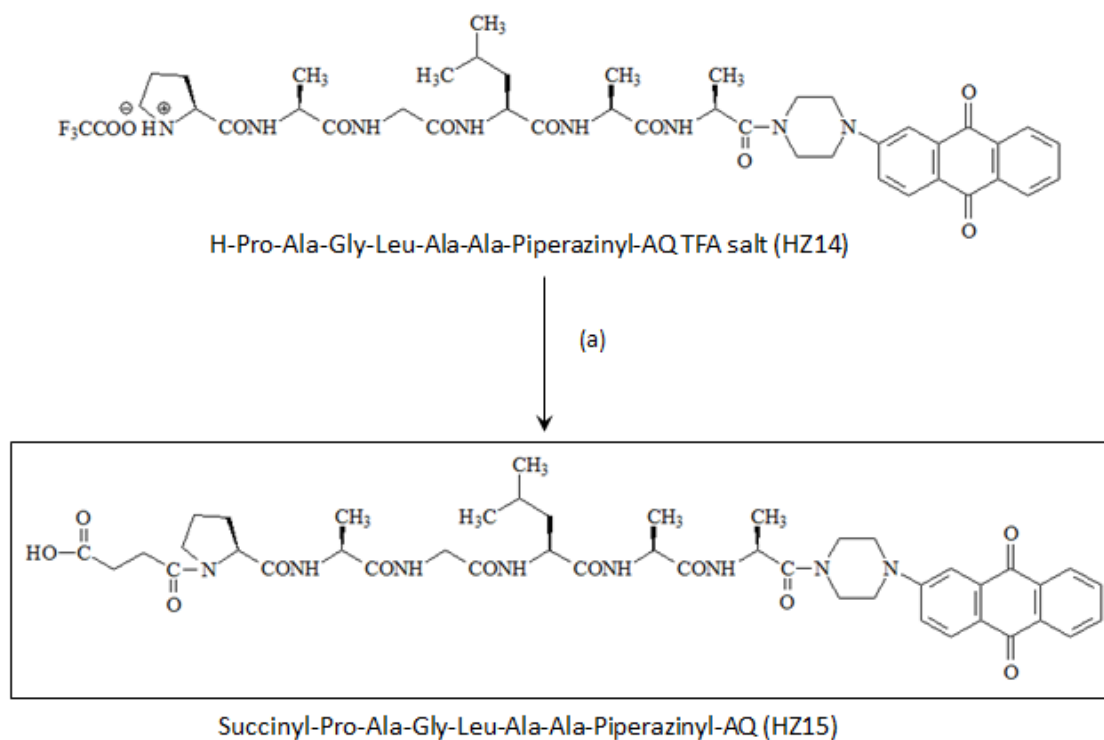
Reagents and conditions: (a) succinic anhydride, DIPEA, dissolved in DMF, RT, 2 days

**Scheme 22.** Synthesis of Succinyl-Pro-Ala-Gly-Leu-Ala-Ala-Piperazinyl-AQ (HZ15)

The TLC (dichloromethane-methanol 6:1) showed that there was no starting material present at the product lane. Column Chromatography was performed to purify the product using dichloromethane-methanol 7:1 solvent system. The solution was evaporated to dryness, and the solid compound Succinyl-Pro-Ala-Gly-Leu-Ala-Ala-Piperazinyl-AQ (HZ15) was precipitated by diethyl ether and collected.

**1.4.10.10 Synthesis of Prodrug 8:**

**Podophyllotoxin-Succinyl-Pro-Ala-Gly-Leu-Ala-Ala-Piperazinyl-AQ (HZ16)**

Podophyllotoxin was used as the active drug of prodrug 8. Podophyllotoxin is a well-known naturally occuring lignan isolated from Podophyllin, a resin extract of Podophyllum species. Podophyllotoxin was commonly used in many Eastern countries, such as China and Japanese, as a folk antiviral remedy for gout, tuberculosis, syphilis and psoriasis (Gordaliza *et al.*, 2004). The application of Podophyllotoxin inhibits the replication cycle of these viruses at early stage. Today, it is still an effective drug in the treatment of venereal warts (condyloma acuminate) caused by human papilloma virus (HPV) (Liu and Hou, 1997).

Another important property of Podophyllotoxin is its antitumor activity that was first described by Kaplan in 1942. Podophyllotoxin and its derivatives were found to be effective in the treatment of genital tumours, lymphomas, lung cancer, multiple myeloma and some other malignant conditions (Castro et al., 2003). Podophyllotoxin acts as microtubule damaging agent like colchicine or vincristine on DNA. There are evidences that showed podophyllotoxin inhibits the polymerization of tubulin. However, the application of podophyllotoxin is often limited by severer toxicity. The podophyllotoxin derivative, etoposide is widely used as antineoplastic drugs with a different mode of action and less toxic (Bohlin and Rosen, 1996). Etoposide is a DNA topoisomerase II inhibitor which forms a DNA-drug-enzyme complex that induces DNA strands break and eventually lead to cell death (Greco and Hainsworth, 1996; Canel et al., 2000).

Podophyllotoxin was attached to the succinyl end of the compound Succinyl-Pro-Ala-Gly-Leu-Ala-Ala-Piperazinyl-AQ (HZ15) to synthesise the podophyllotoxin-based prodrug 8. The reaction was carried out in DMF and acetonitrile (1:1) solution with adding the coupling agents, TEA and TBTU.

During the reaction, there was solid formed in the solution. The reaction mixture was kept at RT overnight **(Scheme 23)**.



Succinyl-Pro-Ala-Gly-Leu-Ala-Ala-Piperazinyl-AQ (HZ15)

Podophyllotoxin

(a)

Podophyllotoxin-Succinyl-Pro-Ala-Gly-Leu-Ala-Ala-Piperazinyl-AQ (HZ16)
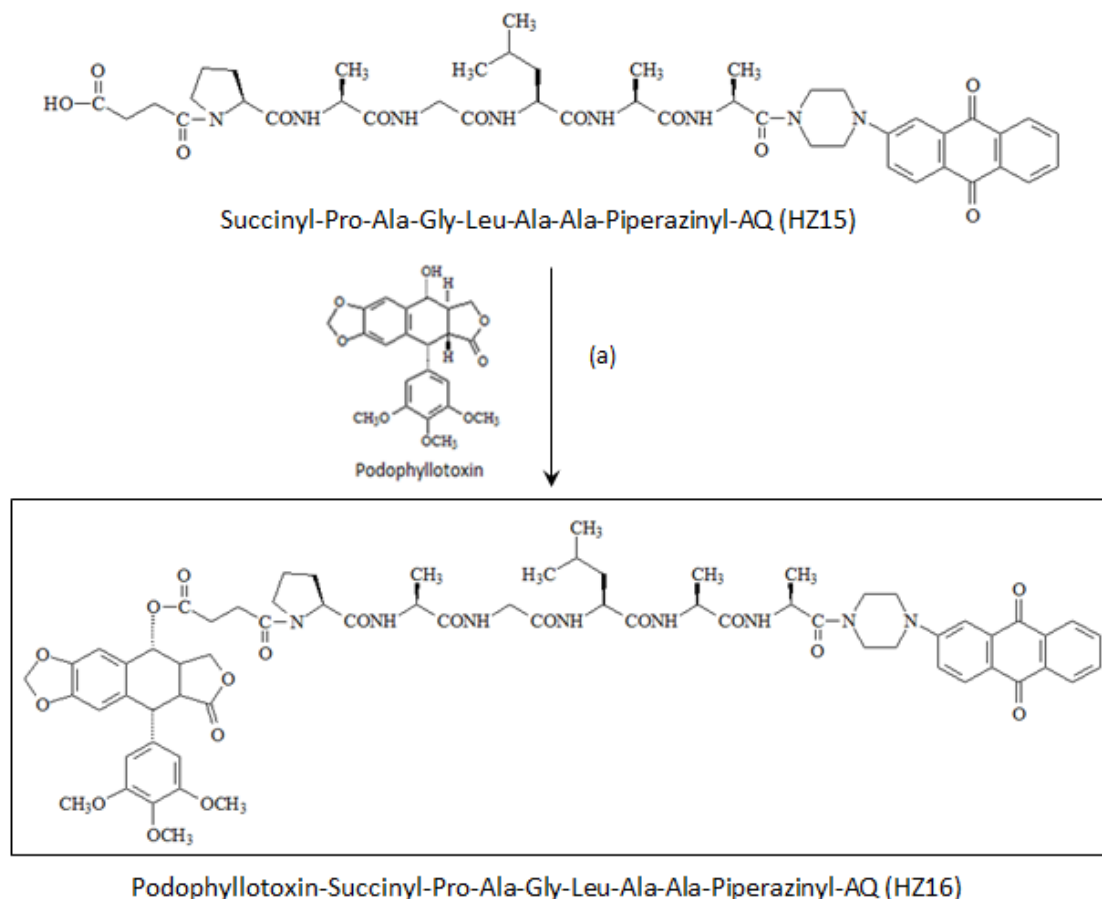
Reagents and conditions: (a) TEA, TBTU, dissolved in DMF & acetonitrile, RT, 48 hours

**Scheme 23.** Synthesis of Prodrug 8: Podophyllotoxin-Succinyl-Pro-Ala-Gly-Leu-Ala-Ala-Piperazinyl-AQ (HZ16)

The reaction solution was checked by TLC (dichloromethane-methanol 8:1) which indicated the reaction has completed. Furthermore, a small amount of the solid in the solution was dissolved in chloroform and checked by TLC which showed that it was the same product as in solution. The mixture was extracted with chloroform and water and then the organic layers were evaporated to dryness. The dried solid was checked by TLC again which showed two main spots, one was the product HZ16 and the other one was the starting material HZ15. The solid was dissolved in acetonitrile followed by the addition of TEA,

TBTU and podophyllotoxin. The reaction was completed after 20 hours by checking the TLC. The solution was evaporated to dryness and dissolved by chloroform in a small volume. A thick TLC plate was used for product purification with a solvent system of dichloromethane-methanol 8:1. The product layer on the TLC plate was collected and dissolved in ethanol. After the filtration, the solution which contained the final product was evaporated, triturated by the addition of diethyl ether and collected. The molecular mass of the synthesised podophyllotoxin peptide prodrug 8 (HZ16) was expected to be 1268 Daltons according to its structure. The electrospray (+) mass spectrum revealed a strong and clear peak at m/z 1286 for the ion $(MNH_4)^+$ which confirmed the mass of 1268 Daltons **(Figure 20)**. Considering the mass spectrum results, the synthesis of podophyllotoxin-based MMP-9 activated prodrug 8 was successful and can be considered as a good candidate for cancer chemotherapy research.
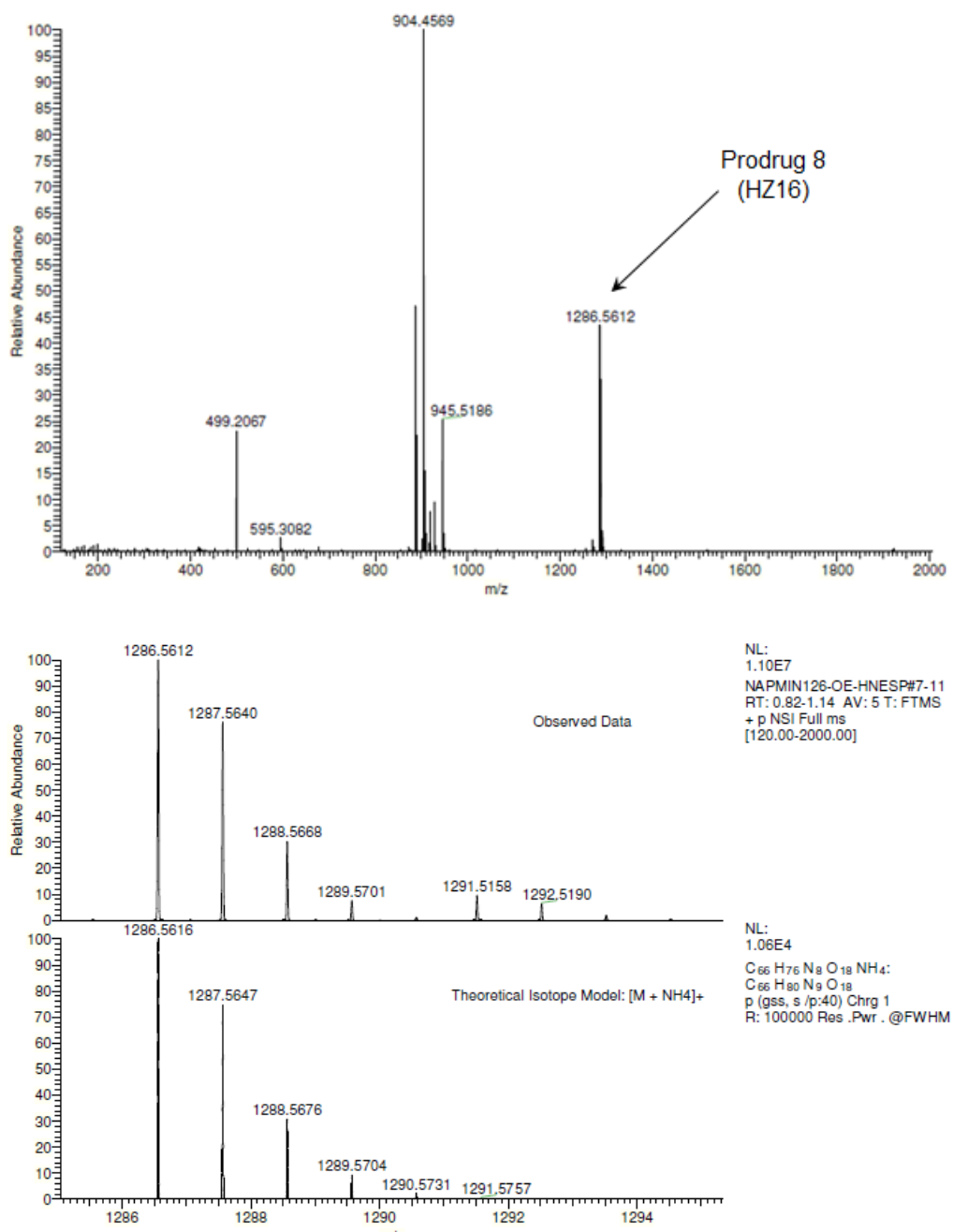
**Figure 20.** Mass Spectrum of Prodrug 8 (HZ16)

According to the chemical structure of the synthesised prodrug 8 (Podophyllotoxin-Succinyl-Pro-Ala-Gly-Leu-Ala-Ala-Piperazinyl-AQ) in this study, the functional group of podopyllotoxin is hydroxyl which forms an ester bond with the carboxyl acid of succinate hexapeptide anthraquinone conjugate. An ester is the most common linkage of tumour activated prodrugs. The ester bond is relatively easy to synthesise, additionally, the functional groups, hydroxyl and

carboxyl acid are widely common in active drugs or chemical linkers. Moreover, esterases that are able to hydrolyse the ester bond are everywhere distributed in the human body (Han & Amidon, 2000). There are four common types of ester bond which are listed shown in **Figure 21**. The half-life of an eater bond may vary from minutes to hours, depends on the structure of TAPs and the esterases activities. The carbamate ester found to be more stable than the other three ester bonds (Liederer & Borchardt, 2006). On the other hand, two TAPs with the same ester bond may also have different half-lives (Mahato *et al.,* 2011).
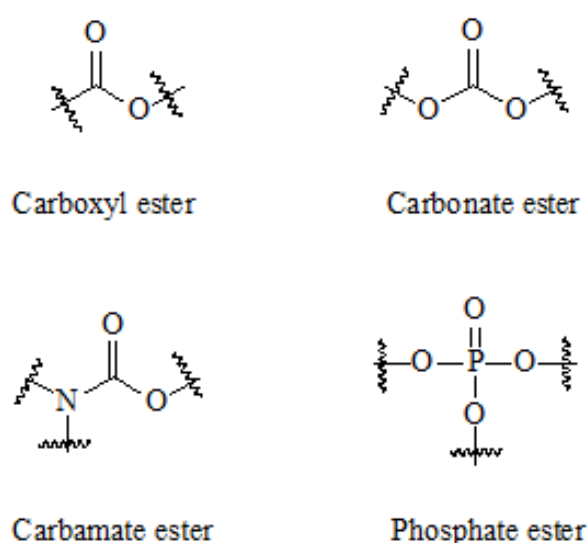


**Figure 21.** Four different types of ester bond
(Adapted from Liederer & Borchardt 2006)

The synthesised prodrug 8 (HZ16) has a carboxyl ester bond and a MMP-9 sensitive peptide substrate. The hexapeptide (Pro-Ala-Gly-Leu-Ala-Ala) is expected to be cleaved by the tumour specific enzyme, MMP-9. The carboxyl ester bond will be hydrolysed by esterase to release the active drug, podophyllotoxin.

The anticipated activation process of synthesised prodrug 8 in cancer cells has been illustrated in **Figure 22**. However, further in vitro and in vivo evaluations are needed, including HPLC studies of the in vitro breakdown in tumour versus

healthy tissues.
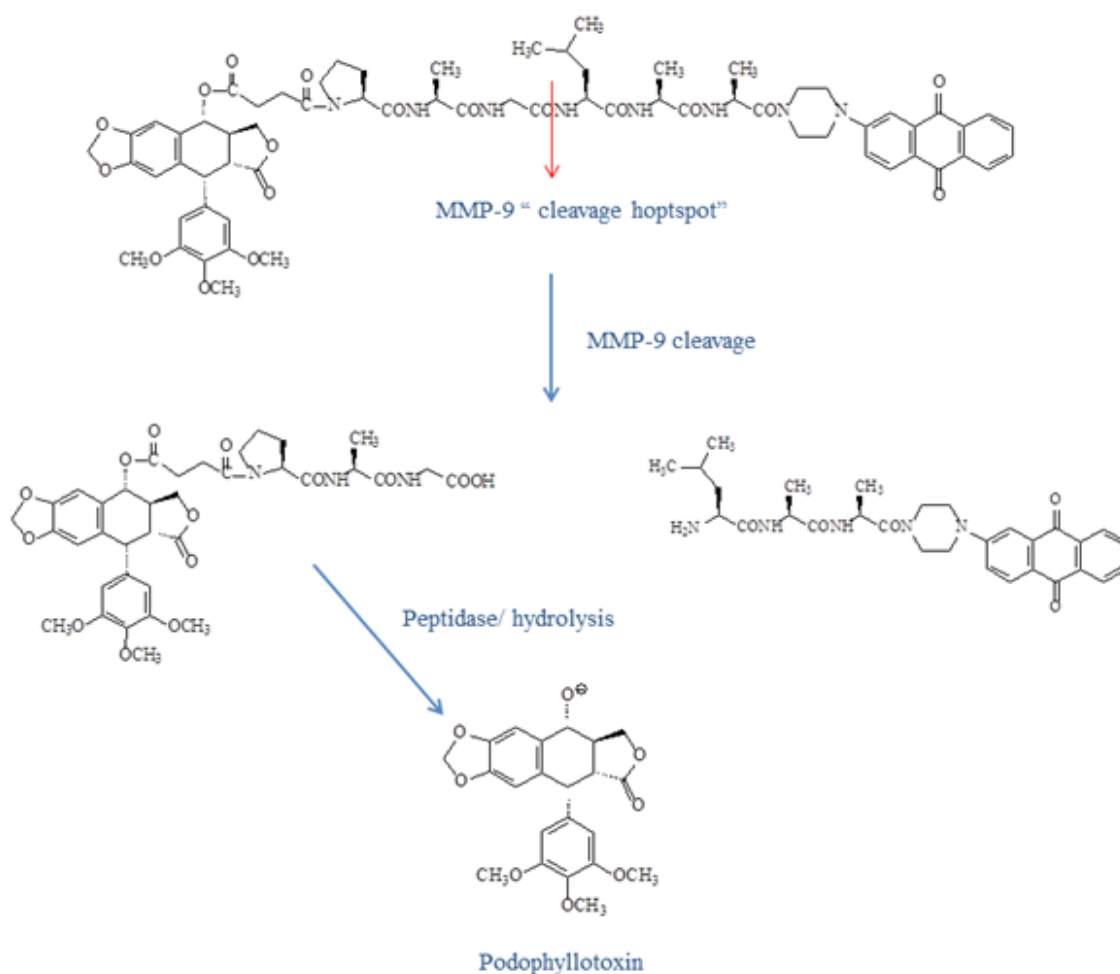


**Figure 22.** The expected activation of synthesized prodrug 8 in vivo

## 1.4.11 HT1080 Cell Culture

The human fibrosarcoma cell line (HT1080) provides a suitable tumour model for

the study of MMPs activated prodrugs (Albright et al., 2005). HT1080 cells are

identified to have overexpressed MMPs, particularly MMP-2 and MMP-9

(Hofmann et al., 2003, Kline et al., 2004).

## 1.4.11.1 Materials for HT1080 cell culture

RPMI 1640 (without L-glutamine), penicillin/streptomycin, L-glutamine, foetal

bovine serum (FBS), Sodium chloride solution, 1× Trypsin/EDTA (prepared in

1:10 dilution with NaCl solution), all purchased from Sigma. HT1080 cells

(obtained from the European Tissue Culture Collection)

## 1.4.11.2 Method for HT1080 cell culture

The HT1080 cells were epithelial adherent cell lines and grown in RPMI 1640 medium with 10% FBS, 1% penicillin/streptomycin, 1% L-glutamine. The cells were regularly examined under an inverted light microscope and passaged by using trypsin solution. The cell culture flaks were kept in a humidified incubator at $37^0C$ with 5% CO2 and 95% air.

## 1.4.12 Fluorescence Studies of Prodrug 3 (HZ43) and Prodrug 7 (HZ57)

The fluorescent labelled Prodrug 7 Carboxyfluorescein-Pro-Ala-Gly-Leu-Pro-GABA-[Propyl-spacer]-AQ (HZ57) and Prodrug 3 FITC-Pro-Ala-Gly-Leu-Pro-GABA-[Propyl-spacer]-AQ (HZ43) allowed the rapid detection of MMP-9 prodrug activation by fluorescence release. The fluorescence of the FITC/Carboxyfluorescein group was internally quenched by the anthraquinone chromophore by fluorescence resonance energy transfer (FRET). The FRET principle is discussed in chapter 3. The cleavage of the MMP-9 specific peptide will result in an increase level of fluorescence.

PBS (Control) and HT1080 homogenate were added to the wells of a 96-well plate in the presence of 10 µM fluorescent labelled Prodrug 3 (HZ43) or Prodrug 7 (HZ57). For comparison, HT1080 homogenate was pre-incubated with CTT (1.3 mM) which is a cyclic peptide gelatinase Inhibitor for MMP-2 and MMP-9 (Ndinguri et al., 2012), for 1 hour before the addition of prodrugs. The fluorescence intensity was measured by a FLUOstar OPTIMA plate reader.
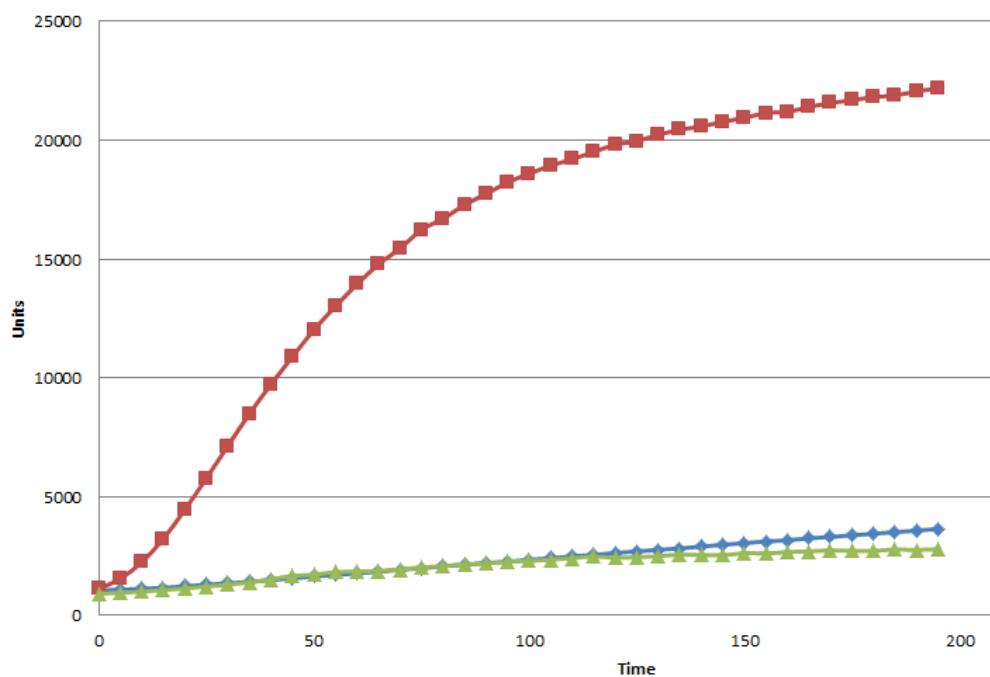
**Figure 23.** Fluorescence released by Prodrug 7 (HZ57) during metabolism. HZ57 (10 µM) was added to HT1080 tumour homogenate (■), PBS buffer (◆), and HT1080 homogenate with pre-incubation of MMP inhibitor CTT (1.3 mM, ▲)

The background levels of fluorescence were shown by the addition of Prodrug 7 (HZ57) into the PBS solution (tissue-free control). It was found that incubation of HZ57 with HT1080 tumour homogenate results in an increased fluorescence due to the cleavage of HZ57. Further evaluation of HZ57 was performed by pre-incubation of HT1080 tumour homogenate with MMP-2/MMP-9 specific inhibitor CTT. From **Figure 23**, the fluorescence of HZ57 was decreased by the CTT treatment.
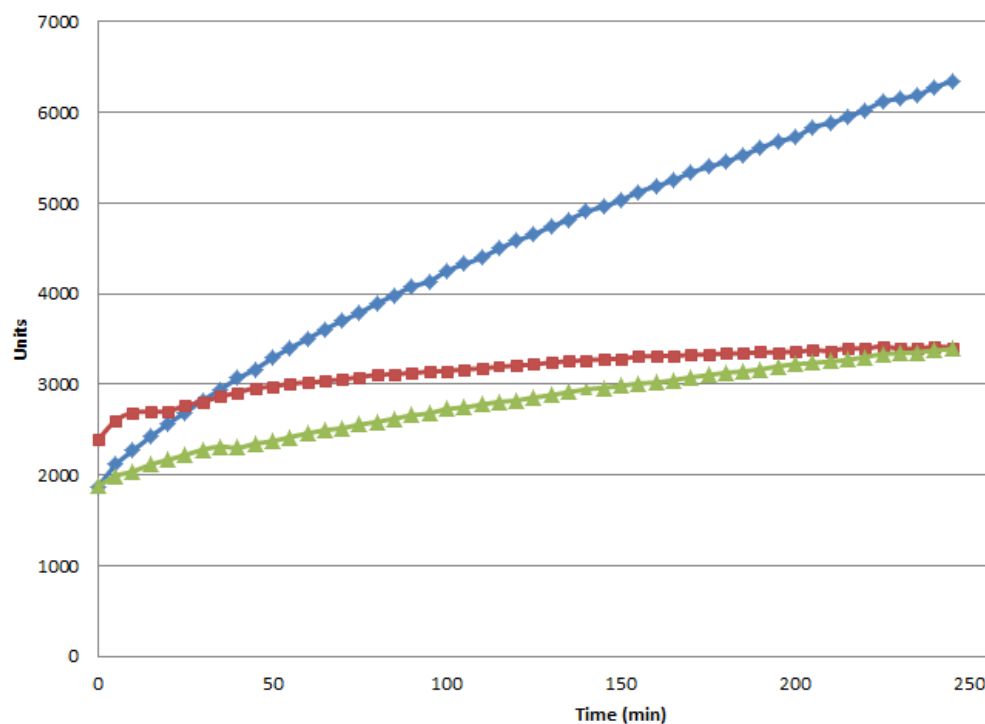
**Figure 24**. Fluorescence released by Prodrug 3 (HZ43) during metabolism. HZ43 (10 μM) was added to HT1080 tumour homogenate (■), PBS buffer (◆), and HT1080 homogenate with pre-incubation of MMP inhibitor CTT (1.3 mM, ▲)

Similarly, the FITC labelled prodrug 3 (HZ43) has an increased fluorescence with incubation of HT1080 tumour homogenate (**Figure 24)**. However, the fluorescence intensity was lower than Prodrug 7 (HZ57) at the same drug concentration of 10 μM. The fluorescence level of HZ43 with CTT treatment showed no significant different with comparison of the tissue-free control.

## 1.5 Conclusion

The over expressed MMP-9 in tumour was used as a promising target for tumour activated prodrugs, and aimed to increase the drug selectivity and decrease the toxicity to other normal cells.

A series of tumour activated prodrugs were synthesised in this study. All prodrugs (1-8) have the MMP-9 cleavable peptide chain in the middle part of the structure. The summarized structures of Prodrugs (1-8) with HZ codes are illustrated in **Table 2**. The red line indicates the MMP-9 cleavage 'hot spot'.

| Code | Structure components |
|------|---------------------|
| Prodrug 1 (HZ32) | Fmoc — Pro Ala Gly ▬ Leu Ala Ala — Propranolol |
| Prodrug 2 (HZ34) | Anthraquinone — Pro Ala Gly ▬ Leu Ala Ala — Propranolol |
| Prodrug 3 (HZ43) | FITC — Pro Ala Gly ▬ Leu Pro — GABA — Anthraquinone |
| Prodrug 4 (HZ45) | Anthraquinone — Pro Ala Gly ▬ Leu Ala Ala — (R)-Ethyl piperidine-3-carboxylate |
| Prodrug 5 (HZ47) | Podophyllotoxin — Pro Ala Gly ▬ Leu Pro — GABA — Anthraquinone |
| Prodrug 6 (HZ54) | Anthraquinone — Pro Ala Gly ▬ Nva Pro — Baclofen |
| Prodrug 7 (HZ57) | Carboxyfluorescein — Pro Ala Gly ▬ Leu Pro — GABA — Anthraquinone |
| Prodrug 8 (HZ16) | Podophyllotoxin — Pro Ala Gly ▬ Leu Ala Ala — Anthraquinone |
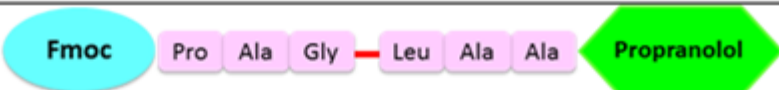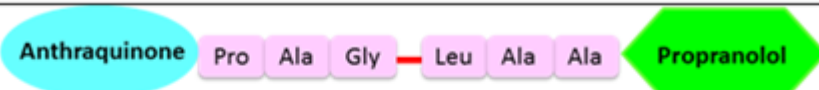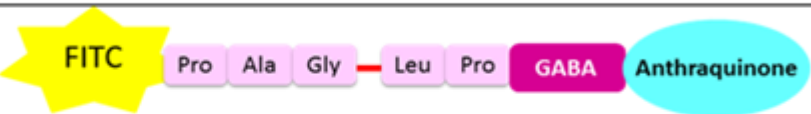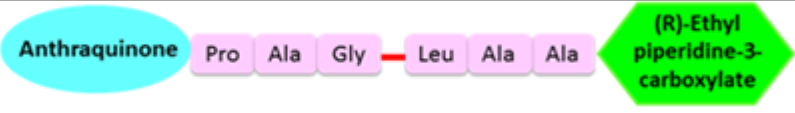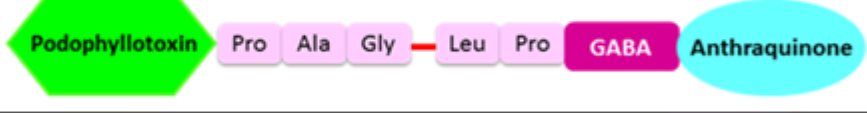
**Table 2.** Summary of selected synthesised MMP-9 activated prodrugs

Prodrugs 1 and 2 have the same active drug propranolol attached to the

hexapeptide substrate (Pro-Ala-Gly-Leu-Ala-Ala). The other side of the peptide was capped by Fmoc (Prodrug 1) or anthraquinone derivative (Prodrug 2). The difference between Prodrug 3 and 7 is the fluorescein compound which attached to the H-Pro-Ala-Gly-Leu-Pro-GABA-spacer-Anthraquinone conjugate. Prodrug 3 used the FITC while Prodrug 7 used 5(6)-Carboxyfluorescein. In Prodrug 4, the GABA antagonist (R)-ethyl piperidine-3-carboxylate was linked to the Anthraquinone-spacer- Pro-Ala-Gly-Leu-Ala-Ala-OH conjugate. Prodrug 5 has a capping group (anthraquinone derivative) and cytotoxic agent (podophyllotoxin) at two sides of peptide chain (Pro-Ala-Gly-Leu-Pro-GABA). The GABA agonist baclofen was attached to Anthraquinone-spacer-Pro-Ala-Gly-Nva-Pro-OH conjugate to form Prodrug 6.

Furthermore, fluorimetric assays evaluated and compared the MMP-9 cleavable substrates of different prodrugs in the HT1080 cancer cell line. The fluorescein labelled Prodrug 3 and 7 were selected for the assay. The results showed that the 5(6)-carboxyfluorescein labelled Prodrug 7 performed much better than the FITC labelled Prodrug 3 during the incubation with the same concentration of HT1080 tumour homogenate.

## 1.6 Structure Library
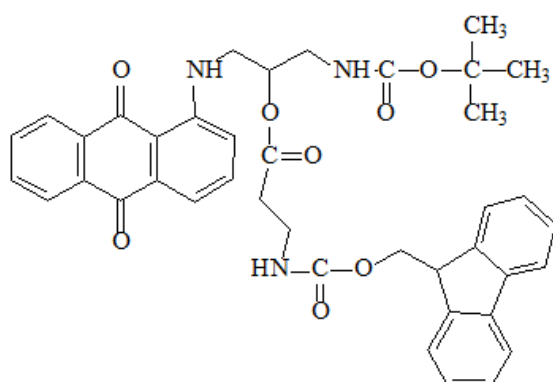
**Fmoc-Ala-[Boc-Spacer]-AQ (HZ26)**
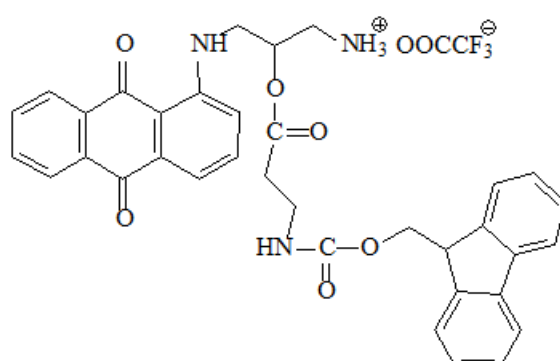
**H-Ala-Spacer-AQ TFA salt (HZ27)**
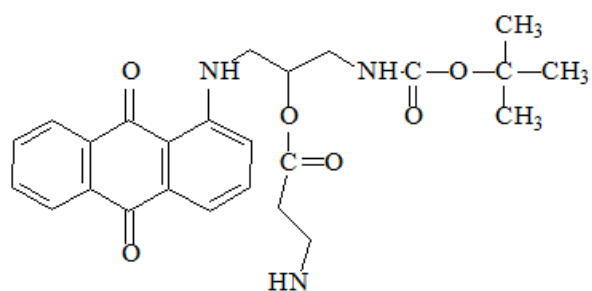
**H-Ala-[Boc-Spacer]-AQ (HZ28)**
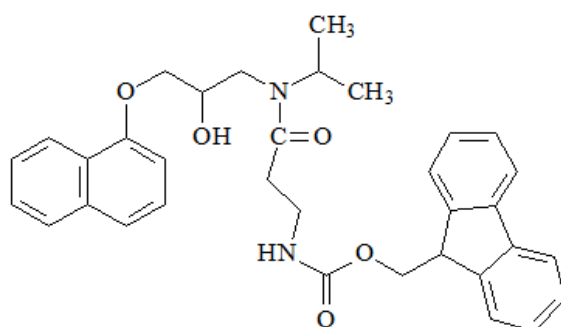
**Fmoc-Ala-Propranolol (HZ29)**
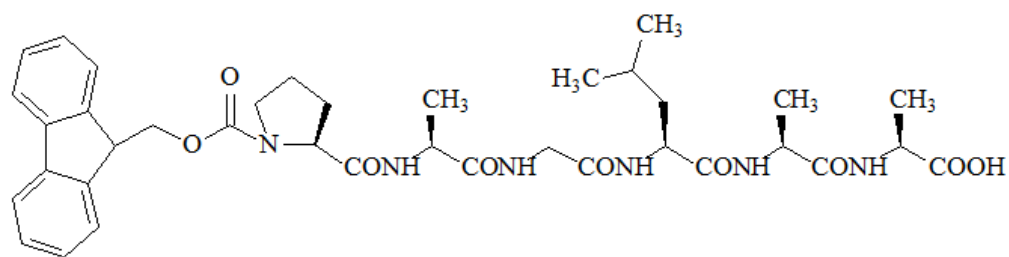
**Fmoc-Pro-Ala-Gly-Leu-Ala-Ala-OH (HZ31)**
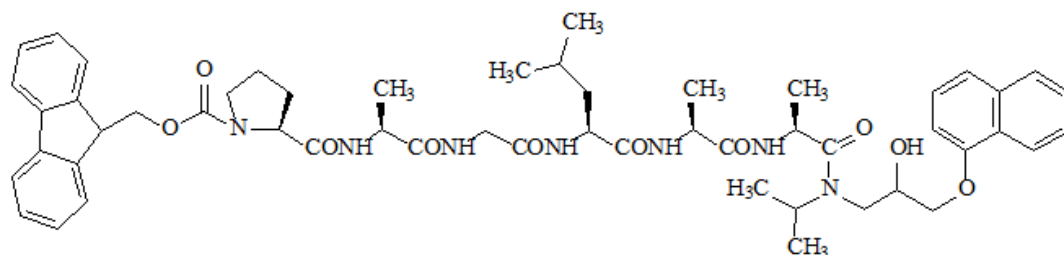


**Fmoc-Pro-Ala-Gly-Leu-Ala-Ala-Propranolol (HZ32)**
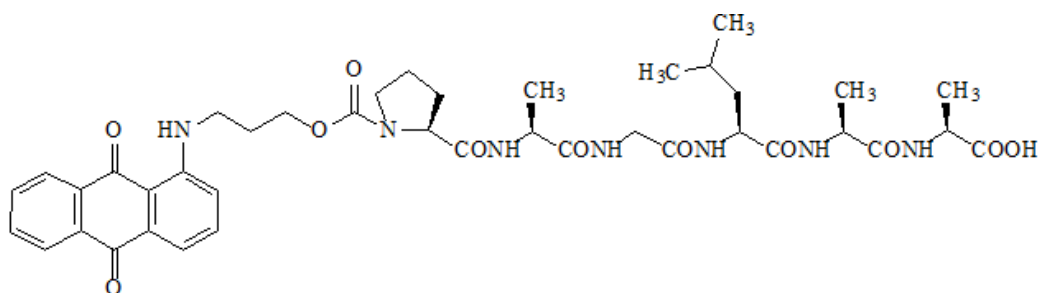


**AQ-Spacer--Pro-Ala-Gly-Leu-Ala-Ala-OH (HZ33)**
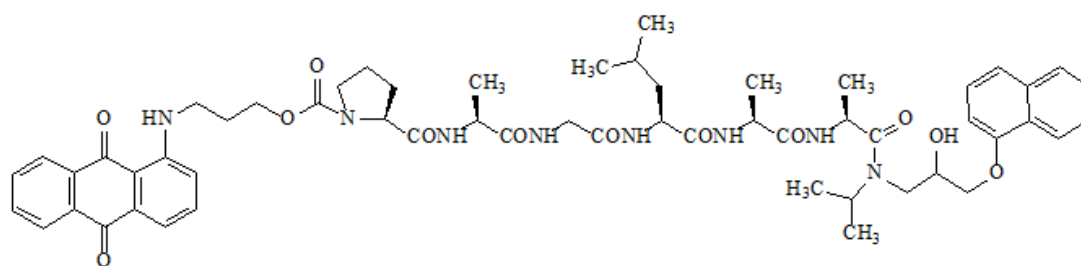


**AQ-Space-Pro-Ala-Gly-Leu-Ala-Ala-Propranolol (HZ34)**
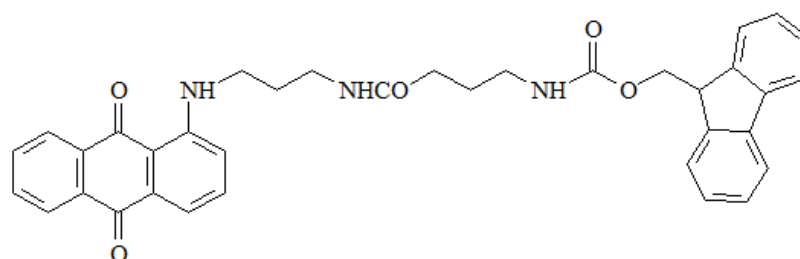


**Fmoc-GABA-[Propyl-spacer]-AQ (HZ35)**
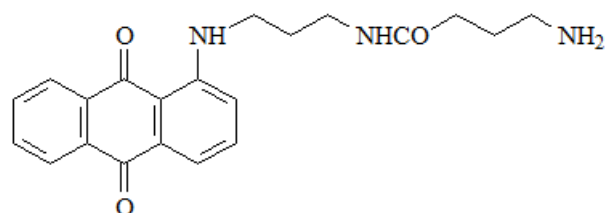
**H-GABA-[Propyl-spacer]-AQ (HZ36)**
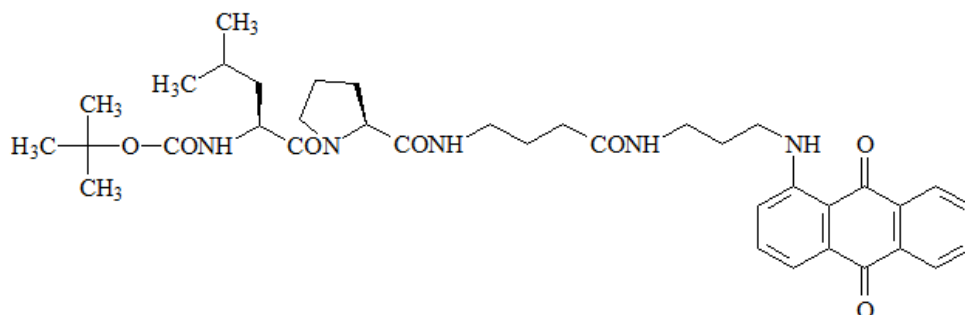


**Boc-Leu-Pro-GABA-[Propyl-spacer]-AQ (HZ37)**
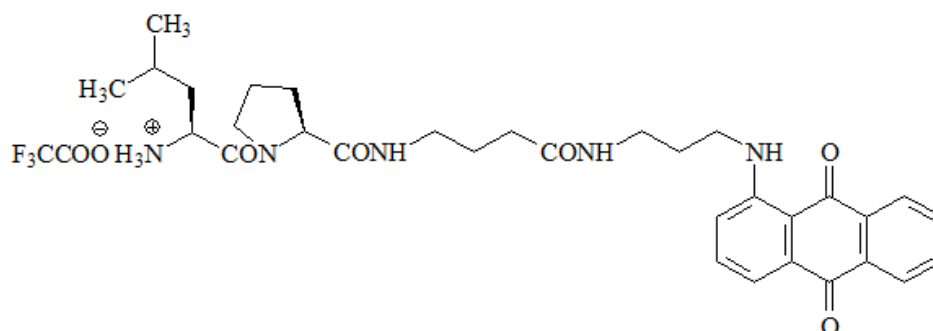


**H-Leu-Pro-GABA-[Propyl-spacer]-AQ TFA salt (HZ38)**
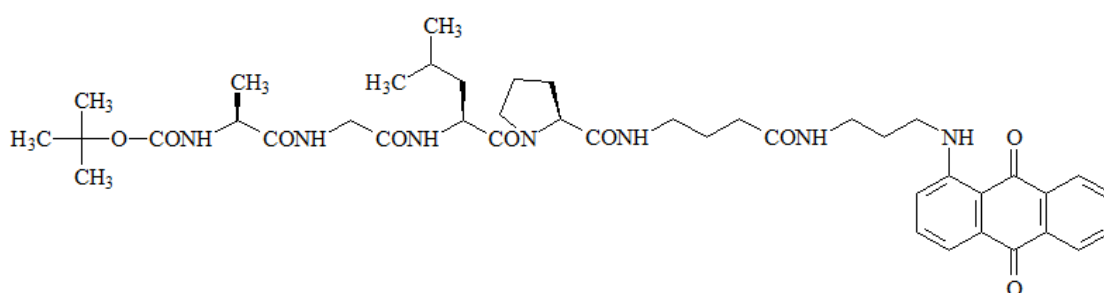


**Boc-Ala-Gly-Leu-Pro-GABA-[Propyl-spacer]-AQ (HZ39)**
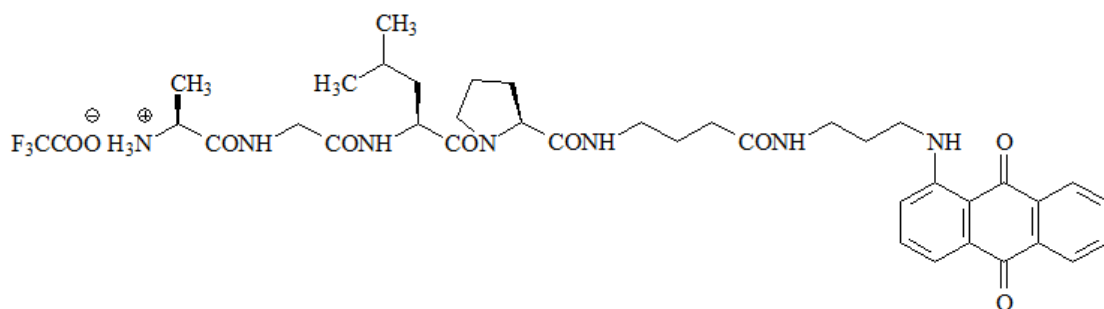
**H-Ala-Gly-Leu-Pro-GABA-[Propyl-spacer]-AQ TFA salt (HZ40)**
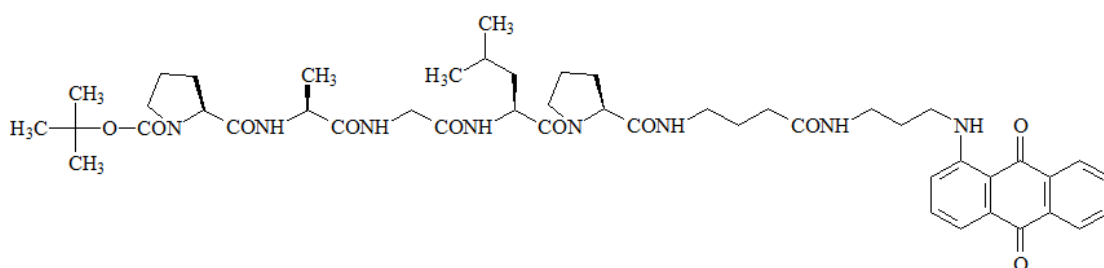


**Boc-Pro-Ala-Gly-Leu-Pro-GABA-[Propyl-spacer]-AQ (HZ41)**
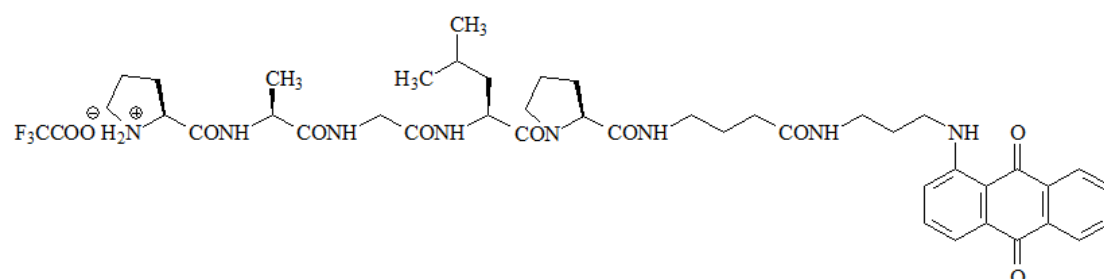


**H-Pro-Ala-Gly-Leu-Pro-GABA-[Propyl-spacer]-AQ TFA salt (HZ42)**
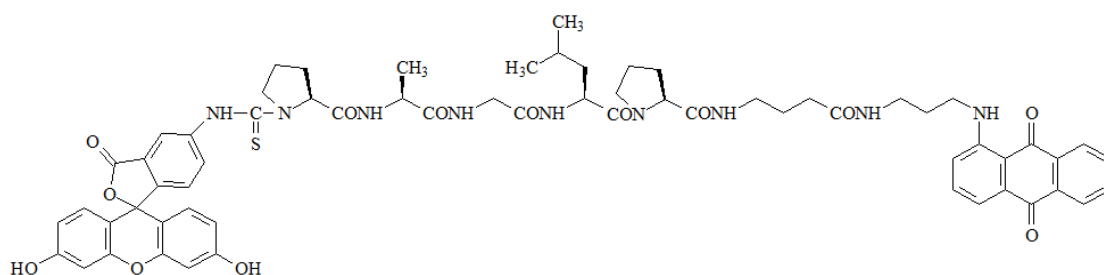


**FITC-Pro-Ala-Gly-Leu-Pro-GABA-[Propyl-spacer]-AQ (HZ43)**
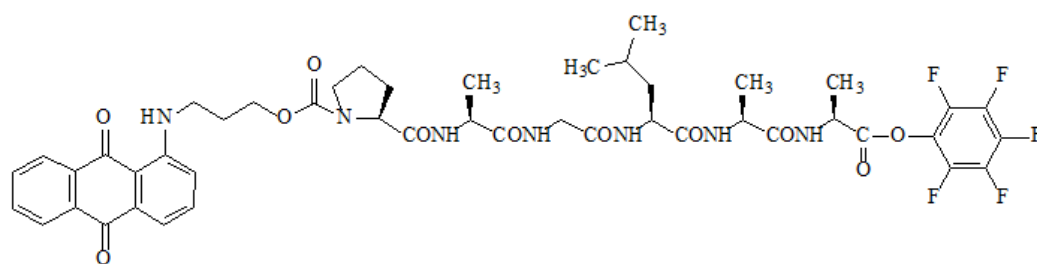


**AQ-[Propyl-spacer]-Pro-Ala-Gly-Leu-Ala-OPFP (HZ44)**
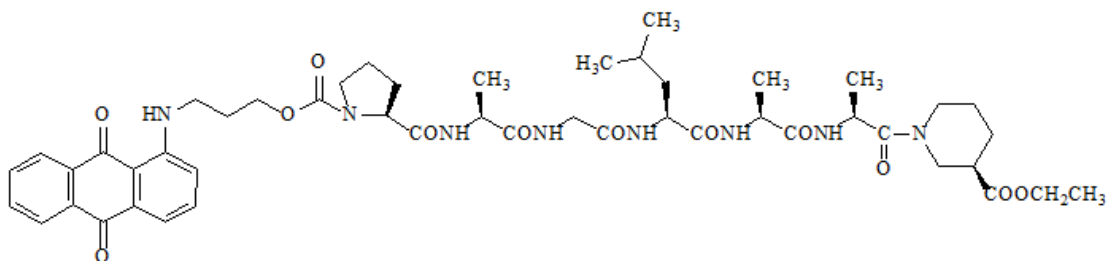
**AQ-[Propyl-spacer]-Pro-Ala-Gly-Leu-Ala-ethylpiperidine-3-carboxylate (HZ45)**
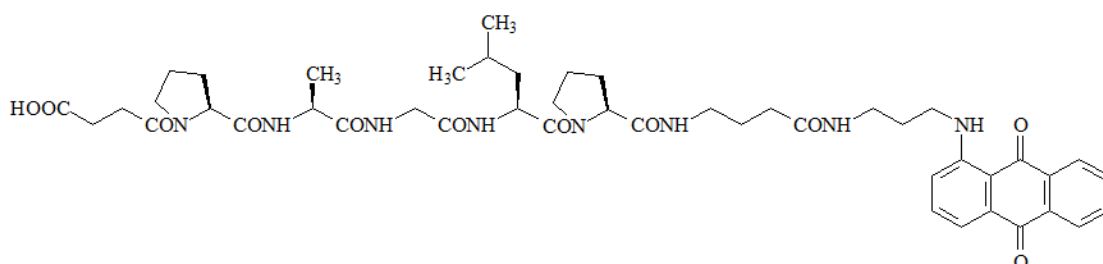


**Succinyl-Pro-Ala-Gly-Leu-Pro-GABA-[Propyl-spacer]-AQ (HZ46)**
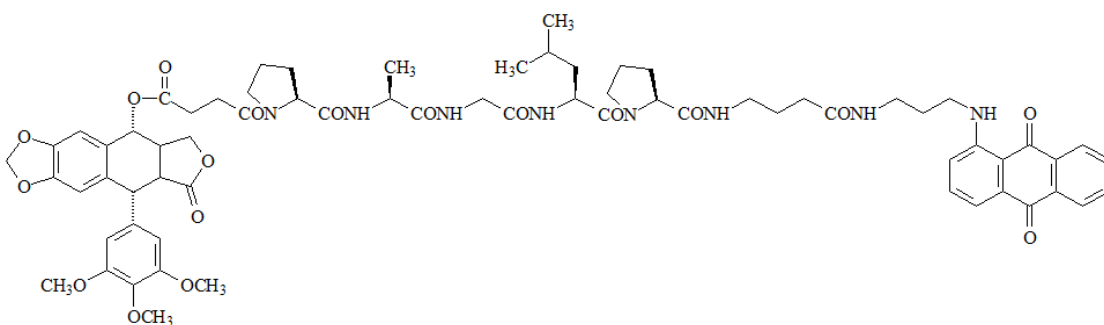


**Podophyllotoxin-Pro-Ala-Gly-Leu-Pro-GABA-[Propyl-spacer]-AQ (HZ47)**
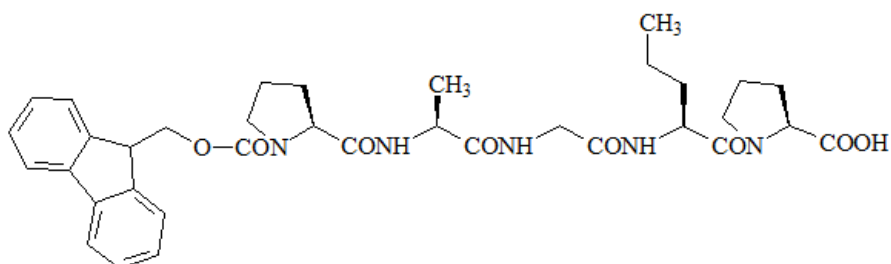


**Fmoc-Pro-Ala-Gly-Nva-Pro-OH (HZ51)**
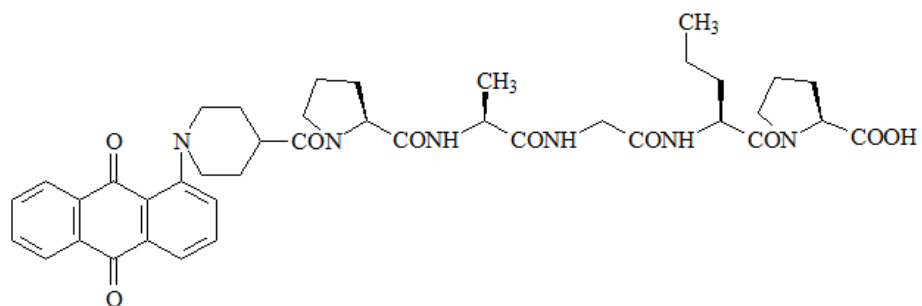
**AQ-Spacer-Pro-Ala-Gly-Nva-Pro-OH (HZ52)**
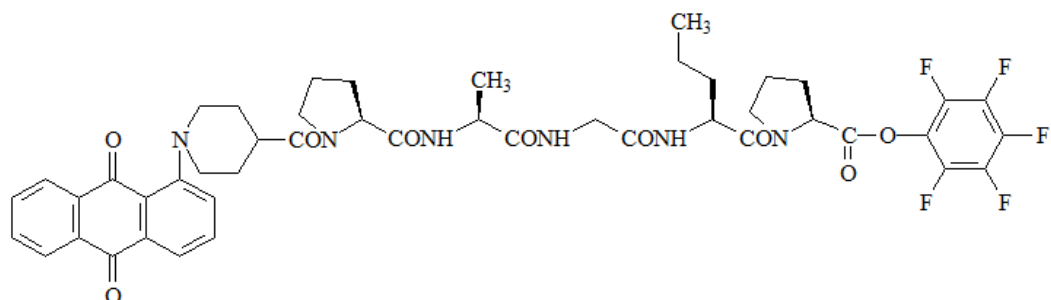


**AQ-Spacer-Pro-Ala-Gly-Nva-Pro-OPFP (HZ53)**
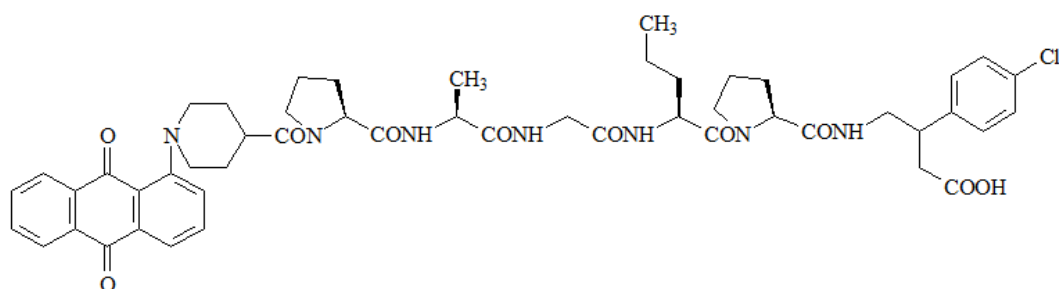


**AQ-Spacer-Pro-Ala-Gly-Nva-Pro-Baclofen (HZ54)**
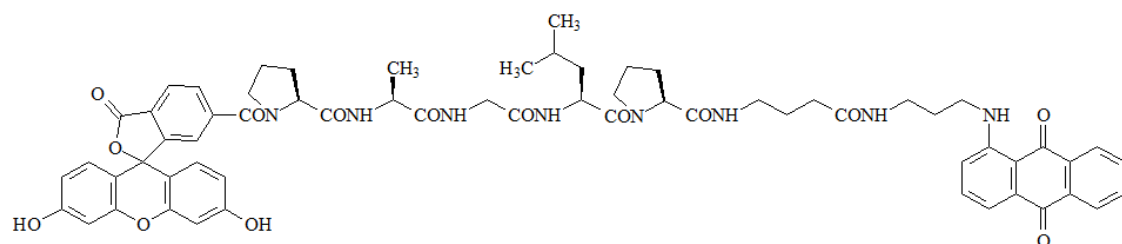


**5(6)-Carboxyfluorescein-Pro-Ala-Gly-Leu-Pro-GABA-[Propyl-spacer]-AQ (HZ57)**
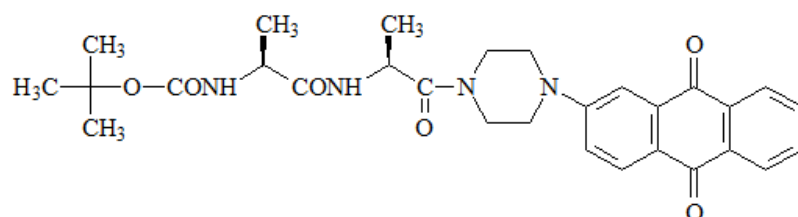


**Boc-Ala-Ala-Piperazinyl-AQ (HZ7)**
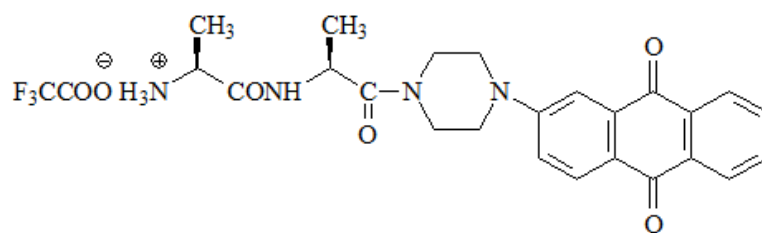
**H-Ala-Ala-Piperazinyl-AQ TFA salt (HZ8)**
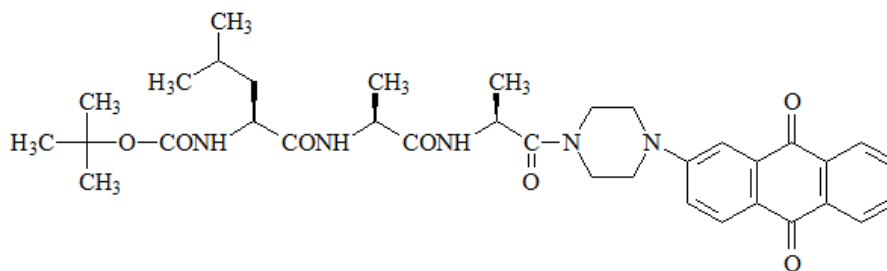


**Boc-Leu-Ala-Ala-Piperazinyl-AQ (HZ9)**
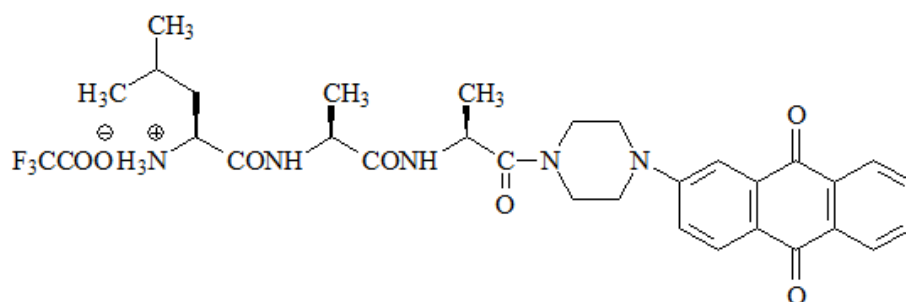


**H-Leu-Ala-Ala-Piperazinyl-AQ TFA (HZ10)**
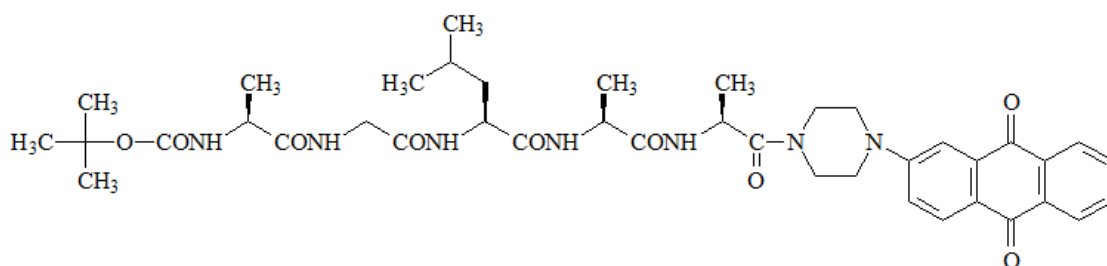


**Boc-Ala-Gly-Leu-Ala-Ala-Piperazinyl-AQ (HZ11)**
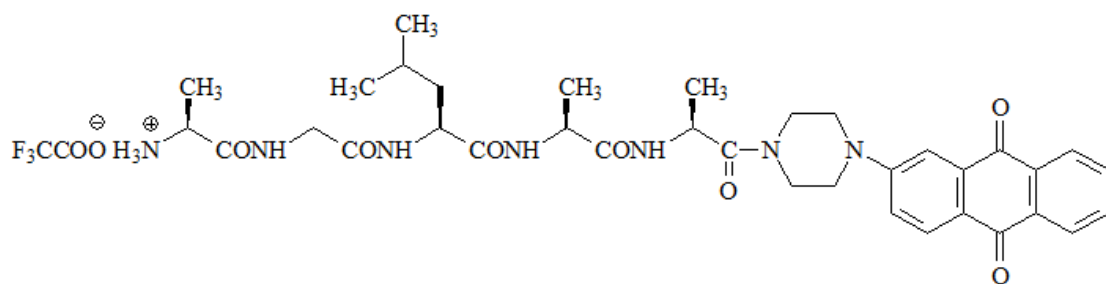
**H-Ala-Gly-Leu-Ala-Ala-Piperazinyl-AQ TFA salt (HZ12)**
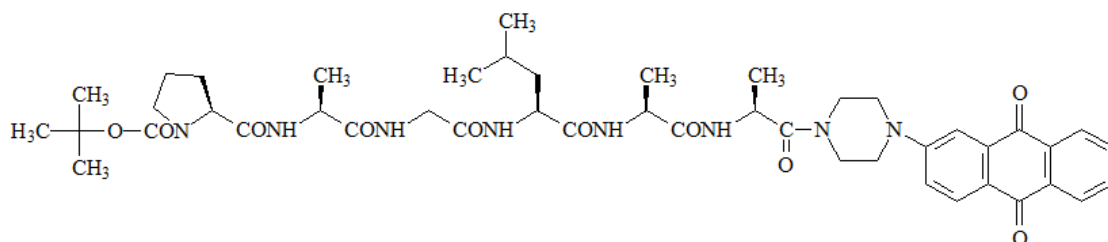


**Boc-Pro-Ala-Gly-Leu-Ala-Ala-Piperazinyl-AQ (HZ13)**
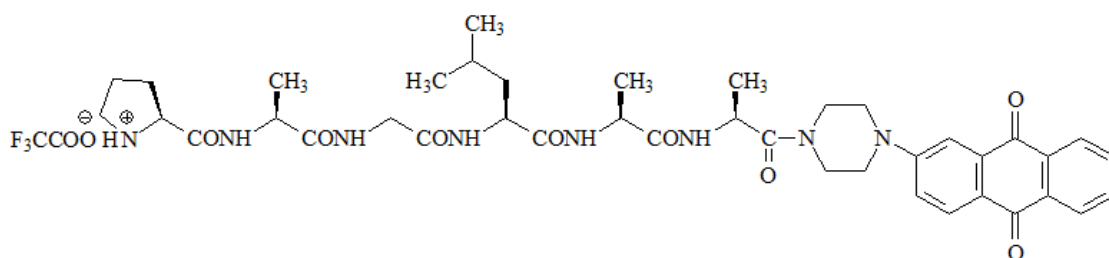


**H-Pro-Ala-Gly-Leu-Ala-Ala-Piperazinyl-AQ TFA salt (HZ14)**
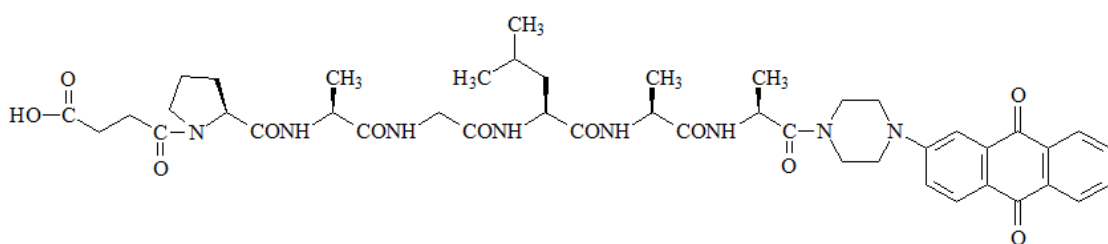


**Succinyl-Pro-Ala-Gly-Leu-Ala-Ala-Piperazinyl-AQ (HZ15)**
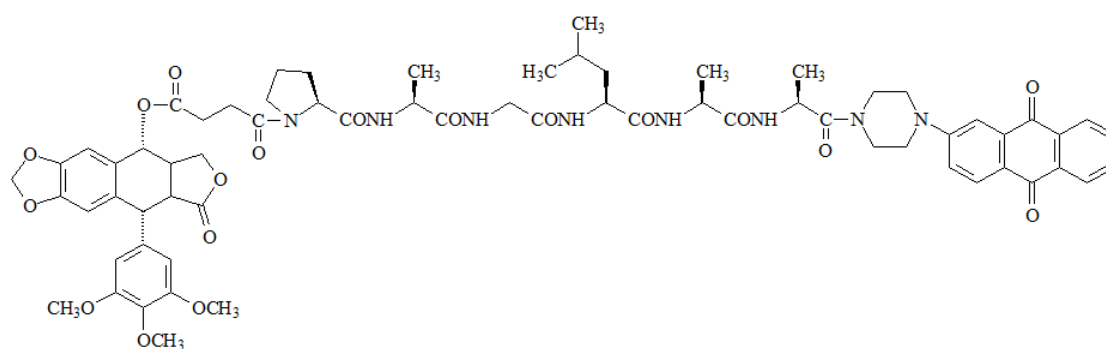


**Podophyllotoxin-Succinyl-Pro-Ala-Gly-Leu-Ala-Ala-Piperazinyl-AQ (HZ16)**

## 1.7 Experimental

## 1.7.1 General methods

## 1.7.1.1 Thin layer chromatography (TLC)

Kieselgel 60 $F_{254}$ pre-loaded aluminium sheets were used for the TLC test. The compounds with colour were self-evident. For colourless compounds, the TLC sheets needed to be placed under the UV light for spots visualization.

## 1.7.1.2 Thick TLC plate

100g of Silica gel 60 $PF_{254}$ and 300 ml of water were mixed well to make smooth slurry. The slurry was then spread onto 20×20 cm glass plates. The thickness of the absorbent silica gel was 1 mm. The plates were then put into the oven and heated at 60 °C for overnight. The plates were stored in a dry, cool and dark place.

Once the Thick TLC plate was used for the purification of compounds, the compounds were first dissolved in a very small volume of organic solution (such as chloroform and dichloromethane). The solution was applied onto the plate by using a Pipette. After the solution has completely dried, the plate was put into the container with the suitable running solvent (about 90 ml) and a cover glass was placed on the top of the container. When the solvent moved no higher than the top of the TLC plate, the plate was removed and dried. The product layer was collected.

## 1.7.1.3 Column chromatography

Silica gel 60 [Merck] mesh 43 – 60 was used for all column chromatography.

## 1.7.1.4 Mass spectrometry

The samples of synthesised pure prodrugs were analysed by the EPSRC

National Mass Spectrometry Service Centre at Swansea and the data was interpreted and compounds were characterized by the author.

### 1.7.1.5 Proton Nuclear Magnetic Resonance (1H NMR)

The samples were dissolved in either deuterated DMSO or deuterated chloroform and transferred to standard NMR testing tubes with a solution height range between 5 and 5.5cm. All experiments were performed by the author using a Bruker AC200 NMR Spectrometer (300 MHz) in Heriot-Watt University, Edinburgh.

### 1.7.2 Chemical synthesis of MMP-9 activated prodrugs

### 1.7.2.1 Synthesis of Boc-Ala-Ala-Piperazinyl-AQ (HZ7)

The compound NU: UB 341 (1 g, 3.4 mmol) and Boc-Ala-Ala-OH (980.54 mg, 3.7 mmol) were dissolved in DMF (10 ml), followed by the addition of TBTU (1209 mg, 3.7 mmol), HOBt (576 mg, 3.7 mmol), and DIPEA (1964.8 µl, 11.2 mmol, 0.742 g/ml). The mixture was left at RT overnight. Mini extraction (dichloromethane and water) was performed for the TLC ($R_f$ 0.714, dichloromethane-methanol 9:1) test. The product solution was extracted. The organic layer was added with anhydrous sodium sulphate and filtered. The filtrate was evaporated using rotary evaporator to a small volume and then performed the column chromatography (4.3 cm × 14.5 cm) with the dichloromethane-methanol 9:1 solvent system. The eluted product was filtered, evaporated to dryness and collected. The dried product was remained in the round bottomed flask for the next de-Boc reaction.

### 1.7.2.2 Synthesis of H-Ala-Ala-Piperazinyl-AQ TFA salt (HZ8)

TFA was added to the Boc-Ala-Ala-Piperazinyl-AQ (HZ7) until the solid was fully

dissolved. The solution was left at RT for 1.15 h. The product (R$_f$ 0.18, chloroform-methanol 9:1) solution was evaporated to dryness and triturated by 10 ml diethyl ether at 5 °C for 1 h. The mixture was filtered, dried and collected. Crude product yield: 1.83 g, 97%

$^1$H NMR spectrum (DMSO-d$_6$, 300 MHz) δ: 1.27 (3H, d, CH$_3$-ala); 1.35 (3H, d, CH$_3$-ala); 3.2-3.75 [11H, m, unresolved, 4×CH$_2$ (piperazine) and NH$_3$]; 3.88 (1H, q, NH$_3$-α-CH); 4.85 (1H, quint, CONH-α-CH); 7.35 (1H, d, H-3 AQ); 7.5 (1H, s, H-1); 7.9 (2H, m, H-6 and H-7 AQ); 8.08 (1H, d, H-4); 8.18 (2H, m, H-5 and H-8 AQ); 8.7 (1H, d, NHCO)

## 1.7.2.3 Synthesis of Boc-Leu-Ala-Ala-Piperazinyl-AQ (HZ9)

The crude H-Ala-Ala-Piperazinyl-AQ TFA salt HZ8 (1.8 g, 3.3 mmol) and Boc-Leu-OSu (1.2 g, 3.4 mmol) were dissolved in DMF (10 ml). DIPEA (1.2 ml, 6.6 mmol, 0.742 g/ml) were added to the solution and left at RT for 3 h. The product (R$_f$ 0.52, chloroform-methanol 9:1) solution was extracted (chloroform and water). The organic layer was filtered, evaporated to dryness and kept in the 250ml round bottomed flask for the next de-Boc reaction.

## 1.7.2.4 Synthesis of H-Leu-Ala-Ala-Piperazinyl-AQ TFA salt (HZ10)

The 250ml round bottomed flask containing Boc-Leu-Ala-Ala-Piperazinyl-AQ (HZ9) was added by TFA until the solid had completely dissolved and reacted at RT for 1.5 h. The product (R$_f$ 0.12, chloroform-methonal 10:1) solution was evaporated to dryness by rotational evaporator. About diethyl ether (10 ml) to precipitate the product at 5 °C for 1 h and the mixture was then filtered, dried and collected. Yield: 1.5 g, 70%.

### 1.7.2.5 Synthesis of Boc-Ala-Gly-Leu-Ala-Ala-Piperazinyl-AQ (HZ11)

H-Leu-Ala-Ala-Piperazinyl-AQ TFA salt HZ10 (1.5 g, 2.3 mmol) and Boc-Ala-Gly-OSu (0.9 g, 2.5 mmol) were dissolved in DMF (10 ml), followed by the addition of DIPEA (800 μl, 4.6 mmol, 0.742 g/ml) and reacted at RT overnight. The reaction was not completed, and Boc-Ala-Gly-OSu (0.79 g, 2.3 mmol) and DIPEA (0.742 g/ml, 400 μl, 2.3 mmol) were added and left at RT for 5 h. The product ($R_f$ 0.44, dichloromethane-methanol 9:1) mixture was extracted (chloroform and water), the organic layer was combined, dried (anhydrous sodium sulphate), filtered, evaporated to dryness for the next reaction.

### 1.7.2.6 Synthesis of H-Ala-Gly-Leu-Ala-Ala-Piperazinyl-AQ TFA salt (HZ12)

TFA was added to the Boc-Ala-Gly-Leu-Ala-Ala-Piperazinyl-AQ (HZ11) in the round bottomed flask until solid was fully dissolved and reacted at RT for 1.5 h. The product ($R_f$ 0.18, dichloromethane-methonal 9:1) solution was evaporated (a few drops of methanol was added to help evaporation) and triturated by diethyl ether (10 ml) at 5 °C for 1 h. The mixture was filtered, evaporated to dryness and collected. Yield: 1.5 g, 83%.

### 1.7.2.7 Synthesis of Boc-Pro-Ala-Gly-Leu-Ala-Ala-Piperazinyl-AQ (HZ13)

The Boc-deprotected dipeptide anthraquinone spacer compound (1.5 g, 1.9 mmol) was dissolved in DMF (10 ml), Boc-Pro-OH (0.5 g, 2.1 mmol), TBTU (0.7 g, 2.1 mmol), HOBt (0.3 g, 2.1 mmol), and DIPEA (1.1 ml, 2.1 mmol, 0.742 g/ml) were added to the solution and left at RT for 1 h. The product ($R_f$ 0.4, dichloromethane-methanol 9:1) solution was extracted (dichloromethane and water). The organic layer was collected, dried (anhydrous sodium sulphate), filtered and evaporated to a small volume for the column chromatography purification (4.3 × 17.5 cm) using dichloromethane-methanol 10:1 solvent

system. The eluted solution was filtered to remove silica gel and then evaporated to dryness and kept in the 250 ml round bottomed flask for the de-Boc reaction.

**1.7.2.8 Synthesis of H-Pro-Ala-Gly-Leu-Ala-Ala-Piperazinyl-AQ TFA salt (HZ14)**

TFA was added to the round bottomed flask which contained Boc-Pro-Ala-Gly-Leu-Ala-Ala-Piperazinyl-AQ (HZ13) until the solid was completely dissolved and the mixture was left at RT for 1 h. The product ($R_f$ 0.1, dichloromethane-methanol 9:1) solution was evaporated to dryness and added with 10 ml diethyl ether. The mixture was cooled at 5 °C for 1.5 h and then filtered, dried and collected. Yield: 1.5 g, 89%.

**1.7.2.9 Synthesis of Succinyl-Pro-Ala-Gly-Leu-Ala-Ala-Piperazinyl-AQ (HZ15)**

H-Pro-Ala-Gly-Leu-Ala-Ala-Piperazinyl-AQ TFA salt HZ14 (300 mg, 0.34 mmol) and succinic acid (50.8 mg, 0.5 mmol) were dissolved in DMF (5 ml), followed by the addition of DIPEA (147.2 µl, 0.85 mmol, 0.742 g/ml) to the solution and reacted at RT over weekend. The product ($R_f$ 0.4, dichloromethane-methanol 6:1; $R_f$ 0.64, butanol-acetate acid-water 4:5:1) solution was extracted, evaporated to a low volume and purified by column chromatography (2.3 cm × 15.6 cm) using dichloromethane-methanol 6:1 solvent system. The product fraction was combined, filtered and evaporated to dryness by rotary evaporator. The product paste was re-dissolved by addition of small volume of ethanol and diethyl ether (10 ml) in a 25 ml round bottomed flask to precipitate the solid product. The solution mixture was cooled at 5 °C for 2 h, filtered, dried in the desiccator, and collected. Yield: 98.7 mg, 33%.

ESMS (+): 871 m/z (100%) (M-H)⁻

## 1.7.2.10 Synthesis of

## Podophyllotoxin-Succinyl-Pro-Ala-Gly-Leu-Ala-Ala-Piperazinyl-AQ (HZ16)

Succinyl-Pro-Ala-Gly-Leu-Ala-Ala-Piperazinyl-AQ HZ15 (90 mg, 0.1 mmol) was dissolved in DMF (2.5 ml) and acetonitrile (2.5 ml), podophylotoxin (43 mg, 0.1 mmol), TBTU (33.13 mg, 0.1 mmol) and TEA (28.7 µl, 0.2 mmol, 0.727 g/ml) were added to the solution and reacted at RT overnight. The TLC showed the reaction was not complete. Additional podophylotoxin (21.37mg, 0.05 mmol), TBTU (16.57 mg, 0.05 mmol) and TEA (14.35 µl, 0.05 mmol, 0.727 g/ml) were added to the solution and left at RT for 5 h. There was solid present in the solution, so the solution was filtered. The solid was orange coloured and was dissolved by chloroform. The filtrate was combined with the dissolved solid and transferred to an evaporating basin and left to dryness overnight. The product was collected and checked by TLC for purity. However, some product had gone back to the starting material. The solid was dissolved in chloroform and added with anhydrous sodium sulphate. The solution was filtered and evaporated to dryness. Acetonitrile (3 ml) was added to dissolve the solid. The reagents, (21.37mg, 0.05 mmol), TBTU (16.57 mg, 0.05 mmol) and TEA (14.35 µl, 0.1 mmol, 0.727 g/ml) were added to the solution and reacted at RT overnight. The product ($R_f$ 0.74, dichloromethane-methanol 8:1) solution was evaporated to dryness, dissolved by chloroform in a very low volume and applied to a thick TLC (90 ml of dichloromethane-methanol (8:1) solvent) plate for purification. The product layer was collected, dissolved in ethanol, filtered and evaporated to dryness in vacuo. 10 ml of diethyl ether was added and the mixture was cooled in 5°C for 1 h. The product was precipitated in ether and the mixture was filtered,

dried in a desiccator and collected. Yield: 57.5 mg, 45%

ESMS (+): 1286 m/z (100%) (M+NH$_4$)$^+$

**1.7.2.11 Synthesis of Fmoc-Ala-[Boc-Spacer]-AQ (HZ26)**

The AQ-spacer-Boc NU: UB 491 (500 mg, 1.26 mmol) was reacted with Fmoc-Ala-OH (432 mg, 1.4 mmol) in dichloromethane (30 ml). DCC (313 mg, 1.5 mmol) and DMAP (15.4 mg, 0.13 mmol) were added and the reaction mixture was stirred for 1 h. The precipitated dicyclohexylurea (DCU) was filtered off and the filtrate was washed with water. The dichloromethane extract was combined, dried by sodium sulfate, and evaporated to dryness. The crude solid was purified by column chromatography using the eluting solvent, dichloromethane: ethyl acetate 7:1. The appropriate fractions were combined, filtered and evaporated to dryness. Diethyl ether was added to precipitate the solid product. The mixture was cooled at 5°C for 1 h. Yield: 392 mg, 45%.

$^1$H NMR spectrum (CDCl$_3$, 300 MHz) δ: 1.48 [(9H, s, CH$_3$ (Boc)]; 1.7 (1H, s); 2.7 (2H, t, AQ-NH-CH$_2$-CH-OCO-CH$_2$); 3.4-3.7 (6H, m, AQ-NH-CH$_2$-CH-CH$_2$ and AQ-NH-CH$_2$-CH-OCO-CH$_2$-CH$_2$); 4.15 [(1H, t, α-CH (Fmoc)]; 4.35 [(2H, d, CH$_2$ (Fmoc)]; 5.0 (1H, s, AQ-NH-CH$_2$-CH); 5.3 (1H, t, NHCO-Boc); 5.79 (1H, s, NHCO-Fmoc); 7.15 (1H, d, H-2); 7.4 (2H, t, H-3 and H-4); 7.5-7.63 (2H, t, H-6 and H-7); 7.63-7.78 [8H, m, CH (Fmoc)]; 8.12 (1H, d, H-5); 8.18 (1H, d, H-8); 9.9 (1H, t, AQ-NH).

**1.7.2.12 Synthesis of H-Ala-Spacer-AQ trifluoroacetate salt (HZ27)**

Fmoc-Ala-[Boc-Spacer]-AQ HZ26 (60 mg, 0.15 mmol) was transferred into a round bottomed flask. TFA was added until all solid dissolved. The reaction was

completed after 10 min. The solution was evaporated to dryness. Diethyl ether was added to precipitate the product. Yield: 50 mg, 98%.

$^1$H NMR spectrum (DMSO-d$_6$, 300 MHz) δ: 2.4-2.65 (2H, t, AQ-NH-CH$_2$-CH-OCO-CH$_2$); 3.05-3.3 (4H, m, AQ-NH-CH$_2$-CH-CH$_2$); 3.3-3.6 (2H, m, CH$_2$-NH-Fmoc); 3.6-3.8 [(1H, t, H-9 (Fmoc)]; 4.1-4.4 [(2H, m, CH$_2$ (Fmoc)]; 5.2 (1H, s, AQ-NH-CH$_2$-CH); 7.2-7.5 [(7H, m, unresolved, H-2(AQ), H-1, H-2, H-4, H-5, H-7 and H-8 (Fmoc)]; 7.5-7.72 (2H, m, H-3 and H-4); 7.73-7.95 [(4H, m, H-3 and H-4 (AQ), H-3 and H-6 (Fmoc)]; 7.95-8.08 (2H, m, H-6 and H-7); 8.08-8.26 (2H, m, H-5 and H-8); 9.75 (1H, t, AQ-NH).

### 1.7.2.13 Synthesis of H-Ala-[Boc-Spacer]-AQ (HZ28)

Fmoc-Ala-AQ HZ26 (150 mg 0.38 mmol) was dissolved in 4 ml of 2% piperidine in DMF. The reaction was completed in 30 min at RT by checking the TLC (R$_f$ 0.17, dichloromethane-methanol 9:1). The reaction solution was purified by extraction (dichloromethane and water) and column chromatography (chloroform-methanol 8:1). The product was collected in an evaporating basin. Yield: 70 mg, 69%.

$^1$H NMR spectrum (DMSO-d$_6$, 300 MHz) δ: 1.4 [(9H, s, CH$_3$ (Boc)]; 2.38-2.52 (2H, m, CH-OCO-CH$_2$); 3.05-3.8 (6H, m, AQ-NH-CH$_2$-CH-CH$_2$ and CH$_2$-NH$_2$); 5.05 (1H, m, AQ-NH-CH$_2$-CH); 7.15-7.25 (1H, t, NHCO); 7.35 (1H, d, H-2); 7.4-7.5 (1H, d, H-4); 7.6-7.7 (1H, t, H-3); 7.8-7.95 (2H, m, H-6 and H-7); 8.12 (1H, d, H-8); 8.2 (1H, d, H-5); 9.78 (1H, t, AQ-NH).

### 1.7.2.14 Synthesis of Fmoc-Ala-Propranolol (HZ29)

Propranolol hydrochloride (1 g, 3.4 mmol) and Fmoc-β-Ala-OH (1.26 g, 4.1 mmol)

were dissolved in 20ml DMF, followed by the addition of TBTU (1.3 g, 4.1 mmol), HOBt (621 mg, 4.1 mmol), and DIPEA (2.7 ml, 16 mmol). The reaction was completed overnight. The crude product ($R_f$ 0.48, dichloromethane- ethyl acetate 1:1) was extracted by dichloromethane and water, dichloromethane/aqueous citric acid and dichloromethane/aqueous sodium bicarbonate. Further purification was done by column chromatography (dichloromethane- ethyl acetate 1:1). The product was dried under vacuum. Yield: 271mg, 14%.

<u>$^1$H NMR spectrum (DMSO-d$_6$, 300 MHz)</u> δ: 1.2-1.45 (6H, dd, C<u>H</u>$_3$); 2.6-2.8 (2H, m, NCO-C<u>H</u>$_2$); 3.5-3.87 [(3H, m, NCO-CH$_2$-C<u>H</u>$_2$ and H-9 (Fmoc)]; 4.05-4.2 (1H, m, C<u>H</u>-CH$_3$); 4.2-4.35 [(4H, m, O-C<u>H</u>$_2$-CH-C<u>H</u>$_2$ (propranolol)]; 4.35-4.45 [(2H, m, C<u>H</u>$_2$ (Fmoc)]; 5.63 [(1H, m, O-CH$_2$-C<u>H</u> (propranolol)]; 6.9 [1H, d, H-2 (propranolol)]; 7.28-7.58 [8H, m, unresolved, H-1, H-2, H-3, H-4, H-5, H-6, H-7 and H-8 (Fmoc)]; 7.6-7.7 [2H, m, H-3 and H-4 (propranolol)]; 7.7-7.9 [4H, m, H-5, H-6, H-7 and H-8 (propranolol)]; 8.25 (1H, d, O<u>H</u>)

## 1.7.2.15 Synthesis of Fmoc-Pro-Ala-Gly-Leu-Ala-Ala-OH (HZ31)

Fmoc-Ala-Wang resin (1 g, 0.72 mmol/g) was used for the SPPS. The resin (1 g) was transferred into a SPPS reaction vessel, added with dichloromethane (10 ml) for swelling the beads and shaken at RT, 650 rpm for 1.5 h. The dichloromethane was drained off and the resin was washed with DMF three times (2 min, 5 ml for each time). Fmoc was removed by the addition of 5 ml of 20% piperidine in DMF to the vessel and shaken for 15 min at RT. This step was repeated for 3 times. The resin was washed with DMF 3 times.

A solution of Fmoc-Ala-OH (448.3 mg, 1.44 mmol), TBTU (439.2 mg, 1.4 mmol), HOBt (209.3 mg, 1.4 mmol) and DIPEA (500.7 µl, and 2.9 mmol, 0.742 g/ml) were dissolved in DMF (20 ml). The solution (10 ml) was transferred into the

vessel and shaken for 30 min. After 30 min, the solution was drained off. Another 10ml stock solution was added and shaken for 30 min. The resin was then Fmoc deprotected for the coupling reaction with next amino acid. The rest of the Fmoc protected amino acids were coupled by the same procedure as above in the order of: Fmoc-Leu-OH (509 mg, 1.44 mmol), Fmoc-Gly-OH (428 mg, 1.44 mmol), Fmoc-Ala-OH (560 mg, 1.8 mmol), and Fmoc-Pro-OH (607.5 mg, 1.8 mmol). Colour test was performed for Fmoc deprotection and amino acid coupling reaction.

TFA (20 ml, 95%) in dichloromethane was prepared. 2-3 ml of the solution was added to the vessel and shaken at RT for 3 min. The solution was drained off and the procedure was repeated for 9 times. The resin was then washed with dichloromethane (×2), methanol (×2), and dichloromethane (×1). All the filtrates and cleavage fractions were combined, transferred into a round bottomed flask and evaporated to a small volume using a rotary evaporator. About 30 ml of diethyl ether was added to precipitate the white solid HZ31 at 5 °C for 1 h. The mixture was filtered and the product was dried in a desiccator. Yield: 176 mg, 34%.

## 1.7.2.16 Synthesis of Fmoc-Pro-Ala-Gly-Leu-Ala-Ala-Propranolol (HZ32)

Fmoc-Pro-Ala-Gly-Leu-Ala-Ala-OH HZ31 (106 mg, 0.15 mmol) was dissolved in DMF (20 ml), propranolol hydrochloride (48 mg, 0.17 mmol), TBTU (52 mg, 0.17 mmol), HOBt (25 mg, 0.17 mmol), and DIPEA (0.742 g/ml, 110 µl, 0.65 mmol) were added to the solution and reacted at RT overnight. The product ($R_f$ 0.43, dichloromethane-ethyl acetate-ethanol 7:2:1) solution was extracted (dichloromethane/ water, dichloromethane/aqueous citric acid, and dichloromethane/aqueous sodium bicarbonate). The organic layer was collected, dried by anhydrous sodium sulphate, filtered and evaporated to a small volume

for the column chromatography purification using dichloromethane-ethyl acetate-ethanol 9:2:1 solvent system. The pure fractions were combined, filtered, evaporated, and precipitated in diethyl ether (10 ml). The white solid product was collected by centrifuging. Yield: 13 mg, 9%.

ESMS (+): 962 m/z (100%) $(M+H)^+$

### 1.7.2.17 Synthesis of AQ-Spacer--Pro-Ala-Gly-Leu-Ala-Ala-OH (HZ33)

The anthraquinone derivative HB8 (64.3 mg, 0.14 mmol) was dissolved in 4ml DMF. The solution was transferred into the SPPS reaction vessel which contained approximate 0.14 mmol of de-Fmoc hexapeptide on resin (HZ31). DIPEA (25 µl, 0.14 mmol) was also added. The mixture was shaken for 1 hour. The resin was washed with DMF 2 time and added with another portion of 64.3mg HB8 and 25µl DIPEA, continued shaking for 1 h. The resin was washed with DMF (×5) and dichloromethane (×3). 15ml of 87% TFA in dichloromethane was measured in a 25ml cylinder. About 2ml solution was added to the resin and shaken for 3-4min. The solution was drained off into a small beaker. This step was repeated 5 times and all fractions were checked by TLC The resin was washed with dichloromethane (×2), methanol (×1), and dichloromethane (×2). All filtrates and fractions were combined and transferred to a round bottomed flask. The solution was evaporated to a small volume and added with diethyl ether (50 ml). The flask was put into fridge at 5°C for cooling overnight. The product was collected by filtration and dried in a desiccator. Yield: 256.8 mg, 98%

### 1.7.2.18 Synthesis of AQ-Space-Pro-Ala-Gly-Leu-Ala-Ala-Propranolol (HZ34)

AQ-Space-Pro-Ala-Gly-Leu-Ala-Ala-OH HZ33 (150 mg, 0.19 mmol) was

dissolved in 60 ml DMF, propranolol hydrochloride (61 mg, 0.21 mmol), TBTU (65.8 mg, 0.21 mmol), HOBt (31.3 mg, 0.21 mmol), and DIPEA (0.742 g/ml, 107 µl, 0.21 mmol) were added to the solution and left to react at RT for 4 hour. The crude product ($R_f$ 0.6, dichloromethane-methanol 9:1) was extracted with dichloromethane/water, dichloromethane/aqueous citric acid, and dichloromethane/aqueous sodium bicarbonate. The organic layers were combined, dried by anhydrous sodium sulphate, evaporated to a low volume and purified by column chromatography (2.1 cm × 11 cm) using dichloromethane ethanol 10:1 eluting solvent. The pure product fractions were combined, filtered and evaporated to dryness by rotational evaporator. The red solid product was precipitated in diethyl ether and the mixture was filtered, dried in a desiccator and collected. Yield: 24 mg, 12%.

ESMS (+): 1069 m/z 100% (M+Na)$^+$

### 1.7.2.19 Synthesis of Fmoc-GABA-[Propyl-spacer]-AQ (HZ35)

The AQ-propyl spacer NU: UB 197 (1500 mg, 5.36 mmol) was dissolved in 50 ml DMF, Fmoc-γaminobutyric acid (2100 mg, 6.4 mmol), TBTU (2100 mg, 6.4 mmol), HOBt (984 mg, 6.4 mmol) and DIPEA (0.742 g/ml, 3.4 ml, 10.7 mmol) were added to the solution and reacted at RT for 1 hour. The crude product ($R_f$ 0.64, dichloromethane-methanol 9:1) solution was poured into water to get red solid precipitate. Further purification was done by column chromatography (dichloromethane-methanol 10:1). The pure fractions were combined, filtered and poured into an evaporating basin. Yield: 2880 mg. 91%.

$^1$H NMR spectrum (DMSO-d$_6$, 300 MHz) δ: 1.7-1.85 (2H, m, AQ-NH-CH$_2$-C$\underline{H}_2$); 2.05-2.15 (2H, m, NHCO-CH$_2$-C$\underline{H}_2$); 2.9-3.05 (2H, m, NHCO-C$\underline{H}_2$); 3.1-3.45 (7H,

m, N<u>H</u>-Fmoc, AQ-NH-C<u>H</u>$_2$-CH$_2$-C<u>H</u>$_2$ and NHCO-CH$_2$-CH$_2$-C<u>H</u>$_2$); 4.17-4.25 [1H, t, H-9 (Fmoc)]; 4.25-4.33 [2H, d, C<u>H</u>$_2$ (Fmoc)]; 7.2-7.48 [(6H, m, unresolved, H-3 (AQ), N<u>H</u>CO, H-1, H-2, H-7 and H-8 (Fmoc)]; 7.6-7.72 [(3H, m, H-4 (AQ), H-4 and H-5 (Fmoc)]; 7.8-7.98 [(4H, m, H-6 and H-7 (AQ), H-3 and H-6 (Fmoc)]; 8.1-8.17 (1H, m, H-8 AQ); 8.17-8.25 (1H, m, H-5 AQ); 9.73 (1H, t, AQ-N<u>H</u>)

### 1.7.2.20 Synthesis of H-GABA-[Propyl-spacer]-AQ (HZ36)

Fmoc-GABA-[Propyl-spacer]-AQ HZ35 (1100 mg, 1.9 mmol) was suspended in 20ml of 20% piperidine in DMF at RT for 1.5 hours. The crude product (Rf 0.14, butanol-acetic acid-water 15:4:1) was extracted with dichloromethane and water. The organic layers were combined, dried by sodium sulfate, evaporated to a small volume and added with diethyl ether. The red precipitate was collected in vacuum. Yield: 400 mg, 59%.

### 1.7.2.21 Synthesis of Boc-Leu-Pro-GABA-[Propyl-spacer]-AQ (HZ37)

H-GABA-[Propyl-spacer]-AQ HZ36 (400 mg, 1.1 mmol) was reacted with Boc-Leu-Pro-OH (396 mg, 1.2 mmol) in DMF by addition of the reagents TBTU (387 mg, 1.2 mmol), HOBt (184 mg, 1.2 mmol), and DIPEA (0.742 g/ml, 629 µl, 3.3 mmol). The reaction had completed in 1 hour 20 min by checking the TLC ($R_f$ 0.6, dichloromethane methanol 5:1). The reaction solution was extracted by dichloromethane and water. The crude product was then purified by column chromatography (3.2 cm × 15.5 cm). The eluting solvent system dichloromethane to methanol 12:1 was used. The appropriate fractions were combined and dried in the round bottomed flask for the next de-Boc reaction.

### 1.7.2.22 Synthesis of H-Leu-Pro-GABA-[Propyl-spacer]-AQ TFA salt (HZ38)

TFA was added to the flask containing Boc-Leu-Pro-GABA-[Propyl-spacer]-AQ

(HZ37) until all solid dissolved. After 40 min, the reaction completed ($R_f$ 0.2, dichloromethane methanol 9:1). TFA was then evaporated off by using the rotary evaporator. Solid product was precipitated in diethyl ether. Yield: 637 mg, 92%.

**1.7.2.23 Synthesis of Boc-Ala-Gly-Leu-Pro-GABA-[Propyl-spacer]-AQ (HZ39)**

H-Leu-Pro-GABA-[Propyl-spacer]-AQ TFA salt HZ38 (600 mg, 0.87 mmol) and Boc-Ala-Gly-OSu (329 mg, 0.96 mmol) were dissolved in DMF with adding DIPEA (0.742 g/ml, 303 µl, 1.74 mmol). After 5 hours, the TLC ($R_f$ 0.56, dichloromethane methanol 9:1) showed the reaction had completed. The solution was extracted by dichloromethane and water. Further purification was performed by column chromatography (3.2 cm × 13.3 cm) using dichloromethane-methanol 12:1 solvent system. The appropriate fractions were combined, dried (using anhydrous sodium sulphate), filtered, and evaporated to dryness for the next reaction.

**1.7.2.24 Synthesis of H-Ala-Gly-Leu-Pro-GABA-[Propyl-spacer]-AQ TFA salt (HZ40)**

TFA was added to the flask of Boc-Ala-Gly-Leu-Pro-GABA-[Propyl-spacer]-AQ (HZ39) until all solids were dissolved. The reaction completed in 45 min by checking the TLC ($R_f$ 0.4, dichloromethane methanol 9:1). TFA was evaporated off and about 6 drops of ethanol was added to the sticky solution by pipetting. 50ml of diethyl ether was then transferred to the flask. The flask was cooled in the fridge overnight. The solid precipitate in diethyl ether was collected. Yield: 512 mg, 72%.

ESMS (+): 704 m/z 100% $(M-CO_2CF_3)^+$

### 1.7.2.25 Synthesis of Boc-Pro-Ala-Gly-Leu-Pro-GABA-[Propyl-spacer]-AQ (HZ41)

H-Ala-Gly-Leu-Pro-GABA-[Propyl-spacer]-AQ TFA salt HZ40 (500 mg, 0.61 mmol) was reacted with Boc-Pro-OH (145 mg, 0.67 mmol) in DMF followed by the addition of TBTU (216 mg, 0.67 mmol), HOBt (103 mg, 0.67 mmol), and DIPEA (0.742 g/ml, 351 μl, 2 mmol). The reaction completed in 1 hour by checking the TLC ($R_f$ 0.6, dichloromethane methanol 9:1). After extraction by dichloromethane and water, column chromatography (3.2 cm × 12 cm) was performed for product purification. The appropriate fractions were combined, filtered and evaporated to dryness and ready for the de-Boc reaction.

### 1.7.2.26 Synthesis of H-Pro-Ala-Gly-Leu-Pro-GABA-[Propyl-spacer]-AQ TFA salt (HZ42)

TFA was added to dissolve Boc-Pro-Ala-Gly-Leu-Pro-GABA-spacer-anthraquinone (HZ41) in a round bottomed flask. The reaction was complete in 45 min monitored by the TLC ($R_f$ 0.3, dichloromethane-methanol 9:1). The solution was then evaporated to dryness by using the rotary evaporator. A few drops of ethanol and diethyl ether (70 ml) were added to the flask. The red solid precipitate was collected by filtration and dried in a vacuum desiccator. Yield: 489 mg, 88%.

ESMS (+): 801 m/z 100% $(M-CO_2CF_3)^+$

### 1.7.2.27 Synthesis of FITC-Pro-Ala-Gly-Leu-Pro-GABA-[Propyl-spacer]-AQ (HZ43)

H-Pro-Ala-Gly-Leu-Pro-GABA-[Propyl-spacer]-AQ TFA salt HZ42 (100mg, 0.11 mmol) and FITC (38.3 mg, 0.1 mmol) were dissolved in 5ml DMF, followed by the addition of DIPEA (0.742 g/ml, 38μl, 0.22 mmol). The reaction was left to

react at RT overnight. The solution was poured into water to get orange precipitate. The crude product (R$_f$ 0.46, dichloromethane-methanol 6:1) was purified by column chromatography using the eluting solvent dichloromethane-methanol 9:1. The pure fractions were combined, filtered and evaporated to dryness. The solid product was scratched off the flask and collected. Yield: 12.5 mg, 9%.

ESMS (-): 1188 m/z 100% (M-H)$^-$

### 1.7.2.28 Synthesis of AQ-[Propyl-spacer]-Pro-Ala-Gly-Leu-Ala-OPFP (HZ44)

AQ-Spacer--Pro-Ala-Gly-Leu-Ala-Ala-OH HZ33 (100 mg, 0,12 mmol) was reacted with PFP (50.3mg, 0.3 mmol), followed by the addition of DCC (61.4 mg, 0.3 mmol) and DMAP (30 mg, 0.24 mmol) in 20ml DMF. The reaction mixture was stirred at RT for 7 hours. The precipitate DCU was filtered off. The crude product (R$_f$ 0.64, dichloromethane-methanol 9:1) was kept in dichloromethane for the next reaction without further purification.

### 1.7.2.29 Synthesis of AQ-[Propyl-spacer]-Pro-Ala-Gly-Leu-Ala-ethyl piperidine-3-carboxylate (HZ45)

(R)-Ethyl piperidine-3-carboxylate (29.5 mg, 0.19 mmol) and DIPEA (0.742 g/ml, 32.6 µl, and 0.19 mmol) were added to the AQ-[Propyl-spacer]-Pro-Ala-Gly-Leu-Ala-OPFP HZ44 (100 mg, 0.124 mmol) in dichloromethane. The reaction was completed in 2.5 hours by checking the TLC (R$_f$ 0.27, dichloromethane-ethyl acetate-ethanol 7:2:1). The solution was washed with water and aqueous sodium bicarbonate. The dichloromethane layers were combined, dried by sodium sulfate, and evaporated to a small volume for column chromatography (dichloromethane-ethyl acetate-ethanol 7:2:1). The pure

fractions were combined, filtered and transferred into an evaporating basin. Yield: 34.8 mg, 30%.

<u>ESMS (+)</u>: 967 m/z 100% (M+Na)$^+$, 983 m/z 100% (M+K)$^+$

## 1.7.2.30 Synthesis of

## Succinyl-Pro-Ala-Gly-Leu-Pro-GABA-[Propyl-spacer]-AQ (HZ46)

H-Pro-Ala-Gly-Leu-Pro-GABA-[Propyl-spacer]-AQ TFA salt HZ42 (200mg, 0.22 mmol) and succinic anhydride (24 mg, 0.24 mmol) were dissolved in DMF (3 ml), followed by the addition of DIPEA (0.742 g/ml, 80 µl, 0.46 mmol). After 4 h, the reaction was completed. The crude product (R$_f$ 0.48, dichloromethane-methanol 4:1) was extracted with dichloromethane and water. Column chromatography (dichloromethane-methanol 4:1) was performed for further purification. The product fractions were combined, filtered and evaporated to dryness by the rotary evaporator. The red solid was added with 50 ml diethyl in the round bottomed flask to precipitate the product. The mixture was cooled at 5 °C overnight, filtered, dried in the desiccator, and collected. Yield: 107 mg, 55%.

## 1.7.2.31 Synthesis of

## Podophyllotoxin-Pro-Ala-Gly-Leu-Pro-GABA-[Propyl-spacer]-AQ (HZ47)

Succinyl-Pro-Ala-Gly-Leu-Pro-GABA-[Propyl-spacer]-AQ HZ46 (80 mg, 0.09 mmol) was dissolved in DMF (1 ml) and acetonitrile (2 ml), followed by the addition of podophyllotoxin (40.5 mg, 0.1 mmol), TEA (26 µl, 0.19 mmol) and TBTU (31.4 mg, 0.19 mmol), and reacted at RT for 3 hours. Acetonitrile was evaporated off first. The crude product (R$_f$ 0.65, dichloromethane-methanol 6:1) in DMF was extracted with dichloromethane and water. The organic layers were combined, dried by anhydrous sodium sulphate, evaporated to a small volume for column chromatography. The eluting solvent dichloromethane-ethyl

acetate-methanol 7:2:1 was used. The product fractions were combined, filtered and evaporated to dryness in an evaporating basin. Yield: 16.3 mg, 14%.

ESMS (+): 1321 m/z 45% (M+Na)$^+$,

## 1.7.2.32 Synthesis of Fmoc-Pro-Ala-Gly-Nva-Pro-Resin (HZ51)

H-Pro-2Cl-Trt resin (1 g, 0.84 mmol/g) was used for the SPPS. The pentapeptide (Fmoc-Pro-Ala-Gly-Nva-Pro-OH) was synthesised using the same method as Fmoc-Pro-Ala-Gly-Leu-Ala-Ala-OH (HZ31). About 23% of the resin (HZ51) was transferred into another resin for the synthesis of HZ52. The rest of 77% resin was treated with 5% TFA in dichloromethane. The cleavage process was done as same as HZ31 synthesis. The white product was precipitated in diethyl ether, filtered, dried in a desiccator and collected. Yield: 233 mg, 42%.

$^1$H NMR spectrum (DMSO-d$_6$, 300 MHz) δ: 1.2-1.4 [6H, m, CH$_3$-CH$_2$-CH$_2$ (Nva) and CH$_3$-CH (Ala)]; 1.4-1.68 [4H, m, 2×CH$_3$-CH$_2$-CH$_2$ (Nva)]; 1.7-2.03 [4H, m, 2×β-CH$_2$ (Pro)]; 2.03-2.3 [4H, m, 2×γ-CH$_2$ (Pro)]; 3.32-3.57 [2H, m, δ-CH$_2$ (Pro)]; 3.6-3.8 [4H, m, 2×CH$_2$ (Gly)]; 3.9-4.32 [5H, m, CH$_2$-(Fmoc), CH (Nva) and α-CH (Pro)]; 4.32-4.55 [2H, m, CH (Ala) and α-CH (Fmoc)]; 7.28-7.48 [4H, m, H-1, H-2, H-7 and H-8 (Fmoc)]; 7.6-7.7 [2H, m, H-4 and H-5 (Fmoc)]; 7.85-7.93 [2H, t, H-3 and H-6 (Fmoc)]; 8.07 [1H, t, CONH (Gly)]; 8.18 [(1H, d, CONH (Ala)]; 8.34 [(1H, d, CONH (Nva)];

## 1.7.2.33 Synthesis of AQ-Spacer-Pro-Ala-Gly-Nva-Pro-OH (HZ52)

Piperidine (15 ml, 20%) in DMF was added to Fmoc-Pro-Ala-Gly-Nva-Pro-Resin HZ51 (23%, 0.19 mmol) on resin. The vessel was shaken for 20 min (3 times, 5 ml each time). The resin was washed 3 times with DMF for the next coupling reaction with TL12. TL12 (65 mg, 1 equivalent), TBTU (59 mg, 0.19 mmol), HOBt

(28.2mg, 0.19 mmol), and DIPEA (67.5 μl, 0.38 mmol, 0.742 g/ml) were dissolved in DMF (8 ml), the solution was added to the de-Fmoc HZ51 resin, and shaken for 1 h. The remaining solution in the vessel was drained off. Another same amount of reagents in DMF was added to the resin and shaken for 1 hour. The resin was washed with DMF (×3) and dichloromethane (×3).

25 ml of 5% TFA in dichloromethane was prepared. Each time 3-4ml of the stock solution was added to the resin and shaken for 8-10 min. All fractions were kept in different beakers for TLC ($R_f$ 0.36, dichloromethane-methanol 9:1) test. The resin was washed with dichloromethane (×3). All filtrates and fractions were combined, evaporated to dryness, precipitated in diethyl ether and collected. Yield: 143 mg, 98%.

ESMS (-): 755 m/z (100%) (M-H)⁻

## 1.7.2.34 Synthesis of AQ-Spacer-Pro-Ala-Gly-Nva-Pro-OPFP (HZ53)

AQ-Spacer-Pro-Ala-Gly-Nva-Pro-OH HZ52 (130 mg, 0.17 mmol), PFP (34.8 mg, 0.19 mmol), DCC (39 mg, 0.19 mmol), and DMAP (21 mg, 0.19 mmol) were dissolved in dichloromethane (10 ml) and refluxed on 40°C water bath for 30 h. The crude product ($R_f$ 0.53, chloroform-methanol 6:1) was extracted with chloroform and water. The organic layers were combined, dried by anhydrous sodium sulphate, and evaporated to dryness. The solid product was kept in the round bottomed flask for the next reaction with baclofen.

## 1.7.2.35 Synthesis of AQ-Spacer-Pro-Ala-Gly-Nva-Pro-Baclofen (HZ54)

The flask which contained pure AQ-Spacer-Pro-Ala-Gly-Nva-Pro-OPFP HZ53 solid (assumed 0.17 mmol) was added with baclofen (36.7 mg, 0.17 mmol), DIPEA (60 μl, 0.34 mmol, 0.742 g/ml) in dichloromethane (15 ml). The mixture was stirred at RT for 40 h. The DCU precipitate was filtered off. The crude

product ($R_f$ 0.46, dichloromethane-methanol 6:1) was purified by column chromatography using the eluting solvent dichloromethane-methanol 9:1. The product was still not pure and further purification was needed. Thick TLC plate (dichloromethane-methanol 6:1) was used. The product layer was scratched off the plate and collected by filtration and dried in an evaporating basin. Yield: 4 mg, 2%.

<u>ESMS (-)</u>: 950 m/z 45% (M-H)⁻

## 1.7.2.36 Synthesis of 5(6)-Carboxyfluorescein-Pro-Ala-Gly-Leu-Pro-GABA-[Propyl-spacer]-AQ (HZ57)

5(6)-Carboxyfluorescein (62 mg, 0.16 mmol) was reacted with H-Pro-Ala-Gly-Leu-Pro-GABA-[Propyl-spacer]-AQ TFA salt HZ42 (150 mg, 0.16 mmol) in DMF (8 ml), followed by the addition of PyBOP (102.3 mg, 0.2 mmol) and DIPEA (91 µl, 0.51 mmol, 0.742 g/ml) to the solution, and reacted with stir at RT for 1 hour. The crude product ($R_f$ 0.37, dichloromethane-methanol 5:1) was extracted with dichloromethane and water. The organic layers were combined, dried by sodium sulfate and evaporated to a small volume. Further purification was done by column chromatography using the eluting solvent dichloromethane-methanol 9:1. The pure product fractions were combined, filtered, and evaporated to dryness in an evaporating basin at RT. Yield: 56.6 mg, 31%.

<u>ESMS (-)</u>: 1159 m/z 100% (M+H)⁺

## 1.8 References

Abdul M, Mccray SD, Hoosein NM. (2008). Expression of gamma-aminobutyric acid receptor (subtype A) in prostate cancer. *Acta Oncol.* **47**, p1546–1550.

Albright, C. F., Graciani, N., Han, W., Yue, E., Stein, R., Lai, Z., Diamond, M., Dowling, R., Grimminger, L., Zhang, S. Y., Behrens, D., Musselman, A., Bruckner, R., Zhang, M., Jiang, X., Hu, D., Higley, A., Dimeo, S., Rafalski, M., Mandlekar, S., Car, B., Yeleswaram, S., Stern, A., Copeland, R. A., Combs, A., Seitz, S. P., Trainor, G. L., Taub, R., Huang, P. & Oliff, A. (2005). Matrix metalloproteinase-activated doxorubicin prodrugs inhibit HT1080 xenograft growth better than doxorubicin with less toxicity. *Mol Cancer Ther,* **4,** p751-760.

Annabi B, Lachambre MP, Plouffe K, Moumdjian R, Béliveau R. (2009). Propranolol adrenergic blockade inhibits human brain endothelial cells tubulogenesis and matrix metalloproteinase-9 secretion. *Pharmacol Res.* **60**(5), p438-445.

Aronica E, Redeker S, Boer K, Spliet WG, van Rijen PC, Gorter JA, Troost D. (2007). Inhibitory networks in epilepsy-associated gangliogliomas and in the perilesional epileptic cortex. *Epilepsy Res.* **74**, p33–44.

Azuma H, Inamoto T, Sakamoto T, Kiyama S, Ubai T, Shinohara Y, Maemura K, Tsuji M, Segawa N, Masuda H, Takahara K, Katsuoka Y, Watanabe M. (2003). Gamma-aminobutyric acid as a promoting factor of cancer metastasis; induction of matrix metalloproteinase production is potentially its underlying mechanism. *Cancer Res.* **63**, p8090-8096.

Balalaie S, Mahdidoust M, Eshaghi-najafabadi R. (2008). 2-(1*H*-Benzotriazole-1-yl)-1,1,3,3-Tetramethyluronium Tetrafluoro Borate (TBTU) as an Efficient Coupling Reagent for the Esterification of Carboxylic acids with Alcohols and Phenols at Room Temperature. *Chinese Journal of Chemistry.* **26**(6), p1141-1144.

Barker J.L., Behar T., Li Y.X., Liu Q.Y., Ma W., Maric D., Maric I., Schaffner A.E., Serafini R., Smith S.V., Somogyi R., Vautrin J.Y., Wen X.L. and Xian H. (1998). GABAergic cells and signals in CNS development. *Perspect. Dev. Neurobiol.* **5**, p305-322.

Bissett D, O'Byrne KJ, von Pawel J, Gatzemeier U, Price A, Nicolson M, Mercier R, Mazabel E, Penning C, Zhang MH, Collier MA, Shepherd FA. (2005). Phase III study of matrix metalloproteinase inhibitor prinomastat in non-small-cell lung cancer. *Journal of Clinical Oncology.* **23**(4), p842–849.

Bohlin L, Rosen B. (1996). Podophyllotoxin derivatives: drug discovery and development. *Drug Discov. Today*, **1**, p343-351.

Bonomi P. (2002). Matrix metalloproteinase and Matrix metalloproteinase inhibitors in lung cancer. *Semin Oncol.* **29**, p78-86.

Brew K, Nagase H. (2010). The tissue inhibitors of metalloproteinases (TIMPs): an ancient family with structural and functional diversity. *Biochim Biophys Acta.* **1803**(1), p55-71.

Campagna-Slater V, Weaver DF (2007). Molecular modelling of the GABA$_A$ ion

channel protein. *J. Mol. Graph. Model.* **25**(5), p721–30.

Candelario-Jalil E, Thompson J, Taheri S, Grossetete M, Adair JC, Edmonds E, Prestopnik J, Wills J, Rosenberg GA. (2011). Matrix metalloproteinases are associated with increased blood-brain barrier opening in vascular cognitive impairment. *Stroke.* **42**(5), p1345-1350.

Canel C, Moraes RM, Dayan FE, Ferreira D. (2000). Podophyllotoxin. *Phytochemistry.* **54**(2), p115-120.

Cao Y. (2001). Endogenous angiogenesis inhibitors and their therapeutic implications. *Int J Biochem Cell Biol.* **33**(4), p357-369.

Castro MA, Miguel del Corral JM, Gordaliza M, Gómez-Zurita MA, de la Puente ML, Betancur-Galvis LA, Sierra J, San Feliciano A. (2003). Synthesis, cytotoxicity and antiviral activity of podophyllotoxin analogues modified in the E-ring. *Eur J Med Chem.* **38**(10), p899-911.

Chen EI, Li W, Godzik A, Howard EW, Smith JW. (2003). A residue in the S2 subsite controls substrate selectivity of matrix metalloproteinase-2 and matrix metalloproteinase-9. *J Biol Chem.* **278**(19), p17158-17163.

Clark IM, Swingler TE, Sampieri CL, Edwards DR. (2009). The regulation of matrix metalloproteinases and their inhibitors. *Int J Biochem Cell Biol.* **40**(6-7), p1362-1378.

Connolly CN, Krishek BJ, McDonald B, Smart TG, Moss SJ (1996). Assembly

and cell surface expression of heteromeric and homomeric g-aminobutyric acid type A receptors. *J Biol Chem.* **271**(1), p89–96.

Curran S, Murray G. (2000). Matrix metalloproteinases: molecular aspects of their roles in tumour invasion and metastasis. *Eur J Cancer.* **36**, p1621-1630.

Denny W. (2001). Prodrug strategies in cancer therapy. *Eur J Med Chem.* **36**, p577-595.

El-Faham A, Albericio F. (2011). Peptide coupling reagents, more than a letter soup. *Chem Rev.* **111**(11), p6557-6602.

Ethell IM, Ethell DW. (2007), Matrix metalloproteinases in brain development and remodeling: synaptic functions and targets. *J Neurosci Res.* **85**(13), p2813-2823.

Fava G, Marucci L, Glaser S, Francis H, De Morrow S, Benedetti A, Alvaro D, Venter J, Meininger C, Patel T, Taffetani S, Marzioni M, Summers R, Reichenbach R, Alpini G. (2005). Gamma-Aminobutyric acid inhibits cholangiocarcinoma growth by cyclic AMP-dependent regulation of the protein kinase A/extracellular signal-regulated kinase 1/2 pathway. *Cancer Res.* **65**(24), p11437-11446.

Filip M, Frankowska M. (2008). GABA$_B$ receptors in drug addiction. *Pharmacol Rep.* **60**, p755–770.

Frølund B, Ebert B, Kristiansen U, Liljefors T, Krogsgaard-Larsen P. (2002). GABA-A receptor ligands and their therapeutic potentials. *Current Topics in Medicinal Chemistry.* **2**(8), p817–832.

Gatto C, Rieppi M, Borsotti P, Innocenti S, Ceruti R, Drudis T, Scanziani E, Casazza A, Taraboletti G, Giavazzi R. (1999). BAY 12-9566, A novel inhibitor of matrix metalloproteinases with antiangiogenic activity. *Clin Cancer Res.* **5**, p3603-3607.

Gialeli C, Theocharis AD, Karamanos NK. (2011). Roles of matrix metalloproteinases in cancer progression and their pharmacological targeting. *FEBS J.* **278**(1), p16-27.

Giavazzi R, Taraboletti G. (2001). Preclinical development of metalloproteasis inhibitors in cancer therapy. *Crit Rev Oncol Hematol.* **37**(1), p53-60.

Gordaliza M, García PA, del Corral JM, Castro MA, Gómez-Zurita MA. (2004). Podophyllotoxin: distribution, sources, applications and new cytotoxic derivatives. *Toxicol.* **44**(4), p441-459.

Greco, F. A., Hainsworth, J. D. (1996). Clinical Studies of Etoposide phosphate. *Semin. Oncol.* **23**(suppl), p45-50.

Gupta SP, Patil VM. (2012). Specificity of binding with matrix metalloproteinases. *EXS.* **103**, p35-56.

Han HK, Amidon GL. (2000). Targeted prodrug design to optimize drug delivery*.*

*AAPS PharmSci.* **2**(1), p1-6.

Hidalgo M, Eckhardt SG. (2001), Development of matrix metalloproteinase inhibitors in cancer therapy. *J Natl Cancer Inst.* **93**(3), p178-193.

Hinnen P, Esken F, Verweij J. (2001). Matix metalloproteinase inhibitors: current developments and future perspectives. *Oncologist.* **6**, p415-427.

Hofmann, U. B., Eggert, A. A., Blass, K., Brocker, E. B. & Becker, J. C. (2003). Expression of matrix metalloproteinases in the microenvironment of spontaneous and experimental melanoma metastases reflects the requirements for tumor formation. *Cancer Res,* **63,** p8221-8225.

Ippolito JE, Merritt ME, Backhed F, Moulder KL, Mennerick S, Manchester JK, Gammon ST, Piwnica-Worms D, Gordon JI. (2006). Linkage between cellular communications, energy utilization, and proliferation in metastatic neuroendocrine cancers. *Proc Natl Acad Sci.* **103**, p12505–12510.

Itoh T, Tanioka M, Yoshida H, Yoshioka T, Nishimoto H, Itohara S. (1998). Reduced angiogenesis and tunour progression in gelatinase A deficient mice. *Cancer Res.* **58**, p1048-1051.

Jacob TC. Moss SJ. Jurd R. (2008). $GABA_A$ receptor trafficking and its role in the dynamic modulation of neuronal inhibition. *Nature Reviews Neuroscience.* **9**, p331-343

Jiang X, Su L, Zhang Q, He C, Zhang Z, Yi P, Liu J. (2012). $GABA_B$ receptor

complex as a potential target for tumor therapy. *J Histochem Cytochem.* **60**(4), p269-279.

Johnson SK. and Haun RS. (2005). The Gamma-Aminobutyric Acid A Receptor π Subunits Is Overexpressed in Pancreatic Adenocarcinomas. *JOP.J Pancreas* **6**(2), p136-142.

Joseph J, Niggemann B, Zaenker KS, Entschladen F. (2002). The neurotransmitter gamma-aminobutyric acid is an inhibitory regulator for the migration of SW 480 colon carcinoma cells. *Cancer Res.* **62**, p6467–6469.

Katzhendler J, Gean KF, Bar-Ad G, Tashma Z, Ben-Snoshan R, Ringel I, Backrack U, Ramu A. (1989). Synthesis of aminoanthraquinone derivatives and their in vitro evaluation as potential anti-cancer drugs. *Eur. J. Med. Chem.* **24**, p23-30.

Kaupmann K, Malitschek B, Schuler V, Heid J, Froestl W, Beck P, Mosbacher J, Bischoff S, Kulik A, Shigemoto R. (1998). GABA(B)-receptor subtypes assemble into functional heteromeric complexes. *Nature.* **396**, p683–687.

Klein G, Vellenga E, Fraaije M, Kamps W, de Bont E. (2004). The possible role of matrix metalloproteinase MMP-2 and MMP-9 in cancer, e.g. acute leukemia. *Crit Rev Oncol Hemat.* **50**, p87-100.

Kline T, Torgov MY, Mendelsohn BA, Cerveny CG, Senter PD. (2004). Novel antitumor prodrugs designed for activation by matrix metalloproteinases-2 and -9. *Mol Pharm.* **1**, p9-22.

Konstantinopoulos PA, Karamouzis MV, Papatsoris AG, Papavassiliou AG. (2008). Matrix metalloproteinase inhibitors as anticancer agents. *Int J Biochem Cell Biol.* **40**(6-7), p1156-1168.

Kridel SJ, Chen E, Kotra LP, Howard EW, Mobashery S, Smith JW. (2001). Substrate hydrolysis by matrix metalloproteinase-9. *J Biol Chem.* **276**(23), p20572-20578.

Lamy S, Lachambre MP, Lord-Dufour S, Béliveau R. (2010). Propranolol suppresses angiogenesis in vitro: inhibition of proliferation, migration, and differentiation of endothelial cells. *Vascul Pharmacol.* **53**(5-6), p200-208.

Lauer-Fields JL, Sritharan T, Stack MS, Nagase H, Fields GB. (2003). Selective hydrolysis of triple-helical substrates by matrix metalloproteinase-2 and -9. *J Biol Chem.* **278**(20), p18140-18145.

Leighl NB, Shepherd F, Paz-Ares L, Douillard JY, Peschel C, Arnold A, Tu D, Galbraith S, Hann K, Seymour L. (2004). Randomized phase II-III study of matrix metalloproteinase inhibitor (MMPI) BMS-275291 in combination with paclitaxel (P) and carboplatin (C) in advanced non-small cell lung cancer (NSCLC): NCIC-CTG BR. 18. *J Clin Oncol.* **22**(14), p7038.

Liederer BM, Borchardt RT. (2006). Enzymes involved in the bioconversion of ester-based prodrugs. *J Pharm Sci.* **95**(6), p1177-1195.

Lim SH, Jeong YI, Moon KS, Ryu HH, Jin YH, Jin SG, Jung TY, Kim IY, Kang SS,

Jung S. (2010). Anticancer activity of PEGylated matrix metalloproteinase cleavable peptide-conjugated adriamycin against malignant glioma cells. *Int J Pharm.* **387**(1-2), p209-214.

Liu C. J, Hou SS. (1997). Current Research Status of Podophyllotoxin Lignans. *Nat. Prod. Res. Develop.* **9**, p81-89.

Liu Y, Li YH, Guo FJ, Wang JJ, Sun RL, Hu JY, Li GC. (2008). Gamma-aminobutyric acid promotes human hepatocellular carcinoma growth through overexpressed gamma-aminobutyric acid A receptor alpha3 subunit. *World J Gastroenterol.* **14**, p7175–7182.

Mahato R, Tai W, Cheng K. (2011). Prodrugs for improving tumor target ability and efficiency. *Adv Drug Deliv Rev.* **63**, p659-70.

Miao Y, Zhang Y, Wan H, Chen L, Wang F. (2010). GABA-receptor agonist, propofol inhibits invasion of colon carcinoma cells. *Biomed Pharmacother.* **64**(9), p583-588.

Mincher DJ, Van Valckenborgh E, Young L, Turnbull A, Di Salvo A, Vanderkerken K. (2008). Design of mechanisms of selective prodrug activation in the bone marrow microenvironment of experimental and human multiple myeloma. *European Journal of Cancer*, **6**(9) p.26-27.

Mincher DJ, Turnbull A, Bibby MC, Double JA, Gilmour PS, Lowe G. (1999). Design and development of a new class of topoisomerase inhibitor: Preliminary in vivo evaluation in experimental colon cancer. *Br. J. Cancer*, **80**(Suppl. 2), p88.

Mincher DJ, Turnbull A, Kay GG, (*Inventors)* (2003). Anthracene derivatives as anti-cancer agents. US Patent US2003130272 A1 [Publication Date: 10-07-2003]; Corresponding to: World Patent WO0144190 A1 [Publication Date: 21-06-2001].

Mincher DJ, Turnbull A, Loadman PM, Van Valckenborgh E, Di Salvo A, Young L, Bibby MC, Vanderkerken K. (2006). Targeting the tumour microenvironment: Design of tissue-specific mechanisms of prodrug activation. *Annals of Oncology*, **17**(Suppl. 3), p34.

Minuk GY, Zhang M, Gong Y, Minuk L, Dienes H, Pettigrew N, Kew M, Lipschitz J, Sun D. (2007). Decreased hepatocyte membrane potential differences and GABAA beta3 expression in human hepatocellular carcinoma. *Hepatology.* **45**, p735–745.

Mizoguchi H, Yamada K, Nabeshima T. (2011). Matrix metalloproteinases contribute to neuronal dysfunction in animal models of drug dependence, Alzheimer's disease, and epilepsy. *Biochem Res Int.* **681385**, p1-10.

Montalbetti CAGN, Falque V. (2005). Amide bond formation and peptide coupling. *Tetrahedron.* **61**, p10827-10852.

Murphy G, Knäuper V. (1997). Relating matrix metalloproteinase structure to function: why the "hemopexin" domain?. *Matrix Biol.* **15**(8-9), p511-518.

Murphy G, Nagase H. (2008). Progress in matrix metalloproteinase research.

*Mol Aspects Med.* **29**(5), p290-308.

Nagase H, Woessner JF Jr. (1999). Matrix metalloproteinases. *J Biol Chem..* **274**(31), p21491-21494.

Ndinguri MW, Bhowmick M, Tokmina-Roszyk D, Robichaud TK, Fields GB. (2012). Peptide-based selective inhibitors of matrix metalloproteinase-mediated activities. *Molecules,* **17,** p14230-48.

Olsen RW, Sieghart W. (2009). GABA$_A$ receptors: subtypes provide diversity of function and pharmacology. *Neuropharmacology.* **56**, p141-148.

Ortega A. (2003). A new role for GABA: inhibition of tumor cell migration. *TRENDS in Pharmacological Sciences.* **24**(4), p151-154.

Pasquier E, Ciccolini J, Carre M, Giacometti S, Fanciullino R, Pouchy C, Montero MP, Serdjebi C, Kavallaris M, André N. (2011). Propranolol potentiates the anti-angiogenic effects and anti-tumor efficacy of chemotherapy agents: implication in breast cancer treatment. *Oncotarget.* **2**(10), p797-809.

Pettersson, S. (2004). Biochemistry of topoisomerase inhibition and cellular mechanism of anthraquinone-amino acid conjugates in vitro. PhD, Edinburgh Napier University.

Rasmussen H, McCann P. (1997). Matrix metalloproteinase inhibition as a novel anticancer strategy: a review with special focus on batimastat and marimastat – correlation with astrocytoma cell invasiveness. *Pharmacol Ther.* **75**, p69-75.

Rawlings ND, Barrett AJ, Bateman A. (2012). *MEROPS*: the database of proteolytic enzymes, their substrates and inhibitors. *Nucleic Acids Res.* 40, D343-D350. Available at: http://merops.sanger.ac.uk/ [accessed: 16th October 2012].

Rautio J, Kumpulainen H, Heimbach T, Oliyai R, Oh D, Järvinen T, Savolainen J. (2008). Prodrugs: design and clinical applications. *Nat Rev Drug Discov.* **7**(3), p255-270.

Ray J. Stetler-Stevenson W. (1994). The role of matrix metalloproteases and their inhibitors in tumour invasion, metastasis and angiogenesis. *Eur Respir J.* **7**, p2062-7202.

Roberts SS, Mendonca-Torres MC, Jensen K, Francis GL, Vasko V. (2009). GABA receptor expression in benign and malignant thyroid tumors. *Pathol Oncol Res.* **15**, p645–650.

Rosenberg GA. (2009). Matrix metalloproteinases and their multiple roles in neurodegenerative diseases. *Lancet Neurol.* **8**(2), p205-216.

Schuller HM, Al-Wadei HA, Majidi M. (2008a). GABA B receptor is a novel drug target for pancreatic cancer. *Cancer.* **112**, p767–778.

Schuller HM, Al-Wadei HA, Majidi M. (2008b). Gamma-aminobutyric acid, a potential tumor suppressor for small airwayderived lung adenocarcinoma. *Carcinogenesis.* **29**, p1979–1985.

Schuller HM, Al-Wadei HA. (2010). Neurotransmitter receptors as central regulators of pancreatic cancer. *Future Oncol.* **6**(2), p221-228.

Sparano JA, Bernardo P, Stephenson P, Gradishar WJ, Ingle JN, Zucker S, Davidson NE. (2004). Randomized phase III trial of marimastat versus placebo in patients with metastatic breast cancer who have responding or stable disease after first-line chemotherapy: Eastern Cooperative Oncology Group trial E2196. *J Clin Oncol.* **22**(23), p4683-4690.

Synowitz M, Ahmann P, Matyash M, Kuhn SA, Hofmann B, Zimmer C, Kirchhoff F, Kiwit JC, Kettenmann H. (2001). GABA(A)-receptor expression in glioma cells is triggered by contact with neuronal cells. *Eur J Neurosci.* **14**, p1294–1302.

Szczaurska K, Mazurkiewicz M, Opolski A. (2003). The role of GABA-ergic system in carcinogenesis. *Postepy Hig Med Dosw.* **57**, p485–500.

Takehara A, Hosokawa M, Eguchi H, Ohigashi H, Ishikawa O, Nakamura Y, Nakagawa H. (2007). Gamma-aminobutyric acid (GABA) stimulates pancreatic cancer growth through overexpressing $GABA_A$ receptor π subunit. *Cancer Res.* **67**(20), p9704-12.

Tallant C, Marrero A, Gomis-Rüth FX. (2010). Matrix metalloproteinases: fold and function of their catalytic domains. *Biochim Biophys Acta.* **1803**(1), p20-28.

Tatsuta M, Iishi H, Baba M, Nakaizumi A, Ichii M, Taniguchi H. (1990). Inhibition by gamma-amino-n-butyric acid and baclofen of gastric carcinogenesis induced

by N-methyl-N'-nitro-N-nitrosoguanidine in Wistar rats. *Cancer Res.* **50**, p4931–4934.

Thaker PH, Yokoi K, Jennings NB, Li Y, Rebhun RB, Rousseau DL Jr, Fan D, Sood AK. (2005). Inhibition of experimental colon cancer metastasis by the GABA receptor agonist nembutal. *Cancer Biol Ther.* **4**, p753–758.

Turnbull, A. (2003). Design and development of novel DNA topoisomerase inhibitors. PhD, Edinburgh Napier University.

Van Valckenborgh E, Mincher D, Di Salvo A, Van Riet I, Young L, Van Camp B, Vanderkerken K. (2005). Targeting an MMP-9-activated prodrug to multiple myeloma-diseased bone marrow: a proof of principle in the 5T33MM mouse model. *Leukemia.* **19**(9), p1628-1633.

Vihinen P, Kähäri VM. (2002). Matrix metalloproteinases in cancer: prognostic markers and therapeutic targets. *Int J Cancer.* **99**(2), p157-166.

Wang T, Huang W, Chen F. (2008). Baclofen, a $GABA_B$ receptor agonist, inhibits human hepatocellular carcinoma cell growth in vitro and in vivo. *Life Sci.* **82**, p536–541.

Watanabe M, Maemura K, Kanbara K, Tamayama T, Hayasaki H. (2002). GABA and GABA receptors in the central nervous system and other organs. Int Rev Cytol. **213**, p1-47.

Watanabe M, Maemura K, Oki K, Shiraishi N, Shibayama Y, Katsu K. (2006).

Gamma-aminobutyric acid (GABA) and cell proliferation: focus on cancer cells. *Histol Histopathol.* **21**(10), p1135-1141.

Woessner JF Jr. (1991). Matrix metalloproteinases and their inhibitors in connective tissue remodeling. *FASEB J.* **5**(8), p2145-2154.

Yong VW. Krekoski CA. Forsyth PA. Bell R. Edwards DR. (1998). Matrixmetalloproteinases and diseases of the CNS. *Neuroendocrine bases of monogamy.* **21**(2), p75-80.

Yong VW, Power C, Forsyth P, Edwards DR. (2001), Metalloproteinases in biology and pathology of the nervous system. *Nat Rev Neurosci.* **2**(7), p502-511.

Young, L. (2006). Novel anticancer agents and oligopeptide drug conjugates: biochemistry of topoisomerase inhibition and MMP-activation. PhD, Edinburgh Napier University.

Young SZ, Bordey A. (2009). GABA's control of stem and cancer cell proliferation in adult neural and peripheral niches. *Physiology (Bethesda).* **24**, p171-185.

Zhang J, Zhang P, Liu X, Fang K, Lin G. (2007). Synthesis and biological evaluation of (R)-N-(diarylmethylthio/sulfinyl)ethyl/propyl-piperidine-3-carboxylic acid hydrochlorides as novel GABA uptake inhibitors. *Bioorg Med Chem Lett.* **17**(13), p3769-3773.

Zhu R, Qin S, He X, Wang F. (2004). $GABA_B$ receptor expression in human

gastric cancer. *Med J Chin PLA.* **29**, p958–960.


Zimmermann AP, Wiegand S, Werner JA, Eivazi B. (2010). Propranolol therapy for infantile haemangiomas: review of the literature. *Int J Pediatr Otorhinolaryngol.* **74**(4), p338-342.


Zucker S, Hymowitz M, Conner C, Zarrabi HM, Hurewitz AN, Matrisian L, Boyd D, Nicolson G, Montana S. (1999). Measurement of matrix metalloproteinases and tissue inhibitors of metalloproteinases in blood and tissues. Clinical and experimental applications. *Ann N Y Acad Sci.* **878**(1), p212-227.

# Chapter 2. Baclofen Based Prodrugs

## 2.1 Abstract

Gamma aminobutyric acids (GABA) are found to play an inhibitory role in most cancers, but the activation of $GABA_B$ receptor has been reported to have contradictory effects on the tumour progression. Baclofen, a $GABA_B$ receptor agonist, is demonstrated to reduce the incidence of some cancers. In this chapter, a series of baclofen based prodrugs and cyclic baclofen prodrugs have been designed and synthesised with the potential to cross the BBB and eventually target brain tumours.

## 2.2  Introduction

### 2.2.1 GABA

GABA is the main inhibitory neurotransmitter throughout the human central nervous system (CNS). It functions via activation of $GABA_A$ and $GABA_B$ receptors. Many studies suggest that GABA is a tumour signalling amino acid in the brain and periphery. In most cases, the levels of GABA content and GAD activity are increased in human tumours (for a review, see Young and Bordey, 2009).

Both $GABA_A$ and $GABA_B$ receptors were found to be overexpressed in different tumours which make them important therapeutic targets for cancer treatment. The GABAB receptors were considered first in this research (described briefly below).

### 2.2.2 GABA$_B$ receptor and tumours

The $GABA_B$ receptor is composed of two subunits GABABR1 and GABABR2.

126

The extracellular domain (ECD) of $GABA_{B1}$ is capable of binding GABA, agonist and antagonist (Jiang *et al.*, 2012). Growing evidence showed that $GABA_B$ receptors are involved in tumour proliferation and migration of tumour cells.

Both GABABR1 and GABABR2 were found to be commonly expressed in human hepatocellular carcinoma (HCC) by RT-PCR (Wang *et al.*, 2008). The expression level of $GABA_B$ receptors were upregulated in human colon cancer cell lines (Thaker *et al.,* 2005) and breast cancer (Jiang *et al.*, 2012). Zhu *et al.,* (2004) detected that in gastric cancer tissue, not only the level of $GBAB_B$ receptors is higher than normal tissues but also there are majority of $GBAB_B$ receptors distributed on the surface of cancer cells.

Schuller *et al.,* (2007) first reported that $GABA_B$ receptors are potent targets for human pancreatic cancer therapy. The Western blotting and cell migration assays in pancreatic ductal adenocarcinoma cell line PANC-1 and BXPC-3 showed that the migration of cells was significantly blocked by GABA and baclofen. The base level DNA synthesis was reduced in two cell lines after incubation with GABA and baclofen by BrdU incorporation assays. GABA and baclofen also inhibited intracellular cAMP signalling by immunoassays. All the data suggested that stimulation of $GABA_B$ receptors may have significant inhibitory effects on the migration of pancreatic tumour cells.

By immunohistochemistry in 70 human thyroid tumour samples, GABABR2 was detected to be differentially expressed between normal, benign, and malignant thyroid tissues. The normal tissues have undetectable expression. Interestingly, the malignant adenomas have the highest expression and benign tumours display an intermediate level. The development of thyroid cancer is thought to be a multi-step process and the high expression of GABABR2 in thyroid adenomas suggests that $GABA_B$ receptors are involved in early stages of thyroid

carcinogenesis (Roberts *et al.,* 2009)

The National Cancer Institute (NCI) data base provides the mRNA level of $GABA_B$ receptors expression in about 60 different cancer cell lines. According to the data, some cell lines of non-small cell lung cancer (HOP-92 and NCI-H226), CNS cancer (SF-268), Melanoma and breast cancer (MDA-MB-231/ATCC) have the high mRNA level of $GABA_B$ receptors (Ross *et al.,* 2000). The breast cancer cell line MCF-7 will be considered in this project for biological testing.

However, there are fewer studies examining the function of $GABA_B$ receptors on tumour cell proliferation than $GABA_A$ receptors.

### 2.2.3 Baclofen and tumours

Baclofen is an agonist of $GABA_B$ receptors. It is a derivative of gamma-butyric acid (**Figure 25**). It is also a licensed drug for the treatment of spasticity (Nielsen *et al.,* 2002).
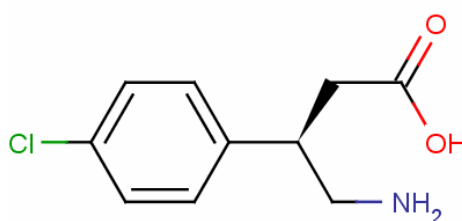


**Figure 25.** Chemical Structure of Baclofen

Several studies revealed that activation of $GABA_B$ receptors by baclofen plays an inhibitory role in most human tumour cell types such as human pancreatic

(Schuller *et al.*, 2008), lung, liver, breast (Azuma *et al.*, 2003), colon (Joseph *et al.,* 2002), and gastric tumours (Tatsuta *et al.*, 1990, 1992) which makes it a promising drug for tumour chemotherapy.

Although the mechanism of baclofen inhibiting tumour cells remains to be determined, there is evidence implied that $GABA_B$ receptor activation may induce the down-regulation of intracellular cyclic adenosine monophosphate (cAMP) and Increase MMP production (Loderwyks *et al.,* 2011).

In contrast, baclofen showed no inhibitory effect on human prostate cancer cells and even promote the invasion (Abdul *et al.*, 2008, Jiang *et al.*, 2012).

## 2.3 Results and discussion

### 2.3.1 Baclofen prodrug design strategy

To increase the drug selectivity, tumour activated prodrug strategies in cancer chemotherapy represent a promising approach (Rautio *et al.* 2008). The prodrugs should be less toxic before activation by tumours.
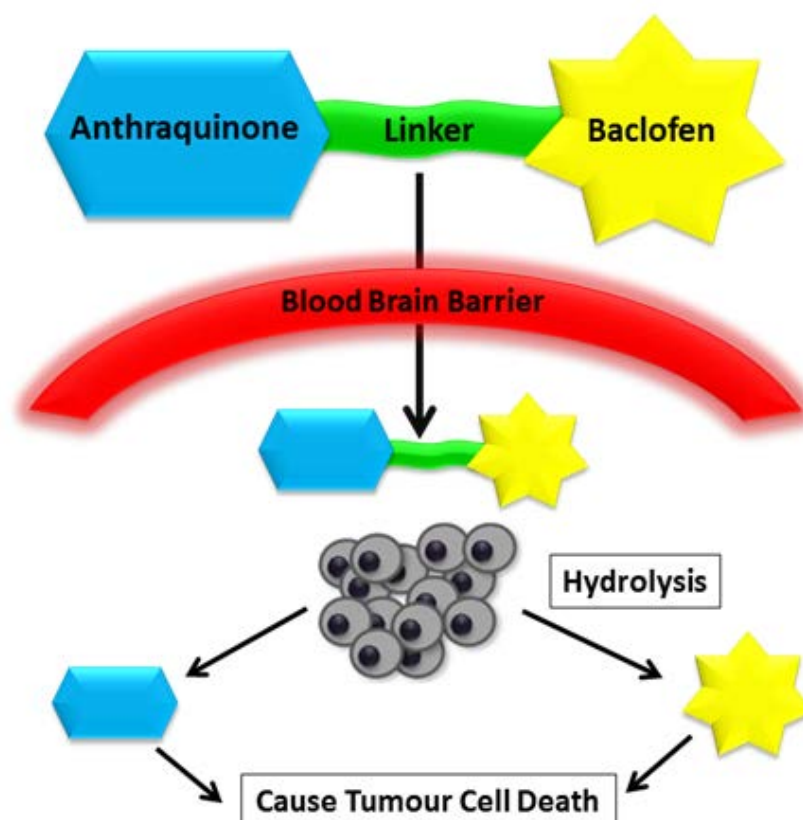


**Figure 26.** General concept of baclofen prodrug design

**Figure 26** shows the general concept of baclofen prodrug design. The baclofen prodrug for brain tumour therapy is designed to have an anthraquinone capping group and a linker connected to baclofen. Because baclofen itself is a polar drug and can poorly absorb across the cell membrane, the designed prodrugs here will increase the lipophilicity and more likely to cross the BBB (Blood Brain Barrier) and target the brain tumour. The acidic environment in tumours will cause the amino peptide linker to be hydrolysed and release the active agent

baclofen.

The uncyclised baclofen prodrugs can be converted into the cyclic baclofen prodrugs using the dehydrating agent acetic anhydride (Abdel-Hafez and Abdel-Wahab, 2008). The cyclic analogues of baclofen should have greater lipophilic properties and the prodrug permeation through the BBB will be improved.

### 2.3.2 Synthesis of AQ-Ahx-Baclofen (HZ68)

1-Chloroanthraquinone was used as the starting material. It was reacted with the 6-aminohexanoic acid using the strong base NaOH in DMSO to form the anthraquinone spacer conjugate (HZ66) as shown in **Scheme 24**.
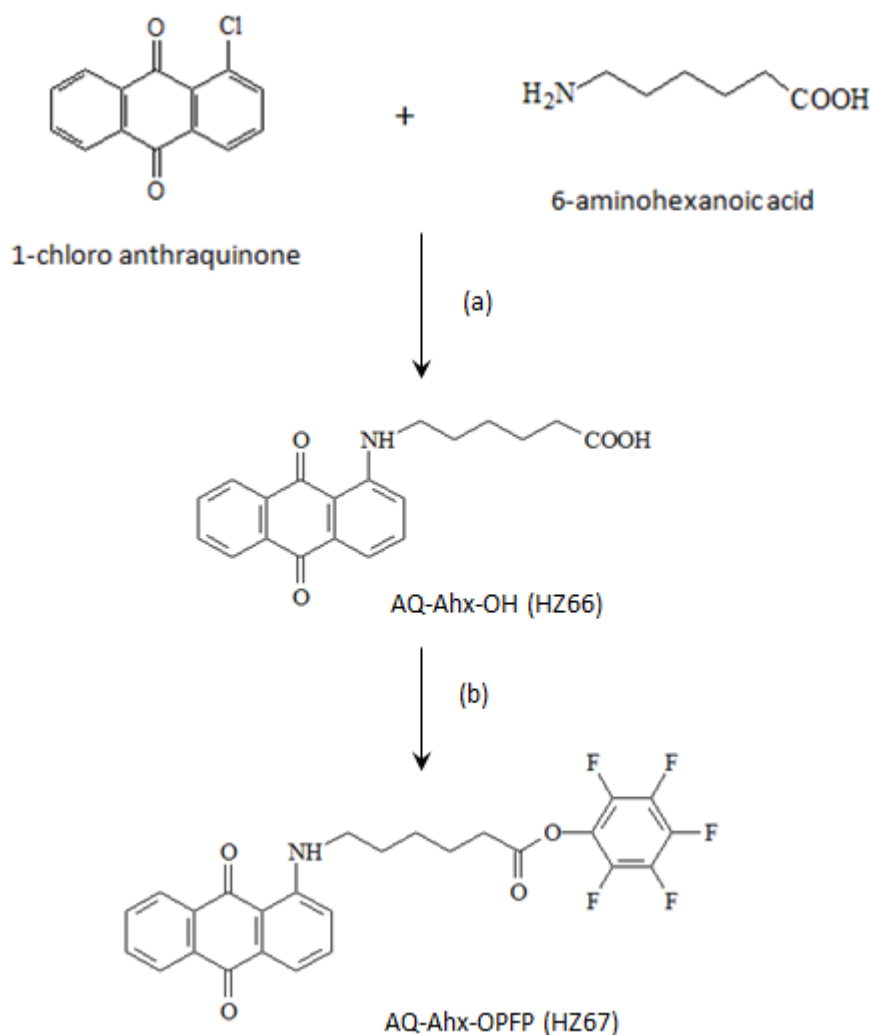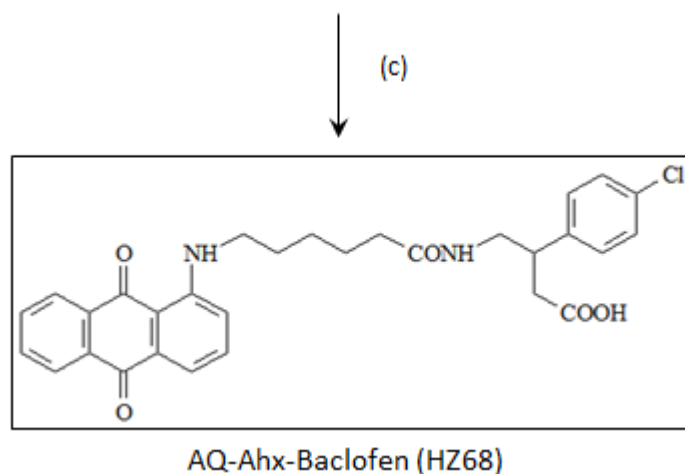
AQ-Ahx-Baclofen (HZ68)

Reagents and Conditions: (a) 6-aminohexanoic acid, NaOH, DMSO, 95°C (b) pentafluorophenol, DCC, DMAP, dichloromethane; (c) baclofen, $NaOH_{(aq)}$, DMF

**Scheme 24.** Outline of Baclofen Prodrug (HZ68) Synthesis

The acid end of AQ-Ahx-OH (HZ66) was converted into a pentafluorophenolate ester (OPFP) before adding the baclofen. The solubility of baclofen is very low in both DMF and DMSO. For the coupling of baclofen, firstly NaOH was dissolved by a drop of water in a round bottomed flask. Secondly, baclofen in DMF was added to the flask. The mixture was heated on the hot water bath (95°C). Another flask with AQ-Ahx-OPFP (HZ67) in DMF was also put on same water bath. The baclofen mixture was slowly added to HZ67 drop wise. The reaction was completed in 5 days by checking the TLC The crude product was extracted and purified by column chromatography. The appropriate fractions were combined, filtered and collected in diethyl ether.

The final product AQ-Ahx-Baclofen (HZ68) was characterized by NMR and its mass spectrum $(M+H)^+$ which has a strong signal at m/z 533 corresponding to a molecular mass of 532 **(Figure 27)**. The $^1H$ NMR spectrum had the amino proton at C-1 of the anthraquinone group that gave a triplet signal at 9.65 ppm. The methylene protons of the hexanoic spacer were identifiable between 1.4 and 3.4 ppm. The anthraquinone protons were fully assigned between 7.42 and 8.25

ppm. Signals for H-2, H-3, H-5 and H-6 of the chlorobenzene group were found from 7.2 to 7.38 ppm.
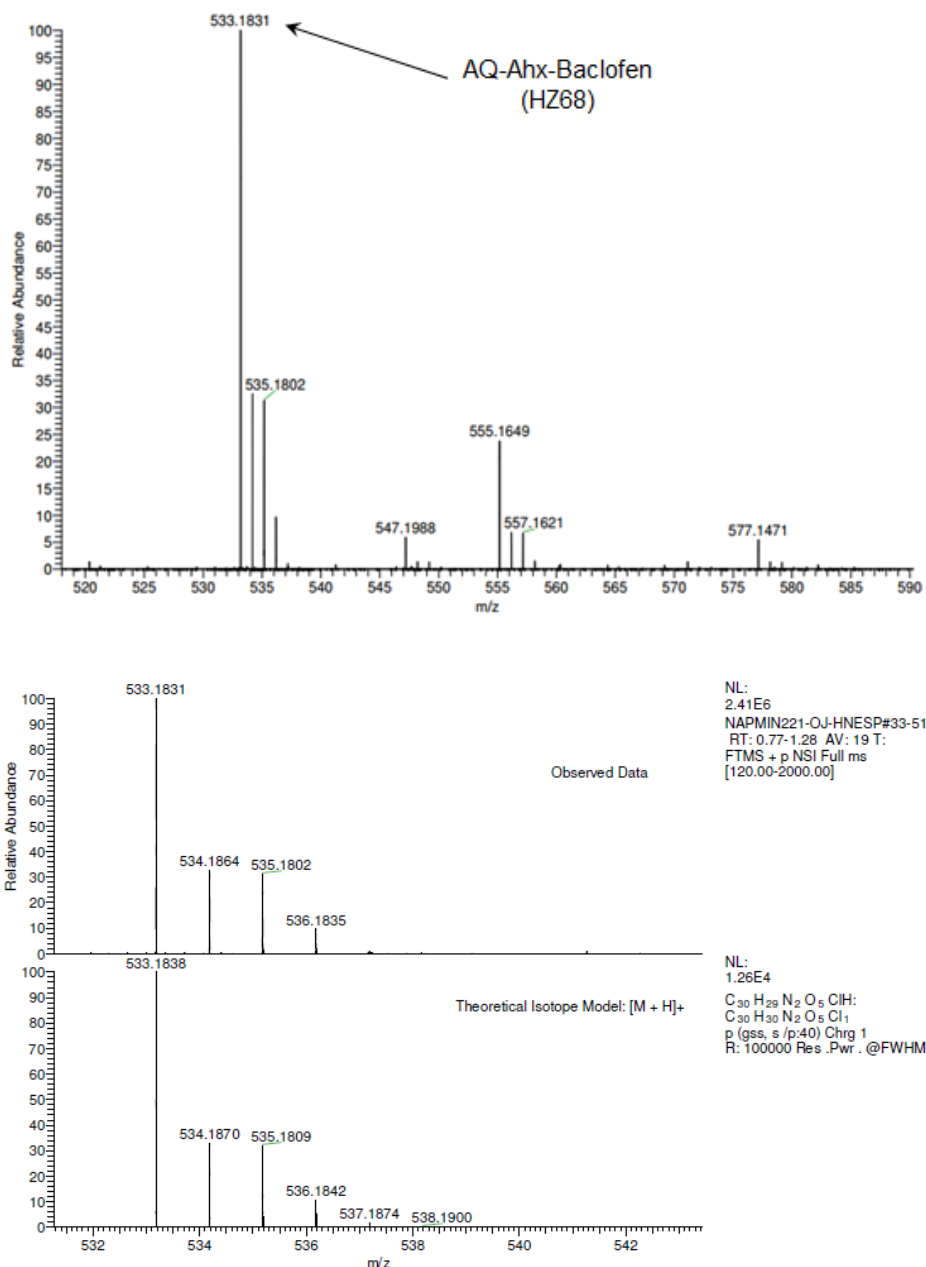


**Figure 27**. The ESI (+) Mass spectrum of prodrug AQ-Ahx-Baclofen (HZ68)

### 2.3.3 Synthesis of AQ-Ahx-cyclic Baclofen (HZ69)

The baclofen prodrug (HZ68) was converted to the cyclic baclofen prodrug AQ-Ahx-cyclic Baclofen (HZ69) using the dehydrating agent acetic anhydride **(Scheme 25)**. The reaction was heated on the water bath and completed in 1

hour by checking the TLC The reaction solution was cooled at RT and poured into distilled water. The precipitated compound was collected. The cyclic baclofen prodrug is expected to have stronger lipophilic properties and enhance the permeation through the BBB with improved therapeutic potency.



AQ-Ahx-Baclofen (HZ68)

(a)

AQ-Ahx-cyclic Baclofen (HZ69)
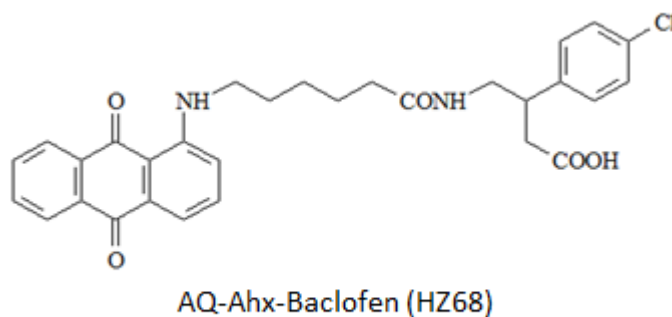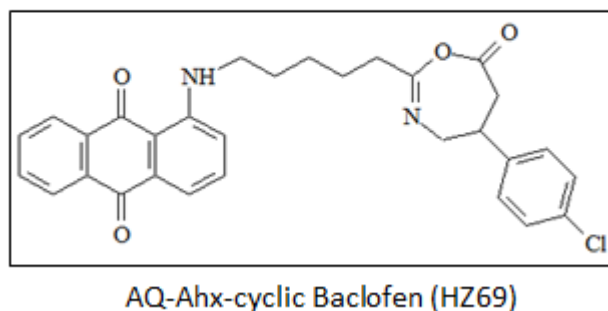
Reagents and Conditions: (a) (Ac)$_2$O reflux

**Scheme 25.** Outline of Baclofen Prodrug (HZ69) Synthesis

The structure of AQ-Ahx-cyclic Baclofen (HZ69) was confirmed by NMR and its ESI (+) Mass spectrum which gave a signal at m/z 515 for the molecular mass of 514. (**Figure 28**) The lactone type structure of HZ69 compound exhibited a multiplet signal at 3.45-3.65 ppm assigned to the methine proton (H-5). The signals at 2.7-2.84 ppm and 3.7-3.8 ppm recognised to be H-6 (O-CO-CH$_2$) and H-4 (C=N-CH$_2$), respectively. The protons of chlorobenzene were also found between 7.15 and 7.4 ppm.
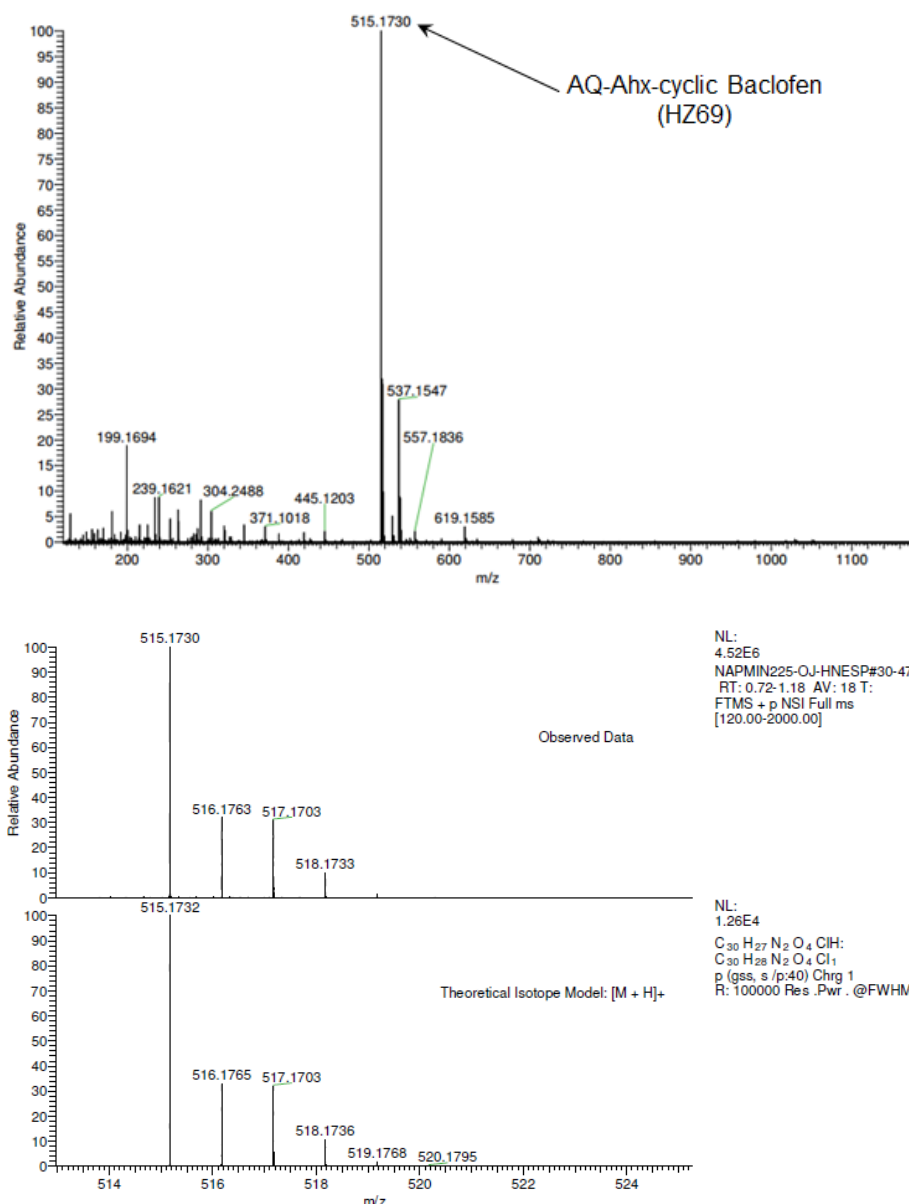
**Figure 28**. ESI (+) Mass spectrum of prodrug AQ-Ahx-cyclic Baclofen (HZ69)

### 2.3.4 Synthesis of AQ-Ava-cyclic Baclofen (HZ75)

The prodrug AQ-Ava-cyclic Baclofen (HZ75) used 5-aminopentanoic acid as the spacer which is shorter than the prodrug AQ-Ahx-cyclic Baclofen (HZ69). The synthesis process was the same as the prodrug HZ69 **(Scheme 25)**. The prodrugs with different spacers were supposed to have varying solubility properties.
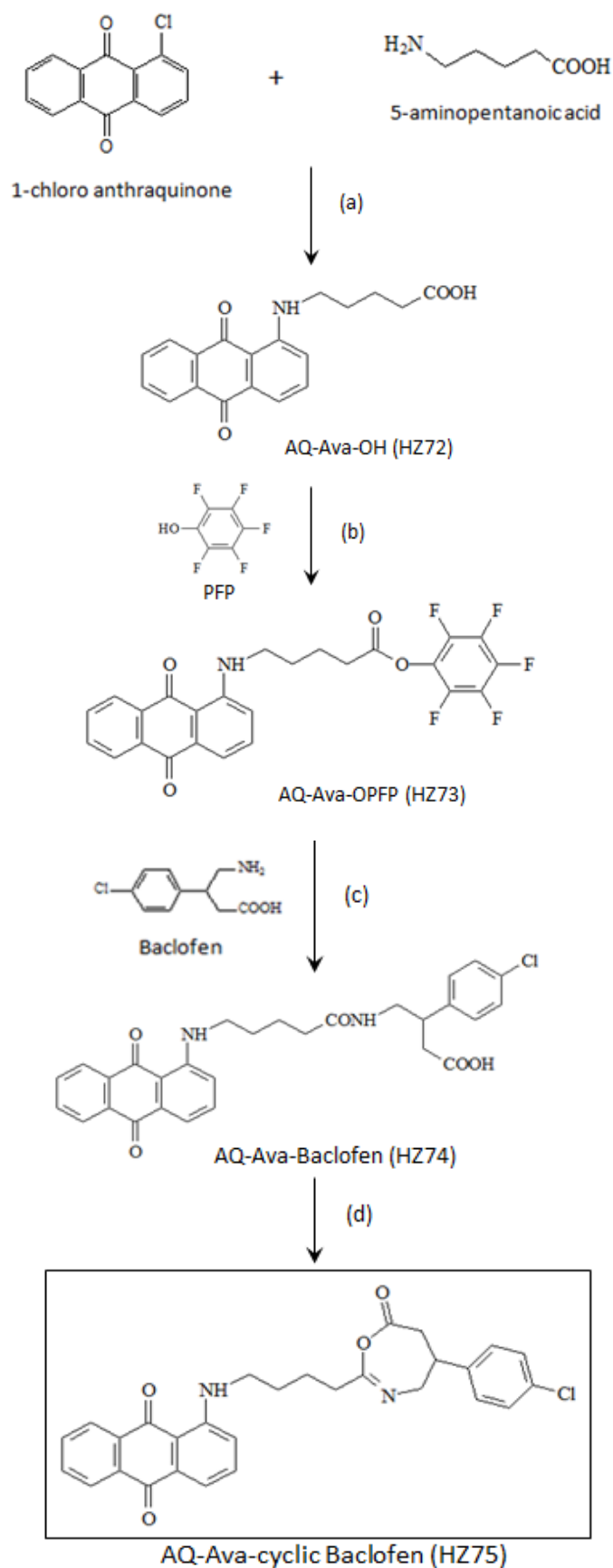
Reagents and Conditions: (a)6-aminohexanoic acid, NaOH, DMSO, 95°C (b)PFP, DCC, DMAP, dichloromethane (c)baclofen, NaOH$_{(aq)}$, DMF (d)(AC)$_2$O reflux

**Scheme 26.** Outline of Baclofen Prodrug (HZ75) Synthesis

The prodrug AQ-Ava-cyclic Baclofen (HZ75) chemical structure was confirmed by its ^{1}H NMR spectrum. The lactone type structure of HZ75 compound gave a multiplet signal at 3.5-3.67 ppm assigned to the methine proton (H-5). The signals at 2.72-3.15 ppm and 3.7-4.38 ppm recognised to be H-6 (O-CO-C$\underline{H}_2$) and H-4 (C=N-C$\underline{H}_2$), respectively. The p-substituted pattern of aromatic protons of the phenyl ring together with the anthraquinone protons showed signals from 7.15-7.22 ppm and from 7.3 to 8.33 ppm. Furthermore, the mass spectrum (M+H)$^+$ showed a signal at m/z 501 corresponding to the molecular mass of 500 for prodrug HZ75 **(Figure 29)**, together with m/z 501 for (M+Na)$^+$.
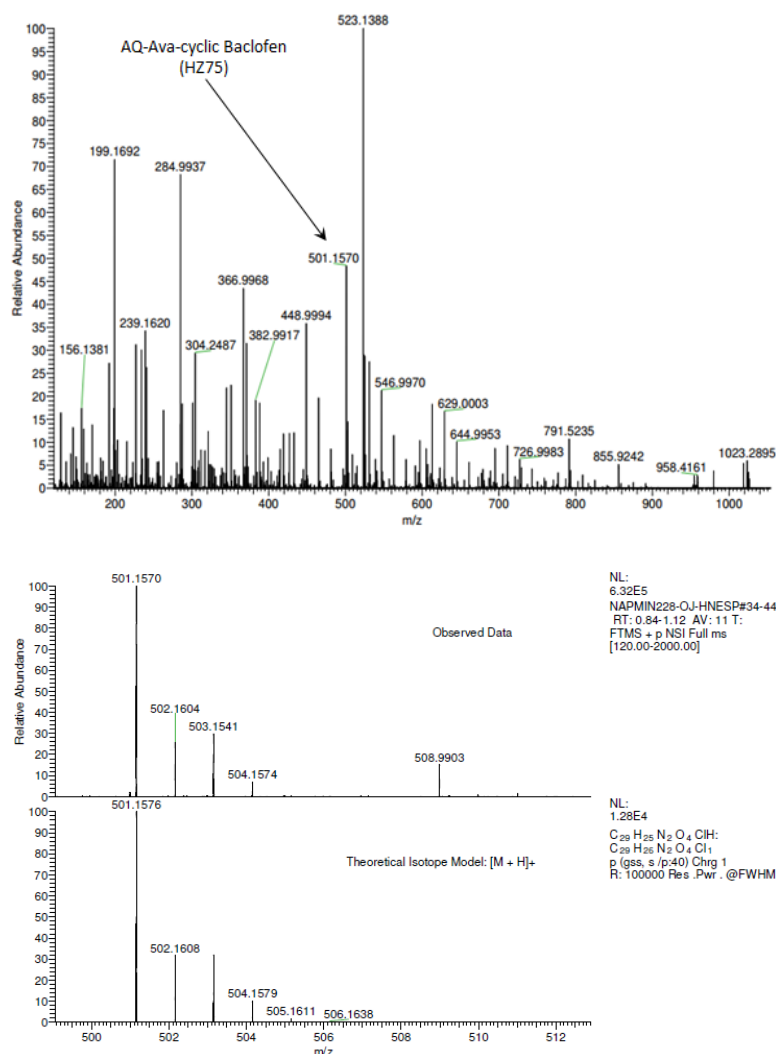


**Figure 29**. ESI (+) Mass spectrum of prodrug AQ-Ava-cyclic Baclofen (HZ75)

### 2.3.5 Synthesis of AQ-GABA-cyclic Baclofen (HZ79)

Gamma-Aminobutyric acid was used to build up the prodrug AQ-GABA-cyclic Baclofen (HZ79) **Scheme 27**. For the chemical structure of HZ79, it has a shorter spacer in the middle than AQ-Ava-cyclic Baclofen (HZ75) and AQ-Ahx-cyclic Baclofen (HZ69).



1-chloroanthraquinone

Gamma-Aminobutyric acid

AQ-GABA-OH (HZ76)

PFP

AQ-GABA-OPFP (HZ77)

Baclofen

AQ-GABA-Baclofen (HZ78)

AQ-GABA-cyclic Baclofen (HZ79)
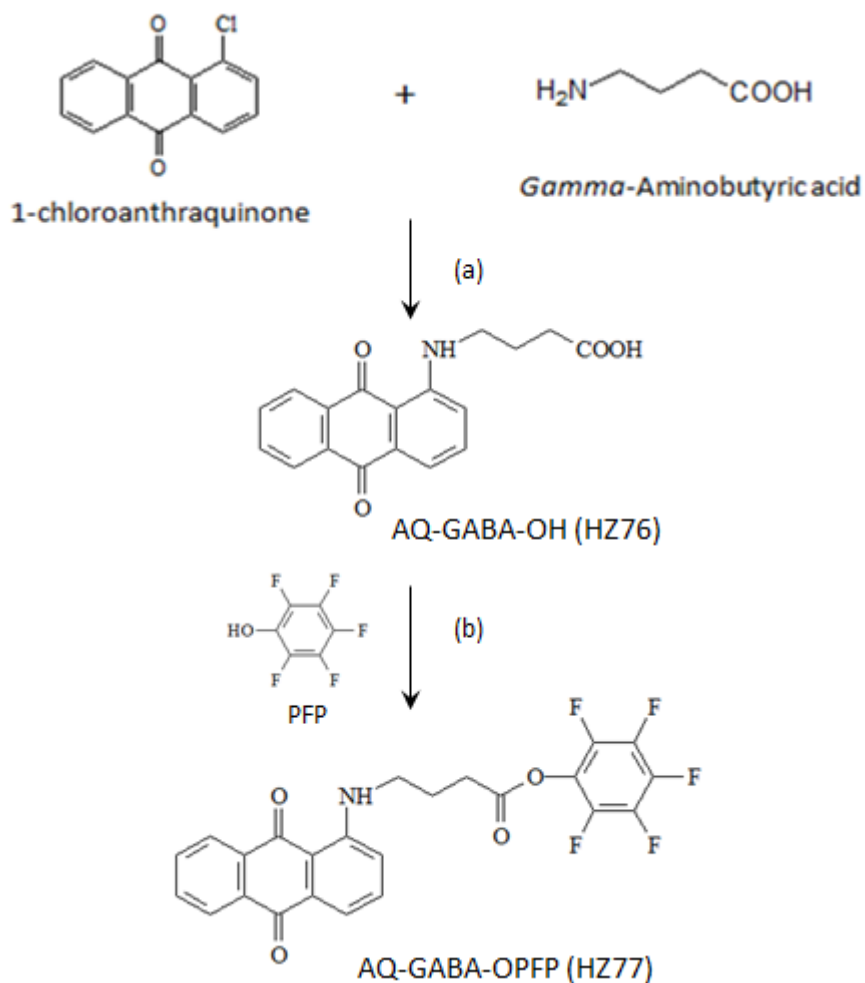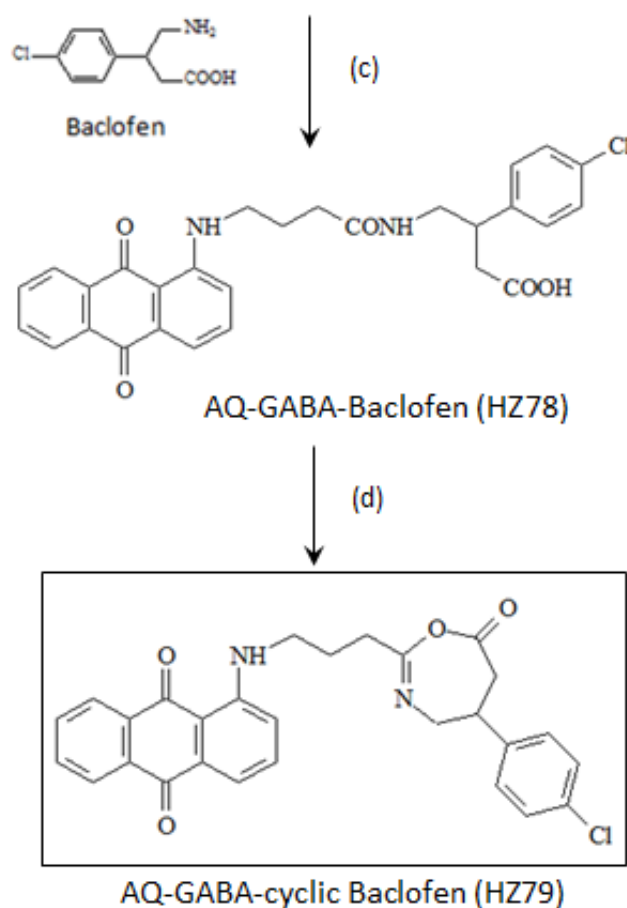
Reagents and Conditions: (a) Gamma-aminobutyric acid, NaOH, DMSO, 95°C (b) pentafluorophenol, DCC, DMAP, dichloromethane; (c) baclofen, NaOH$_{(aq)}$, DMF; (d) (AC)$_2$O

**Scheme 27.** Outline of Baclofen Prodrug (HZ79) Synthesis

The final compound AQ-GABA-cyclic Baclofen (HZ79) was characterized by its mass spectrum (M+H)$^+$ which showed a signal at m/z 487, corresponding to a relative molecular mass of 486 Da **(Figure 30)**.
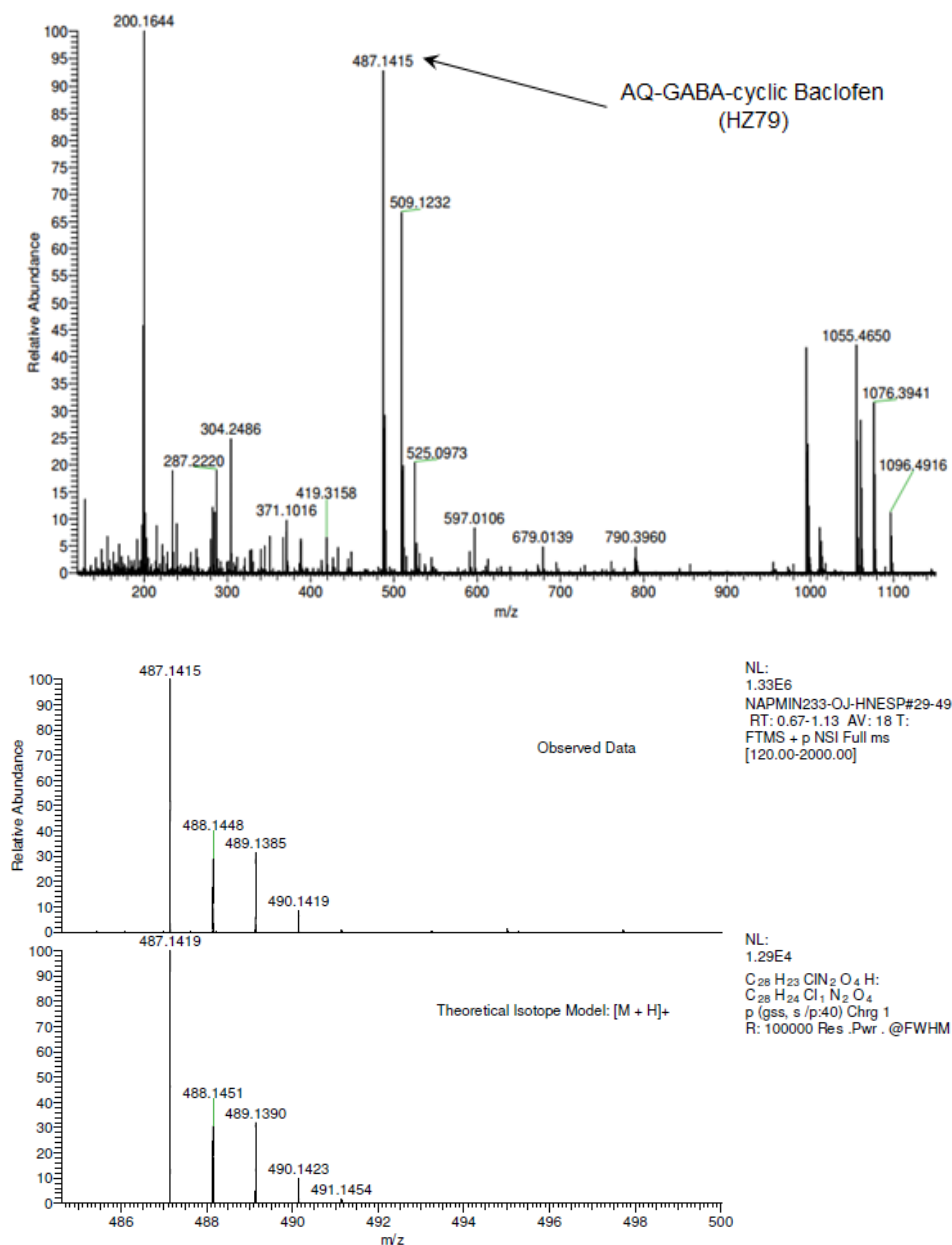
**Figure 30**. ESI (+) Mass spectrum of prodrug AQ-GABA-cyclic Baclofen (HZ79)

## 2.3.6 Synthesis of AQ-[PEG Spacer]-Succinyl-Baclofen (HZ82)

The starting material for the synthesis of prodrug AQ-[PEG Spacer]-Succinyl-Baclofen (HZ82) as shown in **Scheme 28** was the anthraquinone derivative (NU:UB 432). This compound which consists of anthraquinone and polyethylene glycol (PEG) has been used extensively in previous research within this laboratory, particularly in the design of fluorogenic probes (Ding, 2014). The anthraquinone-PEG spacer (NU:UB 432) was reacted

with succinic anhydride in DMF by the addition of DIPEA to the solution (Scheme 5). The reaction was completed overnight. The crude product AQ-[PEG Spacer]-Succinyl (HZ80) was purified by solvent extraction and silica gel column chromatography. The pure HZ80 was collected in diethyl ether. DCC and DMAP were used as standard regents for the addition of PFP to the AQ-[PEG Spacer]-Succinyl (HZ80). The reaction mixture was suspended in dichloromethane. The byprodruct dicyclohexylurea (DCU) was filtered off.
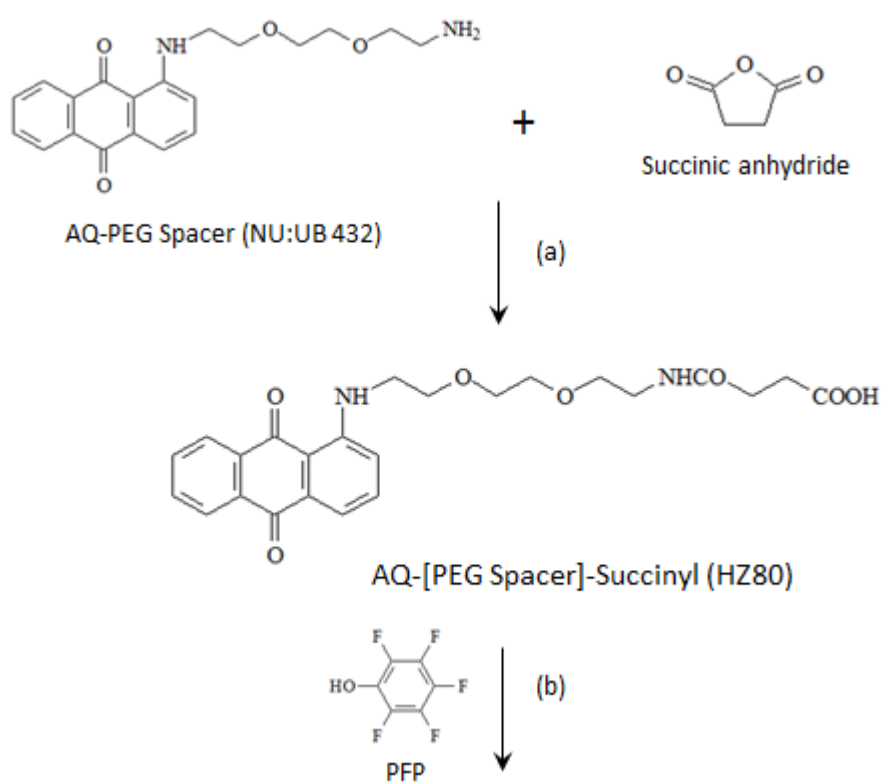


AQ-PEG Spacer (NU:UB 432)

Succinic anhydride

(a)

AQ-[PEG Spacer]-Succinyl (HZ80)

PFP

(b)

AQ-[PEG Spacer]-Succinyl-OPFP (HZ81)

Baclofen

(c)

AQ-[PEG Spacer]-Succinyl-Baclofen (HZ82)

Reagents and Conditions: (a) succinic anydride, DIPEA, DMF; (b) pentafluorophenol, DCC, DMAP, dichloromethane; (c) baclofen, NaOH$_{(aq)}$, DMF

**Scheme 28.** Outline of Baclofen Prodrug (HZ82) Synthesis

Baclofen was finally coupled to the AQ-[PEG Spacer]-Succinyl-OPFP (HZ81). Two round bottomed flask were used. One of them had baclofen, NaOH and water in DMF. Another flask had the AQ-[PEG Spacer]-Succinyl-OPFP (HZ81) in DMF. Both flasks were put on a hot water bath. The baclofen mixture in flask one was added to the HZ81 flask drop wise. The reaction was very slow. By the TLC test, the reaction had mostly completed in 1 week. The mixture was extracted and purified by column chromatography.

Prodrug AQ-[PEG Spacer]-Succinyl-Baclofen (HZ82) was characterized by NMR and its electrospray mass spectrum which gave a signal at m/z 650 for (M+H)$^+$ corresponding to a molecular mass of 649 **(Figure 31)**. The $^1$H NMR spectrum showed signals between 2.15 and 3.8 ppm were assigned to the methylene groups of the PEG spacer. The anthraquinone protons were fully assigned; H-2

at 7.2 ppm, H-4 at 7.45 ppm, H-3 at 7.6-7.7 ppm, H-6 and H-7 gave a multiplet at 7.78-7.95 ppm, H-8 at 8.08-8.15 ppm, H-5 at 8.15-8.25 ppm. The signals at 7.2-7.37 reflected the chlorobenzene protons of baclofen group.
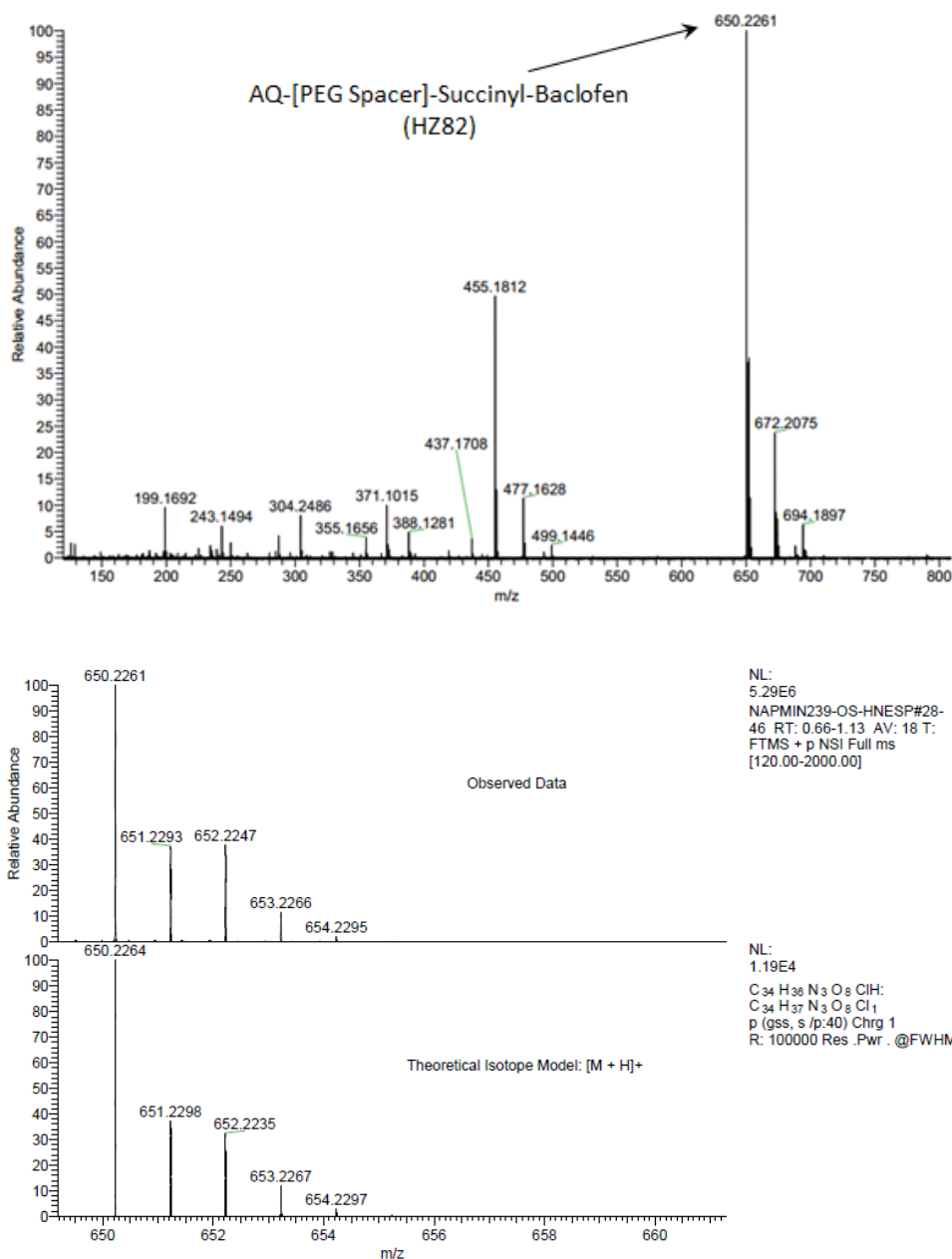


**Figure 31**. ESI (+) Mass spectrum of prodrug AQ-[PEG Spacer]-Succinyl-Baclofen (HZ82)

## 2.3.7 Synthesis of AQ-[PEG Spacer]-Succinyl-cyclic Baclofen (HZ83)

The baclofen prodrug AQ-[PEG Spacer]-Succinyl-Baclofen (HZ82) was further reacted with acetic anhydride to form the lipophilic analogue of baclofen

AQ-[PEG Spacer]-Succinyl-cyclic Baclofen HZ83 **(Scheme 29)**.



AQ-[PEG Spacer]-Succinyl-Baclofen (HZ82)

(a)

AQ-[PEG Spacer]-Succinyl-cyclic Baclofen (HZ83)
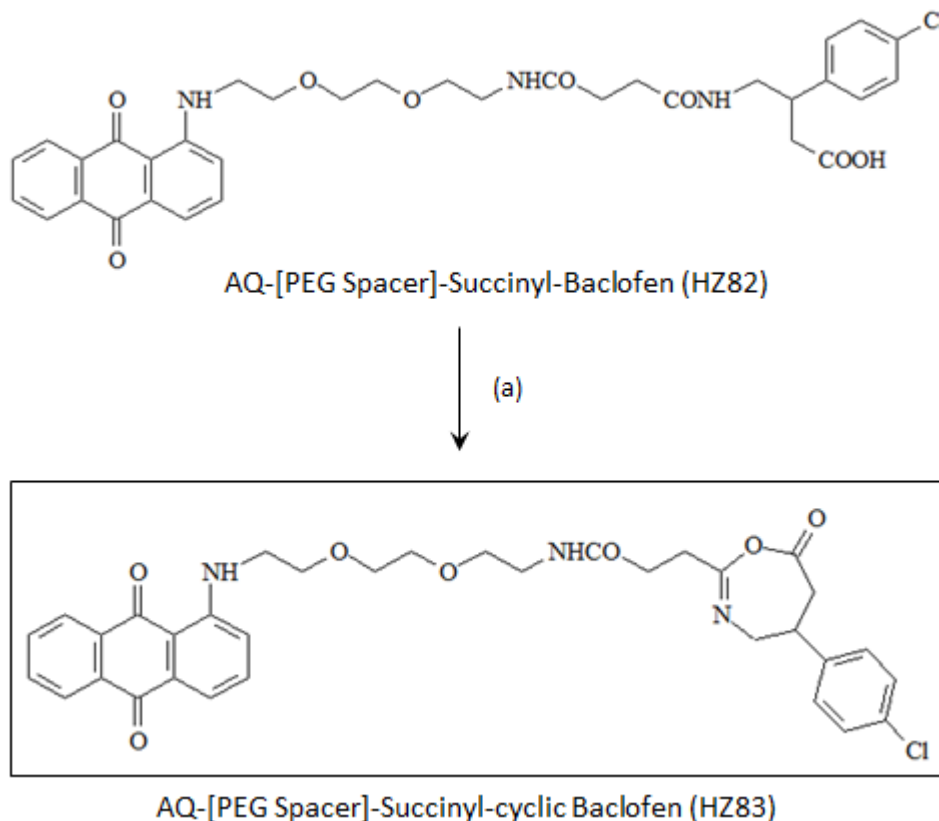
Reagents and Conditions: (a) $(Ac)_2O$

**Scheme 29.** Outline of Baclofen Prodrug (HZ83) Synthesis

The final compound AQ-[PEG Spacer]-Succinyl-cyclic Baclofen (HZ83) was characterised by NMR and mass spectrometry. The lactone type structure of HZ83 compound exhibited a multiplet signal at 3.5-3.7 ppm assigned to the methine proton (H-5). The signals at 2.9-3.25 ppm and 3.8-4.25 ppm recognised to be H-6 (O-CO-C$\underline{H}_2$) and H-4 (C=N-C$\underline{H}_2$), respectively. All of the aromatic protons of anthraquinone were successfully assigned; H-2 appeared at 7.06-7.22 ppm, H-3 and H-4 were found between 7.53-7.68 ppm, H-6 and H-7 at 7.68-7.85 ppm, H-5 and H-8 at 8.22-8.35 ppm. In the mass spectrum **(Figure 32)** of prodrug HZ83, a signal at 632 m/z was assigned to the ion $(M+H)^+$ confirming the molecular mass of 631.
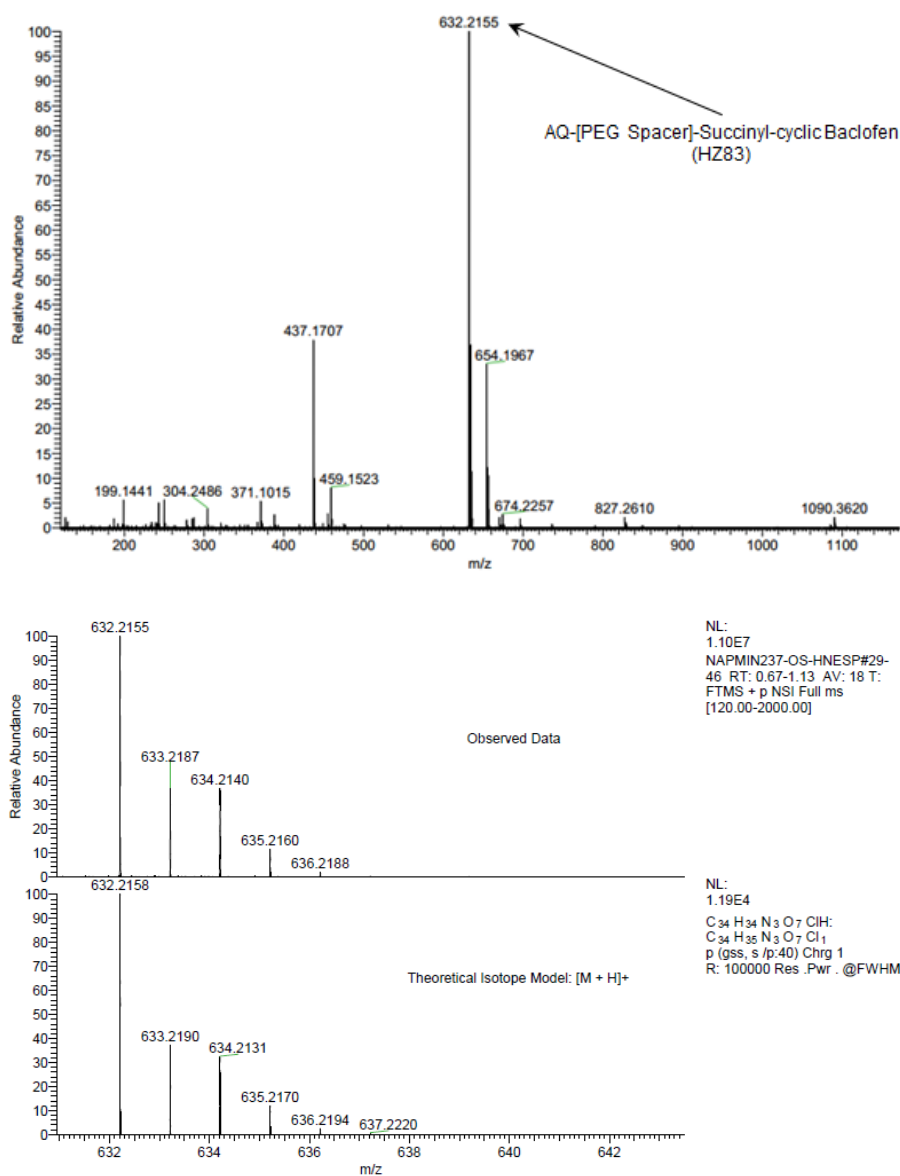
**Figure 32**. ESI (+) Mass spectrum of prodrug AQ-[PEG Spacer]-Succinyl-cyclic Baclofen (HZ83)
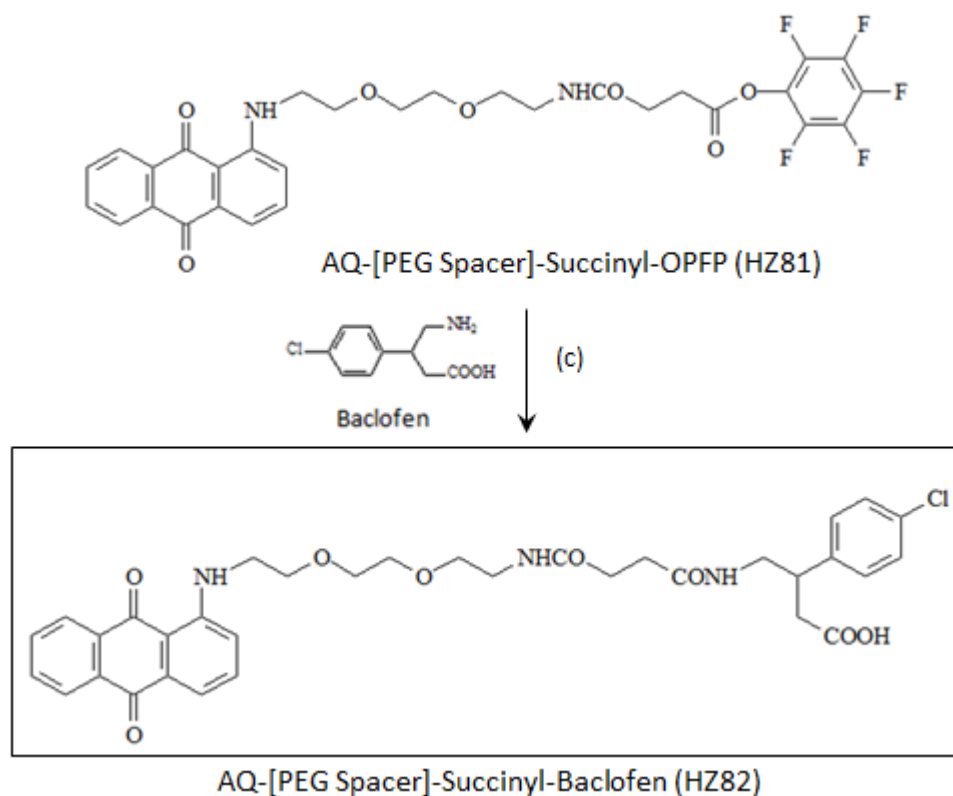
### 2.3.8 Synthesis of AQ-[propyl spacer]-Pro-succinyl-Baclofen (HZ86)

The starting material for the synthesis of prodrug AQ-[propyl spacer]-Pro-succinyl-Baclofen (HZ86) (**Scheme 30**) was the anthraquinone D-proline derivative, NU:UB 46. NU:UB 46 is the D-isomer of one of the leading members of the NU:UB series of spacer-linkedanthraquinone-amino acid conjugates, NU:UB 31. Both NU:UB 31 (L-pro conjugate) and NU:UB 49 (D-pro conjugate) were active in vitro against the MAC15A colon adenocarcinoma cell line, with IC50 values of 2.5 and 3.5µM, respectively, for the L and D isomers. Additionally, NU:UB 31 has broad-spectrum activity in vitro at low micromolar

concentrations in panels of human and animal tumour cell lines, including those of the NCI 60 cell line anticancer drug screen; NU:UB 31 retains activity in cell lines that over-express P-glycoprotein. It is a dual topoisomerase I and II inhibitor and is active in vivo in experimental colon cancer (Mincher et al., 2000; Turnbull, 2003). Previously, NU:UB 31 has successfully been incorporated into a MMP activated prodrug, EV1-FITC (Van Valckenborgh et al., 2005). Here, the D-isomer of NU:UB 31, NU:UB 46, has been conjugated with baclofen via a succinate linker to afford a prodrug with dual topoisomerase inhibiting cytotoxicity together with potential GABA modulating activity. The reactions condition was same as the synthesis of AQ-[PEG Spacer]-Succinyl-Baclofen (HZ82).



AQ-[propyl spacer]-Pro-H

Succinic anhydride

(a)

AQ-[propyl spacer]-Pro-succinyl (HZ84)

(b)
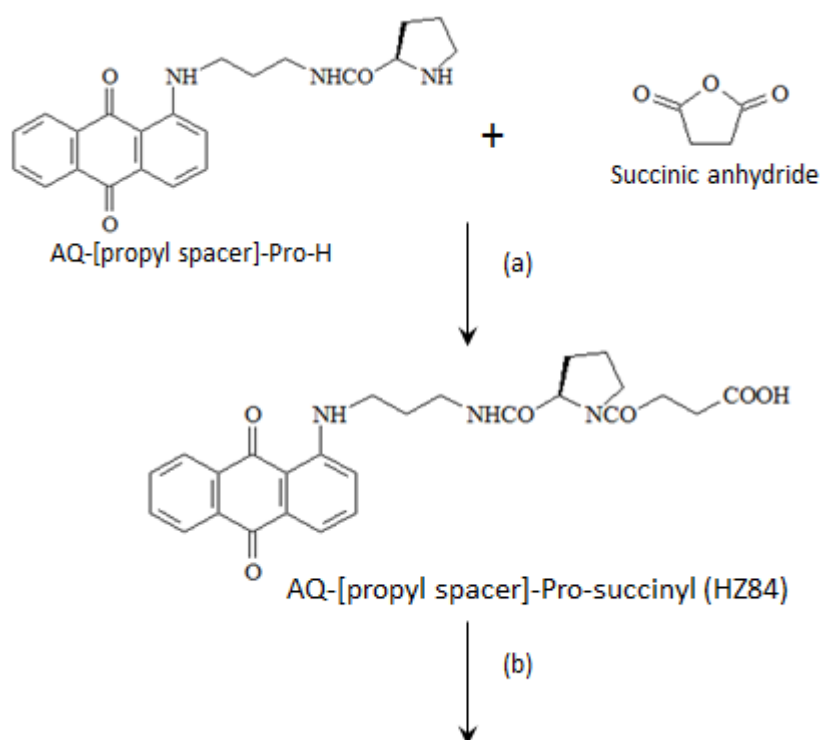
*This synthesis scheme is continued on the next page

AQ-[propyl spacer]-Pro-succinyl-OPFP (HZ85)

(c)

Baclofen

AQ-[propyl spacer]-Pro-succinyl-Baclofen (HZ86)
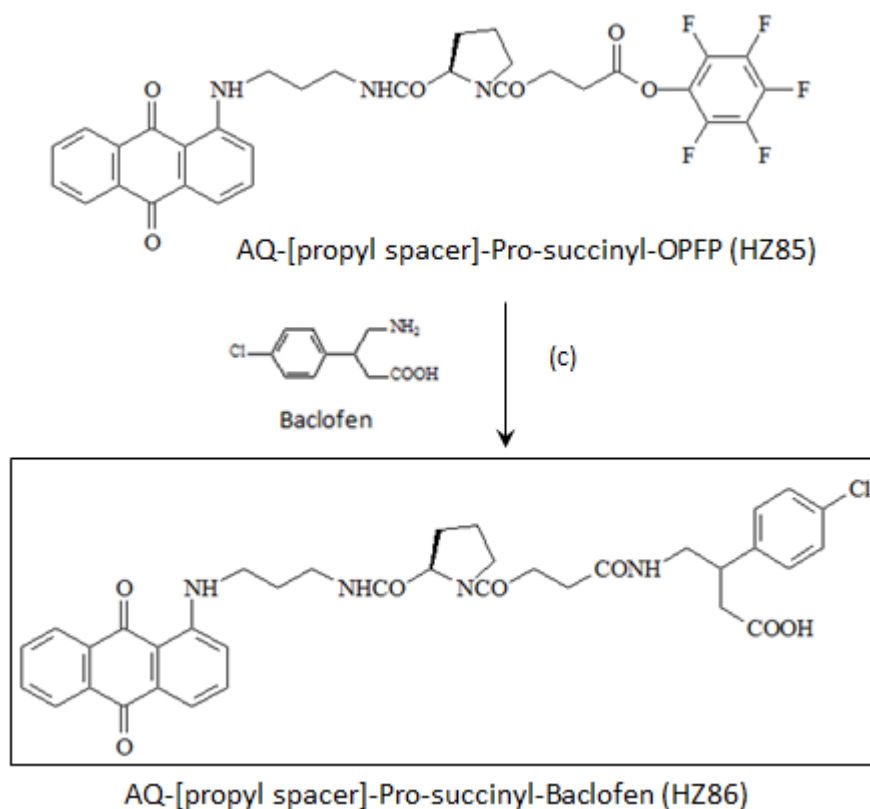
Reagents and Conditions: (a) succinic anhydride, DIPEA, DMF; (b) pentafluorophenol, DCC, DMAP, dichloromethane; (c) baclofen, NaOH$_{(aq)}$, DMF

**Scheme 30.** Outline of Baclofen Prodrug (HZ86) Synthesis

The $^1$H NMR spectrum of AQ-[propyl spacer]-Pro-succinyl-Baclofen (HZ86) showed signals between 1.7 and 4.25 were assigned to the methylene groups of the propyl and proline spacer. The anthraquinone protons were fully assigned; H-2 at 7.05-7.38 ppm, H-3, H-4, H-6 and H-7 gave a multiplet at 7.7-7.95 ppm, H-5 and H-8 gave a quartet between 8.1 and 8.3 ppm. The signals at 7.05-7.38 reflected the chlorobenzene protons of baclofen group.

The mass spectrum (M+H)$^+$ showed a signal at m/z 673 corresponding to the molecular mass of 672 for prodrug HZ86 **(Figure 33)**.
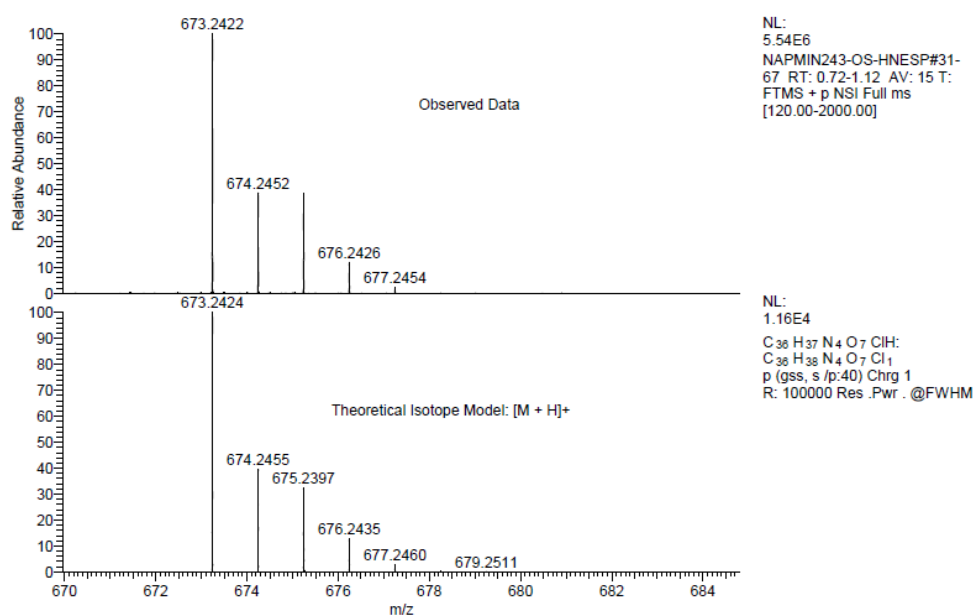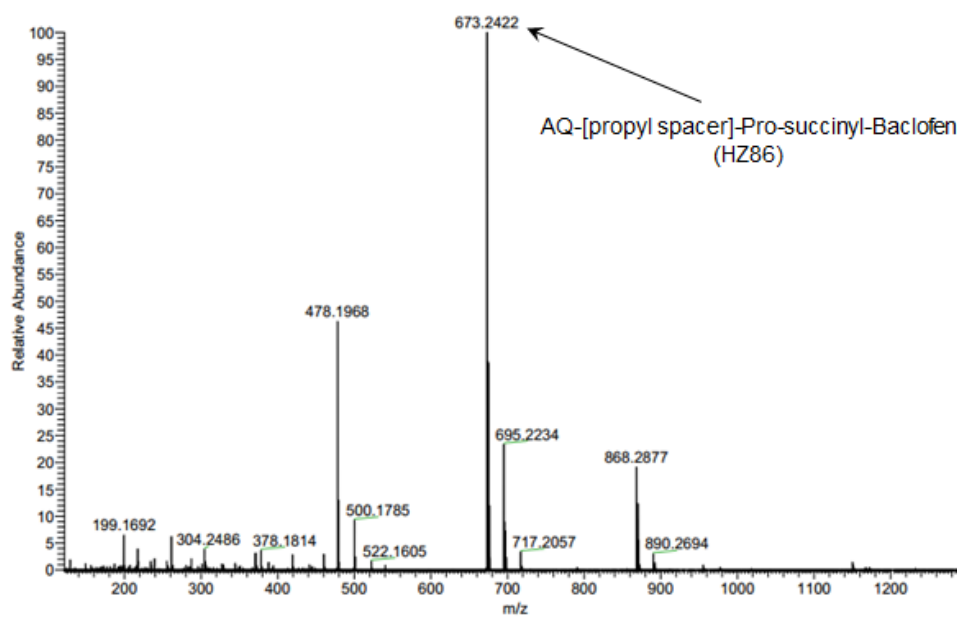
**Figure 33**. ESI (+) Mass spectrum of prodrug AQ-[propyl spacer]-Pro-succinyl-Baclofen (HZ86)

## 2.3.9 Synthesis of AQ-[propyl spacer]-Pro-succinyl-cyclic Baclofen (HZ87)

The prodrug AQ-[propyl spacer]-Pro-succinyl-Baclofen (HZ86) was converted to the cyclic baclofen prodrug AQ-[propyl spacer]-Pro-succinyl-cyclic Baclofen (HZ87) using the dehydrating agent acetic anhydride **(Scheme 31)**.

AQ-[propyl spacer]-Pro-succinyl-Baclofen (HZ86)

(a)

AQ-[propyl spacer]-Pro-succinyl- cyclic Baclofen (HZ87)
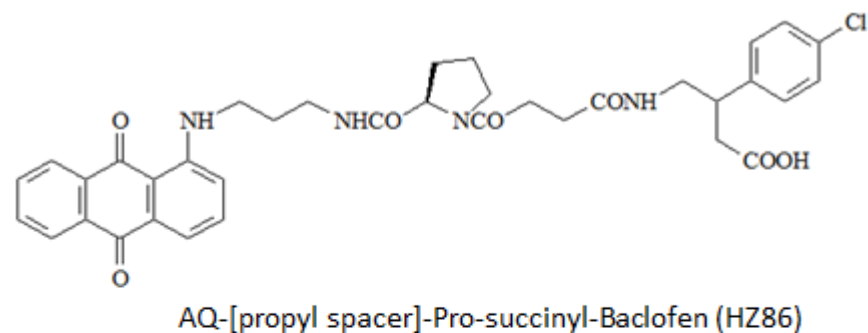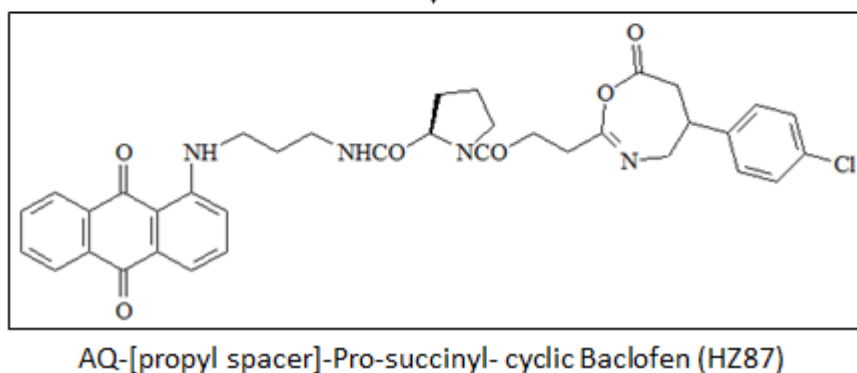
Reagents and Conditions: (a) (Ac)$_2$O

**Scheme 31.** Outline of Baclofen Prodrug (HZ87) Synthesis

**Figure 34** below shows the tumour pH activation of AQ-[propyl spacer]-Pro-succinyl-cyclic Baclofen (HZ87). HZ87 has the cyclic baclofen indicated by the red colour. The acidic environment of the tumour cells will cause the hydrolysis reaction. The cyclic ring will be opened and further hydrolysis to break the prodrug and release anthraquinone-D-proline and baclofen. They are both anticancer agents. So the cyclic baclofen prodrug AQ-[propyl spacer]-Pro-succinyl-cyclic Baclofen (HZ87) is actually a twin drug.
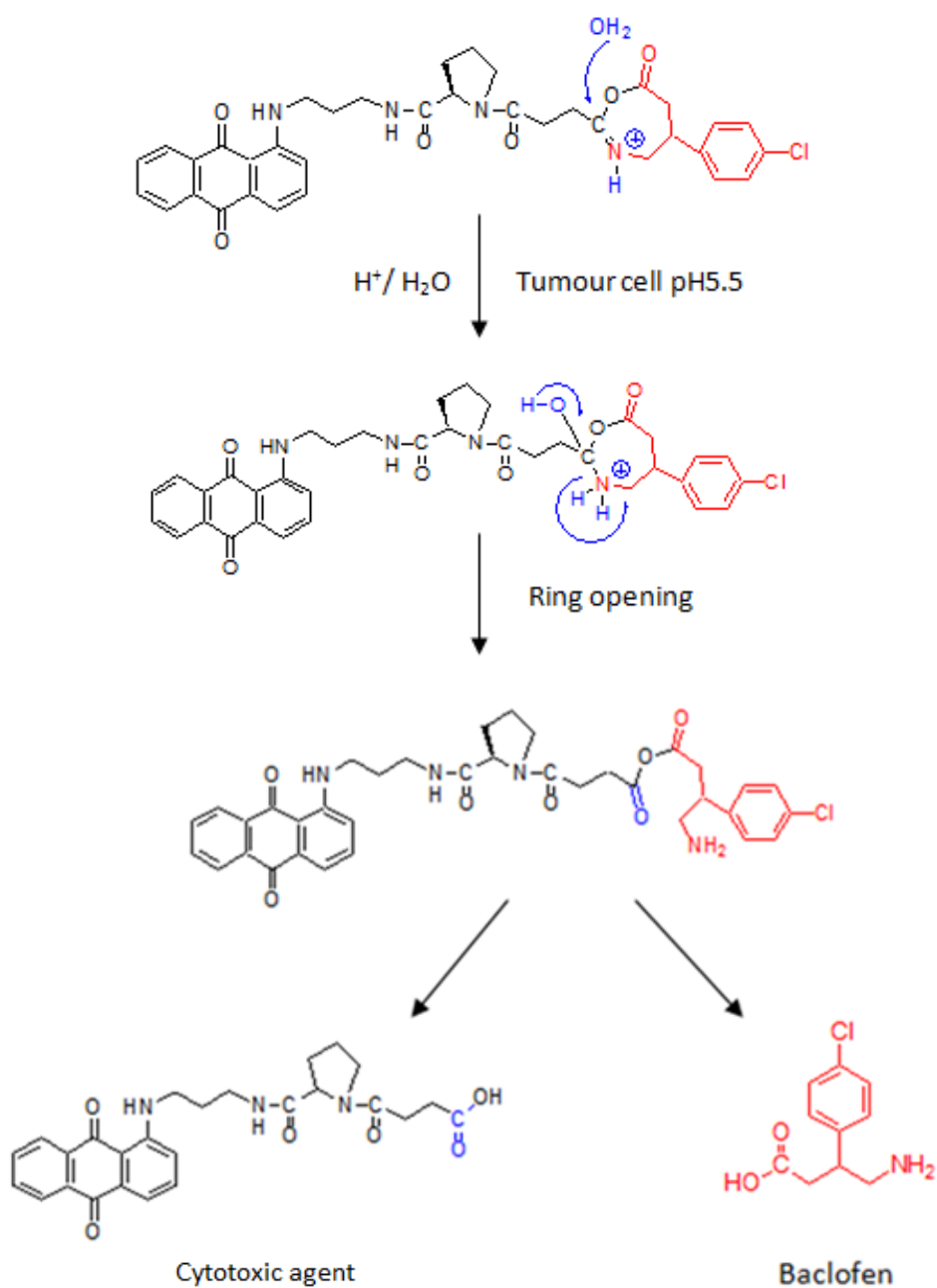
**Figure 34**. Tumour pH (5-6) activation of HZ87

The cyclic baclofen prodrug HZ87 was characterized by NMR and Mass spectroscopy. The structure of HZ87 was confirmed by its ^{1}H NMR spectrum. Most of the aromatic protons of anthraquinone were successfully assigned; H-3 and H-4 appeared at 7.5-7.67 ppm, H-6 and H-7 were found between 7.68-7.84 ppm, H-5 and H-8 at 8.12-8.3 ppm. The protons of chlorobenzene were also found between 6.9 and 7.35 ppm.

For mass spectrum, a signal at m/z 655 for the mono-cation (M+H)$^+$ confirmed the molecular mass of 654 Daltons **(Figure 35)**.
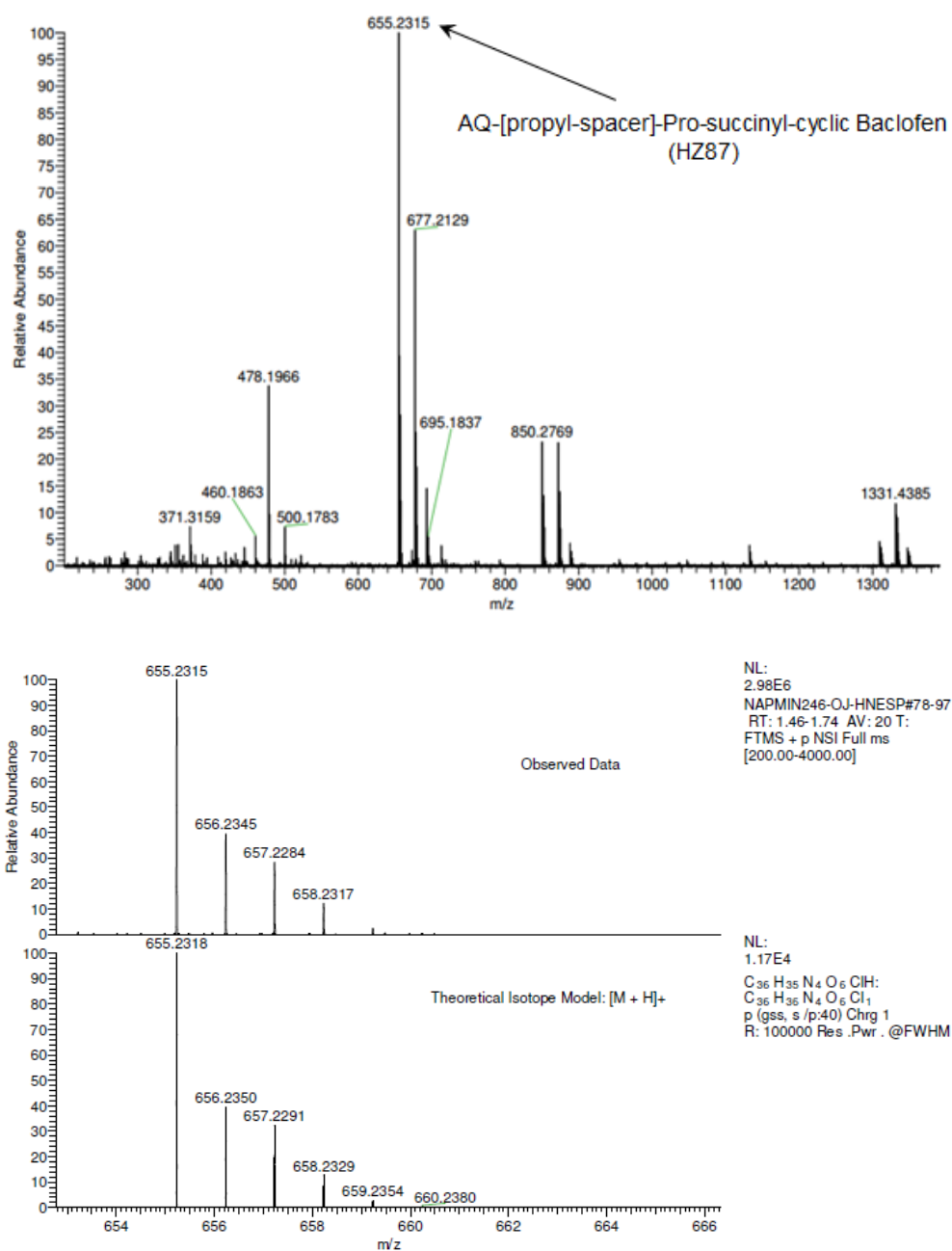


**Figure 35**. ESI (+) Mass spectrum of prodrug
AQ-[propyl-spacer]-Pro-succinyl-cyclic Baclofen (HZ87)

## 2.3.10 Lipophilicity test: Determination of the Distribution Coefficient

Because high lipophilic properties are crucial for the prodrugs to cross the BBB the lipophilicity assay was performed. The prodrugs were partitioned between octanol and PBS. The Eppendorf tubes were shaken for 24 hours. The **Figure**

**36** below is an example of the images of the Eppendorf tubes with prodrugs. The top phases are Octanol used to mimic the lipophilic environment. It can be seen from the colour difference; all the four compounds have more prodrugs in the octanol phase than in the PBS water phase. The concentrations of prodrugs present in each layer were determined from the calibration curves and the distribution coefficient was calculated using the equation given in [**Graph 1~4**]. **Figure 37** is for calculation of distribution coefficient (Leo, Hansch and Elkins, 1971).



|  HZ82 | HZ83 | HZ86 | HZ87 |
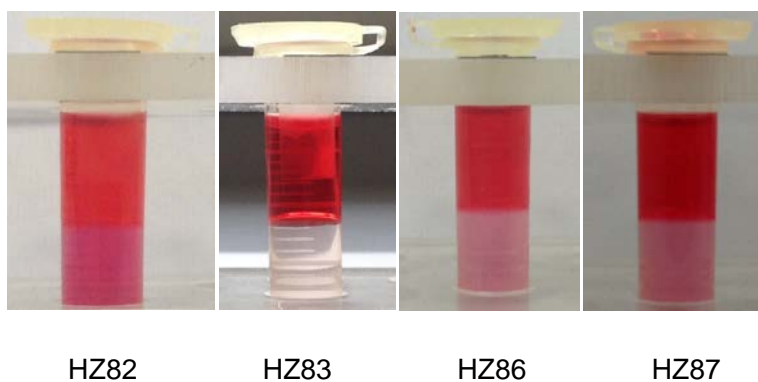
**Figure 36.** Eppendorf tubes of Lipophilicity test

$$\log \ D_{\text{oct/wat}} = \log \left( \frac{[\text{solute}]_{\text{octanol}}}{[\text{solute}]_{\text{water}}^{\text{ionized}} + [\text{solute}]_{\text{water}}^{\text{neutral}}} \right)$$

**Figure 37**. Equation of distribution coefficient

| Run No. | Solvent | Absorbance in cuvette | y=mx+c | Conc. in cuvette (μM) | Dilution Factor | Original conc in eppendorf (μM). | Log D | Log D (Mean ±) |
|---|---|---|---|---|---|---|---|---|
| 1 | Octanol | 0.2126 | y = 0.0187x + 0.0028 | 11.22 | 30(100ul in 3ml) | 336.58 | 0.60 | |
| 1 | PBS (pH7.4) | 0.1041 | y = 0.0167x + 0.0088 | 5.7 | 15(200ul in 3ml) | 85.5 | | |
| 2 | Octanol | 0.1997 | y = 0.0187x + 0.0028 | 10.53 | 30(100ul in 3ml) | 315.9 | 0.74 | |
| 2 | PBS (pH7.4) | 0.0407 | y = 0.0167x + 0.0088 | 1.91 | 30(100ul in 3ml) | 57.3 | | 0.707±0.10 |
| 3 | Octanol | 0.2351 | y = 0.0187x + 0.0028 | 12.4 | 30(100ul in 3ml) | 372.67 | 0.79 | |
| 3 | PBS (pH7.4) | 0.1782 | y = 0.0167x + 0.0088 | 10.14 | 6(500ul in 3ml) | 60.84 | | |

**Graph 1.** Calibration curve and distribution coefficient of HZ82 in both Octanol and PBS
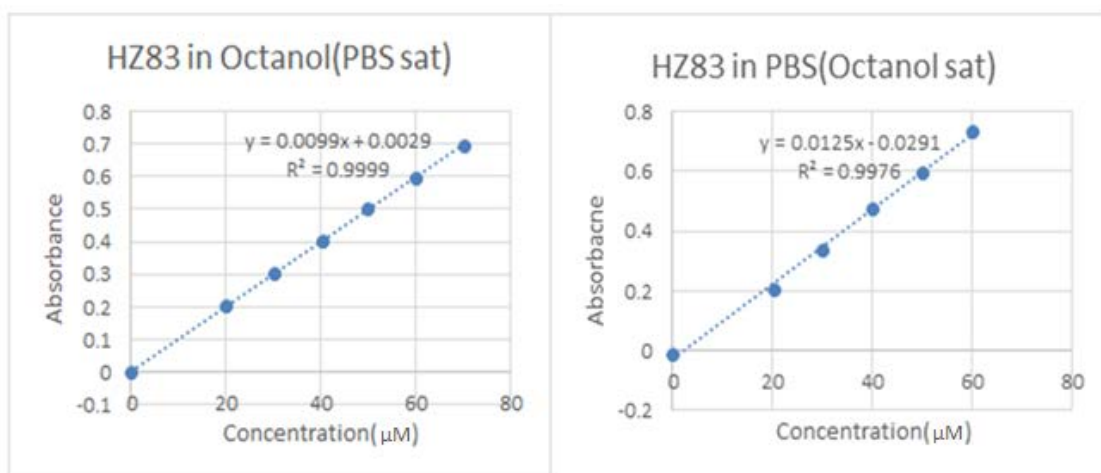
| Run No. | Solvent | Absorbance in cuvette | y=mx+c | Conc. in cuvette (μM) | Dilution Factor | Original conc in eppendorf (μM). | Log D | Log D (Mean ±) |
|---|---|---|---|---|---|---|---|---|
| 1 | Octanol | 0.2583 | y = 0.0099x + 0.0029 | 25.8 | 30 | 774 | 1.84 | |
| 1 | PBS (pH7.4) | 0.0414 | y = 0.0125x - 0.0291 | 5.64 | 2 | 11.28 | | |
| 2 | Octanol | 0.2339 | y = 0.0099x + 0.0029 | 23.3 | 30 | 700 | 1.92 | 1.82±0.10 |
| 2 | PBS (pH7.4) | 0.0239 | y = 0.0125x - 0.0291 | 4.24 | 2 | 8.48 | | |
| 3 | Octanol | 0.1676 | y = 0.0099x + 0.0029 | 16.64 | 30 | 499.1 | 1.72 | |
| 3 | PBS (pH7.4) | 0.031 | y = 0.0125x - 0.0291 | 4.8 | 2 | 9.6 | | |

**Graph 2**. Calibration curve and distribution coefficient of HZ83 in both Octanol and PBS

| Run No. | Solvent | Absorbance in cuvette | y=mx+c | Conc. in cuvette (µM) | Dilution Factor | Original conc in eppendorf (µM). | Log D | Log D (Mean ±) |
|---|---|---|---|---|---|---|---|---|
| 1 | Octanol | 0.301 | y = 0.0075x + 0.0038 | 39.63 | 15(200ul in 3ml) | 594.4 | 0.83 | |
| 1 | PBS (pH7.4) | 0.1044 | y = 0.007x + 0.002 | 14.63 | 6(500ul in 3ml) | 87.77 | | |
| 2 | Octanol | 0.2633 | y = 0.0075x + 0.0038 | 34.6 | 15(200ul in 3ml) | 519 | 0.84 | 0.81±0.03 |
| 2 | PBS (pH7.4) | 0.0906 | y = 0.007x + 0.002 | 12.66 | 6(500ul in 3ml) | 75.94 | | |
| 3 | Octanol | 0.2559 | y = 0.0075x + 0.0038 | 33.61 | 15(200ul in 3ml) | 504.15 | 0.78 | |
| 3 | PBS (pH7.4) | 0.1003 | y = 0.007x + 0.002 | 14.0 | 6(500ul in 3ml) | 84.26 | | |

**Graph 3**. Calibration curve and distribution coefficient of HZ86 in both Octanol and PBS
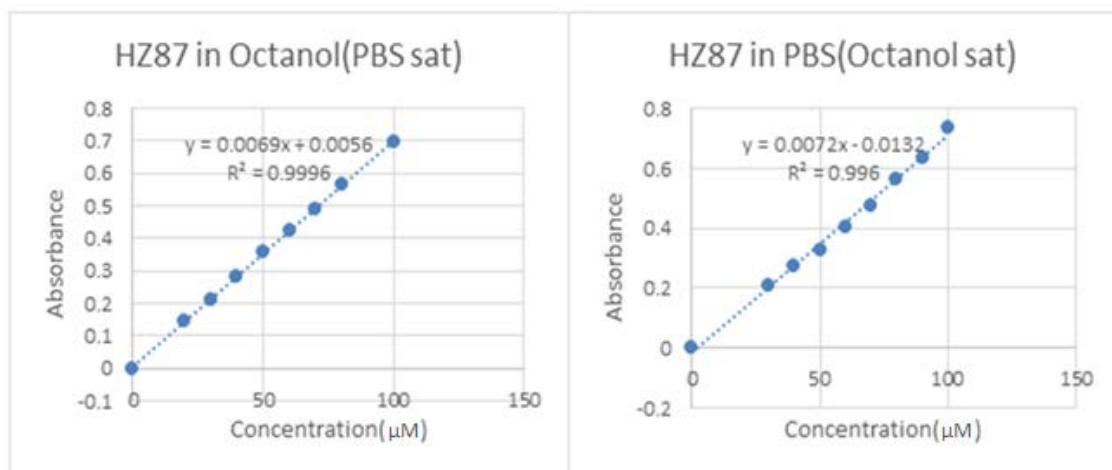
| Run No. | Solvent | Absorbance in cuvette | y=mx+c | Conc. in cuvette ($\mu$M) | Dilution Factor | Original conc in eppendorf ($\mu$M). | Log D | Log D (Mean ±) |
|---|---|---|---|---|---|---|---|---|
| 1 | Octanol | 0.3663 | y = 0.0069x + 0.0056 | 52.28 | 15 | 784.13 | 0.97 | |
| 1 | PBS (pH7.4) | 0.0675 | y = 0.0072x - 0.0132 | 11.2 | 7.5 | 84 | | |
| 2 | Octanol | 0.2914 | y = 0.0069x + 0.0056 | 41.42 | 15 | 621.3 | 0.78 | 0.92±0.12 |
| 2 | PBS (pH7.4) | 0.0361 | y = 0.0072x - 0.0132 | 6.84 | 15 | 102.7 | | |
| 3 | Octanol | 0.3666 | y = 0.0069x + 0.0056 | 52.31 | 15 | 784.65 | 0.99 | |
| 3 | PBS (pH7.4) | 0.0633 | y = 0.0072x - 0.0132 | 10.63 | 7.5 | 79.69 | | |

**Graph 4**. Calibration curve and distribution coefficient of HZ87 in both Octanol and PBS

### 2.3.11 DNA binding assay

The DNA binding properties of the prodrugs were tested by using the ethidium bromide displacement DNA binding assay. Ethidium bromide is a dye that can intercalate into the DNA double helix. The double stranded DNA will be saturated by ethidium bromide binding. The fluorescence of the DNA-bound ethidium bromide can be measured and by competing with the drug, the intensity should decrease with drug concentration and time (Olmsted and Kearns, 1997).

The binding affinity of each compound was determined by the $QE_{50}$ and the binding constant values ($K_{app}$). $QE_{50}$ is the mean concentration of compound that

causes 50% reduction of initial fluorescence intensity. The binding constant can be calculated using the equation: $K_{app} = (K_{EB}[EB])/[Drug]$. The $K_{EB}$ value $(1.0 \times 10^7 M^{-1})$ is the binding constant of ethidium bromide (Ghosh *et al.,* 2010).

The compound will has greater binding affinity if $QE_{50}$ value is smaller and binding constant is bigger. The **Graphs 5~9** below showed both $QE_{50}$ value and binding constant of tested prodrugs.
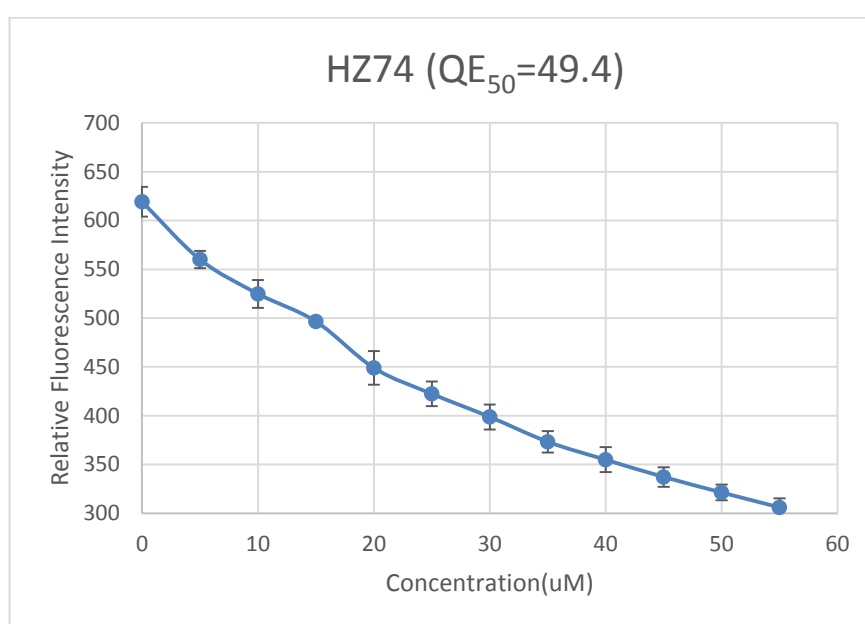


$$K_{app} = (K_{EB}[EB])/[Drug] = (1 \times 10^7 M^{-1} \times 30)/49.4 = 0.61 \times 10^7 M^{-1}$$

**Graph 5**. Variation of relative fluorescence intensity with different concentration of HZ74 in Tris-HCl buffer
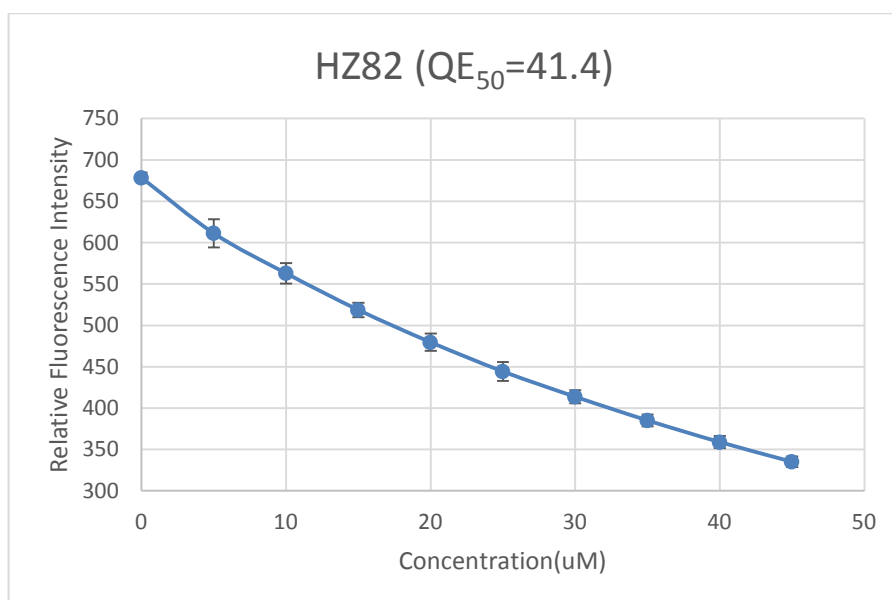
$$K_{app}=0.72 \times 10^7 M^{-1}$$

**Graph 6**. Variation of relative fluorescence intensity with different concentration of HZ82 in Tris-HCl buffer
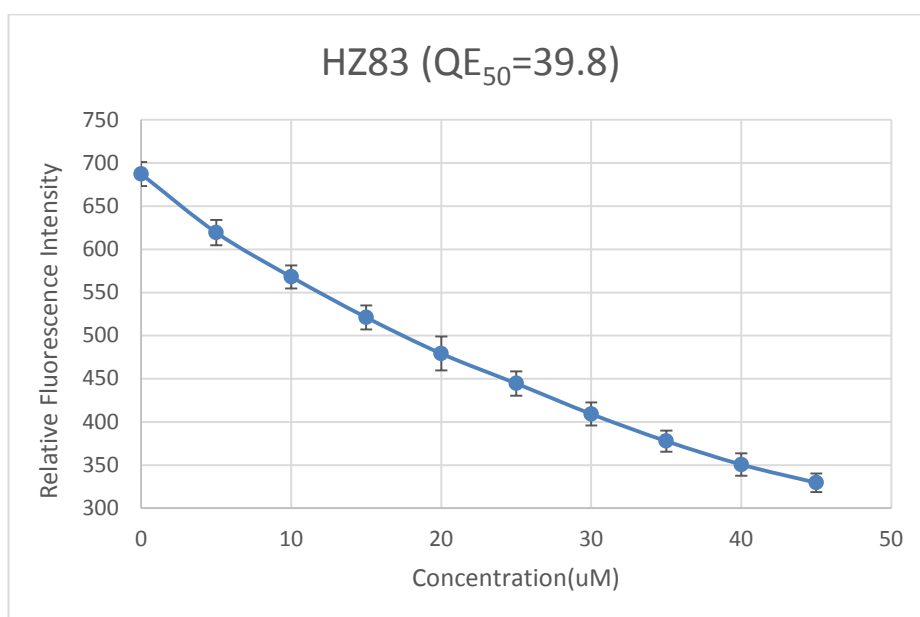


$$K_{app}=0.75 \times 10^7 M^{-1}$$

**Graph 7**. Variation of relative fluorescence intensity with different concentration of HZ83 in Tris-HCl buffer
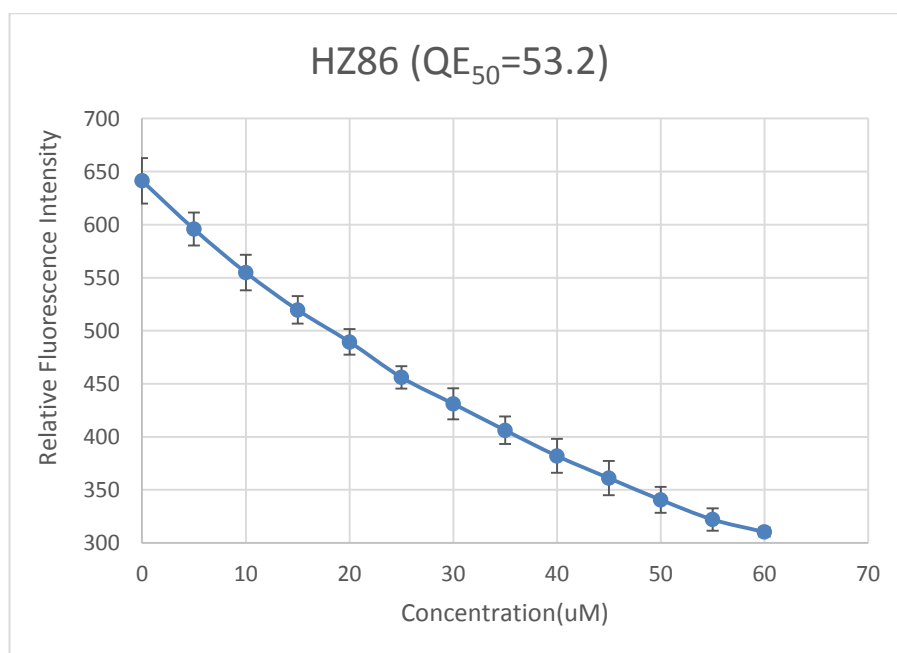
$K_{app}=0.56 \times 10^{7} M^{-1}$

**Graph 8**. Variation of relative fluorescence intensity with different concentration of HZ86 in Tris-HCl buffer
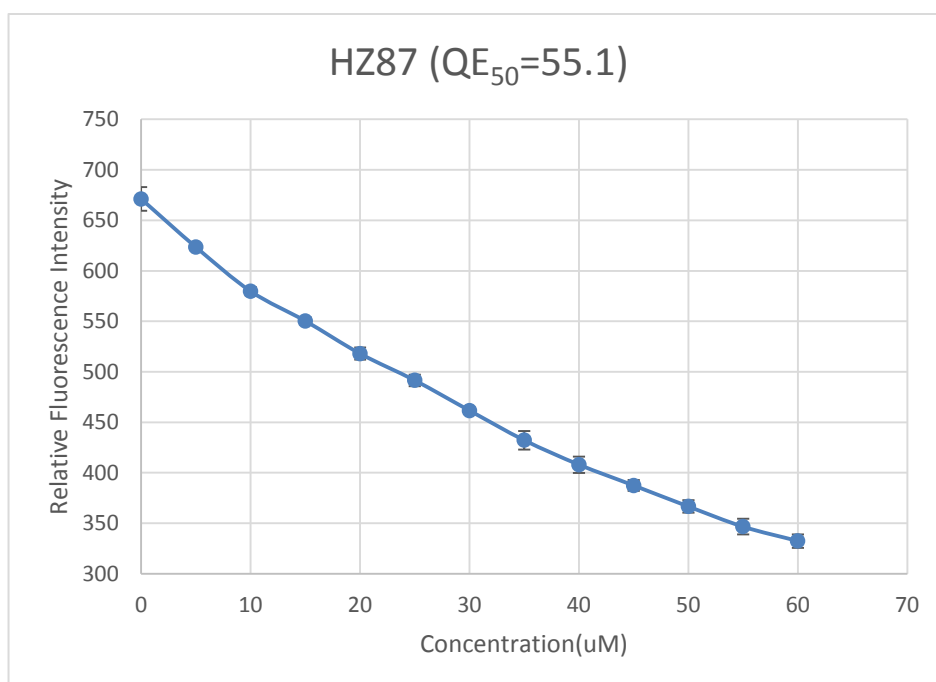


$K_{app}=0.54 \times 10^{7} M^{-1}$

**Graph 9**. Variation of relative fluorescence intensity with different concentration of HZ87 in Tris-HCl buffer

| Drug | $QE_{50}(\mu M)$ | $K_{app}(\times 10^7 M^{-1})$ |
|---|---|---|
| Mitoxantrone | 1.7 | 17.34 |
| HZ74 | 49.4 | 0.61 |
| HZ82 | 41.4 | 0.72 |
| HZ83 | 39.8 | 0.75 |
| HZ86 | 53.2 | 0.56 |
| HZ87 | 55.1 | 0.54 |

**Table 3.** Comparison of drug DNA binding affinity

Mitoxantrone is widely used as a chemotherapeutic drug in the treatment of breast cancer, lymphoma and leukaemia. The nuclear DNA was indicated as the major target of Mitoxantrone based on numerous studies (Mazerski *et al.,* 1998). Mitoxantrone has a planar anthraquinone ring which can intercalate between DNA base pairs and its side chains further bind to the phosphate groups of DNA. This will cause the DNA condensation and thus inhibits DNA replication. Mitoxantrone also shows strong binding affinity to histone proteins besides DNA (Hajihassan and Rabbani-Chadegani, 2009).

The DNA-binding properties of synthesized baclofen based prodrugs were investigated. When comparing the results to the well-known anticancer drug mitoxantrone, as shown in **Table 3** here, the binding constant value of prodrugs HZ74 to HZ87 is much smaller than mitoxantrone, which indicates they all have low DNA binding affinities.

## 2.4 Conclusion

**Table 4** below shows the synthesised baclofen prodrugs (on the left) and cyclic baclofen prodrugs (on the right). The synthesis process was difficult because of the poor solubility of baclofen. The reaction of AQ-spacer-OPFP and baclofen was very slow (up to 10 days). The prodrug structures were characterised by their Mass spectrum, further analysis by NMR was performed. However due to the low yield of prodrugs, some them need to be resynthesised in greater quantities for full NMR analyses.



**Table 4**. List of synthesised baclofen based prodrugs

Because of the difficulty for prodrugs to pass through the blood brain barrier (BBB), the most effective way to make a drug move through a lipophilic barrier is to increase its lipophilicity. Lipophilicity assay was conducted to investigate the

compound's ability to transverse the blood–brain barrier. The lipophilicity assay proved that the prodrugs tested all have high lipophilic properties. This is crucial for the prodrugs to cross the BBB and eventually target the brain tumours. The DNA binding results of prodrugs showed relatively low DNA binding affinities when comparing them to the anticancer drug mitoxantrone.

## 2.5 Structure Library
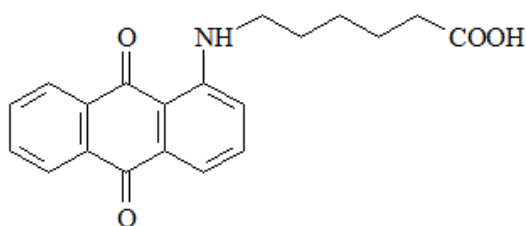


6-(9,10-Dioxo-9,10-dihydro-anthracen-1-ylamino)-hexanoic acid

**AQ-Ahx-OH (HZ66)**
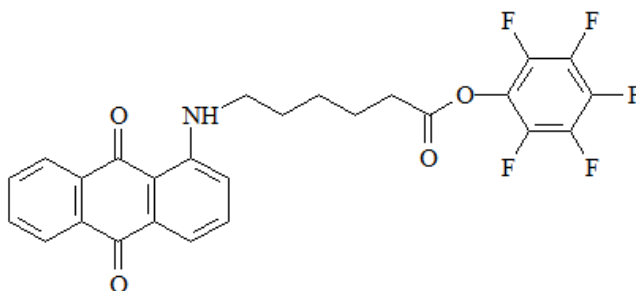


6-(9,10-Dioxo-9,10-dihydro-anthracen-1-ylamino)-hexanoic acid pentafluorophenyl ester

**AQ-Ahx-OPFP (HZ67)**
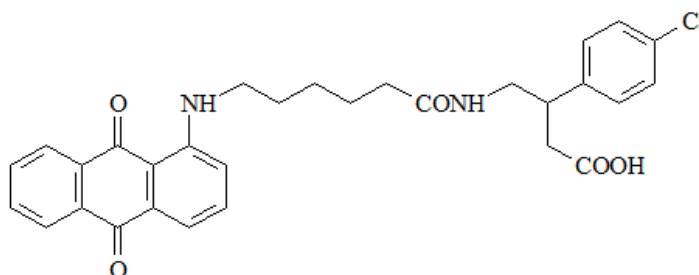


3-(4-Chloro-phenyl)-4-[6-(9,10-dioxo-9,10-dihydro-anthracen-1-ylamino)-hexanoylamino]-butyric acid

**AQ-Ahx-Baclofen (HZ68)**
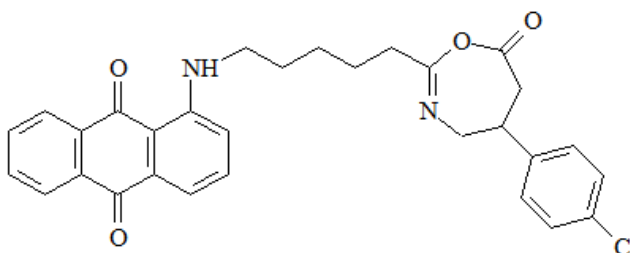


1-{5-[5-(4-Chloro-phenyl)-7-oxo-4,5,6,7-tetrahydro-[1,3]oxazepin-2-yl]-pentylamino}-anthraquinone

**AQ-Ahx-cyclic Baclofen (HZ69)**
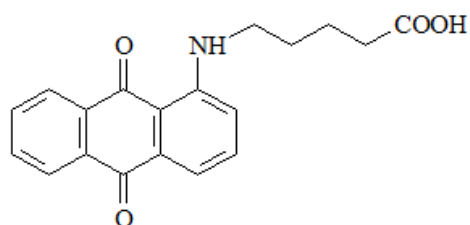
5-(9,10-Dioxo-9,10-dihydro-anthracen-1-ylamino)-pentanoic acid

**AQ-Ava-OH (HZ72)**
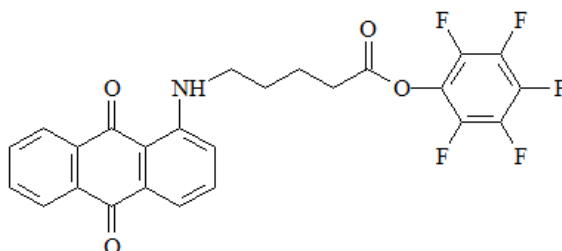


5-(9,10-Dioxo-9,10-dihydro-anthracen-1-ylamino)-pentanoic acid pentafluorophenyl ester

**AQ-Ava-OPFP (HZ73)**
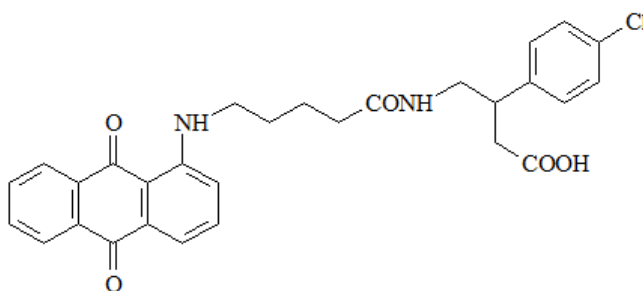


3-(4-Chloro-phenyl)-4-[5-(9,10-dioxo-9,10-dihydro-anthracen-1-ylamino)-pentanoylamino]-butyric acid

**AQ-Ava-Baclofen (HZ74)**
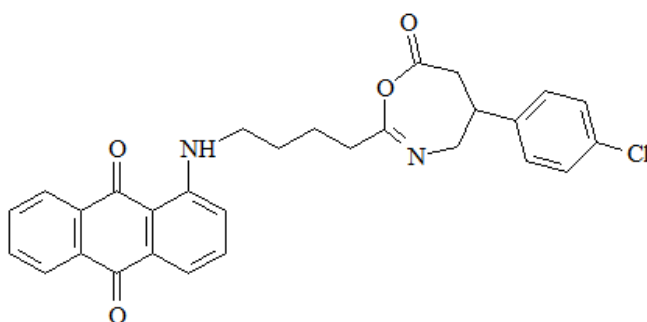


1-{4-[5-(4-Chloro-phenyl)-7-oxo-4,5,6,7-tetrahydro-[1,3]oxazepin-2-yl]-butylamino}-anthraquinone

**AQ-Ava-cyclic Baclofen (HZ75)**

164
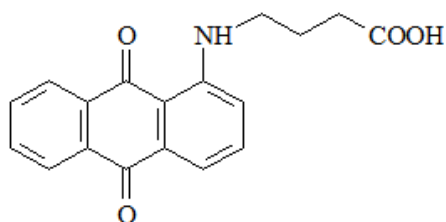
4-(9,10-Dioxo-9,10-dihydro-anthracen-1-ylamino)-butyric acid

**AQ-GABA-OH (HZ76)**
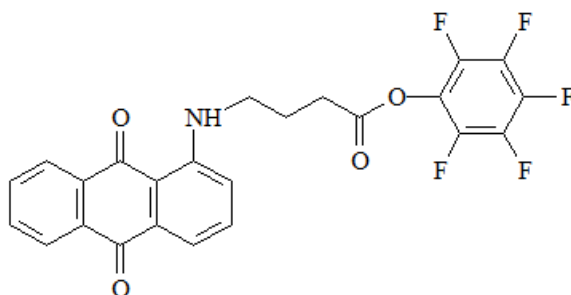


4-(9,10-Dioxo-9,10-dihydro-anthracen-1-ylamino)-butyric acid pentafluorophenyl ester

**AQ-GABA-OPFP (HZ77)**
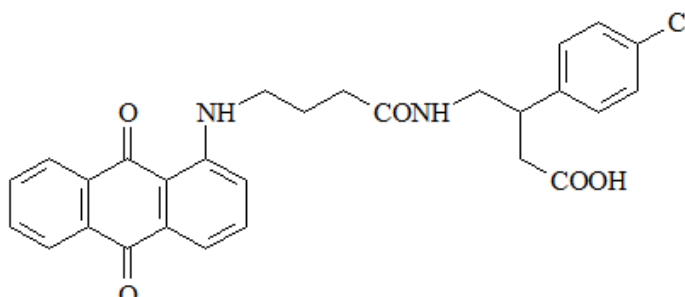


4-(9,10-Dioxo-9,10-dihydro-anthracen-1-ylamino)-butyric acid pentafluorophenyl ester

**AQ-GABA-Baclofen (HZ78)**
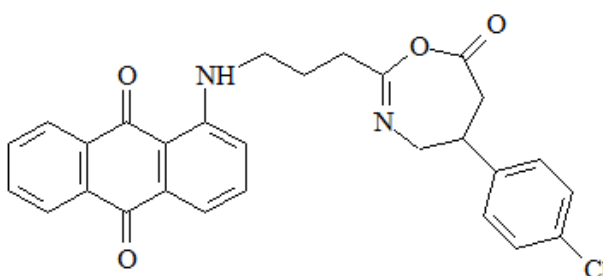


1-{3-[5-(4-Chloro-phenyl)-7-oxo-4,5,6,7-tetrahydro-[1,3]oxazepin-2-yl]-propylamino}-anthraqui
none

**AQ-GABA-cyclic Baclofen (HZ79)**
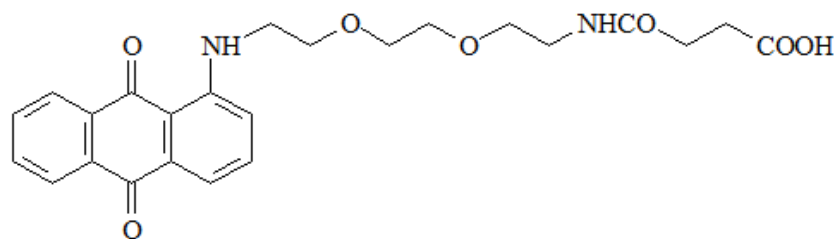
*N*-(2-{2-[2-(9,10-Dioxo-9,10-dihydro-anthracen-1-ylamino)-ethoxy]-ethoxy}-ethyl)-succinamic acid

**AQ-[PEG Spacer]-Succinyl (HZ80)**
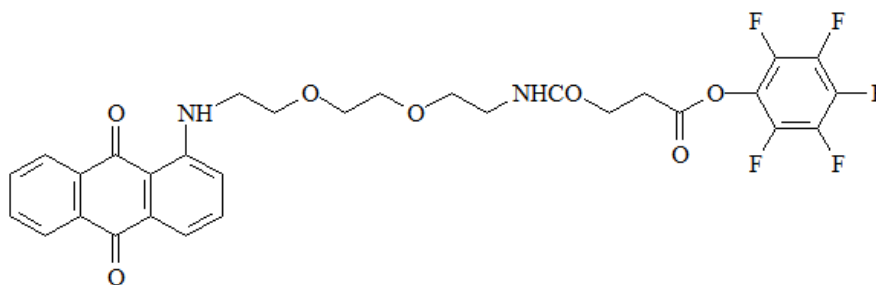


*N*-(2-{2-[2-(9,10-Dioxo-9,10-dihydro-anthracen-1-ylamino)-ethoxy]-ethoxy}-ethyl)-succinamic acid pentafluorophenyl ester

**AQ-[PEG Spacer]-Succinyl-OPFP (HZ81)**
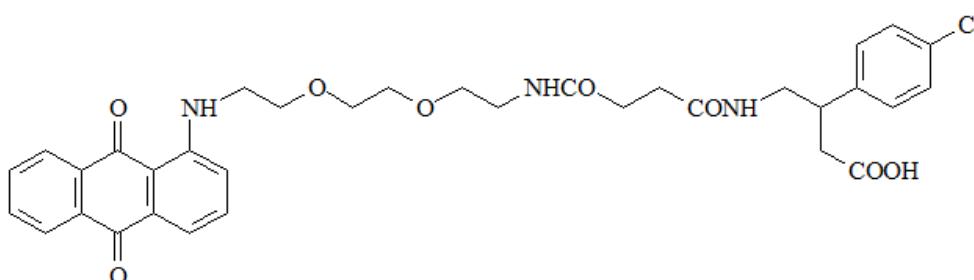


3-(4-Chloro-phenyl)-4-[3-(2-{2-[2-(9,10-dioxo-9,10-dihydro-anthracen-1-ylamino)-ethoxy]-ethoxy}-ethylcarbamoyl)-propionylamino]-butyric acid

**AQ-[PEG Spacer]-Succinyl-Baclofen (HZ82)**
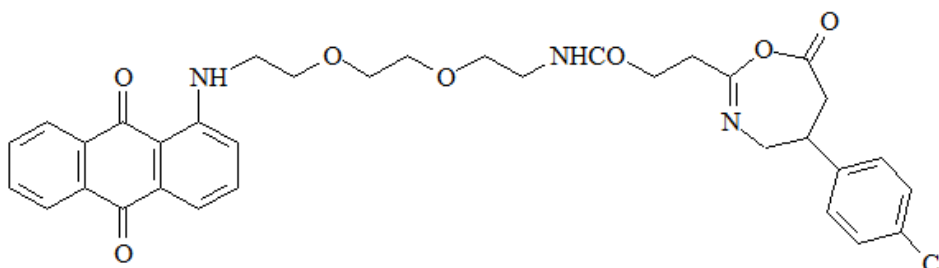


3-[5-(4-Chloro-phenyl)-7-oxo-4,5,6,7-tetrahydro-[1,3]oxazepin-2-yl]-N-(2-{2-[2-(9,10-dioxo-9,10-dihydro-anthracen-1-ylamino)-ethoxy]-ethoxy}-ethyl)-propionamide

**AQ-[PEG Spacer]-Succinyl-cyclic Baclofen (HZ83)**
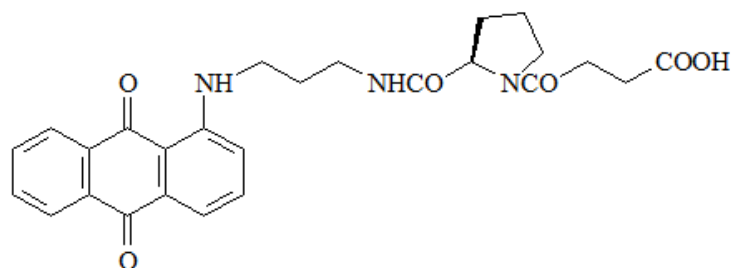
166

4-{2-[3-(9,10-Dioxo-9,10-dihydro-anthracen-1-ylamino)-propylcarbamoyl]-pyrrolidin-1-yl}-4-oxo-butyric acid

**AQ-[propyl spacer]-Pro-succinyl (HZ84)**
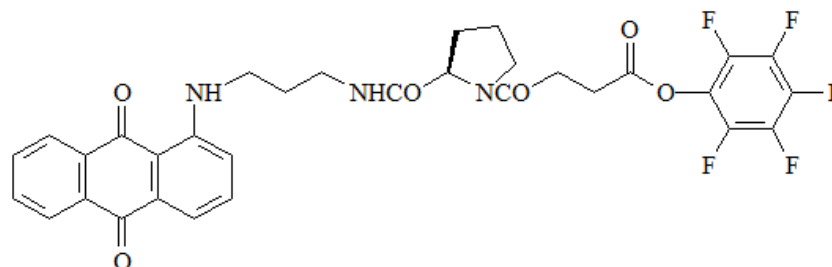


4-{2-[3-(9,10-Dioxo-9,10-dihydro-anthracen-1-ylamino)-propylcarbamoyl]-pyrrolidin-1-yl}-4-oxo-butyric acid pentafluorophenyl ester

**AQ-[propyl spacer]-Pro-succinyl-OPFP (HZ85)**
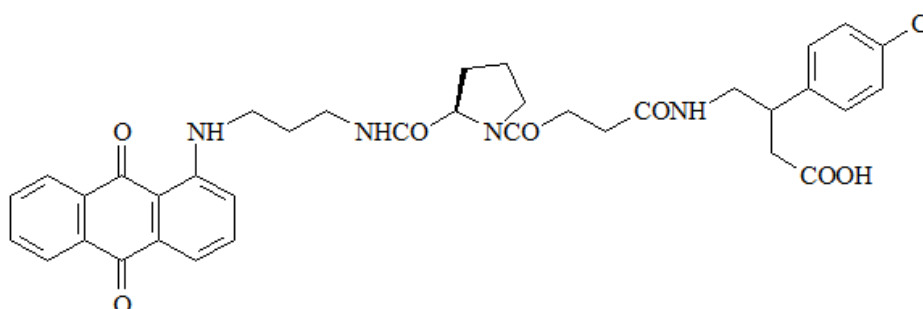


3-(4-Chloro-phenyl)-4-(4-{2-[3-(9,10-dioxo-9,10-dihydro-anthracen-1-ylamino)-propylcarbamoyl]-pyrrolidin-1-yl}-4-oxo-butyrylamino)-butyric acid

**AQ-[propyl spacer]-Pro-succinyl-Baclofen (HZ86)**
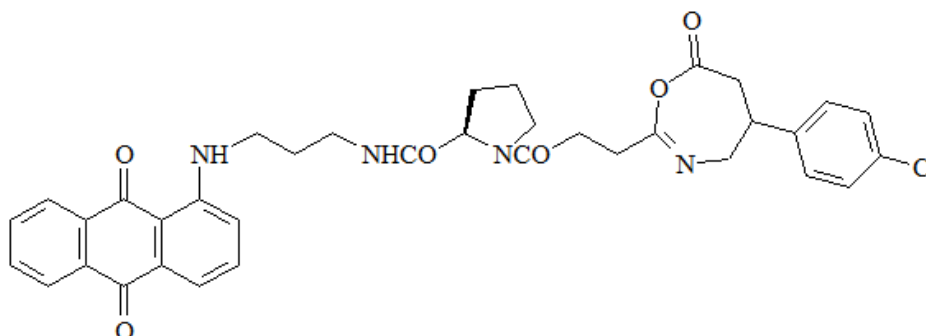


1-{3-[5-(4-Chloro-phenyl)-7-oxo-4,5,6,7-tetrahydro-[1,3]oxazepin-2-yl]-propionyl}-pyrrolidine-2-carboxylic acid [3-(9,10-dioxo-9,10-dihydro-anthracen-1-ylamino)-propyl]-amide

**AQ-[propyl spacer]-Pro-succinyl- cyclic Baclofen (HZ87)**

## 2.6 Experimental

## 2.6.1 DNA binding assay

**Materials for DNA binding assay**

The Tris-HCl buffer (pH7.4) was prepared by dissolving NaCl (25 mM), CaCl$_2$ (1 mM) and Tris-HCl (10 mM) in distilled water (200 ml). The buffer was stored in 4 °C fridge. A stock solution of ethidium bromide 10 mg/ml in distilled water was also prepared and stored at 4 °C for further use. About one centimetre portion of calf thymus DNA was dissolved in Tris-HCl buffer (4 ml) at 4 °C for 24 h. The undissolved DNA was filtered off. The concentration of the DNA stock solution was measured at 260 nm by using the Beckman Coulter DU800 UV/Vis Spectrophotometer. The blank was Tris-HCl buffer (3 ml) in cuvette. The unquantified DNA stock solution (200~300 µl) was added to another cuvette and diluted with buffer to 3 ml. The ideal absorbance should be between 0.4 and 0.7. The absorbance was read three times and the mean value was used to calculate the DNA concentration using the Beer-Lambert Law. The test prodrug (1 mg) was dissolved in DMSO (1 ml) to make a 1 mg/ml stock solution.

**Method for DNA binding assay**

The Perkin Elmer Luminescence Spectrometer LS50B was used to measure the DNA-bound ethidium bromide fluorescence intensity.   The solutions were added into the 3 ml cuvette by order with different final concentrations: 1) 60 µM DNA; 2) 30 µM Ethidium bromide; 3) Tris-HCl buffer up to 3 ml.

Certain volume of test compound to give the final concentration of 5 µM was added into the cuvette. The fluorescence intensity was recorded. After 5 min, another same portion of test compound was added to give the final concentration of 10 µM. The process was repeated until it reached 50%

reduction of the relative fluorescence intensity.

## 2.6.2 Lipophilicity test

**Materials for lipophilicity test**

One tablet of Phosphate Buffered Saline (PBS) was dissolved in distil water (200 ml) to give a solution of 0.01 M phosphate, 0.0027 M KCl and 0.137 M NaCl. PBS buffer (100 ml) and octanol solutions (100 ml) were transferred into a separating funnel and shaken for 24 h. The two layers of octanol-saturated PBS and PBS-saturated octanol solutions were then separated.

**Method for lipophilicity test**

1mg/ml of each compound in DMSO (1 ml) was prepared for creating the calibration curve. A series of standard solutions with concentration of 20 µM, 30 µM, 40 µM, 50 µM, 60 µM and 70 µM were prepared in cuvettes. The absorbance of the solutions was measured. The value should be from 0 to 0.7. Both octanol and PBS calibration curves were prepared. Calibration curves were used to determine the concentration of drugs in two phases.

The test compound (0.5 mg) was put into a 2 ml eppendorf tube. Octanol-saturated PBS (900 µl) and PBS-saturated octanol (900 µl) were added. The tube was shaken for 24 h at RT.

The tube was centrifuged for 2 min to separate the solutions. The upper octanol layer (100 µl or 200 µl) was carefully removed by pipetting and transferred into a 3 ml cuvette and made up to 3 ml by PBS-saturated octanol or octanol-saturated PBS. By measuring the absorbance, the concentration of drug can be determined. The distribution coefficient was calculated.

### 2.6.3 Synthesis of AQ-Ahx-OH (HZ66)

1-Choloroanthraquinone (3 g, 12 mmol) was reacted with 6-aminohexanoic acid (3.24 g, 24 mmol) by the addition of NaOH (1.5 g, 36 mmol) in 70 ml of DMSO. The reaction was heated on a 100°C water bath for 8 h. The solution was cooled to RT and poured into 250 ml of acidic water (HCl was added). The precipitate red compound was collected by filtration. The dried crude product ($R_f$ 0.31, dichloromethane-methanol 9:1) was purified by column chromatography using the eluting solvent chloroform and methanol 10:1. The pure product fractions were combined, filtered and evaporated. The red solid compound was collected from diethyl ether (60 ml). Yield: 558 mg, 16.6%.

### 2.6.4 Synthesis of AQ-Ahx-OPFP (HZ67)

The starting compound AQ-Ahx-OH HZ66 (400 mg, 1.19 mmol) and PFP (327 mg, 1.78 mmol) were dissolved in 50 ml of dichloromethane, followed by the addition of coupling reagents DCC (490 mg, 2.38 mmol) and DMAP (435 mg, 3.57 mmol). The reaction completed in 4 h by checking the TLC ($R_f$ 0.73, dichloromethane-ethyl acetate 5:1). DCU precipitate was filtered off. The product was purified by column chromatography using dichloromethane and ethyl acetate 6:1. The product fractions were combined, filtered and evaporated to dryness. Hexane (40 ml) was used to precipitate the solid compound. Yield: 245 mg, 41%.

$^1$H NMR spectrum (CDCl$_3$, 300 MHz) δ: 1.58-1.7 (2H, m, AQ-NH-CH$_2$-CH$_2$-C<u>H</u>$_2$); 1.8-1.98 (4H, m, AQ-NH-CH$_2$-C<u>H</u>$_2$-CH$_2$-C<u>H</u>$_2$); 2.75 (2H, t, AQ-NH-CH$_2$-CH$_2$-CH$_2$-CH$_2$-C<u>H</u>$_2$); 3.4 (2H, q, AQ-NH-C<u>H</u>$_2$); 7.1 (1H, d, H-2); 7.52-7.63 (2H, m, H-3 and H-4); 7.7-7.8 (2H, m, H-6 and H-7); 8.28 (2H, m, H-5 and H-8); 9.8 (1H, t, AQ-N<u>H</u>)

### 2.6.5 Synthesis of AQ-Ahx-Baclofen (HZ68)

Two round bottomed flasks were used. One of them had AQ-Ahx-OPFP HZ67 (200 mg, 0.4 mmol) in 10 ml of DMF. The other one had NaOH (14 mg, 0.36 mmol), $H_2O$ (about 20 µl) and baclofen (94 mg, 0.44 mmol) in DMF (10 ml). The two flasks were both refluxed on the hot water bath (90°C). The baclofen solution was added to the flask of HZ67 by drop wise. The reaction was checked by TLC ($R_f$ 0.22, dichloromethane-methanol 6:1) and had mostly completed in 5 days. The reaction solution was extracted between dichloromethane and water (1:4, 300 ml). The organic phase was dried by anhydrous sodium sulphate, filtered, and evaporated to a small volume. The crude product was purified by column chromatography using the eluting solvent dichloromethane methanol 12:1. The pure fractions were combined, filtered, evaporated to dryness and collected. Yield: 53.6 mg, 25%.

<u>$^1$H NMR spectrum (DMSO-$d_6$, 300 MHz) δ</u>: 1.4-1.68 (4H, m, AQ-NH-CH$_2$-CH$_2$-C<u>H$_2$</u>-C<u>H$_2$</u>); 2.0-2.1 (2H, m, AQ-NH-CH$_2$-C<u>H$_2$</u>); 2.4-2.55 (2H, m, C<u>H$_2$</u>-COOH); 3.17-3.4 (5H, m, unresolved, AQ-NH-C<u>H$_2$</u>, CONH-C<u>H$_2$</u> and C<u>H</u>-Benzene-Cl); 7.2-7.29 [(3H, q, H-2 (AQ), H-3 and H-5 (Benzene-Cl)]; 7.29-7.38 [(2H, d, H-2 and H-6 (Benzene-Cl)]; 7.42 (1H, d, H-4); 7.6-7.7 (1H, t, H-3); 7.75-7.96 (3H, m, unresolved, CON<u>H</u>, H-6 and H-7); 8.05-8.25 (2H, m, H-5 and H-8); 9.65 (1H, t, AQ-N<u>H</u>)

<u>ESMS (+)</u>: 533 m/z 100% (M+H)$^+$

### 2.6.6 Synthesis of AQ-Ahx-cyclic Baclofen (HZ69)

AQ-Ahx-Baclofen HZ68 (25 mg, 0.05 mmol) was dissolved in acetic anhydride (3 ml) and refluxed on 95 °C water bath for 1 hour. The solution was cooled to RT and poured into distilled water. The precipitated product ($R_f$ 0.6,

dichloromethane-methanol 6:1) was collected by centrifuge. Yield: 14 mg, 54%.

$^1$H NMR spectrum (CDCl$_3$, 300 MHz) δ: 1.55-1.68 (2H, m, AQ-NH-CH$_2$-CH$_2$-C$\underline{H}_2$); 1.72-1.9 (4H, m, AQ-NH-CH$_2$-C$\underline{H}_2$-CH$_2$-C$\underline{H}_2$); 2.7-2.84 (1H, m, O-CO-C$\underline{H}_2$); 2.93-3.08 (3H, m, O-CO-C$\underline{H}_2$ and AQ-NH-CH$_2$-CH$_2$-CH$_2$-CH$_2$-C$\underline{H}_2$); 3.38-3.45 (2H, q, AQ-NH-C$\underline{H}_2$); 3.45-3.65 (1H, m, C$\underline{H}$-Benzene-Cl); 3.7-3.8 (1H, q, C=N-C$\underline{H}_2$); 4.25-4.35 (1H, q, C=N-C$\underline{H}_2$); 7.05-7.15 (1H, d, H-2); 7.15-7.23 [(2H, q, H-3 and H-5 (Benzene-Cl)]; 7.3-7.4 [(2H, q, H-2 and H-6 (Benzene-Cl)]; 7.52-7.65 (2H, m, H-3 and H-4); 7.7- 7.82 (2H, m, H-6 and H-7); 8.3 (2H, m, H-5 and H-8); 9.8 (1H, t, AQ-N$\underline{H}$)

ESMS (+): 515 m/z 100% (M+H)$^+$

## 2.6.7 Synthesis of AQ-Ava-OH (HZ72)

1-Choloroanthraquinone (4 g, 17 mmol), 5-aminopentanoic acid (6 g, 51 mmol) and NaOH (2.7 g, 68 mmol) were suspended in 90 ml of DMSO. The reaction was heated on 100°C water bath for 10 h. The mixture was poured into the 300 ml of acidic water (HCl was added). The red precipitate was collected by filtration. The crude compound (R$_f$ 0.42, dichloromethane-methanol 9:1) was purified by column chromatography using solvent system dichloromethane and methanol 9:1. The appropriate fractions were combined, filtered and evaporated to dryness. The product was precipitated in diethyl ether (70 ml) and collected. Yield: 909 mg, 17%.

$^1$H NMR spectrum (CDCl$_3$, 300 MHz) δ: 1.8-1.95 (4H, m, AQ-NH-CH$_2$-C$\underline{H}_2$-C$\underline{H}_2$); 2.5 (2H, t, AQ-NH-CH$_2$-CH$_2$-CH$_2$-C$\underline{H}_2$); 3.32-3.45 (2H, q, AQ-NH-C$\underline{H}_2$); 7.0-7.1 (1H, d, H-2); 7.5-7.65 (2H, m, H-3 and H-4); 7.68-7.8 (2H, m, H-6 and H-7); 8.2-8.33 (2H, m, H-5 and H-8); 9.75 (1H, t, AQ-N$\underline{H}$)

### 2.6.8 Synthesis of AQ-Ava-OPFP (HZ73)

AQ-Ava-OH HZ72 (800 mg, 2.5 mmol), PFP (684 mg, 3.75 mmol), DCC (1030 mg, 5 mmol) and DMAP (915 mg, 7.5 mmol) were dissolved in dichloromethane (60 ml). The reaction had completed in 4 h by checking the TLC ($R_f$ 0.67, dichloromethane- ethyl acetate 5:1). The DCU precipitate was filtered off. The product was purified by column chromatography using dichloromethane and ethyl acetate 5:1. The product fractions were combined, filtered and evaporated to dryness. Hexane (40 ml) was used to precipitate the solid compound. Yield: 610 mg, 50%.

$^1$H NMR spectrum (CDCl$_3$, 300 MHz) δ: 1.9-2.1 (4H, m, AQ-NH-CH$_2$-C$\underline{H}_2$-C$\underline{H}_2$); 2.78-2.85 (2H, t, AQ-NH-CH$_2$-CH$_2$-CH$_2$-C$\underline{H}_2$); 3.4-3.5 (2H, q, AQ-NH-C$\underline{H}_2$); 7.1 (1H, d, H-2); 7.55-7.68 (2H, m, H-3 and H-4); 7.7-7.83 (2H, m, H-6 and H-7); 8.25-8.35 (2H, m, H-5 and H-8); 9.82 (1H, t, AQ-N$\underline{H}$)

### 2.6.9 Synthesis of AQ-Ava-Baclofen (HZ74)

Two round bottomed flasks were used. One of them had AQ-Ava-OPFP HZ73 (500 mg, 1 mmol) in DMF. The other one had NaOH (36 mg, 0.9 mmol), H$_2$O (about 15 µl) and baclofen (235 mg, 1.1 mmol) in DMF. The two flasks were both refluxed on the hot water bath (90ºC). The baclofen solution was added to the flask of HZ73 by drop wise. The reaction was checked by TLC ($R_f$ 0.75, dichloromethane methanol 9:1) and had mostly completed in 8 days. The reaction solution was extracted between dichloromethane and water (1:5, 200 ml). The organic phase was dried by anhydrous sodium sulphate, filtered, and evaporated to a small volume. The crude product was purified by column chromatography using the eluting solvent dichloromethane and methanol 13:1. The pure fractions were combined, filtered, evaporated to dryness and collected.

Yield: 110 mg, 21%.

$^1$H NMR spectrum (DMSO-d$_6$, 300 MHz) δ: 1.5-1.6 (4H, m, AQ-NH-CH$_2$-CH$_2$-CH$_2$); 2.1 (2H, t, AQ-NH-CH$_2$-CH$_2$-CH$_2$-CH$_2$); 2.4-2.5 (2H, m, CH$_2$-COOH); 3.2-3.4 (5H, m, unresolved, AQ-NH-CH$_2$, CONH-CH$_2$, and CH-Benzene-Cl); 7.2-7.28 [(3H, m, H-2, H-3 and H-5 (Benzene-Cl)]; 7.28-7.34 [(2H, m, H-2 and H-6 (Benzene-Cl)]; 7.4-7.48 (1H, d, H-4); 7.6-7.7 (1H, t, H-3); 7.8-7.95 (3H, m, CONH, H-6 and H-7); 8.1-8.17 (1H, d, H-8); 8.17-8.25 (1H, d, H-5); 9.67 (1H, t, AQ-NH)

ESMS (+): 517 m/z 100% (M-H)$^-$

## 2.6.10 Synthesis of AQ-Ava-cyclic Baclofen (HZ75)

AQ-Ava-Baclofen HZ74 (60 mg, 0.12 mmol) was dissolved by acetic anhydride (3 ml) and refluxed on water bath (95ºC) for 1 h. The solution was cooled to RT and poured into distilled water. The precipitate product (R$_f$ 0.55, dichloromethane-methanol 6:1) was collected by centrifuge. Yield: 48 mg, 80%.

$^1$H NMR spectrum (CDCl$_3$, 300 MHz) δ: 1.6 (2H, m, AQ-NH-CH$_2$-CH$_2$-CH$_2$); 1.85-2.0 (4H, m, AQ-NH-CH$_2$-CH$_2$); 2.72-2.85 (1H, dd, O-CO-CH$_2$); 2.95-3.15 (3H, m, O-CO-CH$_2$ and AQ-NH-CH$_2$-CH$_2$-CH$_2$-CH$_2$); 3.38-3.5 (2H, m, AQ-NH-CH$_2$); 3.5-3.67 (1H, q, CH-Benzene-Cl); 3.7-3.8 (1H, dd, C=N-CH$_2$); 4.26-4.38 (1H, dd, C=N-CH$_2$); 7.05-7.15 (1H, d, H-2); 7.15-7.22 [(2H, m, H-3 and H-5 (Benzene-Cl)]; 7.3-7.4 [(2H, q, H-2 and H-6 (Benzene-Cl)]; 7.54-7.68 (2H, m, H-3 and H-4); 7.7-7.83 (2H, m, H-6 and H-7); 8.25-8.33 (2H, m, H-5 and H-8); 9.8 (1H, t, AQ-NH)

ESMS (+): 501 m/z 100% (M+H)$^+$

## 2.6.11 Synthesis of AQ-GABA-OH (HZ76)

1-Choloroanthraquinone (3 g, 12 mmol), gamma-aminobutyric acid (3.8 g, 37 mmol), NaOH (1.44 g, 36 mmol) and DMSO (80 ml) were transferred into a round bottomed flask. The flask was put on a 100ºC water bath and heated for 6 h. The solution mixture was poured into the 300ml of acidic water (HCl was added). The red precipitate ($R_f$ 0.27, dichloromethane-methanol 9:1) was filtered and purified by column chromatography using solvent system dichloromethane and methanol 11:1. The pure product fractions were combined, filtered and evaporated to dryness by using the rotational evaporator. The red solid product was precipitated in diethyl ether (50 ml) and the mixture was filtered, dried in a desiccator and collected. Yield: 605 mg, 20%.

## 2.6.12 Synthesis of AQ-GABA-OPFP (HZ77)

AQ-GABA-OH HZ76 (500 mg, 1.6 mmol), PFP (442 mg, 2.4 mmol), DCC (659 mg, 3.2 mmol) and DMAP (586 mg, 4.8 mmol) were dissolved in dichloromethane (50 ml). The reaction had completed in 7 h by checking the TLC ($R_f$ 0.7, dichloromethane- ethyl acetate 4:1). The DCU precipitate was filtered off. The product was purified by column chromatography using dichloromethane and ethyl acetate 4:1. The product fractions were combined, filtered and evaporated to dryness. Hexane (40 ml) was used to precipitate the solid compound. Yield: 335 mg, 44%.

## 2.6.13 Synthesis of AQ-GABA-Baclofen (HZ78)

Two round bottomed flasks were used. One of them had AQ-GABA-OH HZ77 (300 mg, 0.63 mmol) in DMF (15 ml). The other one had NaOH (23 mg, 0.57 mmol), $H_2O$ (about 15 µl) and baclofen (148 mg, 0.69 mmol) in 10ml of DMF. The two flasks were both refluxed on the hot water bath (90ºC). The baclofen solution

was added to the flask of HZ77 by drop wise. The reaction was checked by TLC (Rf 0.35, dichloromethane- methanol 6:1) and had mostly completed in 10 days. The reaction solution was extracted between dichloromethane and water (1:5, 200 ml). The organic phase was dried by anhydrous sodium sulphate, filtered, and evaporated to a small volume. The crude product was purified by column chromatography using the eluting solvent dichloromethane and methanol 13:1. The pure fractions were combined, filtered, evaporated to dryness and collected. Yield: 43 mg, 14%.

### 2.6.14 Synthesis of AQ-GABA-cyclic Baclofen (HZ79)

AQ-GABA-Baclofen HZ78 (25 mg, 0.05 mmol) was dissolved by acetic anhydride (5 ml) and refluxed on water bath (95ºC) for 1 h. The solution was cooled to RT and poured into distilled water. The precipitate product (R$_f$ 0.45, dichloromethane-methnol 6:1) was collected by centrifuge. Yield: 11.7 mg, 48%. ESMS (+): 487 m/z 100% (M+H)$^+$

### 2.6.15 Synthesis of AQ-[PEG Spacer]-Succinyl (HZ80)

Succinic anhydride (249 mg, 2.7 mmol) and anthraquinone derivative (800 mg, 2.26 mmol) were dissolved in DMF (40 ml) followed by the addition of the DIPEA (864 µl, 5 mmol, 0.742 mg/ml) and reacted at RT overnight. The product (R$_f$ 0.27, dichloromethane-methanol 9:1) solution was extracted by dichloromethane and water (1:5, 200 ml). The organic layer was collected, dried by anhydrous sodium sulphate, filtered and evaporated to a small volume for the column chromatography purification using dichloromethane-ethyl acetate-ethanol 6:2:1 solvent system. The pure fractions were combined, filtered, evaporated, and precipitated in diethyl ether (50 ml). The solid product was collected. Yield: 520 mg, 61%.

**2.6.16 Synthesis of AQ-[PEG Spacer]-Succinyl-OPFP (HZ81)**

AQ-[PEG Spacer]-Succinyl HZ80 (450 mg, 0.73 mmol), PFP (200 mg, 1.1 mmol), DCC (300 mg, 1.46 mmol) and DMAP (267 mg, 2.19 mmol) were dissolved in dichloromethane (60 ml). The reaction had completed in 6 h by checking the TLC ($R_f$ 0.75, dichloromethane- ethyl acetate 4:1). The DCU precipitate was filtered off. The product was purified by column chromatography using dichloromethane and ethyl acetate 5:1. The product fractions were combined, filtered and evaporated to dryness. Hexane (50 ml) was used to precipitate the solid compound. Yield: 250 mg, 53%.

**2.6.17 Synthesis of AQ-[PEG Spacer]-Succinyl-Baclofen (HZ82)**

Two round bottomed flasks were used. One of them had AQ-[PEG Spacer]-Succinyl-OPFP HZ81 (200 mg, 0.32 mmol) in 15 ml of DMF. The other one had NaOH (11 mg, 0.29 mmol), $H_2O$ (about 15 µl) and baclofen (110 mg, 0.35 mmol) in DMF (8 ml). The two flasks were both refluxed on the hot water bath (90ºC). The baclofen solution was added to the flask of HZ81 by drop wise. The reaction was checked by TLC ($R_f$ 0.38, dichloromethane-methanol 6:1) and had mostly completed in 8 days. The reaction solution was extracted between dichloromethane and water (1:3, 200 ml). The organic phase was dried by anhydrous sodium sulphate, filtered, and evaporated to a small volume. The crude product was purified by column chromatography using the eluting solvent dichloromethane and methanol 10:1. The pure fractions were combined, filtered, evaporated to dryness and collected. Yield: 120 mg, 56%.

^{1}H NMR spectrum (DMSO-d$_6$, 300 MHz) δ: 2.15-2.4 (4H, m, unresolved, AQ-NH-CH$_2$-C$\underline{H}_2$ and CONH-C$\underline{H}_2$); 2.4-2.55 (2H, m, C$\underline{H}_2$-COOH); 3.1-3.3 (4H, m, NHCO-C$\underline{H}_2$-C$\underline{H}_2$); 3.32-3.48 (2H, m, AQ-NH-C$\underline{H}_2$); 3.5-3.7 (7H, m,

CH-Benzene-Cl, AQ-NH-$C_2H_4$-O-$C_2H_4$-O-C$\underline{H}_2$ and AQ-NH-$C_2H_4$-O-$C_2\underline{H}_4$); 3.7-3.8 (2H, q, C$\underline{H}_2$-NHCO); 7.2-7.37 [(4H, m H-2, 3, 5, 6 (Benzene-Cl)]; 7.45 (1H, d, H-4); 7.6-7.7 (1H, t, H-3); 7.78-7.95 (4H, m, unresolved, N$\underline{H}$CO, CON$\underline{H}$, H-6 and H-7); 8.08-8.15 (1H, d, H-8); 8.15-8.25 (1H, d, H-5); 9.79 (1H, t, AQ-N$\underline{H}$)

<u>ESMS (+)</u>: 650 m/z 100% (M+H)$^+$

## 2.6.18 Synthesis of AQ-[PEG Spacer]-Succinyl-cyclic Baclofen (HZ83)

AQ-[PEG Spacer]-Succinyl-Baclofen HZ82 (60 mg, 0.09 mmol) was dissolved by acidic anhydride (5 ml) and refluxed on water bath (95ºC) for 1 h. The solution was cooled to RT and poured into distilled water. The precipitate product ($R_f$ 0.55, dichloromethane-methanol 6:1) was collected by centrifuge. Yield: 37 mg, 65%.

<u>$^1$H NMR spectrum (CDCl$_3$, 300 MHz) δ</u>: 2.45-2.52 (2H, t, AQ-NH-$CH_2$-C$\underline{H}_2$); 2.68-2.78 (2H, q, NHCO-C$\underline{H}_2$); 2.9-3.0 (1H, dd, O-CO-C$\underline{H}_2$); 3.15-3.25 (1H, dd, O-CO-C$\underline{H}_2$); 3.45-3.7 (7H, m, unresolved, AQ-NH-C$\underline{H}_2$, NHCO-C$\underline{H}_2$-C$\underline{H}_2$, and C$\underline{H}$-Benzene-Cl); 3.7-3.8 (4H, m, AQ-NH-$C_2H_4$-O-$C_2\underline{H}_4$); 3.8-3.9 (3H, m, C=N-C$\underline{H}_2$ and C$\underline{H}_2$-NHCO); 4.16-4.27 (1H, dd, C=N-C$\underline{H}_2$); 6.45 (1H, t, N$\underline{H}$CO); 7.06-7.22 [(3H, m, H-2 (AQ), H-3 and H-5 (Benzene-Cl)]; 7.25-7.4 [(2H, q, H-2 and H-6 (Benzene-Cl)]; 7.53-7.68 (2H, m, H-3 and H-4); 7.68-7.85 (2H, m, H-6 and H-7); 8.22-8.35 (2H, m, H-5 and H-8); 9.93 (1H, t, AQ-N$\underline{H}$)

<u>ESMS (+)</u>: 632 m/z 100% (M+H)$^+$

## 2.6.19 Synthesis of AQ-[propyl spacer]-Pro-succinyl (HZ84)

Anthraquinone-spacer-D-Pro (400mg, 1.1 mmol) and succinic anhydride (127 mg, 1.3 mmol) were dissolved in 30 ml of DMF followed by the addition of DIPEA (0.742 mg/ml, 420 µl, 2.2 mmol) and reacted at RT overnight. The product ($R_f$ 0.25, dichloromethane methanol 9:1) solution was extracted by dichloromethane

and water (1:3, 300 ml). The organic layer was collected, dried by anhydrous sodium sulphate, filtered and evaporated to a small volume for the column chromatography purification using dichloromethane-ethanol 7:1 solvent system. The pure fractions were combined, filtered, evaporated, and precipitated in 40 ml of diethyl ether. The solid product was collected. Yield: 218 mg, 42%.

### 2.6.20 Synthesis of AQ-[propyl spacer]-Pro-succinyl-OPFP (HZ85)

AQ-[propyl spacer]-Pro-succinyl HZ84 (200 mg, 0.42 mmol), PFP (116 mg, 0.63 mmol), DCC (173 mg, 0.84 mmol) and DMAP (154 mg, 1.26 mmol) were dissolved in dichloromethane (40 ml). The reaction had completed in 4 h by checking the TLC ($R_f$ 0.8, dichloromethane- ethyl acetate 5:1). The DCU precipitate was filtered off. The product was purified by column chromatography using dichloromethane and ethyl acetate 5:1. The product fractions were combined, filtered and evaporated to dryness. Hexane (50 ml) was used to precipitate the solid compound. Yield: 120 mg, 44%

### 2.6.21 Synthesis of AQ-[propyl spacer]-Pro-succinyl-Baclofen (HZ86)

Two round bottomed flasks were used. One of them had AQ-[propyl spacer]-Pro-succinyl-OPFP HZ85 (100 mg, 0.16 mmol) in DMF (20 ml). The other one had NaOH (5.6 mg, 0.14 mmol), $H_2O$ (about 10 µl) and baclofen (38 mg, 0.18 mmol) in DMF (8 ml). The two flasks were both refluxed on the hot water bath (90ºC). The baclofen solution was added to the flask of HZ85 by drop wise. The reaction was checked by TLC ($R_f$ 0.43, dichloromethane-methanol 6:1) and had mostly completed in 6 days. The reaction solution was extracted between dichloromethane and water (1:5, 300 ml). The organic phase was dried by anhydrous sodium sulphate, filtered, and evaporated to a small volume. The crude product was purified by column chromatography using the eluting solvent

dichloromethane and methanol 14:1. The pure fractions were combined, filtered, evaporated to dryness and collected. Yield: 96 mg, 89%.

<u>$^{1}$H NMR spectrum (DMSO-d$_6$, 300 MHz)</u> δ: 1.7-2.0 (6H, m, unresolved, AQ-NH-CH$_2$-C<u>H$_2$</u>, β-C<u>H$_2$</u> and γ-C<u>H$_2$</u>); 2.1-2.7 (6H, m, unresolved, NCO-C<u>H$_2$</u>-C<u>H$_2$</u> and C<u>H$_2$</u>-COOH); 3.1-3.3 (4H, m, AQ-NH-CH$_2$-CH$_2$-C<u>H$_2$</u> and CONH-C<u>H$_2$</u>); 3.3-3.8 (5H, m, unresolved, C<u>H</u>-Benzene-Cl, AQ-NH-C<u>H$_2$</u> and δ-C<u>H$_2$</u>); 4.25 (1H, m, α-C<u>H</u> pro); 7.05-7.38 [(5H, m H-2, 3, 5, 6 (Benzene-Cl) and H-2 (AQ)]; 7.4 (1H, t, CON<u>H</u>); 7.65 (1H, t, N<u>H</u>CO); 7.7-7.95 (4H, m, H-3, H-4, H-6 and H-7); 8.1-8.3 (2H, q, H-5 and H-8); 9.72 (1H, t, AQ-N<u>H</u>)

<u>ESMS (+)</u>: 673 m/z 100% (M+H)$^+$

## 2.6.22 Synthesis of AQ-[propyl spacer]-Pro-succinyl- cyclic Baclofen (HZ87)

AQ-[propyl spacer]-Pro-succinyl-Baclofen HZ86 (50 mg, 0.07 mmol) was dissolved by acetic anhydride (5 ml) and refluxed on water bath for 1 hour. The solution was cooled to RT and poured into distilled water. The precipitate product (R$_f$ 0.71, dichloromethane-methanol 9:1) was collected by centrifuge. Yield: 37 mg, 80%.

<u>$^{1}$H NMR spectrum (CDCl$_3$, 300 MHz)</u> δ: 1.75-2.1(6H, m, unresolved, AQ-NH-CH$_2$-C<u>H$_2$</u>, β-C<u>H$_2$</u> and γ-C<u>H$_2$</u>); 2.35-2.95 (6H, m, unresolved, NCO-C<u>H$_2$</u>-C<u>H$_2$</u> and O-CO-C<u>H$_2$</u>,); 3.15-3.9 (7H, m, unresolved, AQ-NH-C<u>H$_2$</u>-CH$_2$-C<u>H$_2$</u>, C<u>H</u>-Benzene-Cl and C=N-C<u>H$_2$</u>); 4.0-4.3 (1H, m, α-C<u>H</u>); 4.68-4.75 (2H, m, δ-C<u>H$_2$</u>); 6.9-7.35 [(5H, m H-2, 3, 5, 6 (Benzene-Cl) and H-2 (AQ)]; 7.45 (1H, t, N<u>H</u>CO); 7.5-7.67 (2H, m, H-3 and H-4); 7.68-7.84 (2H, m, H-6 and H-7); 8.12-8.3 (2H, m, H-5 and H-8); 9.75 (1H, t, AQ-N<u>H</u>)

<u>ESMS (+)</u>: 655 m/z 100% (M+H)$^+$

## 2.7 References

Abdel-Hafez AA1, Abdel-Wahab BA. (2008). 5-(4-Chlorophenyl)-5,6-dihydro-1,3-oxazepin-7(4H)-one derivatives as lipophilic cyclic analogues of baclofen: design, synthesis, and neuropharmacological evaluation. *Bioorg Med Chem.* **16**(17), p7983-7991

Abdul M, Mccray SD, Hoosein NM. (2008). Expression of gammaaminobutyric acid receptor (subtype A) in prostate cancer. *Acta Oncol.* **47**, p1546–1550.

Azuma H, Inamoto T, Sakamoto T, Kiyama S, Ubai T, Shinohara Y, Maemura K, Tsuji M, Segawa N, Masuda H, Takahara K, Katsuoka Y, Watanabe M. (2003). Gamma-aminobutyric acid as a promoting factor of cancer metastasis; induction of matrix metalloproteinase production is potentially its underlying mechanism. *Cancer Res.* **63**(23), p8090-8096.

Ding, Y. (2014) Design and synthesis and evaluation of novel endoprotease-activated prodrugs and fluorogenic probes with theranostic applications in chemotherapy. PhD, Edinburgh Napier University.

Ghosh R, Bhowmik S, Bagchi A, Das D, Ghosh S. (2010). Chemotherapeutic potential of 9-phenyl acridine: biophysical studies on its binding to DNA. *Eur Biophys J.* **39**(8) p1243-1249.

Jiang X, Su L, Zhang Q, He C, Zhang Z, Yi P, Liu J. (2012), GABAB receptor complex as a potential target for tumor therapy. *J Histochem Cytochem.* **60**(4), p269-279.

Joseph J, Niggemann B, Zaenker KS, Entschladen F. (2002). The neurotransmitter gamma-aminobutyric acid is an inhibitory regulator for the migration of SW 480 colon carcinoma cells. *Cancer Res.* **62**(22), p6467-6469.

Hajihassan Z, Rabbani-Chadegani A. (2009). Studies on the binding affinity of anticancer drug mitoxantrone to chromatin, DNA and histone proteins. *J Biomed Sci*. **16**(31), p1-7.

Leo A, Hansch C, and Elkins D (1971). "Partition coefficients and their uses". *Chem Rev.* **71**(6), p525-616.

Lodewyks C, Rodriguez J, Yan J, Lerner B, Lipschitz J, Nfon C, Rempel JD, Uhanova J, Minuk GY. (2011). GABA-B receptor activation inhibits the in vitro migration of malignant hepatocytes. *Can J Physiol Pharmacol.* **89**(6), p393-400.

Mazerski J, Martelli S, Borowski E. (1998). The geometry of intercalation complex of antitumor mitoxantrone and ametantrone with DNA: molecular dynamics simulations. *Acta Biochim. Pol.* **45**(1), p1–11.

Mincher DJ, Turnbull A, Pettersson S, Bibby MC, Double JA. (2000). NU:UB 31: A novel in vivo-active dual topoisomerase I and II inhibitor with high selectivity in colon carcinoma. *Clinical Cancer Research*, **6**(Suppl.), p249.

Nielsen JF, Hansen HJ, Sunde N, Christensen JJ. (2002). Evidence of tolerance to baclofen in treatment of severe spasticity with intrathecal baclofen. *Clinical neurology and neurosurgery.* **104**(2). p142–145.

Olmsted J. III and Kearns D.R. (1997) Mechanism of ethidium bromide fluorescence enhancement on binding to nucleic acid. *Biochemistry.* **16**(16), p3647-3654.

Rautio J, Kumpulainen H, Heimbach T, Oliyai R, Oh D, Järvinen T, Savolainen J. (2008). Prodrugs: design and clinical applications.. *Nat Rev Drug Discov.* **7**(3), p255-270.

Roberts SS, Mendonça-Torres MC, Jensen K, Francis GL, Vasko V. (2009). GABA receptor expression in benign and malignant thyroid tumors. *Pathol Oncol Res.* **15**(4), p645-50.

Ross DT1, Scherf U, Eisen MB, Perou CM, Rees C, Spellman P, Iyer V, Jeffrey SS, Van de Rijn M, Waltham M, Pergamenschikov A, Lee JC, Lashkari D, Shalon D, Myers TG, Weinstein JN, Botstein D, Brown PO. (2000). Systematic variation in gene expression patterns in human cancer cell lines. Available: http://dtp.cancer.gov/mtweb/targetinfo?moltid=GC15136&moltnbr=5734. Last accessed 9th May 2014.

Schuller HM, Al-Wadei HA, Majidi M. (2008). GABA B receptor is a novel drug target for pancreatic cancer. Cancer. **112**(4), p767-78.

Tatsuta M, Iishi H, Baba M, Nakaizumi A, Ichii M, Taniguchi H. (1990). Inhibition by gamma-amino-n-butyric acid and baclofen of gastric carcinogenesis induced by N-methyl-N'-nitro-N-nitrosoguanidine in Wistar rats. *Cancer Research.* **50**(16), p4931–4934.

Tatsuta M, Iishi H, Baba M, Taniguchi H. (1992). Attenuation by the GABA receptor agonist baclofen of experimentalcarcinogenesis in rat colon by azoxymethane. *Oncology.* **49**(3), p241–245.

Thaker PH, Yokoi K, Jennings NB, Li Y, Rebhun RB, Rousseau DL Jr, Fan D, Sood AK. (2005). Inhibition of experimental colon cancer metastasis by the GABA-receptor agonist nembutal. *Cancer Biol Ther.* **4**(7), p753-758.

Turnbull, A. (2003). Design and development of novel DNA topoisomerase inhibitors. PhD, Edinburgh Napier University.

Van Valckenborgh E, Mincher D, Di Salvo A, Van Riet I, Young L, Van Camp B, Vanderkerken K. (2005). Targeting an MMP-9-activated prodrug to multiple myeloma-diseased bone marrow: a proof of principle in the 5T33MM mouse model. *Leukemia*, **19**(9), p1628-1633

Wang T, Huang W, Chen F. (2008). Baclofen, a GABAB receptor agonist, inhibits human hepatocellular carcinoma cell growth in vitro and in vivo. *Life Sci.* **82**(9-10), p536-541.

Zhu R, Qin S, He X, Wang F. (2004). GABAB receptor expression in human gastric cancer. *Med J Chin PLA.* **29**. p958–960.

# Chapter 3 Legumain Activated GABA Prodrugs

## 3.1 Abstract

Legumain represents a recently identified lysosomal protease that is upregulated in most human cancers. Legumain activity is thought to promote tumour invasion and metastasis. Consequently, legumain is a promising target for probe design in cancer diagnosis.

A quenched activity-based probe for legumain Rho-Pro-Ala-Asn-GABA-[Propyl spacer]-AQ (HZ101) was chemically synthesised. The probe comprises the fluorochrome Rhodamine B, a legumain specific peptide substrate and the dark quencher anthraquinone. This probe is highly selective for legumain due to the asparagine residue at the P1 position. Peptide cleavage by legumain relieves the self-quenching of the probe and generates fluorescence. The evaluation of probe activity by MTT, HPLC and lipophilicity assays demonstrated that HZ101 is an ideal biomarker for the imaging and diagnosis of human breast cancer and is a potential prodrug for the delivery of GABA to tumours to modulate the $GABA_B$ receptor response.

## 3.2  Introduction

### 3.2.1 Legumain

Legumain, an asparaginyl endopeptidase, is a member of the C13 cysteine protease family and was first identified in plants (Ishii, 1993). Mammalian legumain has been discovered in the liver, spleen and kidney. Legumain has been proposed to play an important role in the degradation of the extracellular matrix (Morita *et al.,* 2007). Each legumains is first produced as a pro-enzyme (50-60 kDa), which is converted into the active form by auto cleavage under acidic conditions (pH 4.0 to 5.8). The size of mature active legumain varies from

30 kDa to 40 kDa. Legumain is irreversibly denatured at a pH of 7 or higher (Chen *et al.*, 1997, Chen *et al.,* 2001). In cells, mammalian legumain is mainly localized in the endo-lysosomal system. The acidic pH environment of lysosomes facilitates legumain activity (Dall and Brandstetter, 2015).

### 3.2.2 Legumain Substrate Specificity

The crystal structure of legumain provides insights into its substrate specificity. The S1 pocket of legumain has a dual charge character and is consequently an ideal binding site for the asparagine at the P1 substrate position (Dall and Brandstetter, 2013).

Legumain has less selectivity at other substrate positions. A peptide library was constructed to determine the optimal substrate sequences for the P3-P2-P1 positions. The tripeptide Thr-Ala-Asn was identified as the ideal substrate for *Schistosoma* legumain whereas human legumain prefers a proline (Pro) residue at P3. These observations suggest that legumain substrate specificity is species dependent (Mathieu *et al.,* 2002). At the P1' position, amino acids with small side chains such as Gly and Ala, are tolerated, but proline is excluded (Schwarz *et al.*, 2002).

The endogenous cystatin E/M is the most potent inhibitor of legumain and also serves as a tumour suppressor. The auto-activation of prolegumain is inhibited by cystatin E/M in both intra- and extracellular environments (Smith *et al.,* 2012). The crystal structure of the legumain-cystatin complex revealed that cystatin acts as a substrate and the cleavage product remains bound to the legumain active site. The development of legumain inhibitors has been considered. Recently, a series of aza-peptidyl inhibitors with non-natural amino acids were

synthesised. It was found that inhibitors with small alkyl groups in the P3 position had the improved inhibitory activity (Lee and Bogyo, 2012).

### 3.2.3 Legumain expression in tumours

Several studies have shown that legumain is highly expressed in tumours *in vitro and in vivo*, such as colorectal, prostate, gastric, ovarian, and breast cancers (Zhen *et al.,* 2015).

Immunohistochemical and western blotting methods have revealed that the expression of legumain is increased in primary colorectal cancer compared with normal mucosa. Patients with lower legumain expression and weak staining have a better survival rate. These findings suggest that legumain may play a greater role in the early development of colorectal cancers and that its prognostic importance should be considered (Murthy *et al.*, 2005).

The expression and activity of legumain in melanoma were first addressed in 2010. The endogenous cystatin E/M was detected to inhibits the legumain activity and suppresses tumour growth and metastasis (Briggs *et al.*, 2010). Legumain expression has also been confirmed in prostate cancer by RT-PCR and Western blot. An immunohistochemical study revealed that a vesicular staining pattern of legumain was associated with prostate tumour invasion and metastasis (Ohno *et al.*, 2013). In gastric cancer, legumain is over-expressed and is significantly correlated with tumour cell invasion and malignant transformation. Legumain has been proposed as a biomarker to predict the prognosis for metastasis in gastric cancer (Guo *et al.*, 2013).

Gawend *et al.* (2007) investigated legumain expression in breast cancer. Non-neoplastic breast tissues exhibited a pattern of negative or low staining pattern for legumain, whereas a positive vesicular pattern was observed in

invasive breast tumour cells by immunohistochemistry. Another study supported the hypothesis that targeting tumour associated macrophages and reducing their density in tumour tissues leads to a reduction of tumour mass. Macrophages are responsible for the secretion of many tumour invasive factors such as MMP-9, VEGF, and TNF-α. Legumain overexpressed by tumour-associated macrophages was used as the target molecule and a legumain based DNA vaccine was used to target tumour associated macrophages (Luo *et al.*, 2006). In ovarian cancer, patients with high legumain expression had a worse prognosis and survival rate. Legumain was found to be upregulated in ovarian cancer tissues at both the mRNA and protein levels (Wang *et al.*, 2012).

### 3.2.4 Legumain Activated Prodrugs

The protease activated prodrug approach for cancer therapy was first described in 1980 (Carl *et al.,* 1980). The created prodrugs aim to be locally activated by tumour-associated protease and have less toxicity to normal cells.

Legubicin (as shown in **Figure 38**) was designed as the legumain activated prodrug for cancer chemotherapy (Liu *et al.,* 2003). The prodrug was synthesized by addition of a peptide extension (Boc-Ala-Ala-Asn-Leu) to the amino group of doxorubicin. The Boc protecting group at the $NH_2$ terminus prevented the hydrolysis of peptide component. After cleavage by legumain, the prodrug will be converted into two molecules Boc-Ala-Ala-Asn-OH and Leu-doxorubicin.
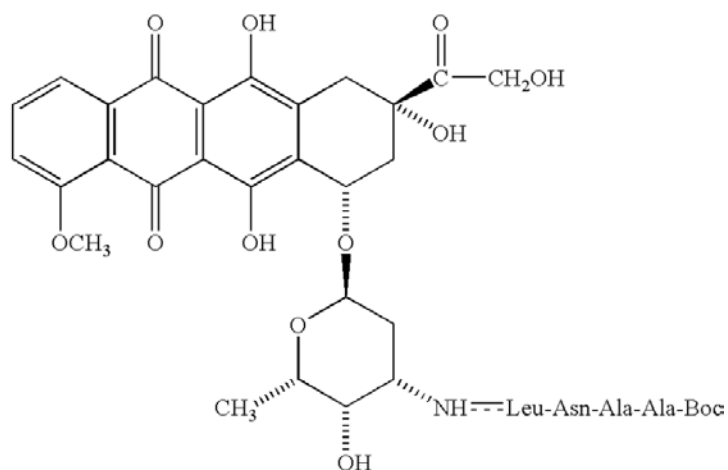
**Figure 38. Chemical structure of**
***N*-(-*t*-Butoxycarbonyl-L-alanyl-L-alanyl-L-asparaginyl-L-leucyl)doxorubicin**
**(Legubicin) prodrug**

The cytotoxicity of legubicin was analysed in vitro. On tumour cells not expressing legumain, the cytotoxic effect of legubicin was less than 1% compared with doxorubicin. In contrast, on legumain positive cells, the effect of legubicin with conversion to Leu-doxorubicin was similar to doxorubicin. This result indicated that the peptide conjugation on legubicin prodrug had successfully eliminated the cytotoxic effect of doxorubicin (liu *at al.,* 2003).

The in vitro effects of legubicin were investigated on mice model with CT26 colon carcinoma. The injection of legubicin at 5 mg/kg three times in 2 days to mice arrested the tumour growth. The weight of mice was monitored during the therapy and there was no evidence of weight loss which indicated that legubicin was tolerated in mice and has little toxicity. Moreover, the organs that express legumain such as liver and kidney were not injured. At the same dose, doxorubicin was fatal to mice and failed to produce similar antitumour effect as legubicin. The TUNEL assays showed that the apoptotic index of legubicin was higher that doxorubicin.
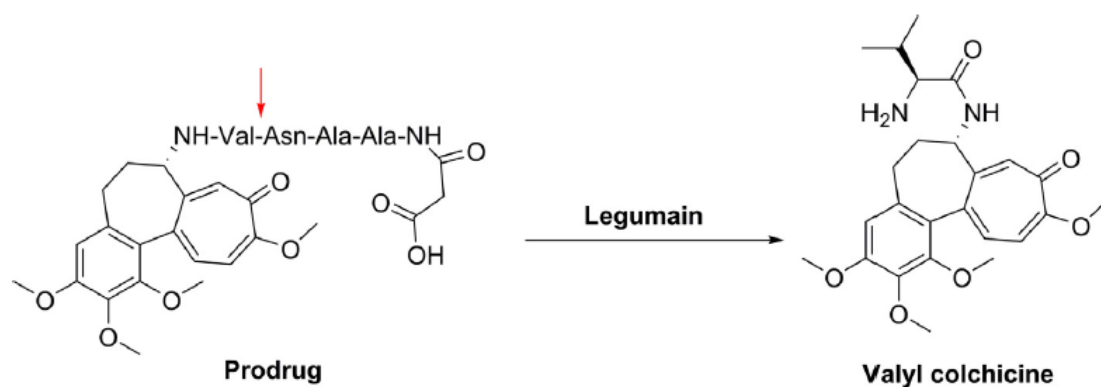
**Figure 39.** legumain cleavable colchicine prodrug

**Figure 39** shows another example of a legumain-cleavable prodrug incorporating colchicine as the cytotoxic agent (Smith *et al.,* 2014). The synthesised prodrug has the legumain peptide substrate Val-Asn-Ala-Ala. The amino acid valine was linked to deacetyl colchicine to increase the lipophilicity of the released active agent after legumain cleavage. The prodrug activity was investigated by MTT assay on the colorectal cell lines HCT116 and SW620. The legumain activity in HCT116 showed approximately 25% higher than SW620 cell line. At the same prodrug concentration (10 μM), the cell viability for HCT116 was lower than in SW620 cells. Furthermore, the legumain inhibitor cystatin E/M was able to reduce the toxicity of the colchicine prodrug by approximately 33% in legumain over-expressing cell line M38L (Smith *et al.,* 2014).

### 3.2.5 Legumain Activated Probes

In 2013, (Edgington *et al.,* 2013) developed a legumain probe (LE28) that is fluorescently quenched. The chemical structure of LE28 was shown in **Figure 40.**
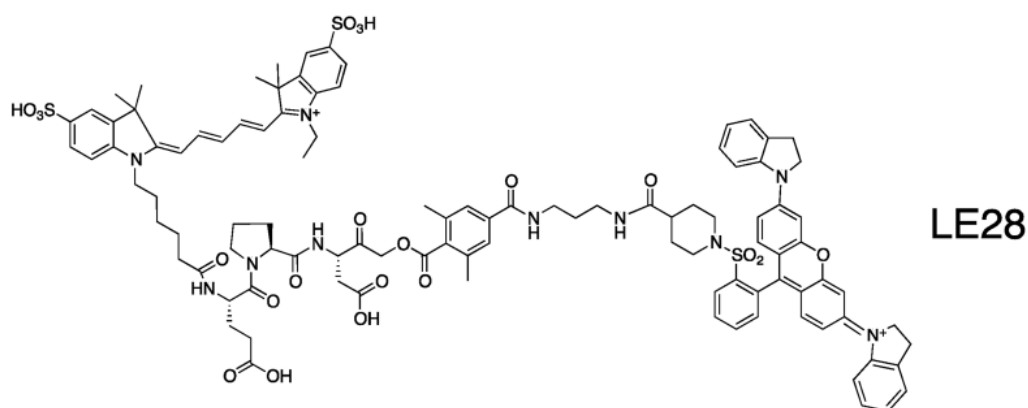
**Figure 40.** Chemical structure of LE28
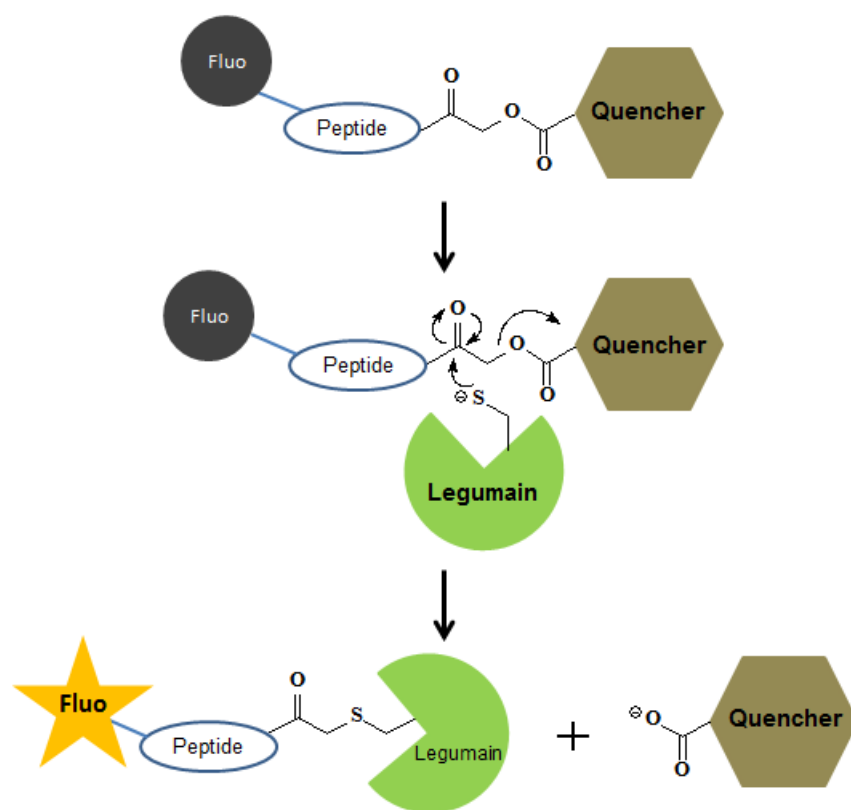


**Figure 41.** Mechanism of LE28 binding to legumain

The mechanism of LE28 has been illustrated in **Figure 41.** The catalytic thiol in the active site of legumain attacks the acyloxymethyl ketone of LE28 and results in loss of quenching group. The probe covalently binds to legumain and becomes fluorescent. LE28 was found to be highly quenched. The capacity of LE28 bind to legumain was tested by incubation of RAW cell extracts with

increasing concentrations (0-5 µM) of LE28 at pH 4.5. The proteins were resolved by fluorescent SDS-PAGE and a legumain size at 36 kDa was observed.

In vivo imaging with LE28 was first performed on healthy nude mice. The mice were injected with LE28 and the fluorescence was imaged on an IVIS machine. LE28 already started to produce low fluorescence at early time (5-25 min) of injection. After 1 hour, the fluorescent imaging intensity in the kidney became strong and continued to increase. The major organs were collected after 8 hours of injection and a biochemical analysis was performed. Kidney appeared to have the highest LE28 labelling. Liver had a lesser level of LE28 labelling than kidney. The imaging ability of LE28 on tumour cells was evaluated using the HCT-116 (human colorectal carcinoma cells) and tumour bearing mice. The injected mice were monitored for 28 hours. After 30 min of injection, the fluorescence signal of LE28 became detectable. The fluorescent imaging intensity reached the maximal value at 7 hours and remained constant until 28 hours. The probe LE28 effectively imaged the legumain activity in normal tissues and tumours. Future efforts on design of the fluorescently quenched probe target legumain for different tumour types have great importance (Edgington *et al.,* 2013).

Another recent study developed a new MRI contrast agent Gd-NBCB-TTDA-Leg(L) and a near-infrared fluorescent probe CyTE777-Leg(L)-CyTE807 for detection of legumain activity in tumours (Chen *et al.,* 2014). Both of the two compounds have the same legumain specific substrate peptide Leg(L). The MTT assay evaluated the cytotoxicity of Gd-NBCB-TTDA-Leg(L) and CyTE777-Leg(L)-CyTE807 on colon carcinoma cell line. They all showed low cytotoxicity even at high concentrations. The in vitro

and in vivo MR imaging were carried out for Gd-NBCB-TTDA-Leg(L), the results indicated that the new MRI contrast agent attained 55.3 fold higher imaging enhancement than control. In vivo optical imaging of the NIR fluorescent probe CyTE777-Leg(L)-CyTE807 showed efficiently fluorescent intensity.

## 3.3 Results and Discussion

### 3.3.1 Design of Legumain activated Probe HZ101

Fluorescent probes have been developed as powerful tools for *in vivo* imaging of tumour microenvironment (Ueno and Nagano, 2011). The probe designed in this study for fluorescence imaging is based on the FRET principle (**Figure 42**).
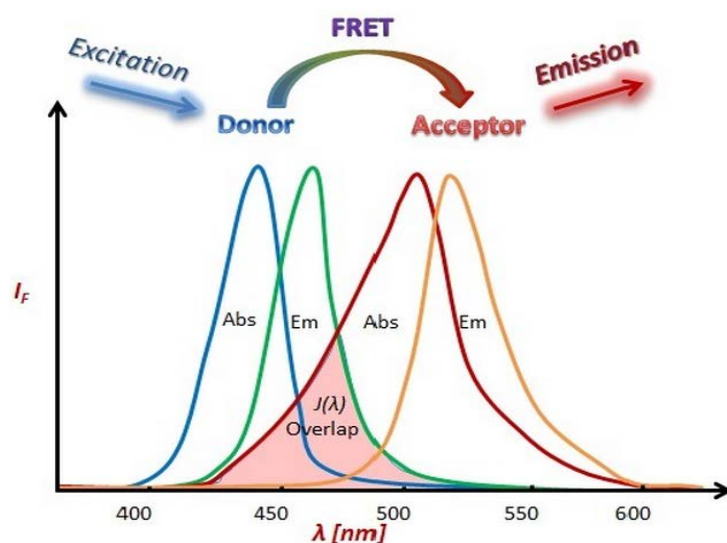


**Figure 42.** Schematic of the FRET process

FRET (Fluorescence Resonance Energy Transfer) is one of the most commonly exploited mechanisms for the design of fluorescent probes. FRET is the process of energy transfer from an excited donor to an acceptor through dipole-dipole interactions. The transfer of energy reduces the fluorescence intensity of the donor (Demchenko, 2010). The emission spectrum of the donor should overlap with the acceptor absorption spectrum, whereas, the absorption spectra of the donor and acceptor should be well separated. The donor is a fluorophore with brightness comparable to that of the acceptor dye. The linker between the donor and acceptor is selected to prevent fluorescence quenching (Kobayashi *et al.,* 2010).
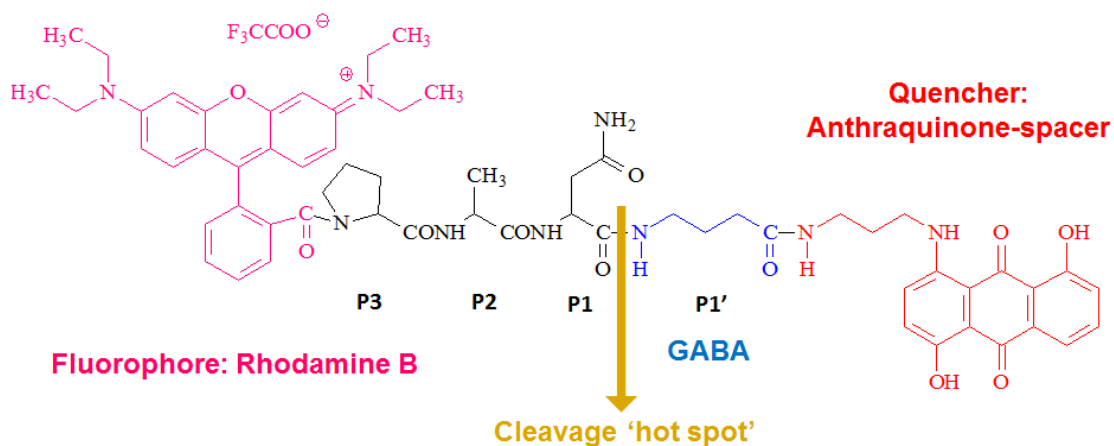
**Figure 43.** Designed structure of the legumain activated probe (HZ101)

The legumain activated probe (HZ101) designed here **Figure 43** contains a legumain specific substrate (Pro-Ala-Asn↓) in the middle. The arrow denotes the cleavage site adjacent to the carboxy terminus of asparagine. The C-terminal side of asparagine at the P1 site is cleaved by legumain in a number of substrates. One side of the substrate (N-terminus) was attached to rhodamine B as the fluorophore. The quenching group anthraquinone spacer was added to the other side (C-terminus) of the tripeptide substrate.

The designed probe HZ101 (Rho-Pro-Ala-Asn-GABA-[Propyl spacer]-AQ) aims to exploit the proteolytic activity of overexpressed legumain in the breast cancer cell line MCF-7. The fluoro group of rhodamine B can be silenced by the dark quenching group of the anthraquinone spacer due to the principle of FRET. After peptide cleavage by legumain, which is indicated by fluorescence restoration, the anthraquinone spacer is further activated by aminopeptidases to release the ligand GABA.
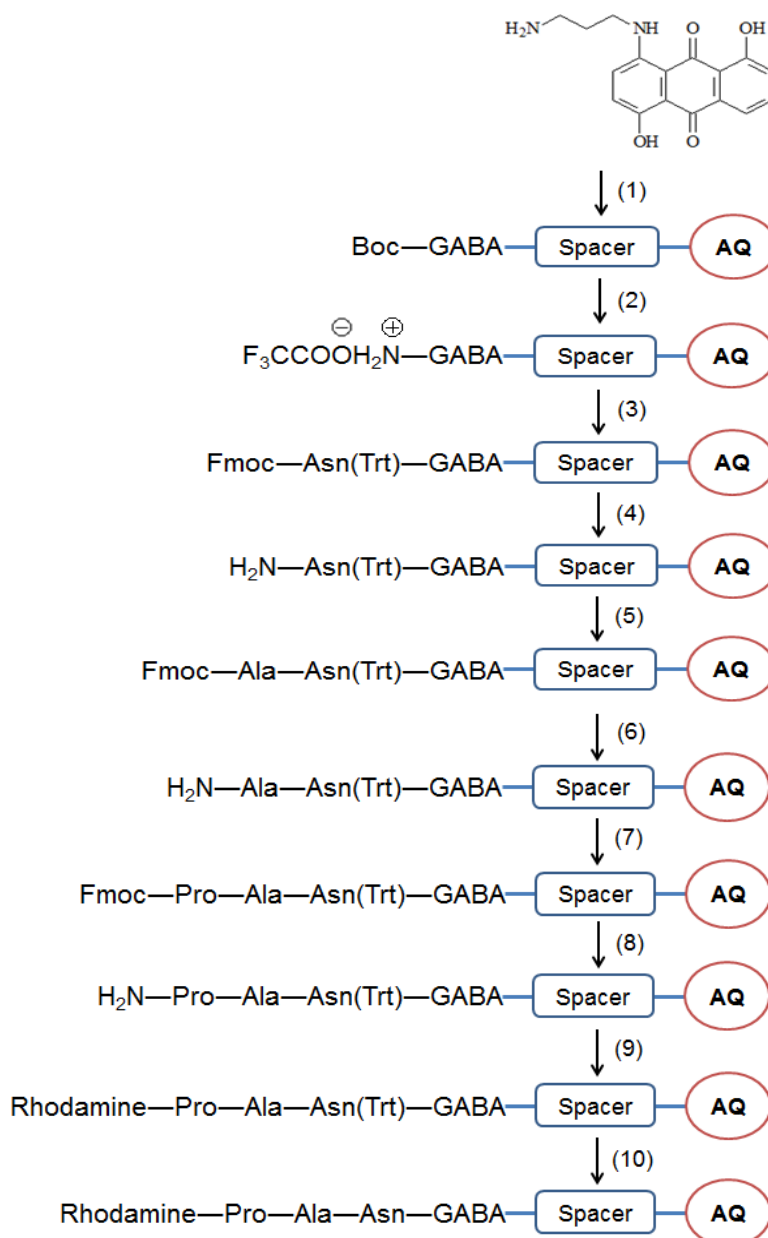
**Reagents and conditions:** (1) Boc-GABA-OH, PyBOP , DIPEA, in DMF, RT(2) TFA, RT (3) Fmoc-Asn(Trt)-OH, TBTU, HOBt, DIPEA, DMF, RT, (4) 20% piperidine in DMF, RT (5) Fmoc- Ala-OH, TBTU, HOBt, DIPEA, DMF, RT (6) 20% piperidine in DMF, RT (7) Fmoc-Pro-OH, TBTU, HOBt, DIPEA, DMF, RT (8) 20% piperidine in DMF, RT (9) Rhodamine B, TBTU, HOBt, DIPEA, DMF (10) TFA, RT

**Scheme 32.** Overview of the synthesis of the legumain activated prodrug (HZ101)

**Scheme 32** presents the overall scheme of the whole synthesis of the legumain prodrug HZ101. The tetrapeptide (Pro-Ala-Asn(Trt)-GABA) was built on the anthraquinone spacer by solution phase peptide synthesis. The trityl protecting group of asparagine was removed at the last step after adding rhodamine B to the tetrapeptide anthraquinone conjugate H-Pro-Ala-Asn(Trt)-GABA-[Propyl spacer]-AQ.

### 3.3.2 Synthesis of H-[Propyl spacer]-AQ (HZ103)

The starting point in the synthesis of the legumain targeted theranostic prodrug (HZ101) as shown in **Scheme 33** was the preparation of the aminoanthraquinone (HZ103), which serves as both the quencher of the rhodamine fluorophore in FRET for diagnostic applications and a DNA binding cytotoxic agent in anticancer therapeutics.

In general, the introduction of hydroxy groups into the anthracenedione ring system enhances cytotoxic potency; hydroxylation of the nucleus, as in the case of mitoxantrone may be expected to increase cytotoxicity due to stronger binding to DNA and slower dissociation kinetics due to the presence of the hydroxyl groups (Smith*et al.*, 1990).

Here, the strategy adopted for the synthesis of the 4, 8-dihydroxylated aminoanthraquinone-spacer compound (HZ 103) was based on the controlled mono-amination of leuco-1,4,5-trihydroxyanthraquinone (leuco-5-hydroxyquinizarin). The methods were based on the reported regiospecific amination of this leuco-trihydroxyanthraquinone by Morris, Mullah and Sutherland (1986), who synthesised a series of aminohydroxyanthraquinones from leuco-5-hydroxyquinizarin. It was found that if the *leuco*-intermediates were oxidised and then hydrolysed using HCl or NaOH, they each gave 5-hydroxyquinizarin. However, if these intermediates were stirred with triethylamine in dichloromethane in the presence of air, the aminoanthraquinones were formed. These conditions were adopted for the synthesis of HZ103.
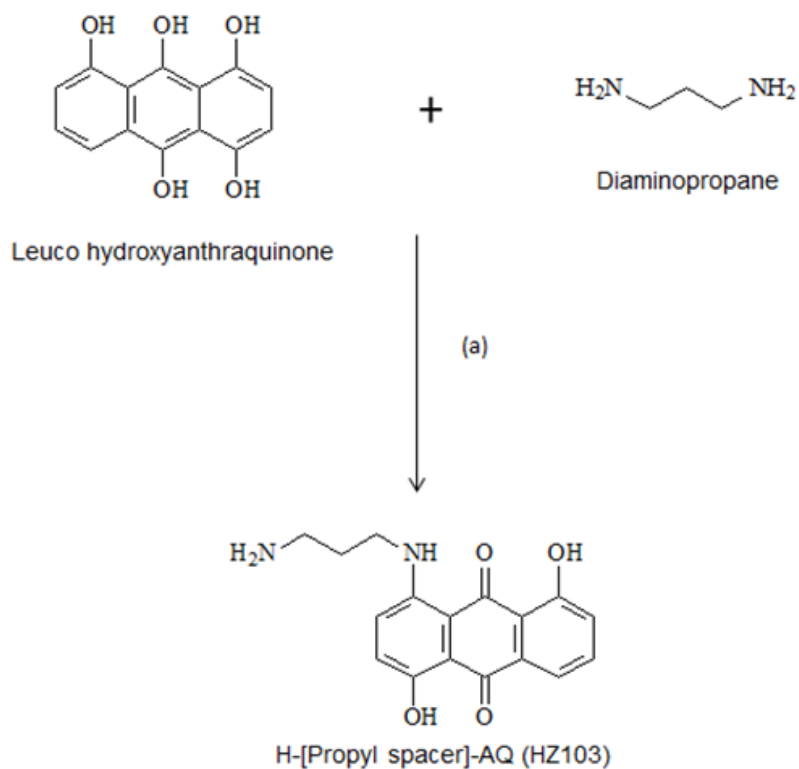
Reagents and Conditions: (a) $CH_2Cl_2$, water bath (1 hour), then $Et_3N$ (0.5 ml) and $O_2$ for 2 hours

**Scheme 33.** Outline of HZ103 synthesis

Leuco-1,4,5-trihydroxyanthraquinone was reacted with diaminopropane in dichloromethane. The reaction mixture was refluxed in $60^o\,C$ water bath for 1 hour. Triethylamine was then added to the reaction. The mixture was oxidized by $O_2$ for 2 hours. The brown insoluble solid was removed by filtration and the remaining solution was extracted with dichloromethane and water. The organic layers were combined and dried. The dark blue product H-[Propyl spacer]-AQ (HZ103) was collected for the next reaction.

### 3.3.3 Synthesis of Boc-GABA-[Propyl spacer]-AQ (HZ104)

The coupling reaction of H-[Propyl spacer]-AQ (HZ103) and Boc-GABA-OH was performed in DMF by the addition of reagents PyBOP and DIPEA (**Scheme 34**).
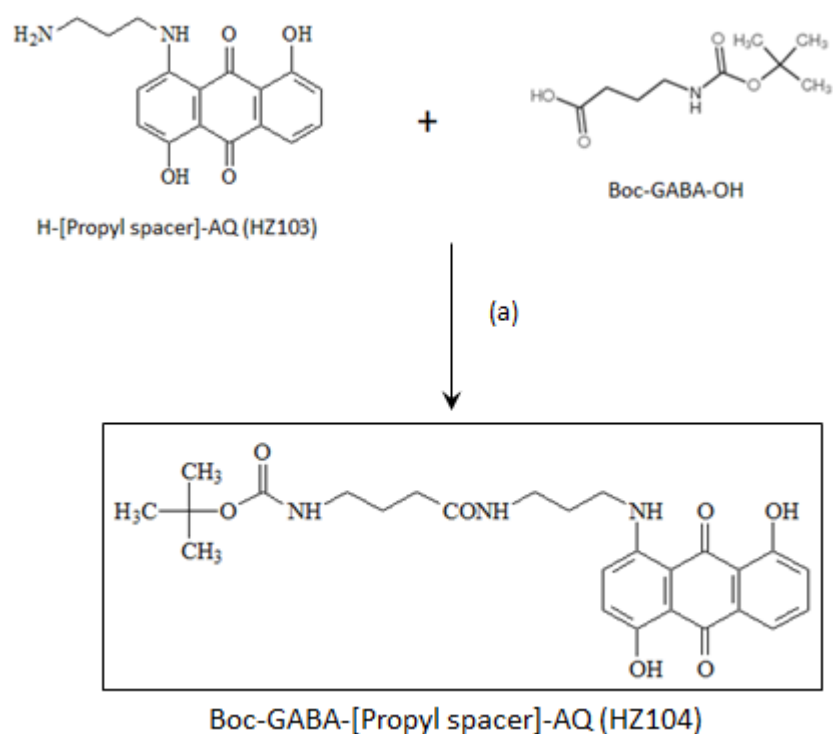
Reagents and Conditions: (a) PyBOP, DIPEA, in DMF

**Scheme 34.** Outline of HZ104 synthesis

The reaction was monitored by TLC and pure HZ104 was obtained by silica gel chromatography and collection of appropriate fractions. The product Boc-GABA-[Propyl spacer]-AQ (HZ104) was then used in the de-protection reaction.

### 3.3.4 Synthesis of H-GABA-[Propyl spacer]-AQ TFA Salt (HZ105)

The Boc protecting group of Boc-GABA-[Propyl spacer]-AQ (HZ104) was removed by using TFA (**Scheme 35**). After confirmation of Boc removal by TLC the excess TFA was removed by evaporation.
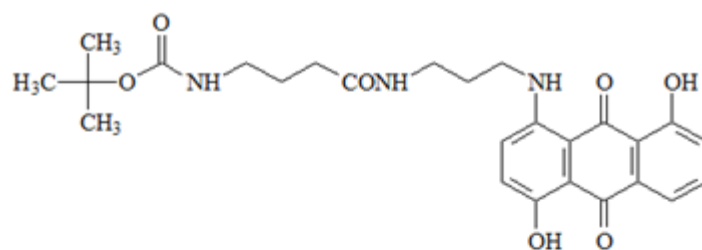
Boc-GABA-[Propyl spacer]-AQ (HZ104)

(a)
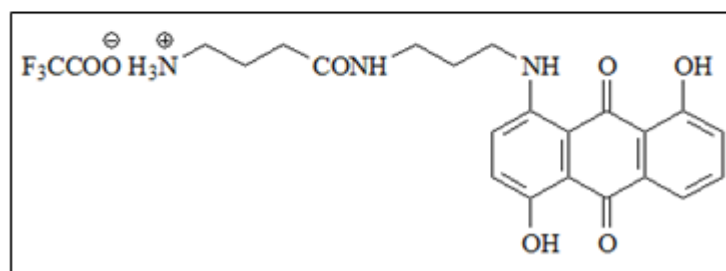
H-GABA-[Propyl spacer]-AQ TFA salt (HZ105)

Reagents and Conditions: (a) TFA

**Scheme 35.** Outline of HZ105 synthesis

To obtain pure H-GABA-[Propyl spacer]-AQ TFA salt (HZ105) for HPLC analysis, further purification was performed using thick layer chromatography. The compound H-GABA-[Propyl spacer]-AQ TFA salt (HZ105) was characterised by NMR. The ^{1}H NMR spectrum revealed signals between 1.7 and 3.4 were assigned to the methylene groups of the GABA and propyl spacer. The anthraquinone protons were fully assigned; H-2 and H-3 gave a 2-proton multiplet at 7.18 to 7.3 ppm, H-7 was a doublet at 7.3 to 7.4 ppm, and H-6 was a multiplet between 7.58 and 7.7 ppm.

### 3.3.5 Synthesis of H-Pro-Ala-Asn(Trt)-GABA-[Propyl spacer]-AQ (HZ99)

The amino acid coupling reaction with the anthraquinone spacer compound (HZ105) was performed by solution phase peptide synthesis as shown in

**Scheme 36**.



H-GABA-[Propyl spacer]-AQ TFA salt (HZ105)

Solution phase peptide synthesis

H-Pro-Ala-Asn(Trt)-GABA-[Propyl spacer]-AQ (HZ99)
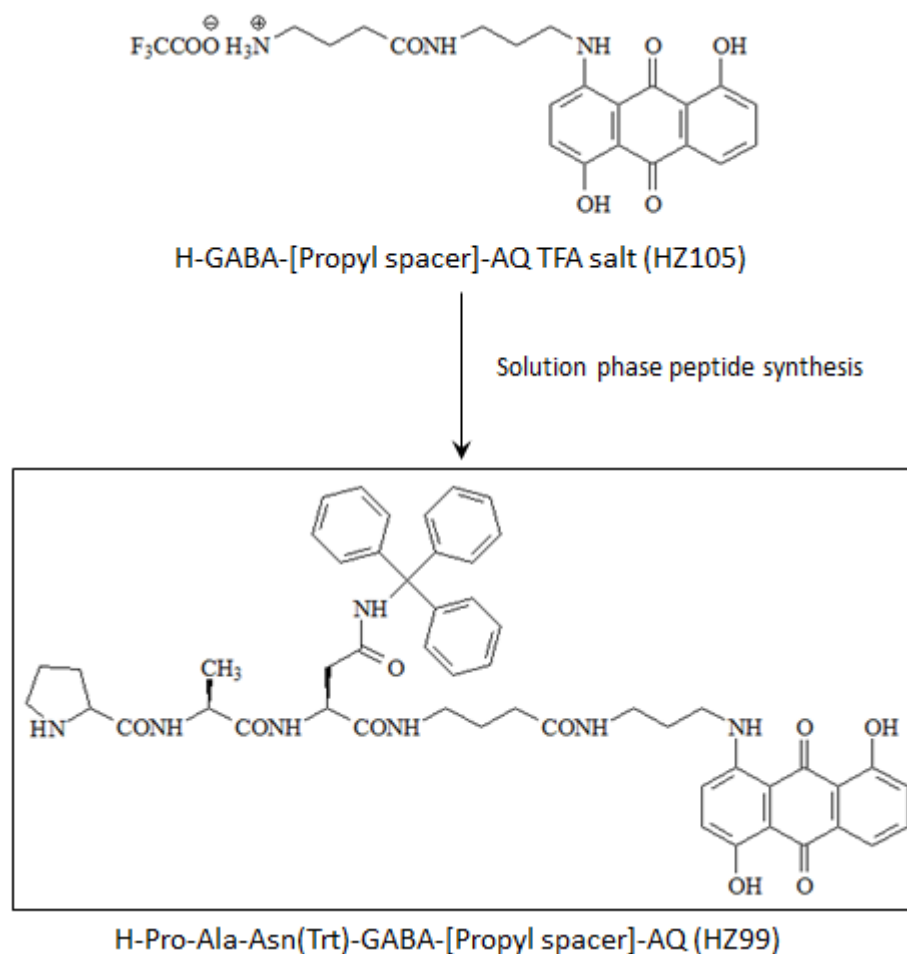
**Scheme 36.** Outline of HZ99 synthesis

HZ105 was reacted with Fmoc-Asn-OH in DMF, followed by the addition of the coupling reagents TBTU, HOBt, and DIPEA. The product Fmoc-Asn-spacer-anthraquinone was treated with 20% piperidine in DMF to remove the Fmoc protecting group. The next amino acid was added using the same method. The solution phase peptide synthesis produced the substrate conjugate Pro-Ala-Asn-GABA-Spacer-anthroquinone (HZ99).

### 3.3.6 Synthesis of Rho-Pro-Ala-Asn(Trt)-GABA-[Propyl spacer]-AQ (HZ100)

The fluorescent agent rhodamine B was coupled with H-Pro-Ala-Asn(Trt)-GABA-[Propyl spacer]-AQ (HZ99) in DMF using the reagents

PyBOP and DIPEA (**Scheme 37**).
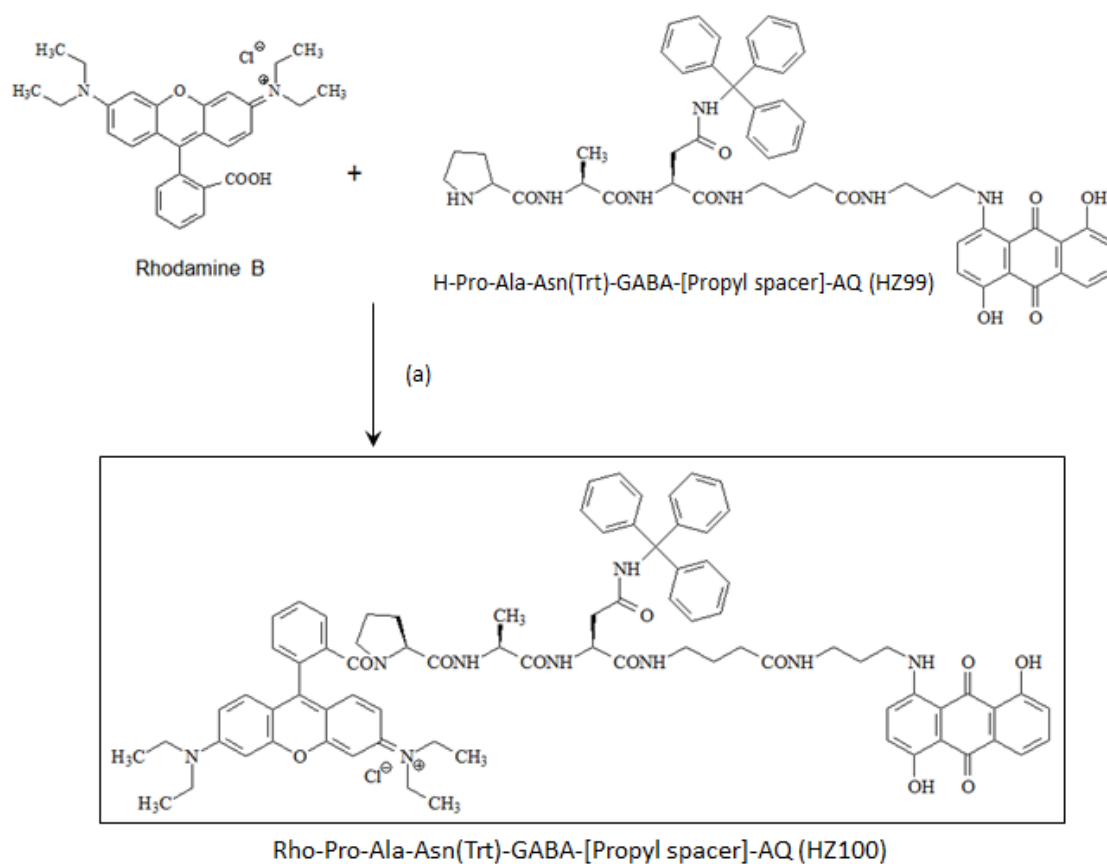


Reagents and Conditions: (a) PyBOP, DIPEA, in DMF

**Scheme 37.** Outline of HZ100 synthesis

The reaction was considered successful if monitoring of the TLC plate under the light of a UV lamp (360 nm) revealed an absence of fluorescent spots in the product lane. Rho-Pro-Ala-Asn(Trt)-GABA-[Propyl spacer]-AQ (HZ100) was further purified by silica gel chromatography. Chloroform to methanol (8:1) was used as the solvent system. The product was collected under vacuum.

### 3.3.7 Synthesis of Rho-Pro-Ala-Asn-GABA-[Propyl spacer]-AQ (HZ101)

The N-protecting group triphenylmethyl (trityl) on the asparagine of Rho-Pro-Ala-Asn(Trt)-GABA-[Propyl spacer]-AQ (HZ100) was removed by TFA treatment. The synthesis of HZ101 was illustrated in **Scheme 38**.

Rho-Pro-Ala-Asn(Trt)-GABA-[Propyl spacer]-AQ (HZ100)

(a)

Rho-Pro-Ala-Asn-GABA-[Propyl spacer]-AQ (HZ101)
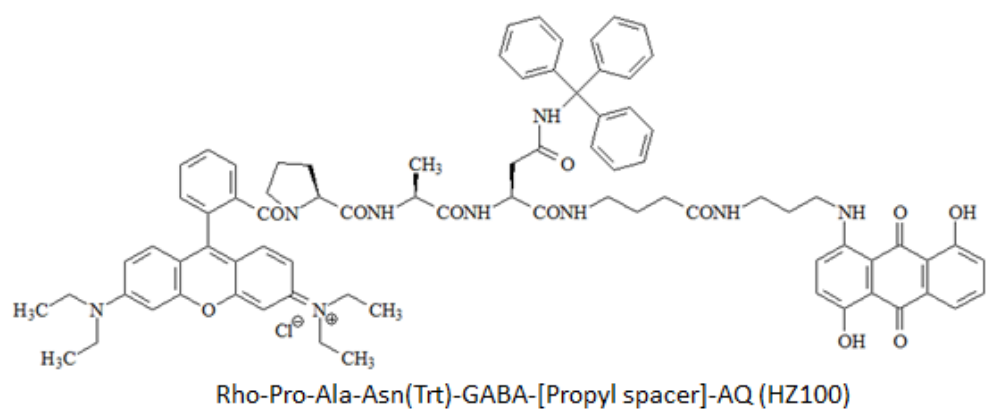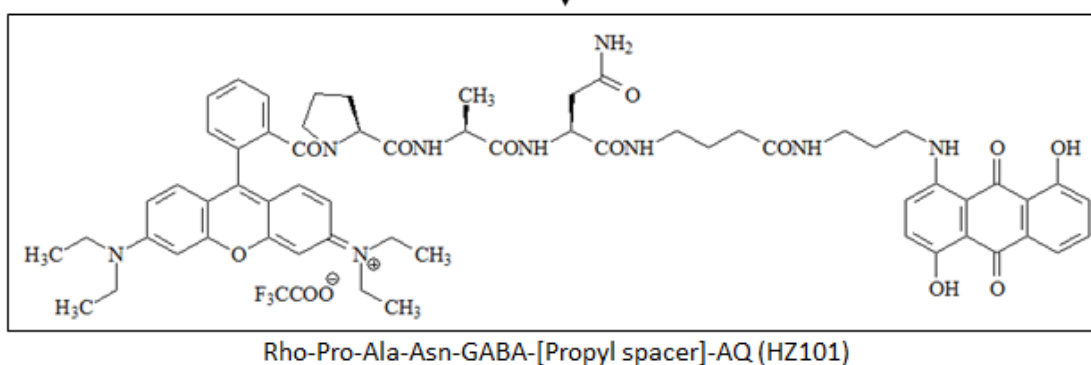
Reagents and Conditions: (a) TFA

**Scheme 38.** Outline of legumain activated prodrug (HZ101) synthesis

After confirmation of reaction completion by TLC, the reaction solution was evaporated to dryness. The solid compound was precipitated in diethyl ether. To obtain a high purity of Rho-Pro-Ala-Asn-GABA-[Propyl spacer]-AQ (HZ101) for HPLC analysis, further purification by thick layer chromatography was performed. Dichloromethane to methanol (6:1) was used as the solvent system for thick layer chromatography.

**Mass Spectral characterization of HZ101**

The Rho-Pro-Ala-Asn-GABA-[Propyl spacer]-AQ (HZ101) was successfully characterised by nanoelectrospray positive ionisation mass spectrometry (**Figure 44**). The signal at m/z 1104 in the nanoelectrospray positive ion mass

spectrum for the species $(M-CO_2CF_3)^+$ corresponds to a molecular mass of 1217 Da. In addition, the observed data and theoretical isotope model were in good agreement.
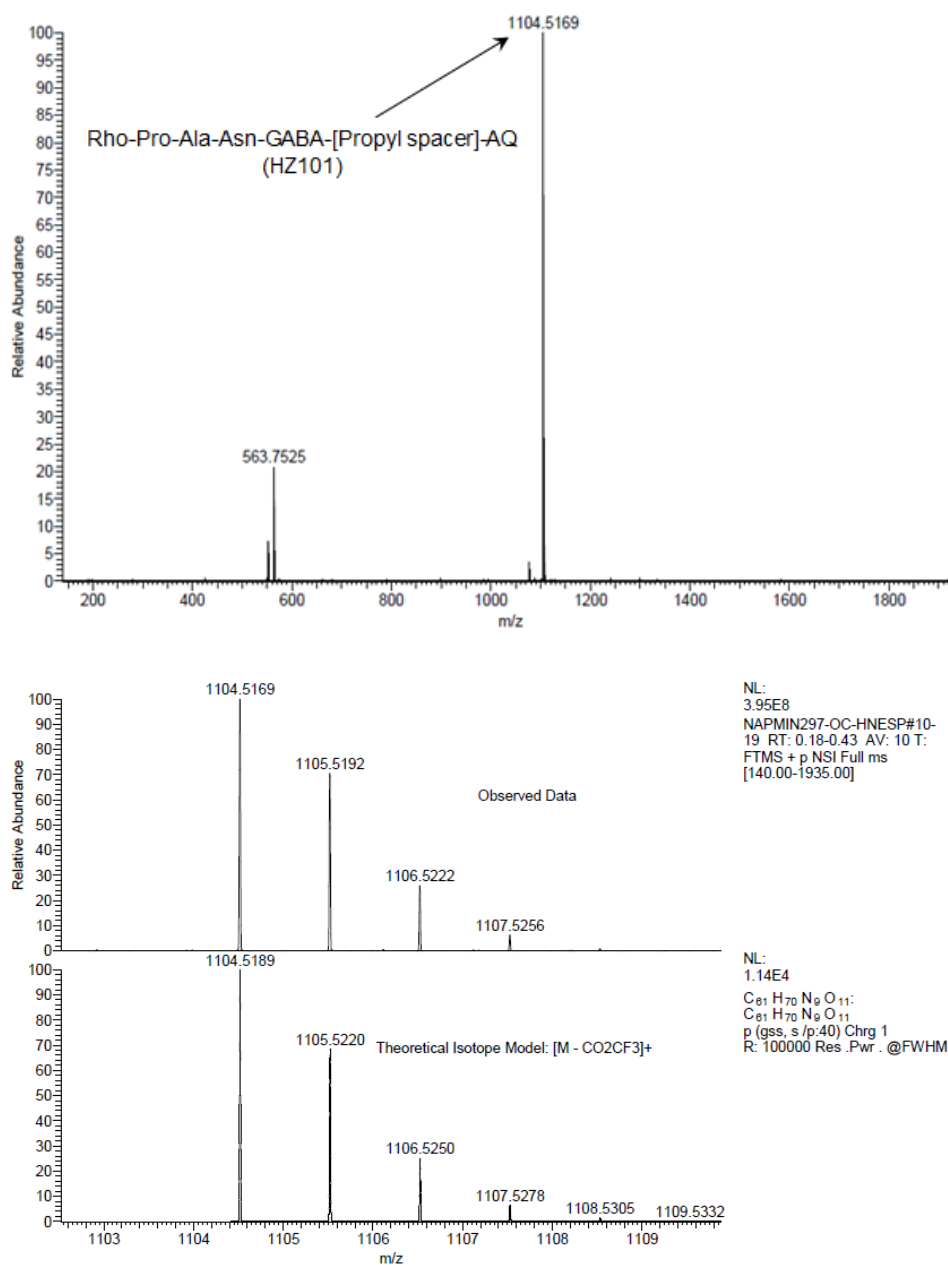


**Figure 44.** ESI (+) Mass spectrum of Probe:
Rho-Pro-Ala-Asn-GABA-[Propyl spacer]-AQ (HZ101)

### 3.3.8 Legumain PCR results

The legumain expression in MCF-7 cells was determined by end-point PCR. Before the PCR experiment, RNA was extracted from the MCF-7 cells. The

isolated RNA was then used for cDNA synthesis. As shown in **Figure 45,** beta actin was used as the positive control.
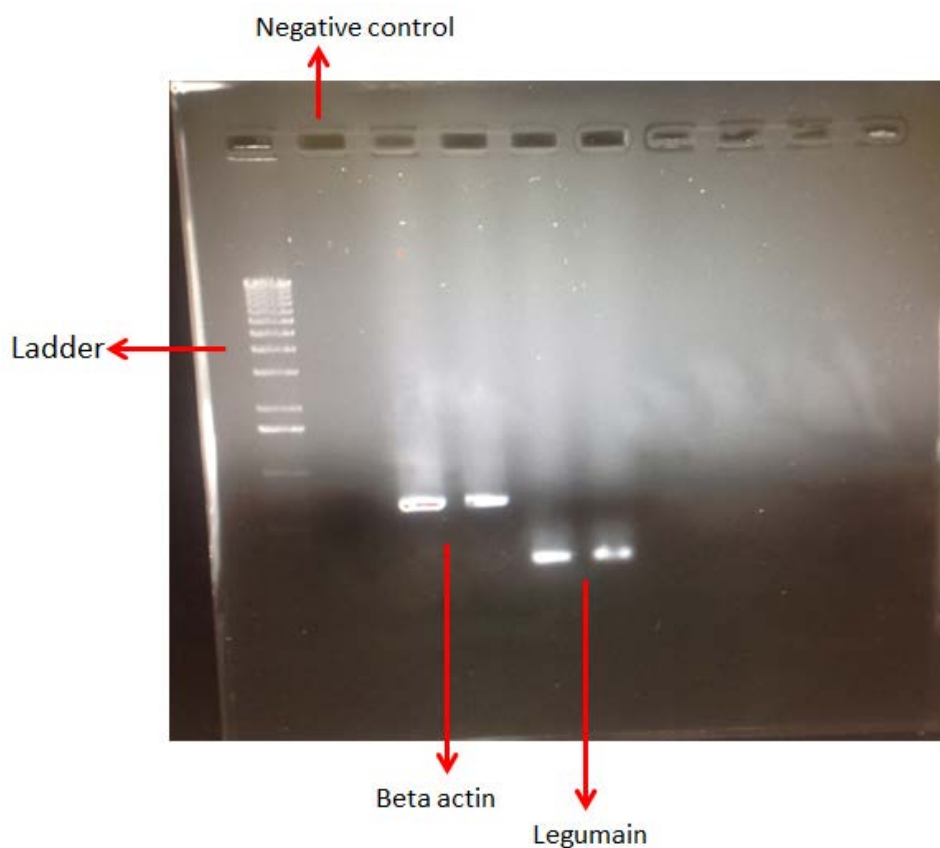


**Figure 45.** PCR results for legumain

The legumain primers were designed using the program Primer-BLAST to amplify only the legumain transcript.

Forward primer: Sequence (5'→3'): ATCCGGCAAAGTCCTGAAGAG

Reverse primer: Sequence (5'→3'): ATGAACCACCTGCCGGATAAC

From **Figure 45** above, it is obvious to see the brands of legumain which indicate the presence of legumain expression in the breast cancer (MCF-7) cell line.

### 3.3.9 HZ101 Activity Study: Fluorophore Quenching Study

In **Figure 46**, the graph showed that the highest relative fluorescence intensity of

rhodamine B is 825 at the wavelength of at 577nm.
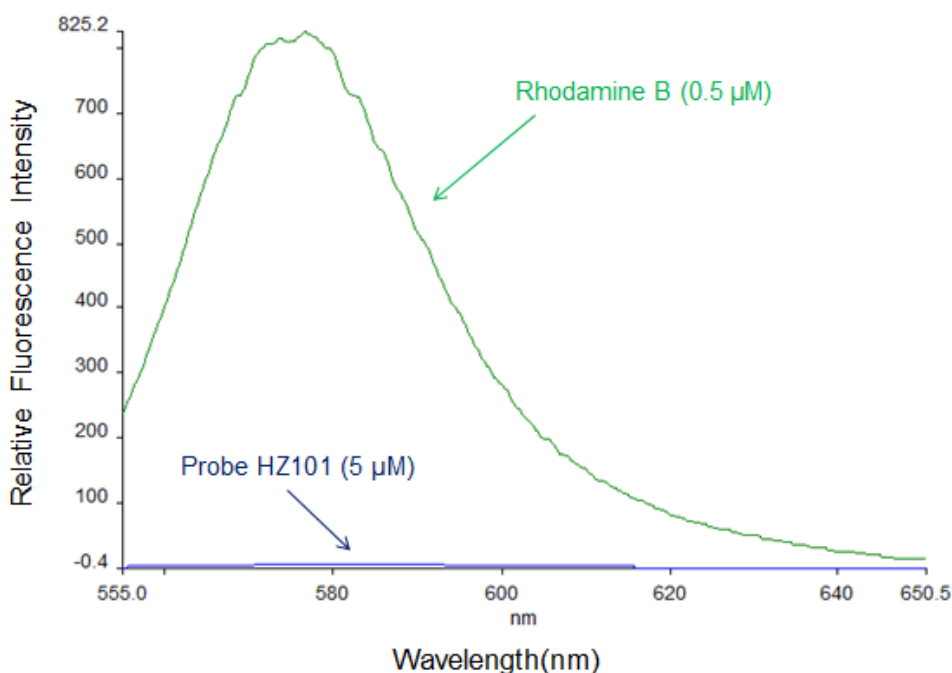


**Figure 46.** Comparison of fluorescence intensities of rhodamine B (0.5 µM) and probe HZ101 (5 µM) in legumain assay buffer, pH 5.0. Excitation/Emission (nm): 550/590.

By contrast, the fluorogenic probe HZ101 had a maximum relative fluorescence intensity of 5, at a wavelength of 580 nm, demonstrating excellent quenching of rhodamine fluorescence by the aminodihydroxyanthraquinone chromophore. There was a 165 fold difference between the two compounds. In addition, the concentration of HZ101 (5 µM) was 10 times higher than that of rhodamine B (0.5 µM) in the fluorophore quenching study. This result determines the high efficiency of the anthraquinone spacer in quenching the fluorophore rhodamine B in the probe HZ101.

### 3.3.10 HZ101 Fluorimetric Assay

The legumain activated prodrug (HZ101) was incubated with recombinant human legumain (40 ng) at 37ºC in 96 well plates (**Figure 47**). The total volume of each well was 100 µl. The concentration of HZ101 was varied from 5 µM, 10

µM, 25 µM, 50 µM to 100 µM. At concentrations of 5 µM and 10 µM, the fluorescence intensity of HZ101 increased significantly during the first 30 min and gradually reached a maximum value (550) with in the next 30 min. At the concentration of 25 µM, the maximum fluorescence intensity was only 350. When the concentration was increased to 50 µM and 100 µM, the fluorescence intensity of HZ101 remained unchanged at 250 and 200, respectively, between 3 min and 120 min.
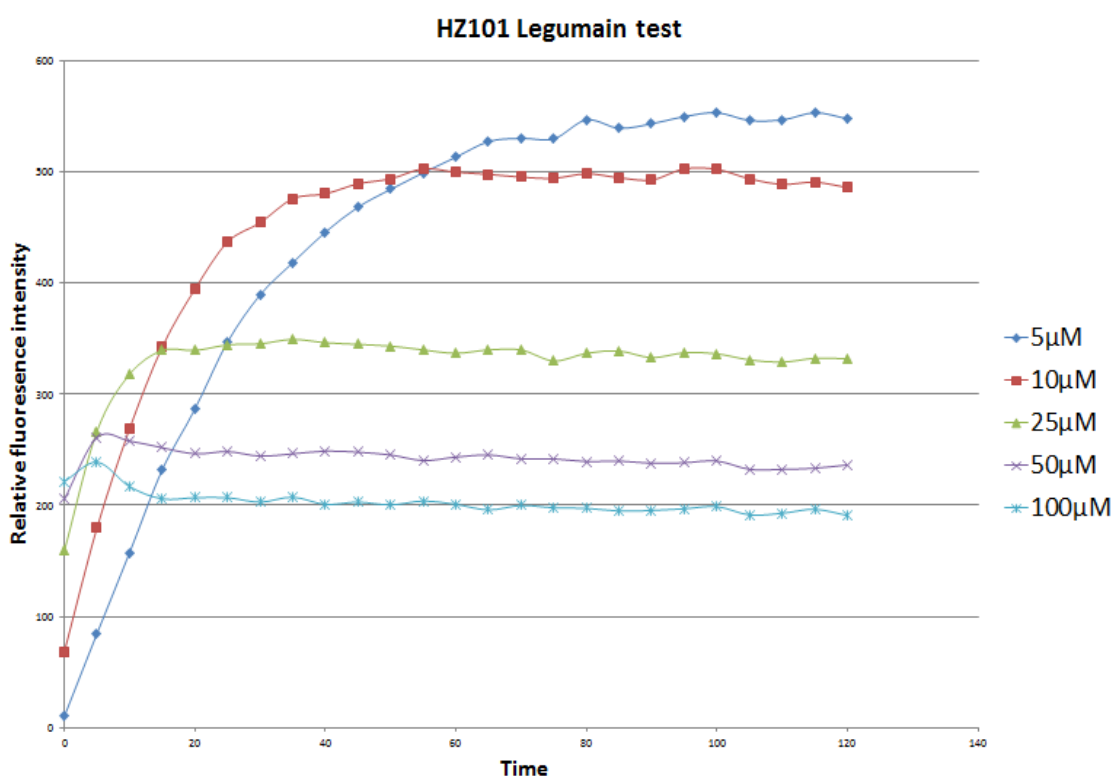


**Figure 47.** Relative fluorescence intensity released by HZ101 during the incubation with legumain. pH 5.0. Excitation: 544, Emission: 590, Gain: 800.

### 3.3.11 HZ101 Cytotoxicity Assays

The MTT cell proliferation assay has been widely used to estimate the number of viable cells in 96-well plates during cell culture. MTT (3-(4,5-dimethylthiazol-2-yl)-2,5-diphenyltetrazolium bromide) is a yellow reagent that can be cleaved by living cells to produce a dark blue formazan product (Ciapetti et al., 1993). The quantity of formazan (directly proportional to

the number of viable cells) is measured by recording the absorbance at 550 nm using a plate reading spectrophotometer.

As shown in **Figure 48**, the wells in lane 1 contained fresh medium only as the blank control. The MCF-7 cell suspension was pipetted into each well of the 96-well plate from lanes 2 to 12. The plate was incubated at 37 °C and 5% $CO_2$ overnight before treatment with HZ101. Drug dilutions were added to the wells from lanes 3 to 7 to achieve final drug concentrations of 1 µM, 5 µM, 25 µM, 50 µM and 100 µM. Lanes 8 to 12 were loaded with the same array of HZ101 concentrations. For the lane 2, cell culture was added as a control.
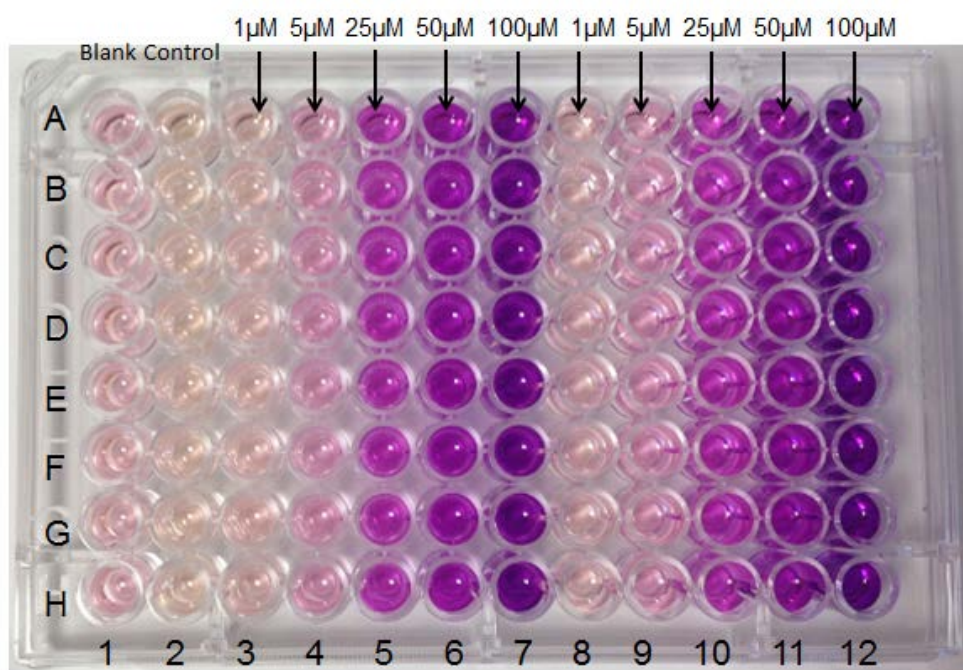


**Figure 48.** MCF-7 cells incubated with HZ101 on a 96-well plate

The plate was incubated for 72 hours at 37 °C and then centrifuged at 1000rpm for 5 min. The cells were washed with NaCl before MTT treatment. The MTT solution was pipetted into each well, including the control (**Figure 49**). The plate was returned to the incubator for 4 hours and then centrifuged for 5 min. The

medium was removed by pipetting and DMSO was added to each well. The plate was shaken gently and placed in the incubator for 30min. The plate was read at 550 nm in a plate reader.
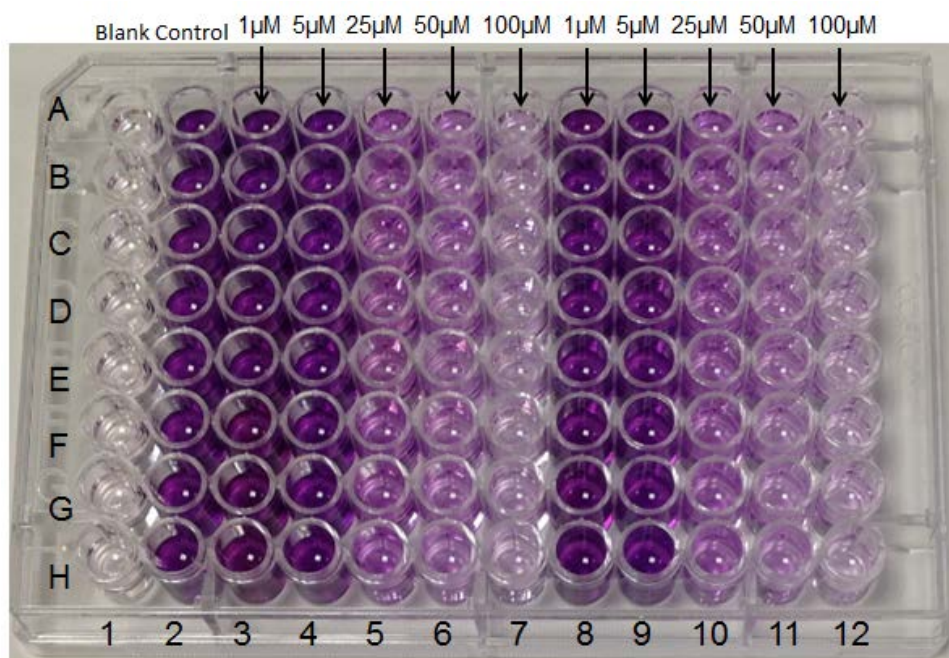


**Figure 49.** MCF-7 cells incubated with HZ101 on a 96-well plate after MTT treatment

Baclofen and GABA were incubated with the MCF-7 breast cancer cell line. The MTT results in **Graph 10** show that after 72 hours of incubation, the cell viability in both the baclofen and GABA groups did not differ significantly between concentrations of 1 µM to 100 µM. Even at the highest concentration of 100 µM, more than 90% of the cells remained alive, which indicates that baclofen and GABA had no cytotoxic effect on MCF-7 cells. However, to obtain statistically significant data, the chemosensitivity of the MTT assays had to be determined twice (n = 3 for the MTT assay).
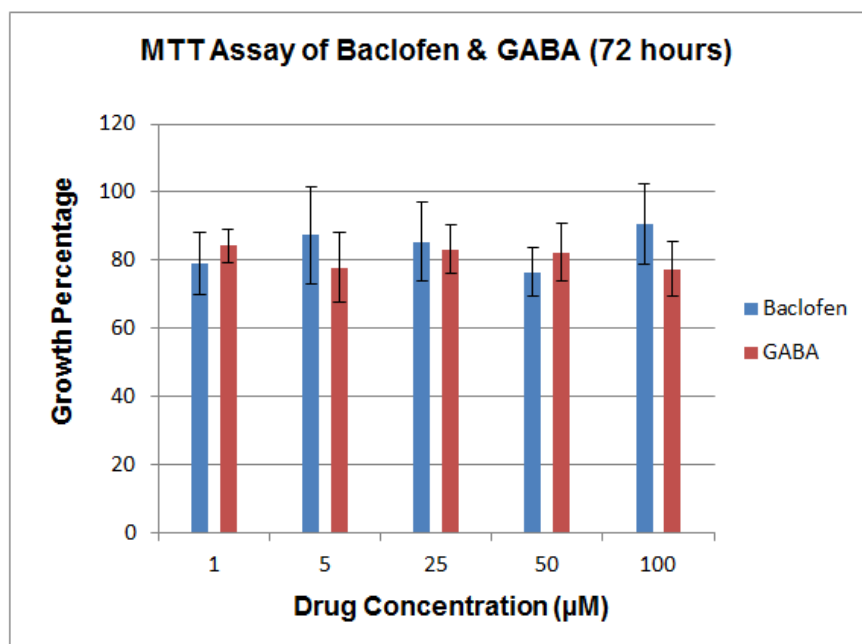
**Graph 10.** MTT cell proliferation assay of Baclofen and GABA (measured at

550nm, n=3)
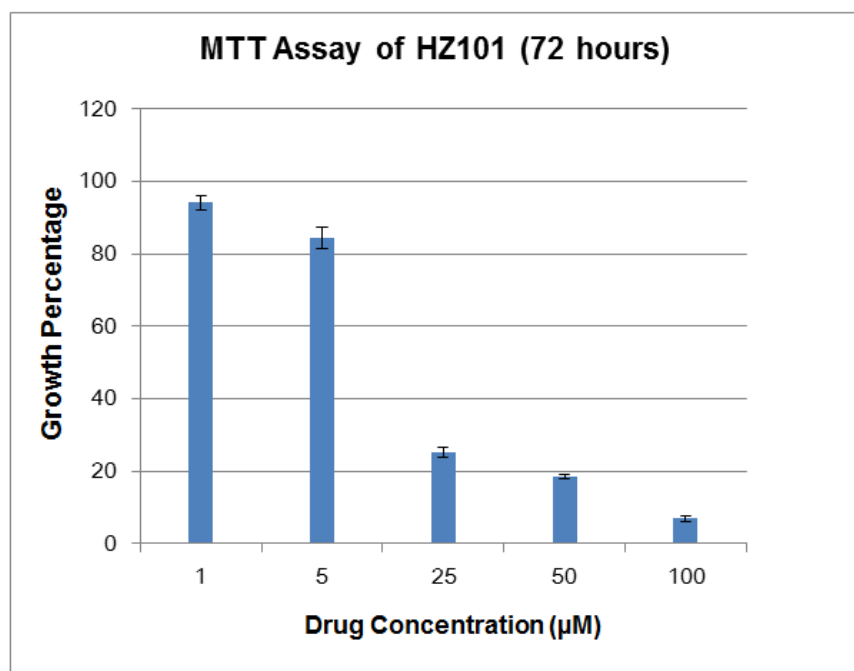


**Graph 11.** MTT cell proliferation assay of HZ101 (measured at 550nm, n=3)

The cytotoxicity of the legumain activated probe HZ101 against MCF-7 breast

cancer cells was evaluated by MTT assay. As shown in **Graph 11** after 72 hours

of incubation with HZ101 (at the concentration of 1 µM), more than 95% of cells

remained alive. The percentage of living cells decreased slightly to 85% when the concentration of HZ101 was 5 µM. At concentrations of 25 µM and 50 µM, only 25% and 18% of living cells were detected, respectively. At the highest concentration 100 µM of HZ101, the percentage of living cells dropped to 6%. According to this MTT results, HZ101 has low cytotoxicity, which makes it a good biomarker probe for breast cancer diagnosis and treatment.

### 3.3.11.1 Cytotoxicity Assays of HZ105 and HZ93

More studies are required into the stability of the GABA conjugates. The GABA anthraquinone conjugates were designed as templates for delivering the ligand GABA upon protease-mediated cleavage of GABA from the template. However, it is possible that the intact GABA conjugates may exert a cytotoxic effect, given that many anthraquinone-amino acid conjugates are known to be cytotoxic (members of the NU:UB series). To date it is not possible to identify the structures responsible for conferring toxicity. HPLC analysis of the stability of the AQ-GABA conjugates is necessary to determine whether or not the GABA is removed upon exposure to cancer cells and if so, on what timescale. The GABA conjugates here were only moderately potent (above single figure micromolar concentrations) but perhaps exposure times of greater than the 48 hours employed are necessary to observe fuller cytotoxic effects. In other words, it may be necessary to allow time for the GABA to be released.

The trend in cytotoxic potency observed in this study, however, correlates well with many reported studies of anthracenediones. Cheng and Zee-Cheng (1983) reported that the more OH side chains present in the anthraquinone ring the greater the cytotoxicity. Moreover, studies showed that removal of both OH groups in MTX to afford ametantrone reduced activity more than ten-fold (Cavalletti *et al.*, 1996). Hydroxyl groups according to Cheng and Zee-Cheng

(1978) do not necessarily improve intercalation itself but add to the overall DNA binding affinity where strong DNA binding is major driver for the intercalating agents to have long residence times between the base pairs to exert their cytotoxic effects.

Compounds were tested for their cytotoxicity to compare the effects of there being two, one or no hydroxyl groups in the anthraquinone structure as show in **Table 5.** The $IC_{50}$ value is the concentration of drug at which 50% of the cell population dies. From the data, the compound (HZ105) with two hydroxyl groups in the anthraquinone has the higher $IC_{50}$ value than compound (AL4) with one hydroxyl group and the $IC_{50}$ value of AL4 is higher than the compound (HZ93) with no hydroxyl groups. These results indicate that the presence of hydroxyl groups in the anthraquinone increased the drug toxicity.

| Tested Compound Structure | Synthesis Code | $IC_{50}$ µM |
|---|---|---|
|  | Mitoxantrone | 0.005 |
|  | HZ93 | 68 |
|  | AL4 | 38 |
|  | HZ105 | 27 |
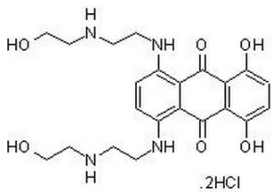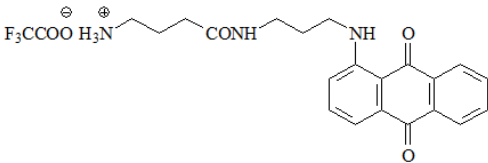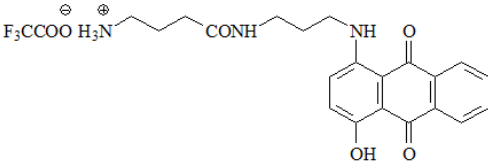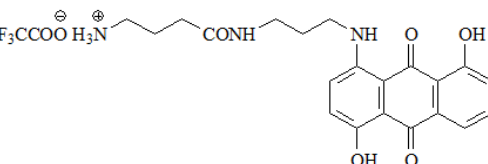
**Table 5.** $IC_{50}$ values of the tested compounds against MCF 7 cells (n = 3), 48 h.

## 3.3.12 HPLC Analysis of HZ101 and Its Metabolites

Further analysis of probe HZ101 activity was carried out by HPLC. Peptide cleavage of the probe HZ101 by legumain releases two potential compounds HZ105 and Rho-PAN-OH as illustrated in **Figure 51**. In order to determine a proper wavelength for the UV detecting HPLC assay, a UV spectrum of HZ101, HZ105 and Rho-PAN-OH was produced (**Figure 52**). The wavelength of 585 nm was selected, where the absorbance of HZ105 and Rho-PAN-OH were at identical value. The absorbance of HZ101 is higher than that of its metabolites.
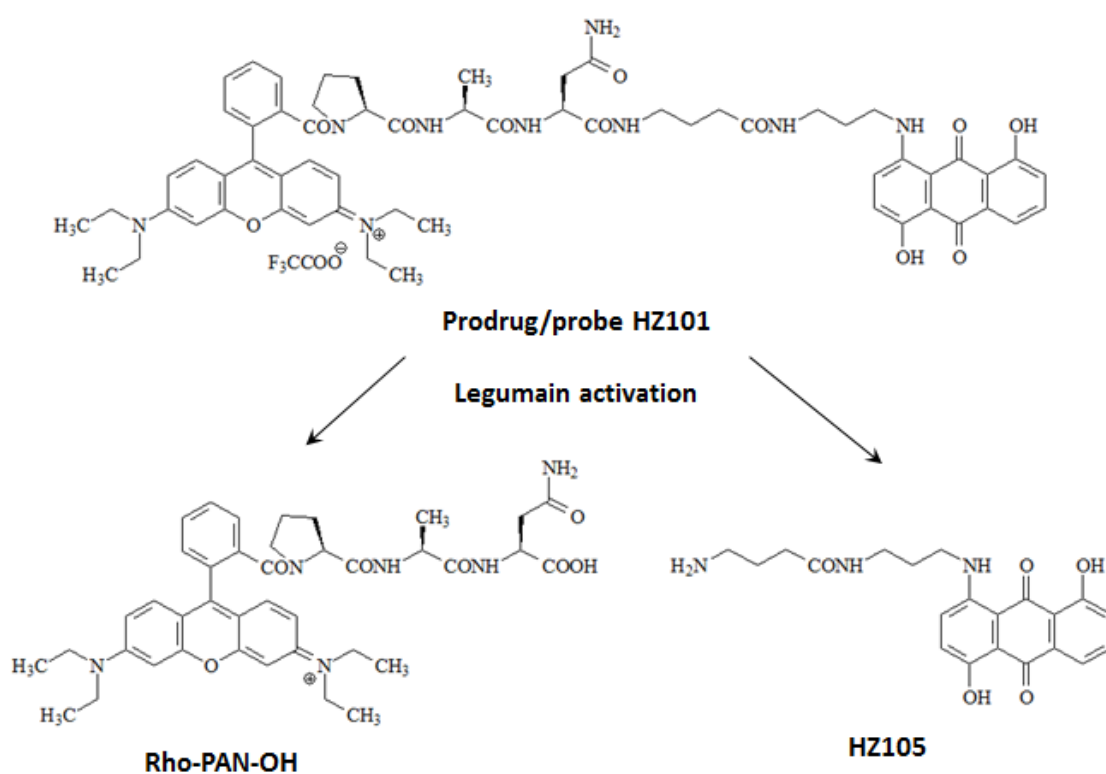


**Figure 51.** HZ101 and its metabolites after legumain activation

| Scan | Position | Use | Sample Name | Description |
|------|----------|-----|-------------|-------------|
| 1 | 1 | ☑ | Sample 1-1 | Blank (50% ACN in Water) |
| 2 | 2 | ☑ | Sample 2-2 | HZ105 50µM |
| 3 | 3 | ☑ | Sample 3-3 | HZ101 50µM |
| 4 | 4 | ☑ | Sample 4-4 | Rho-PAN-OH 50µM |
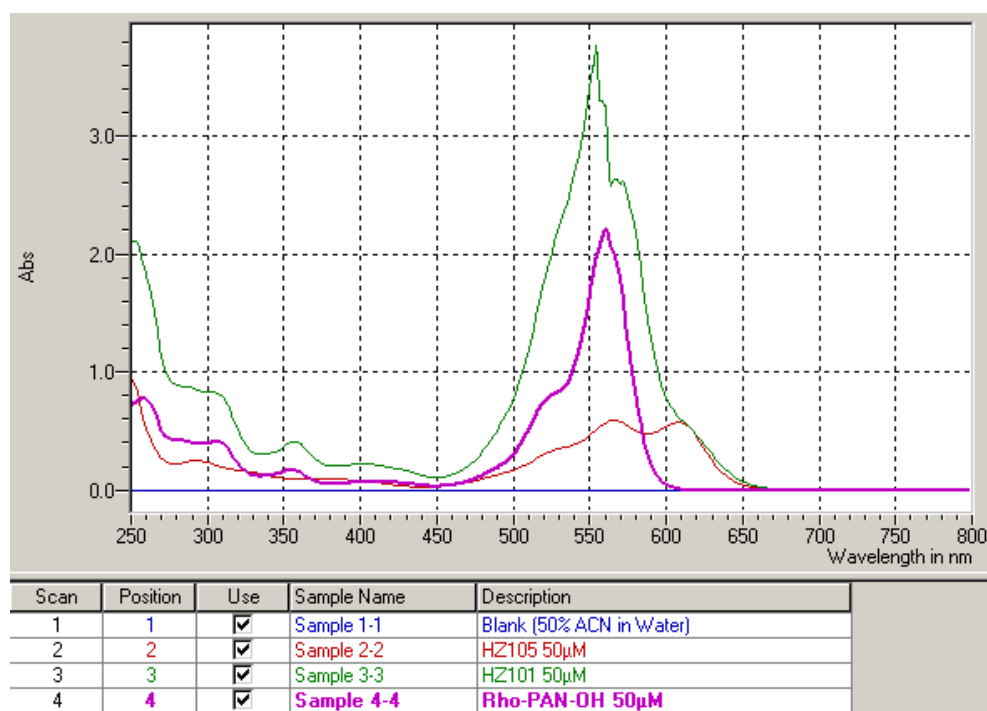
**Figure 52.** The UV spectra of HZ101, HZ105 and Rho-PAN-OH at same concentration (50 µM)

During the HPLC analysis, stock solutions of compound were prepared in 100% DMSO. The drug solutions needed for HPLC were further diluted in 50% acetonitrile in $dH_2O$. HPLC was performed using a Waters 2695 instrument (Napier University). The mobile phase A was acetonitrile with 0.01% TFA and mobile phase B was $H_2O$. A reverse-phase column (C18 HiChrom HIRPB-250A; 25 cm × 4.6 mm) was used with gradients developed over a 42 min period as shown in (**Table 6**). Samples were injected onto the column in volumes of 25 µl with a flow rate of 1 ml/min and a column temperature of 25ºC. The UV detector of the HPLC system recorded the absorbance at the wavelength of 585 nm.

| Time | Mobile Phase A (%) | Mobile Phase B (%) |
|:---:|:---:|:---:|
| 0 | 40 | 60 |
| 15 | 80 | 20 |
| 28 | 80 | 20 |
| 29 | 40 | 60 |
| 42 | 40 | 60 |

Mobile Phase A: Acetonitrile with 0.01% TFA
Mobile Phase B: $H_2O$

**Table 6.** HPLC gradient mobile phase composition

The retention times of the legumain activated probe HZ101 and its potential metabolites (HZ105 and Rho-PAN-OH) determined by HPLC analysis were essential for the identification of metabolites produced during the cleavage of probe HZ101 in legumain assay buffer. Because all compounds were dissolved in 50% acetonitrile in $H_2O$, a solution of 50% acetonitrile in $H_2O$ was tested first as the blank control.

The probe Rho-Pro-Ala-Asn-GABA-[Propyl spacer]-AQ (HZ101) was analysed by HPLC with different concentrations of 1 µM, 5 µM, 10 µM, 25 µM and 50 µM. As shown in **Figure 53**, the five chromatograms all have the same retention time of the peak which is 12.4 min. A calibration curve was created with the peak absorbance on the y-axis and the concentration of HZ101 on the x-axis. The $R^2$ value was 0.9996. These data indicate that the HPLC column was in good condition and the operation of the experiment was accurate.

The calibration curve for the probe HZ101 is shown in **Figure 54**. The curve equation (y = 51255 x + 5149.5) provided the source to calculate the precise concentration of probe HZ101 when area was the only certain value.
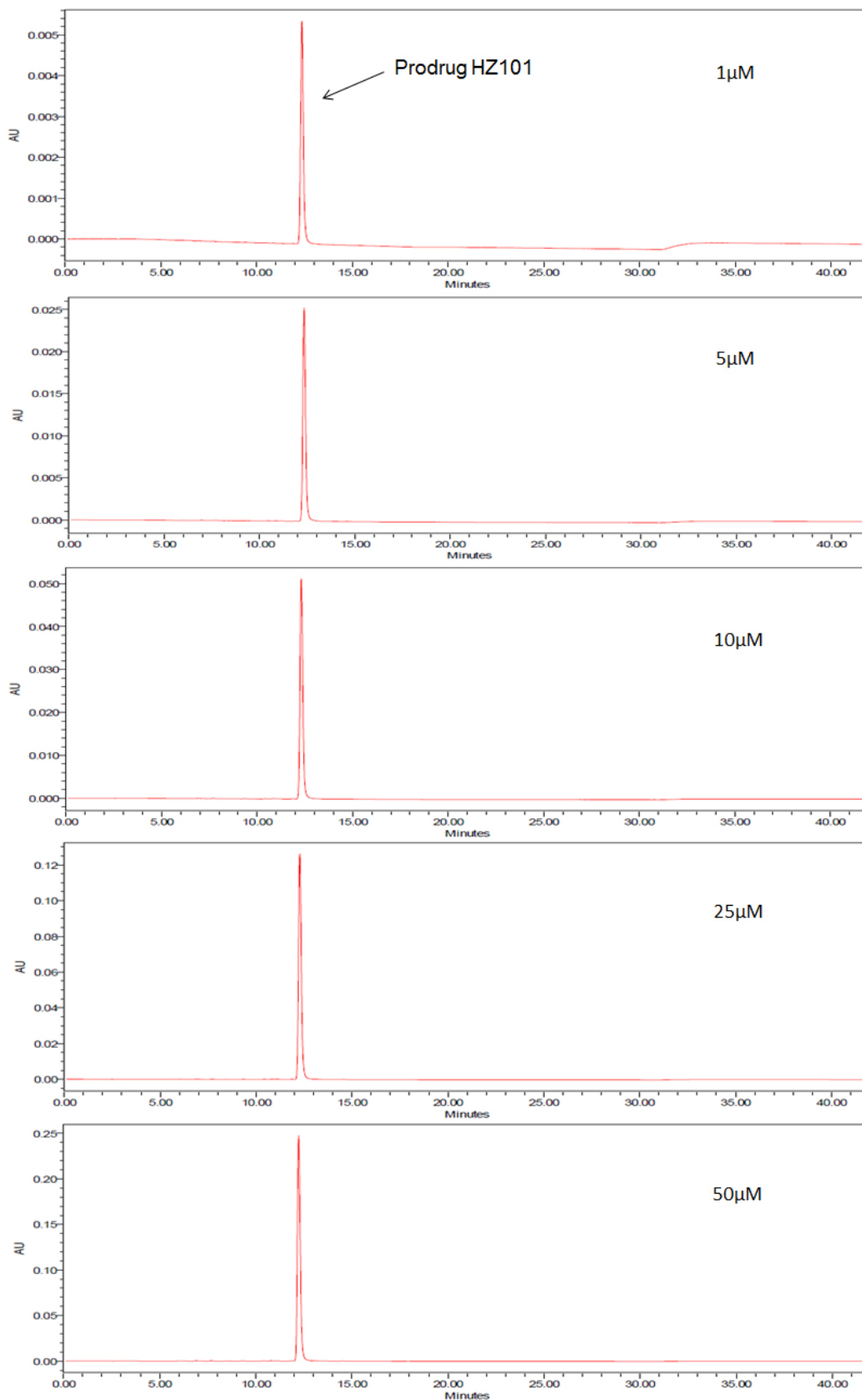
**Figure 53.** HPLC chromatograms of 1 μM, 5 μM, 10 μM, 25 μM and 50 μM

probe HZ101. RT: 12.4 min
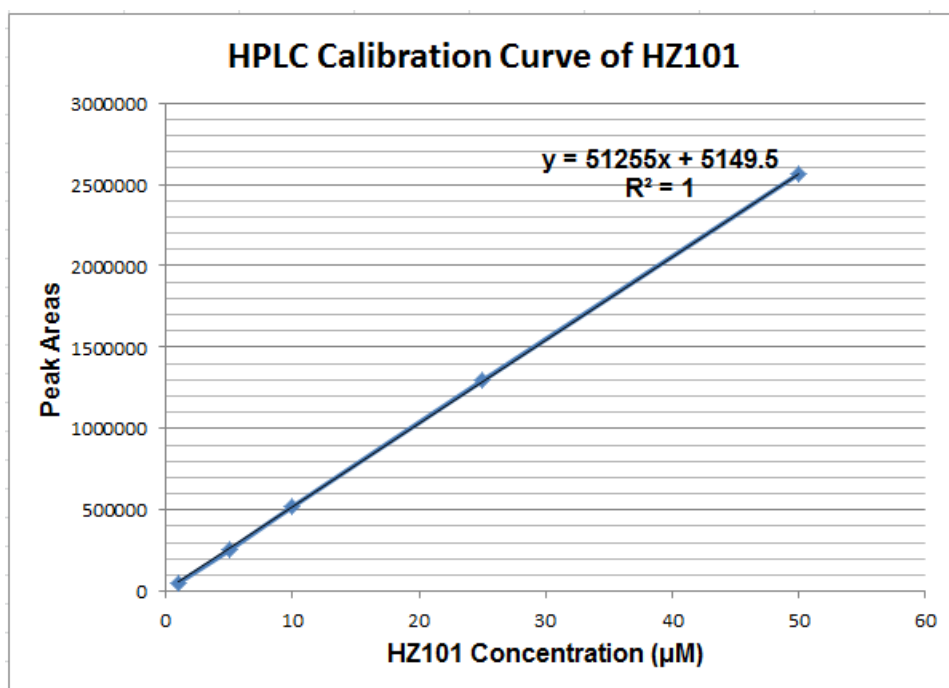
**Figure 54.** HPLC calibration curve for probe HZ101

The HPLC analysis of H-GABA-[Propyl spacer]-AQ (HZ105) is displayed in **Figure 55**. HZ105 is one of the metabolites from the legumain cleavage of probe HZ101. Five different concentrations (1 µM, 5 µM, 10 µM, 25 µM and 50 µM) of HZ105 were analysed and the retention time of the peak was 6.2 min. The calibration curve is shown in **Figure 56.**
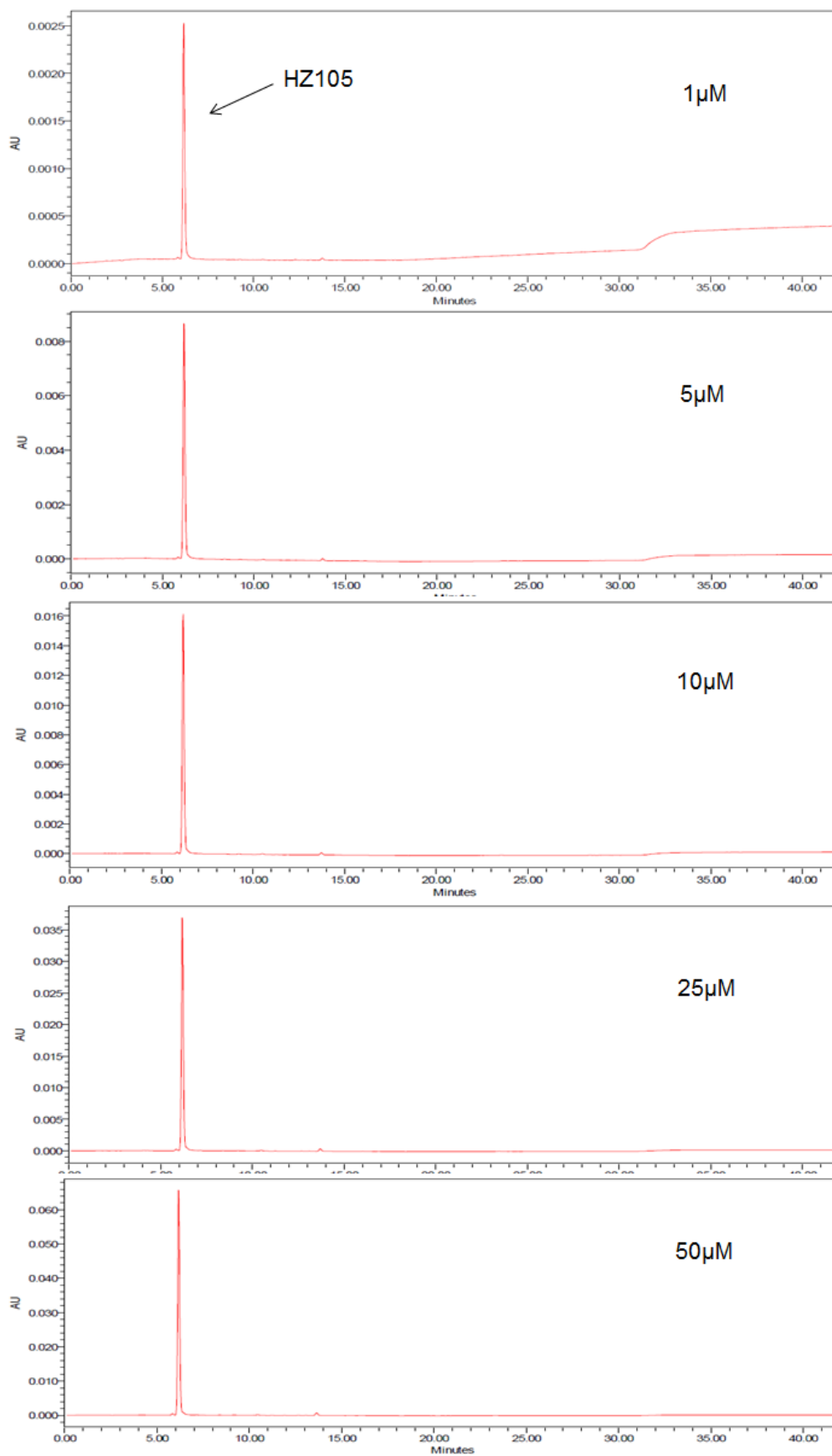
**Figure 55.** HPLC chromatograms of 1 μM, 5 μM, 10 μM, 25 μM, 50 μM HZ105
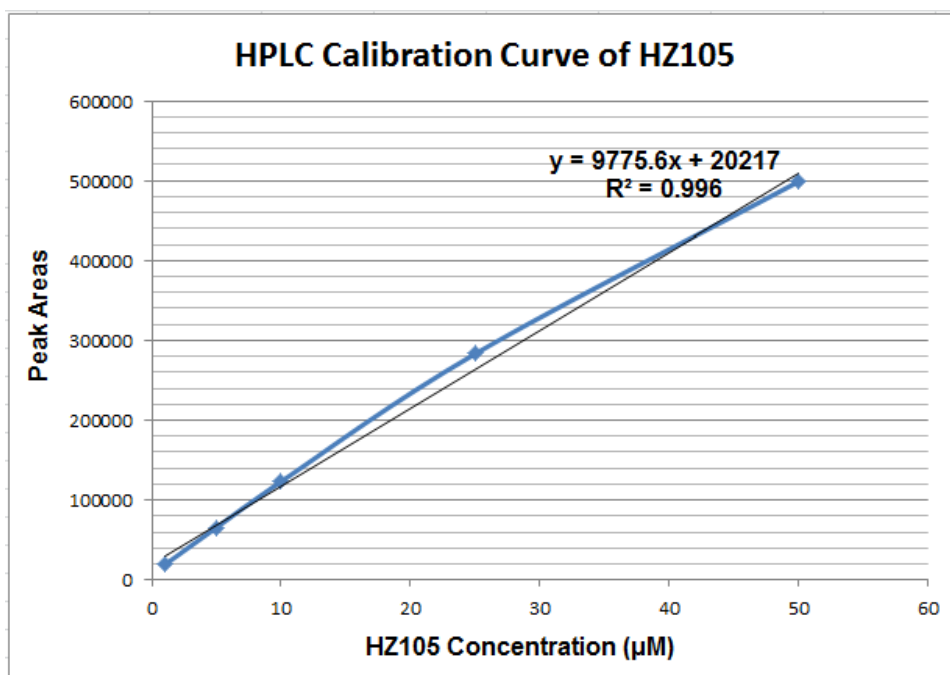
**Figure 56.** HPLC calibration curve for HZ105

The compound Rho-PAN-OH (Rhodamine B-Pro-Ala-Asn-OH) is the other metabolite from the legumain cleavage of probe HZ101 and was characterised by HPLC at the concentration of 50 µM. According to its HPLC chromatogram (**Figure 57**), the retention time of the peak was 7.26 min.
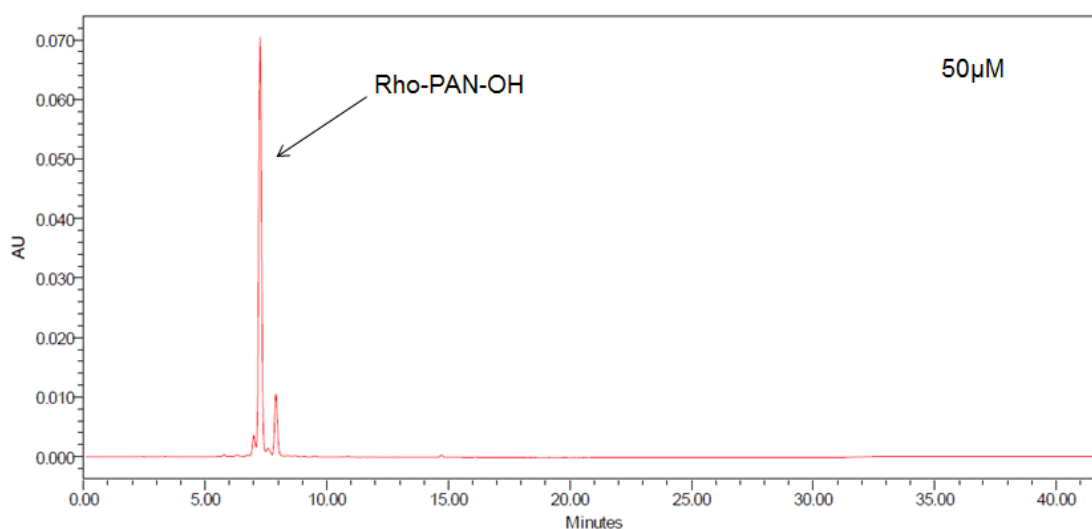


**Figure 57.** HPLC chromatograms of Rho-Pan-OH

A mixture of HZ101 and its metabolites HZ105 and Rho-Pan-OH was analysed by HPLC as shown in the chromatogram (**Figure 58**). At a wavelength of 585 nm, the peak absorbance of HZ105 and Rho-Pan-OH were nearly identical. The peak absorbance of probe HZ101 was nearly 4 times higher than those of the other two peaks. The three peaks were well separated using the designed HPLC mobile phase composition and the same conditions were considered in later drug-legumain assay.
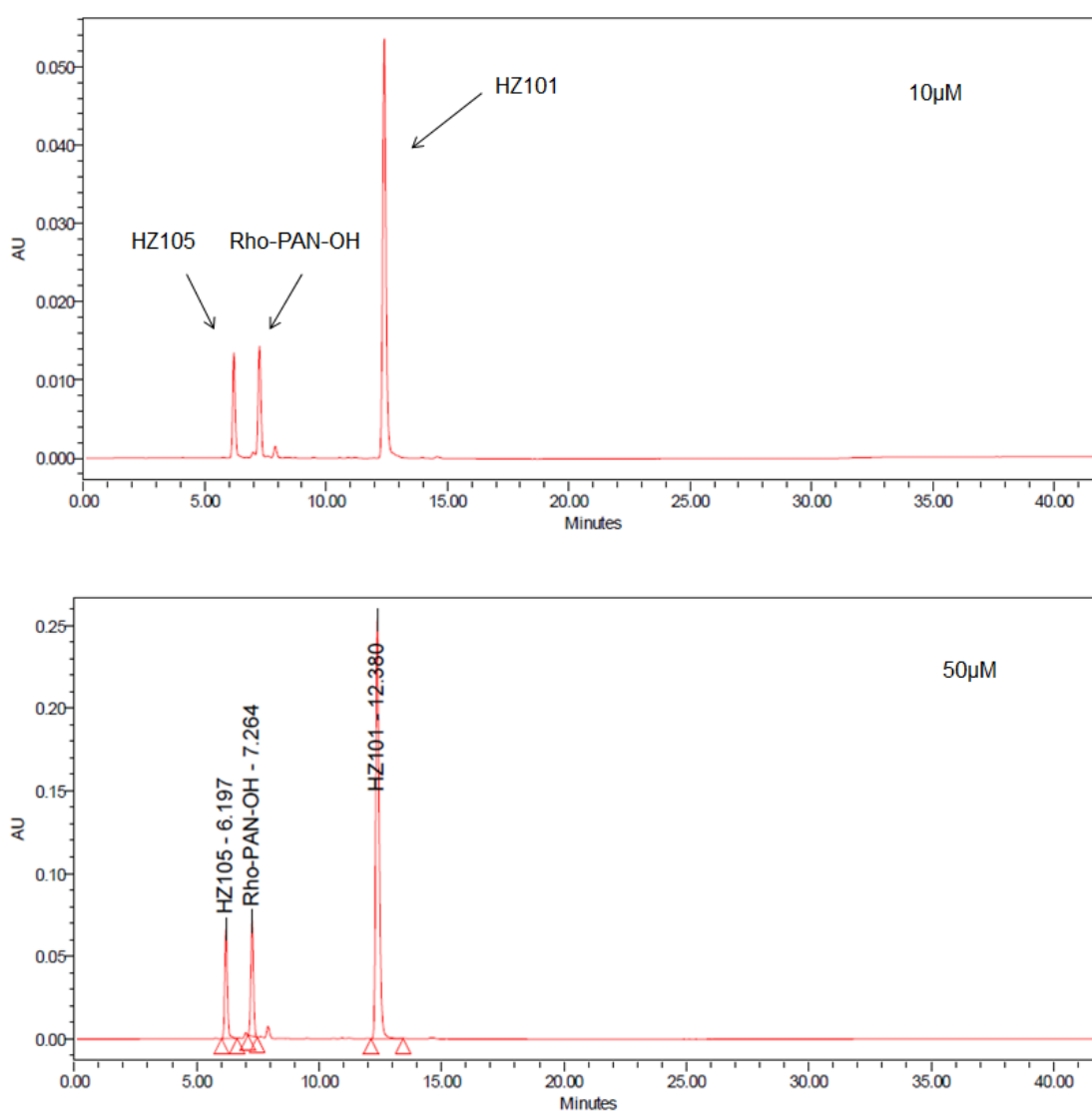


**Figure 58.** HPLC chromatograms of the mixture of HZ101, HZ105 and Rho-Pan-OH at concentration of 10 µM and 50 µM

The probe HZ101 was incubated with legumain in the assay buffer for 3 hours.

The mixture of legumain, MES and NaCl in assay buffer might be risky for the HPLC column because of its low pH and salt content and attempts were made to remove these components before the HPLC analysis. The buffer solution was poured into a clean evaporating basin. The evaporating basin was transferred to a fume cupboard and the solution was evaporated at room temperature. The dried solid in the evaporating basin was suspended in methanol and the mixture was transferred to Eppendorf tubes and centrifuged for 10 min at 1000 rpm. The supernatant was removed to a new evaporating basin and dried at room temperature. The solid was re-dissolved in 50% acetonitrile in $H_2O$ to a concentration of 30 µM (HZ101 before cleavage) and prepared for HPLC analysis.

In **Figure 59**, the HPLC chromatogram of probe HZ101 after 3 hours of incubation with legumain is shown. The concentration of HZ101 during the incubation was 10 µM which is the optimal concentration for legumain activation according to the fluorimetric assay (see **Figure 47**). The appearance of the peaks for Rho-Pan-OH and HZ105 clearly indicated that probe HZ101 was cleaved by legumain and converted into the two anticipated metabolites.
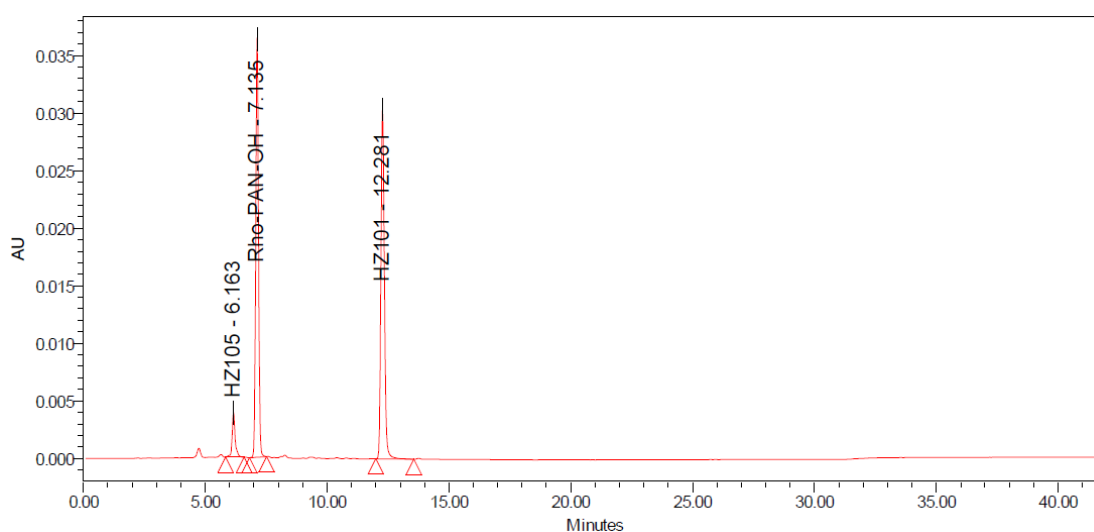


**Figure 59.** HPLC chromatogram of HZ101 (10µM) after 3 hours of incubation with rh-legumain

After 24 hours' of incubation of probe HZ101 with legumain, the probe was mostly cleaved into two compounds HZ105 and Rho-Pan-OH. As shown in **Figure 60**, the peak for probe HZ101 was very small and the absorbance value decreased to 0.001, whereas the absorbance values of the other two peaks were 0.012 and 0.04. Thus, HPLC analysis of HZ101 indicated that the probe was successfully activated by legumain and that the cleavage site was at the carboxyl end of asparagine. The HZ101 was converted into the anthraquinone quenching group HZ105 and the released fluoro group (Rho-Pan-OH).
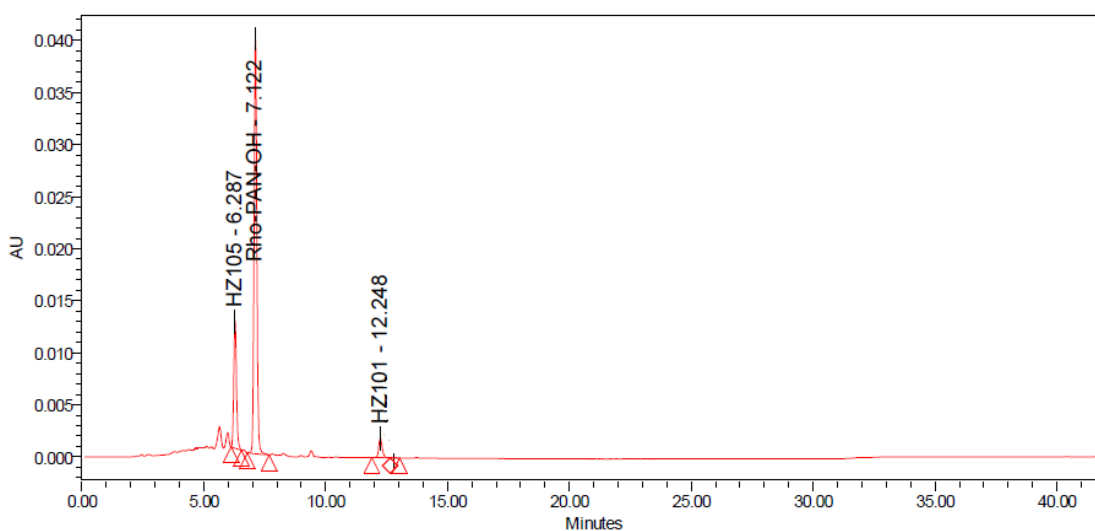


**Figure 60.** HPLC chromatogram of HZ101 (10µM) after 24 hours incubation with rh-legumain

### 3.3.13 Lipophilicity Assay

The partition coefficient of a chemical compound provides a measurement of its preference for the lipophilic or hydrophilic phases (Liu et al., 2011). A certain balance of lipophilicity and hydrophilicity is required for a drug to successfully pass through biological membranes. The most widely used model for lipophilicity is the partitioning of a compound between PBS buffer (pH 7.4) and octanol. The partition coefficient (LogP) refers to the unionised (neutral) form of the

compound. In the case of ionisable compounds, the term 'distribution coefficient (LogD)' is often used. The distribution coefficient takes into account the solution pH, which is important for the analysis of drug lipophilicity in biological environments. LogD is the logarithm of the ratio of the concentrations of the ionised form of the compound in water and octanol media.

In the experiment, the compounds were distributed between octanol and PBS in the Eppendorf tubes and shaken for 24 hours. The concentrations of the compounds in each layer were determined from the calibration curves by UV spectroscopic methods and the distribution coefficient was calculated. **Figure 61 to 63** shows the calibration curves for HZ101, HZ105 and Rho-PAN-OH in the two phases PBS and octanol. The distribution coefficient was 1.2 for probe HZ101 (**Table 7**) and 0.49 for HZ105 (**Table 8**). Rho-PAN-OH is hydrophilic and has a negative value of LogD which was -0.75 (**Table 9**).



**Figure 61.** Calibration curves for HZ101 in octanol and PBS

| Run No. | Solvent | Absorbance in cuvette | y=mx+c | Conc. in cuvette (mM) | Dilution Factor | Original conc. in Eppendorf (mM). | Log D | Log D (Mean ±) |
|---|---|---|---|---|---|---|---|---|
| 1 | Octanol | 1.04 | y = 0.0941x + 0.0487 | 10.55 | 30(100µl in 3ml) | 316.5 | | |
| 1 | PBS (pH7.4) | 0.1 | y = 0.0572x + 0.0058 | 1.65 | 15(200µl in 3ml) | 24.7 | 1.1 | |
| 2 | Octanol | 1.18 | y = 0.0941x + 0.0487 | 12 | 30(100µl in 3ml) | 361 | | 1.2 (± 0.1) |
| 2 | PBS (pH7.4) | 0.07 | y = 0.0572x + 0.0058 | 1.12 | 15(200µl in 3ml) | 16.8 | 1.3 | |
| 3 | Octanol | 1.27 | y = 0.0941x + 0.0487 | 13 | 30(100µl in 3ml) | 389.8 | | |
| 3 | PBS (pH7.4) | 0.12 | y = 0.0572x + 0.0058 | 2 | 15(200µl in 3ml) | 30 | 1.1 | |

**Table 7.** Distribution coefficient LogD of HZ101
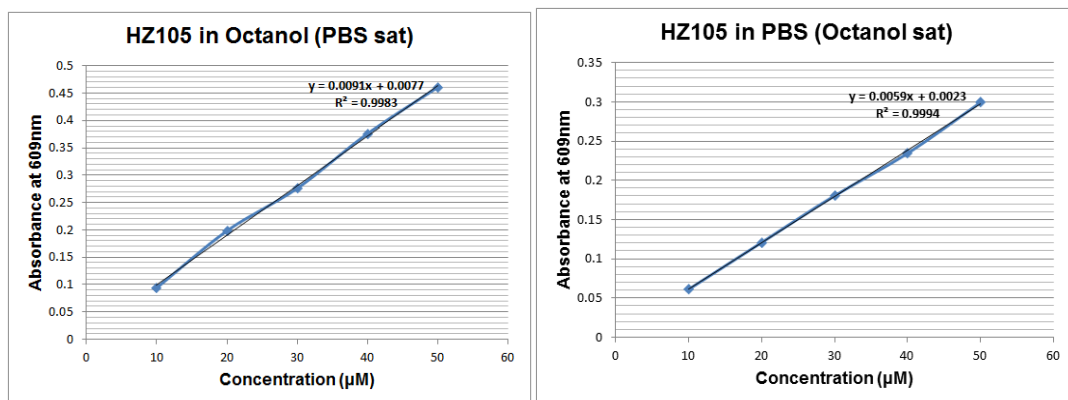


**Figure 62.** Calibration curves for HZ105 in octanol and PBS

| Run No. | Solvent | Absorbance in cuvette | y=mx+c | Conc. in cuvette (mM) | Dilution Factor | Original conc. in Eppendorf (mM). | Log D | Log D (Mean ±) |
|---------|---------|----------------------|--------|----------------------|-----------------|-----------------------------------|-------|----------------|
| 1 | Octanol | 0.34 | y = 0.0091x + 0.0077 | 36.5 | 15(200µl in 3ml) | 547.7 | | |
| 1 | PBS (pH7.4) | 0.07 | y = 0.0059x + 0.0023 | 11.5 | 15(200µl in 3ml) | 172.5 | 0.5 | |
| 2 | Octanol | 0.38 | y = 0.0091x + 0.0077 | 41 | 15(200µl in 3ml) | 615 | | 0.49 |
| 2 | PBS (pH7.4) | 0.08 | y = 0.0059x + 0.0023 | 13.2 | 15(200µl in 3ml) | 198 | 0.49 | (±0.01) |
| 3 | Octanol | 0.37 | y = 0.0091x + 0.0077 | 39.8 | 15(200µl in 3ml) | 597 | | |
| 3 | PBS (pH7.4) | 0.08 | y = 0.0059x + 0.0023 | 13.2 | 15(200µl in 3ml) | 198 | 0.48 | |

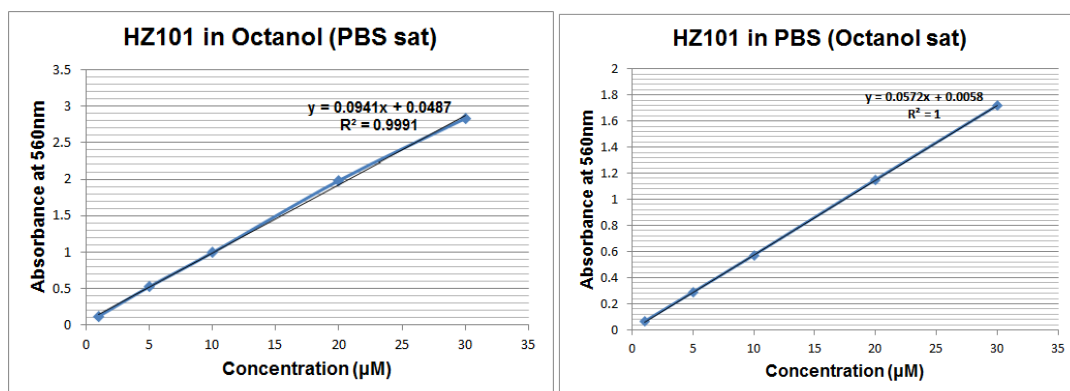**Table 8.** Distribution coefficient LogD of HZ105
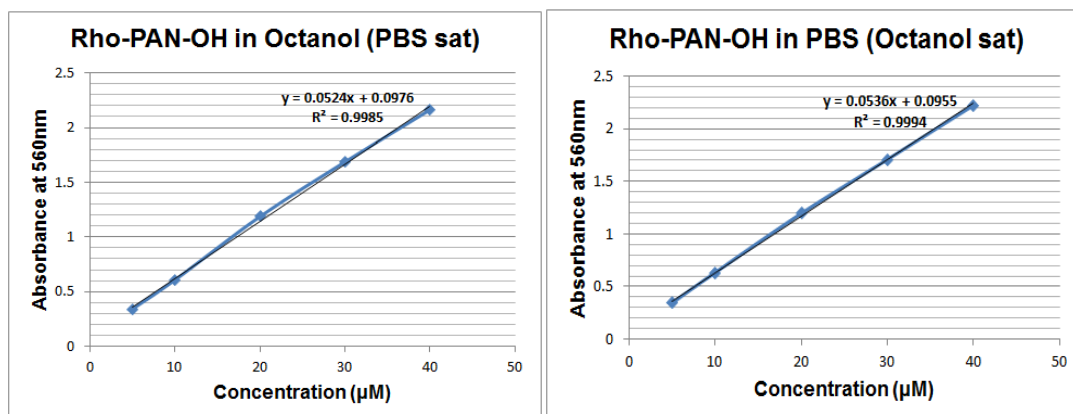


**Figure 63.** Calibration curves for Rho-PAN-OH in octanol and PBS

| Run No. | Solvent | Absorbance in cuvette | y=mx+c | Conc. in cuvette (mM) | Dilution Factor | Original conc in Eppendorf (mM). | Log D | Log D (Mean ±) |
|---|---|---|---|---|---|---|---|---|
| 1 | Octanol | 0.31 | y = 0.0524x + 0.0976 | 4.11 | 15(200µl in 3ml) | 61.65 | -0.72 | |
| 1 | PBS (pH7.4) | 0.67 | y = 0.0536x + 0.0955 | 10.7 | 30(100µl in 3ml) | 321 | | |
| 2 | Octanol | 0.39 | y = 0.0524x + 0.0976 | 5.58 | 15(200µl in 3ml) | 83.7 | -0.77 | - 0.75 (±0.02) |
| 2 | PBS (pH7.4) | 0.97 | y = 0.0536x + 0.0955 | 16.3 | 30(100µl in 3ml) | 489 | | |
| 3 | Octanol | 0.38 | y = 0.0524x + 0.0976 | 5.4 | 15(200µl in 3ml) | 81 | -0.77 | |
| 3 | PBS (pH7.4) | 0.95 | y = 0.0536x + 0.0955 | 16 | 30(100µl in 3ml) | 478 | | |

**Table 9.** Distribution coefficient LogD of Rho-PAN-OH

## 3.4 Conclusion

Legumain, an asparaginyl endopeptidase, is overexpressed in the majority of human tumours and is associated with tissue invasion and metastasis. An acidic environment is optimal for legumain proteolytic activity. Legumain has a unique enzyme substrate specificity towards the asparagine residue in the P1 position. Based on these properties, legumain is an attractive candidate for prodrug or probe design in the therapeutic or diagnostic applications.

A legumain-activated probe, HZ101, was designed, synthesised and evaluated. The chemical structure of HZ101 (Rho-Pro-Ala-Asn-GABA-[Propyl spacer]-AQ) consists of a fluoro group (rhodamine B), a legumain-specific peptide substrate and a quenching aminodihydroxyanthraquinone spacer compound. The synthesis of HZ101 began with the reaction of leuco-1,4,5-trihydroxyhydroxyanthaquinone and diaminopropane to produce H-[Propyl spacer]-AQ (HZ103). The amino acid GABA was added to HZ103 as the anthraquinone-quenching group to form H-GABA-[Propyl spacer]-AQ TFA salt (HZ105). As the potential active agent and/or template for the release of GABA, the tripeptide Pro-Ala-Asn was attached to HZ105 by solution phase peptide synthesis. The product, H-Pro-Ala-Asn(Trt)-GABA-[Propyl spacer]-AQ (HZ99), was then reacted with rhodamine B. The N-protecting group triphenylmethyl (trityl) on the asparagine of HZ100 was removed by TFA treatment to yield the final compound probe HZ101, which was characterised by mass spectrometry.

The biochemical properties of HZ101 were evaluated. The fluorimetric assay showed that incubation of HZ101 with legumain resulted in increased fluorescence intensity with time. The best result was obtained at a HZ101

concentration of 10 µM. This concentration was later considered in the HPLC analysis. The MTT assay revealed that probe HZ101 had relatively poor cytotoxicity against breast cancer cell lines, supporting its potential as a good candidate prodrug and biomarker probe. HPLC analysis of HZ101 and its two metabolites (HZ105 and Rho-Pan-OH) confirmed the retention times of the three compounds. Furthermore, HZ101 was incubated with legumain for 3 hours and 24 hours. The results demonstrated that HZ101 was successfully cleaved by legumain at the proposed site. The lipophilicity tests confirmed that the probe HZ101 has a good balance of lipophilic and hydrophilic properties, which is crucial to allow the probe to cross biological barriers and eventually target tumours.

## 3.5 Structure Library
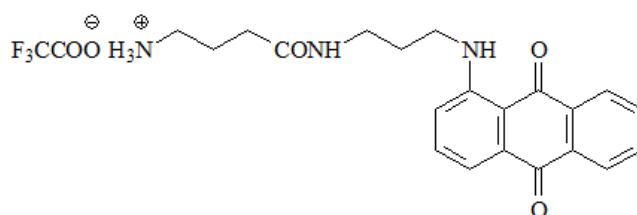


**H-GABA-[Propyl spacer]-AQ TFA salt (HZ93)**
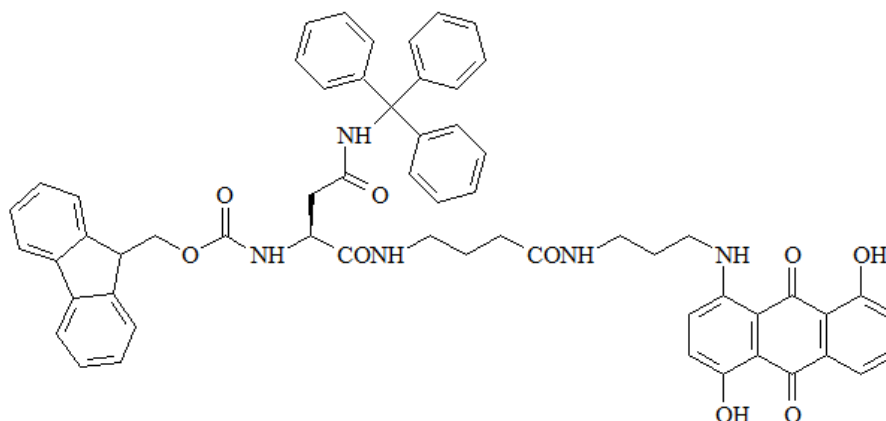


**Fmoc-Asn(Trt)-GABA-[Propyl spacer]-AQ (HZ94)**
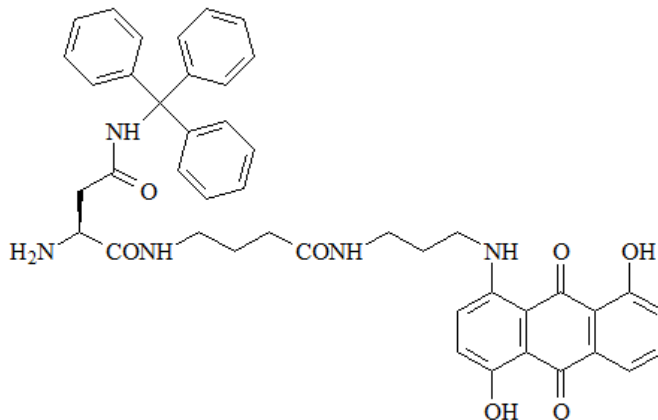


**H-Asn(Trt)-GABA-[Propyl spacer]-AQ (HZ95)**
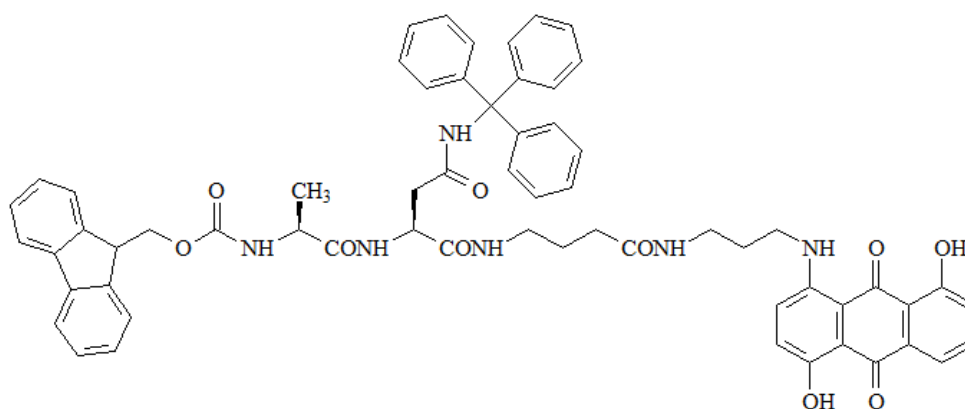


**Fmoc-Ala-Asn(Trt)-GABA-[Propyl spacer]-AQ (HZ96)**
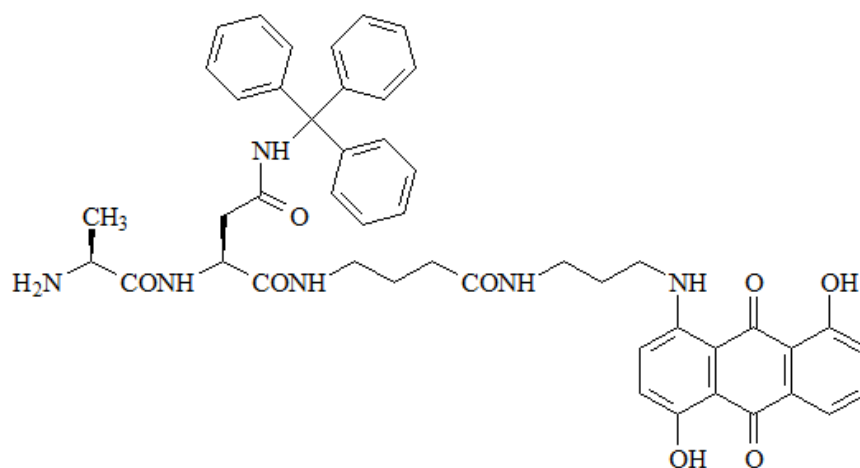
**H-Ala-Asn(Trt)-GABA-[Propyl spacer]-AQ (HZ97)**
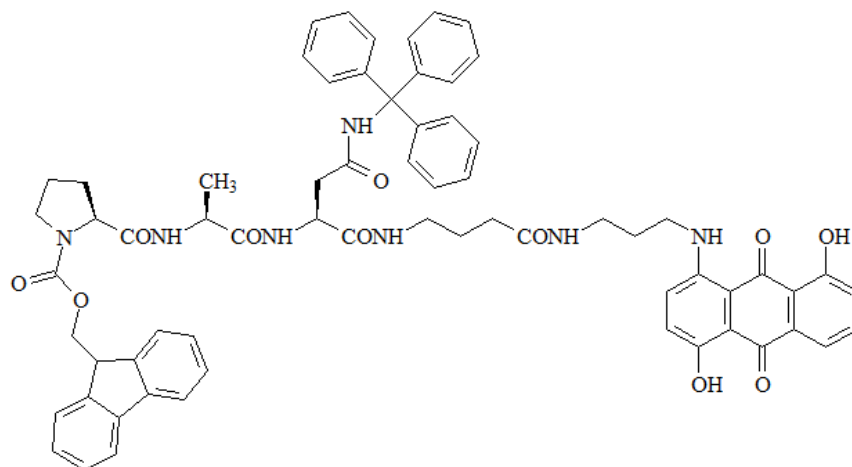


**Fmoc-Pro-Ala-Asn(Trt)-GABA-[Propyl spacer]-AQ (HZ98)**
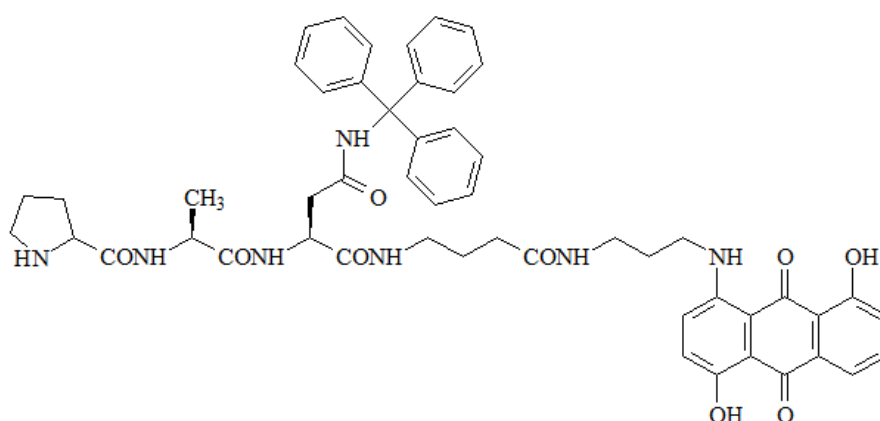


**H-Pro-Ala-Asn(Trt)-GABA-[Propyl spacer]-AQ (HZ99)**
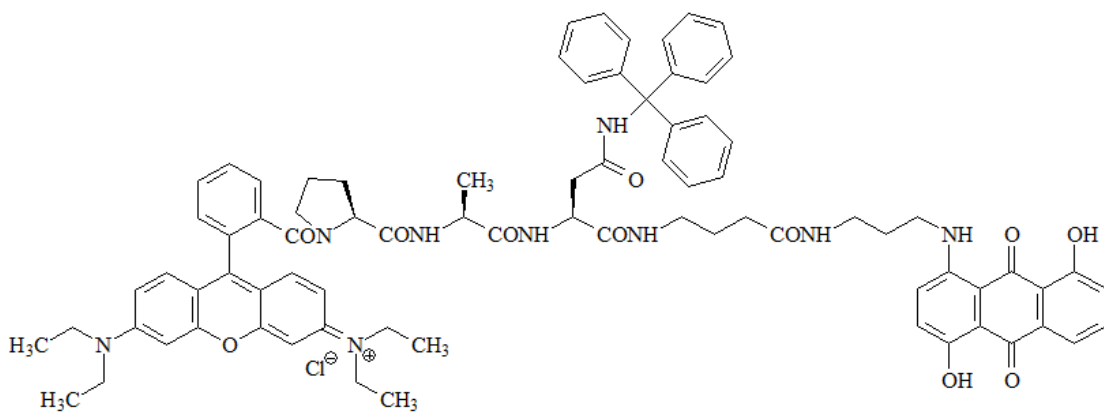
**Rho-Pro-Ala-Asn(Trt)-GABA-[Propyl spacer]-AQ (HZ100)**
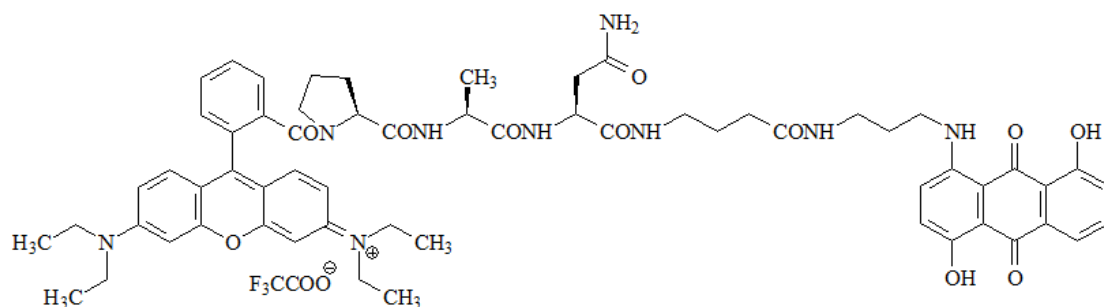


**Rho-Pro-Ala-Asn-GABA-[Propyl spacer]-AQ (HZ101)**
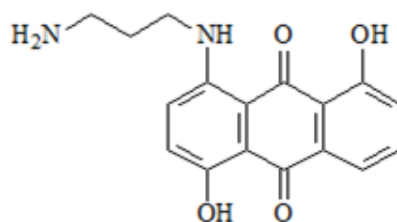


**H-[Propyl spacer]-AQ (HZ103)**
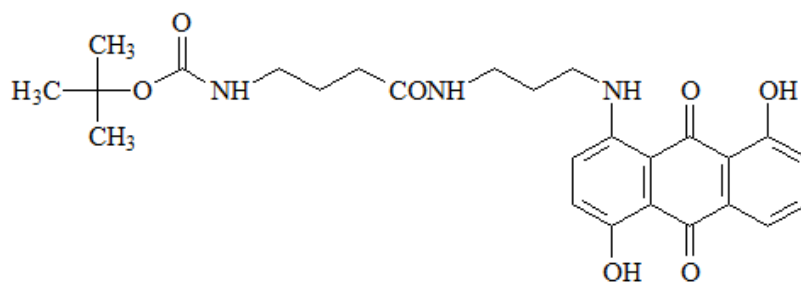


**Boc-GABA-[Propyl spacer]-AQ (HZ104)**
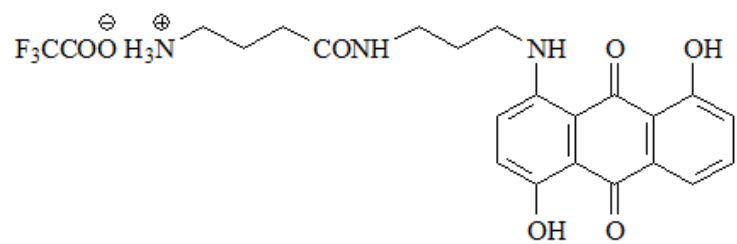
**H-GABA-[Propyl spacer]-AQ TFA salt (HZ105)**

### 3.6 Experimental

### 3.6.1 Synthesis of Fmoc-Asn(Trt)-GABA-[Propyl spacer]-AQ (HZ94)

H-GABA-[Propyl spacer]-AQ TFA salt HZ105 (400 mg, 0.78 mmol) was dissolved in DMF, followed by the addition of Fmoc-Asn-OH (513 mg, 0.86 mmol), TBTU (276 mg, 0.86 mmol), HOBt (132 mg, 0.86 mmol), and DIPEA (449 µl, 2.58 mmol). The reaction was allowed to proceed at RT for 4 h and was monitored by TLC in chloroform: methanol (9:1): $R_f$ 0.5. The reaction solution was extracted with chloroform and water. The organic layers were combined and poured into an evaporating basin and left to dry in a fume cupboard overnight. The solid crude product was collected. Yield: 730 mg, 96%.

### 3.6.2 Synthesis of H-Asn(Trt)-GABA-[Propyl spacer]-AQ (HZ95)

Fmoc-Asn(Trt)-GABA-[Propyl spacer]-AQ HZ94 (730 mg, 0.74 mmol) was suspended in 20% piperidine in DMF for 3 h. TLC was performed in chloroform: methanol (9:1): $R_f$ 0.1. The solution was extracted with chloroform and water. The organic layers were combined and dried by rotary evaporator. The crude HZ95 was purified by silica gel chromatography (4.3 cm × 9.5 cm) and eluted with dichloromethane-methanol (6:1). The appropriate fractions were collected, filtered and evaporated to dryness. Yield: 503 mg, 90%

ESMS (+): 754 m/z 100% (M-2H+H)$^+$

### 3.6.3 Synthesis of Fmoc-Ala-Asn(Trt)-GABA-[Propyl spacer]-AQ (HZ96)

H-Asn(Trt)-GABA-[Propyl spacer]-AQ HZ95 (500mg, 0.66mmol), Fmoc-Ala-OH (227 mg, 0.73 mmol), TBTU (230 mg, 0.72 mmol), HOBt (109 mg, 0.72 mmol) and DIPEA (373 µl, 2.16 mmol) were dissolved in DMF and the reaction mixture was allowed to proceed at RT overnight. TLC was performed in chloroform-methanol (9:1): $R_f$ 0.4. The solution was extracted with

dichloromethane and water. The crude products in organic layers were collected. Yield: 595 mg, 86%.

### 3.6.4 Synthesis of H-Ala-Asn(Trt)-GABA-[Propyl spacer]-AQ (HZ97)

The crude Fmoc-Ala-Asn(Trt)-GABA-[Propyl spacer]-AQ HZ96 (595 mg, 0.57 mmol) was suspended in 20% piperidine in DMF for 2 h. The reaction solution was extracted with dichloromethane and water. The organic layers were combined, dried and evaporated to a small volume ($\sim$ 3 ml) for further purification by column chromatography (4.3 cm$\times$151 cm). The solid product was collected. Yield: 356 mg, 76%.

### 3.6.5 Synthesis of Fmoc-Pro-Ala-Asn(Trt)-GABA-[Propyl spacer]-AQ (HZ98)

A quantity of 356mg, 0.43mmol of H-Ala-Asn(Trt)-GABA-[Propyl spacer]-AQ HZ97, Fmoc-Pro-OH (160 mg, 0.47 mmol), TBTU (153 mg, 0.48 mmol), HOBt (73 mg, 0.48 mmol) and DIPEA (248 µl, 1.44 mmol) were dissolved in DMF. The reaction was complete in 3 h confirmed by TLC in chloroform-methanol (6:1): $R_f$ 0.8. After extraction with chloroform and water, the organic layers were combined, and dried by rotary evaporation. The crude product was retained in the round-bottom flask for the next Fmoc de-protection reaction.

### 3.6.6 Synthesis of H-Pro-Ala-Asn(Trt)-GABA-[Propyl spacer]-AQ (HZ99)

H-Ala-Asn(Trt)-GABA-[Propyl spacer]-AQ HZ98 was dissolved in 20% piperidine in DMF for 2.5 h. TLC was performed in chloroform-methanol (6:1): $R_f$ 0.2. The solution was extracted with dichloromethane and water and the organic layers were combined and dried by rotary evaporation. The crude HZ99 was purified by silica gel chromatography (4.3 cm $\times$ 13.5 cm) and eluted with

chloroform-methanol (10:1). The appropriate fractions were collected, filtered and evaporated to dryness. Yield: 336mg.

<u>ESMS (+)</u>: 922 m/z 100% $(M-2H+H)^+$

### 3.6.7 Synthesis of Rho-Pro-Ala-Asn(Trt)-GABA-[Propyl spacer]-AQ (HZ100)

Rhodamine B (150 mg, 0.31 mmol), PyBop (253 mg, 0.49 mmol) and DIPEA (120 µl, 0.7 mmol) were dissolved in DMF. A stir bar was placed in the round-bottom flask to aid dissolving. After 15 min of stirring, H-Pro-Ala-Asn(Trt)-GABA-[Propyl spacer]-AQ HZ99 (320 mg, 0.35 mmol) was added to the reaction. The reaction was complete in 1 h as confirmed by TLC in chloroform-methanol (6:1): $R_f$ 0.45. The solution was poured into an evaporating basin to dry overnight. HZ100 was further purified by silica gel chromatography (4.3 cm×13 cm) using chloroform-methanol (8:1) as the solvent system. The fractions containing pure HZ100 were combined, filtered and evaporated to dryness. Yield: 380 mg, 79%.

### 3.6.8 Synthesis of Rho-Pro-Ala-Asn-GABA-[Propyl spacer]-AQ (HZ101)

Rho-Pro-Ala-Asn(Trt)-GABA-[Propyl spacer]-AQ HZ100 (380 mg, 0.28 mmol) was treated with TFA at RT for 1 h. The reaction was monitored by TLC in chloroform-methanol (6:1): $R_f$ 0.1. The solution was evaporated to dryness and a few drops of ethanol were added to the flask. Diethyl ether was then poured into the flask to dissolve the precipitated solid compound HZ101. The mixture was stored in the flask in a refrigerator overnight. The mixture was filtered and the product was dried in the desiccator and collected. Yield: 275 mg, 81%

<u>ESMS (+)</u>: 1104 m/z 100% $(M-CO_2CF_3)^+$

### 3.6.9 Synthesis of H-[Propyl spacer]-AQ (HZ103)

Leuco-hydroxyl anthraquinones (1 g, 3.7 mmol) and diaminopropane (1 ml) were suspended in dichloromethane (50 ml). The reaction solution was refluxed in a 60°C water bath. After 1 h, trimethylamine (0.5 ml) was added to the reaction. The round-bottom flask with the reaction mixture was removed from the water bath. After oxidation by pumping air into the flask, the colour of the compound became dark blue. The paste solid was filtered, extracted (dichloromethane-water), and dried. The crude product was collected. Yield: 200 mg, 17%.

### 3.6.10 Synthesis of Boc-GABA-[Propyl spacer]-AQ (HZ104)

H-[Propyl spacer]-AQ HZ103 (200 mg, 0.64 mmol), Boc-GABA-OH (143 mg, 0.7 mmol), PyBop (399 mg, 0.77 mmol) and DIPEA (256 µl, 1.5 mmol) were dissolved in DMF. The reaction was complete in 2 h as confirmed by TLC in chloroform-methanol (6:1): $R_f$ 0.7. After extraction with chloroform and water, the crude HZ104 was purified by column chromatography with an elution system of dichloromethane and water (6:1). The appropriated fractions were combined, filtered and dried. The solid was collected. Yield: 150 mg, 47%

### 3.6.11 Synthesis of H-GABA-[Propyl spacer]-AQ TFA salt (HZ105)

HZ104 (150 mg, 0.3 mmol) was treated with TFA for 1 h. TLC was performed in chloroform-methanol (3:1): $R_f$ 0.9. The solution was evaporated to dryness and further purification was performed by thick layer chromatography. The solvent system dichloromethane-methanol (9:1) was used. The product layer was scratched off the plate and the solid HZ105 was collected by filtration and evaporation. Yield: 70 mg, 45%.

$^1$H NMR spectrum (DMSO-d$_6$, 300 MHz) δ: 1.7-1.85 (4H, m, AQ-NH-CH$_2$-C<u>H</u>$_2$ and NH$_3$-CH$_2$-C<u>H</u>$_2$); 2.15-2.3 (2H, t, NH$_3$-CH$_2$-CH$_2$-C<u>H</u>$_2$); 2.72-2.9 (2H, t, NH$_3$-C<u>H</u>$_2$); 3.12-3.25 [7H, m, unresolved, AQ-NH-C<u>H</u>$_2$-CH$_2$-C<u>H</u>$_2$ and NH3 (exchanged)]; 7.18-7.3 (2H, m, H-2 and H-3); 7.3-7.4 (1H, d, H-7); 7.58-7.7 (2H, m, H-6 and H-5); 8.1(1H, t, N<u>H</u>CO); 9.8 (1H, t, AQ-N<u>H</u>)

ESMS (+): 398 m/z 100% (M-CO$_2$CF$_3$)$^+$

### 3.6.12 Synthesis of Boc-GABA-Propyl-AQ (HZ92)

The staring material H-Propyl-AQ NU:UB 197 (500 mg, 1.79 mmol) and Boc-GABA-OH (399 mg, 1.97 mmol) were dissolved in DMF (25 ml), followed by the addition of the coupling reagents TBTU (630 mg, 1.97 mmol), HOBt (300 mg, 1.97 mmol) and DIPEA (1024 µl, 6.5 mmol). The reaction was complete in 4 h as determined by TLC (R$_f$ 0.45). The reaction solution was extracted with dichloromethane and water. The organic layers were combined and poured into an evaporating basin to dry overnight. The crude product was purified by column chromatography (3.2 cm × 15 cm) using the solvent system dichloromethane-methanol (14:1). The appropriate fractions were combined, filtered and collected for the next de-protection reaction.

### 3.6.13 Synthesis of H-GABA-Propyl-AQ TFA salt (HZ93)

Boc-GABA-Propyl-AQ (HZ92) was dissolved in TFA for 40 min. After confirming the reaction b TLC, the solution was evaporated to a small volume (approximately 2 ml). Then diethyl ether (50 ml) was added to the flask to precipitate the product HZ93. The solid was collected by filtration. Yield: 450 mg, 52%.

$^1$H NMR spectrum (DMSO-d$_6$, 300 MHz) δ: 1.7-1.9 (4H, m, AQ-NH-CH$_2$-C<u>H</u>$_2$ and

NH$_3$-CH$_2$-C$\underline{H_2}$); 2.18-2.38 (2H, m, NH$_3$-CH$_2$-CH$_2$-C$\underline{H_2}$); 2.75-2.9 (2H, m, NH$_3$-C$\underline{H_2}$); 3.15-3.28 (2H, q, AQ-NH-CH$_2$-CH$_2$-C$\underline{H_2}$); 3.28-3.5 (2H, q, AQ-NH-C$\underline{H_2}$); 7.26 (1H, d, H-2); 7.45 (1H, d, H-4); 7.6-7.7 (1H, t, H-3); 7.8-7.95 (2H, m, H-6 and H-7); 8.05-8.16 (2H, m, H-5 and H-8); 8.16-8.27 (1H, t, CON$\underline{H}$); 9.7 (1H, t, AQ-N$\underline{H}$)

### 3.6.14 HZ101 Fluorimetric Assay

**Materials**

- Activation buffer: 50 mM sodium acetate, 100 mM NaCl, pH 4.0

- Assay buffer: 50 mM MES hydrate, 250 mM NaCl, pH 5.0

- Recombinant human legumain (R&D systems): The stock (10 µl) was diluted in activation buffer (100 µl) and stored at -80 ℃. The stock was incubated for 2 h at 37 ℃ before assaying. The aliquots were then diluted to 1ng/µl in assay buffer.

- Drug stock solutions:1mg/ml in DMSO

- FluoStar Omega multi-mode microplate reader

**Method**

A 96-well plate was used for the assay. Wells A1～C1 contained assay buffer (100 µl), A2～C2 contained assay buffer (98.78 µl) and HZ101 (1.22 µl, 10 µM), and A3～C3 contained assay buffer (58.78 µl), HZ101 (1.22 µl, 10 µM) and rh-legumain (40 µl, 1 ng/µl).

The plate was read in a FluoStar Omega multi-mode microplate reader and spectra were recorded every 5 min for 2 h.

### 3.6.15 Cytotoxicity assays

**Method for MCF-7 cell culture**

MCF-7 mammary carcinoma cells were grown in 75 cm$^2$ flask containing 30 ml of RPMI 1640 medium supplemented with 10% FBS, 1% penicillin/streptomycin and 1% L-glutamine at 37ºC in the incubator (5% $CO_2$). The MCF-7 cells were adherent to the flask. Fresh medium was supplied every two to three days and the cells were passaged weekly.

The cells were harvested when needed. The medium was poured out and the cells were washed with sodium chloride 3 times. After washing, 10% trypsin in NaCl was added to the flask and incubated for 8min at 37 ºC to suspend the cells. The mixture was poured into a 50 ml tube and centrifuged for 2 min at 2000 rpm. The pelleted cells were then collected for MTT assays or passaged and resuspended in fresh medium.

### 3.6.16 MTT Assay

**Materials for MTT assay**

The stock solution (1mM) of HZ101 in DMSO was sterilised by filtration. Further dilutions were prepared to obtain concentrations of 100, 50, 25, 5, and 1 µM in phenol red free RPMI medium. The cells were seeded, counted and diluted to achieve a cell suspension of 1.4×10$^4$ cells/ml.

**Methods for MTT assay**

The wells in lane 1 of a 96-well plate contained 200 µl of medium only as a blank control. In lanes 2 to 12, 150µl of cell suspension (1.4×10$^4$ cells/ml) was pipetted into each well. The plate was incubated at 37 ºC, 5% $CO_2$ overnight before treatment with HZ101 compounds. The final drug concentrations in lanes 3 to 7 were 1, 5, 25, 50, 100µM. If needed, 50 µl of the correct drug dilution was added

to individual wells to achieve the above concentrations. Lanes 8 to 12 were loaded in the same manner as HZ101. In lane 2, 50 µl of cell culture was added as a control.

After incubation for 72 hours at 37 ºC, the plate was centrifuged at 1000 rpm for 5 min. The cells were washed with NaCl before MTT treatment. Then, 2 ml of MTT (5 mg/ml in 0.01 M PBS) was added to 5ml of RPMI medium. The solution (50 µl) was pipetted into each well, including the control. The plate was returned to the incubator for 4 hours and then centrifuged at 1000rpm for 5 min. The medium was removed by pipetting and DMSO (150 µl) was added to each well. The plate was shaken gently and placed in the incubator for 30min. The plate was read at 550 nm in a plate reader.

## 3.7 References

Briggs JJ, Haugen MH, Johansen HT, Riker AI, Abrahamson M, Fodstad O, Maelandsmo GM, Solberg R. (2010). Cystatin E/M suppresses legumain activity and invasion of human melanoma. *BMC Cancer*, **10**, p17.

Carl PL, Chakravarty PK, Katzenellenbogen JA, Weber MJ. (1980). Protease-activated "prodrugs" for cancer chemotherapy. *Proc Natl Acad Sci USA*, **77**, p2224-2228.

Cavalletti E, Giuliani FC, Hacker MP, Krapcho AP. (1996). *U.S. Patent No. 5,587,382*. Washington, DC: U.S. Patent and Trademark Office.

Chen JM, Dando PM, Rawlings ND, Brown MA, Young NE, Stevens RA, Hewitt E, Watts C, Barrett AJ. (1997). Cloning, isolation, and characterization of mammalian legumain, an asparaginyl endopeptidase. *J Biol Chem*, **272**, p8090-8098.

Chen JM, Fortunato M, Stevens RA, Barrett AJ. (2001). Activation of progelatinase A by mammalian legumain, a recently discovered cysteine proteinase. *Biol Chem,* **382**, p777-783.

Chen YJ, Wu SC, Chen CY, Tzou SC, Cheng TL, Huang YF, Yuan SS, Wang YM. (2014). Peptide-based MRI contrast agent and near-infrared fluorescent probe for intratumoral legumain detection. *Biomaterials*, **35**, p304-315.

Cheng CC, Zee-Cheng RK. (1978). Antineoplastic agents. Structure-activity relationship study of bis(substituted aminoalkylamino) anthraquionones. *Journal*

*of Medicinal Chemistry*, **3**(21), p291-294.

Cheng CC, Zee-Cheng RK. (1983). The design, synthesis and development of a new class of potent antineoplastic anthraquinones. *Progress in Medicinal Chemistry*, **20**(2), p83-118.

Ciapetti G, Cenni E, Pratelli L, Pizzoferrato A. (1993). In vitro evaluation of cell/biomaterial interaction by MTT assay. *Biomaterials*, **14**, p359-364.

Dall E, Brandstetter H. (2013). Mechanistic and structural studies on legumain explain its zymogenicity, distinct activation pathways, and regulation. *Proc Natl Acad Sci U S A*, **110**, p10940-10945.

Dall E, Brandstetter H. (2015). Structure and function of legumain in health and disease. *Biochimie.* **122**, p126-150.

Demchenko AP. (2010). The concept of lambda-ratiometry in fluorescence sensing and imaging. *J Fluoresc*, **20**, p1099-1128.

Edgington LE, Verdoes M, Ortega A, Withana NP, Lee J, Syed S, Bachmann MH, Blum G, Bogyo M. (2013). Functional imaging of legumain in cancer using a new quenched activity-based probe. *J Am Chem Soc.* **135**, p174-182.

Gawenda J, Traub F, Luck HJ, Kreipe H, Von Wasielewski R. (2007). Legumain expression as a prognostic factor in breast cancer patients. *Breast Cancer Res Treat.* **102**, p1-6.

Guo P, Zhu Z, Sun Z, Wang Z, Zheng X, Xu H. (2013). Expression of legumain correlates with prognosis and metastasis in gastric carcinoma. *PLoS One*, 8, e73090.

Ishii S. (1993). Asparaginylendopeptidase: an enzyme probably responsible to post-translational proteolysis and transpeptidation of proconcanavalin A. *Seikagaku*. **65**, p185-189.

Kobayashi H, Ogawa M, Alford R, Choyke PL, Urano Y. (2010). New strategies for fluorescent probe design in medical diagnostic imaging. *Chem Rev*. **110**, p2620-2640.

Lee J, Bogyo M. (2012). Synthesis and evaluation of aza-peptidyl inhibitors of the lysosomal asparaginyl endopeptidase, legumain. *Bioorg Med Chem Lett*. **22**, p1340-1343.

Liu C, Sun C, Huang H, Janda K, Edgington T. (2003). Overexpression of legumain in tumors is significant for invasion/metastasis and a candidate enzymatic target for prodrug therapy. *Cancer Res*. **63**, p2957-2964.

Liu X, Testa B, Fahr A. (2011). Lipophilicity and its relationship with passive drug permeation. *Pharm Res.* **28**, p962-977.

Luo Y, Zhou H, Krueger J, Kaplan C, Lee SH, Dolman C, Markowitz D, Wu W, Liu C, Reisfeld RA, Xiang R. (2006). Targeting tumor-associated macrophages as a novel strategy against breast cancer. *J Clin Invest.* **116**, p2132-2141.

Mathieu MA, Bogyo M, Caffrey CR, Choe Y, Lee J, Chapman H, Sajid M, Craik CS, Mckerrow JH. (2002). Substrate specificity of schistosome versus human legumain determined by P1-P3 peptide libraries. *Mol Biochem Parasitol.* **121**, p99-105.

Morita Y, Araki H, Sugimoto T, Takeuchi K, Yamane T, Maeda T, Yamamoto Y, Nishi K, Asano M, Shirahama-Noda K, Nishimura M, Uzu T, Hara-Nishimura I, Koya D, Kashiwagi A, Ohkubo I. (2007). Legumain/asparaginyl endopeptidase controls extracellular matrix remodeling through the degradation of fibronectin in mouse renal proximal tubular cells. *FEBS Lett.* **581**(7), p1417-1424.

Morris GA, Mullah KB, Sutherland JK. (1986). Some experiments with aminohydroxyanthraquinones. *Tetrahedron.* **42**(12), p3303-3309.

Murthy RV, Arbman G, Gao J, Roodman GD, Sun XF. (2005). Legumain expression in relation to clinicopathologic and biological variables in colorectal cancer. *Clin Cancer Res.* **11**, p2293-2299.

Ohno Y, Nakashima J, Izumi M, Ohori M, Hashimoto T, Tachibana M. (2013). Association of legumain expression pattern with prostate cancer invasiveness and aggressiveness. *World J Urol.* **31**, p359-364.

Schwarz G, Brandenburg J, Reich M, Burster T, Driessen C, Kalbacher H. (2002). Characterization of legumain. *Biol Chem.* **383**, p1813-6.

Smith R, Johansen HT, Nilsen H, Haugen MH, Pettersen SJ, Maelandsmo GM, Abrahamson M, Solberg R. (2012). Intra- and extracellular regulation of activity

and processing of legumain by cystatin E/M. *Biochimie*. **94**, p2590-2599.

Smith RL, Astrand OA, Nguyen LM, Elvestrand T, Hagelin G, Solberg R, Johansen HT, Rongved P. (2014). Synthesis of a novel legumain-cleavable colchicine prodrug with cell-specific toxicity. *Bioorg Med Chem*. **22**, p3309-3315.

Smith PJ, Morgan SA, Fox ME, Watson JV. (1990) Mitoxantrone-DNA binding and the induction of topoisomerase II associated DNA damage in multi-drug resistant small cell lung cancer cells. *Biochem Pharmacol*. **40**(9), p2069-2078.

Ueno T, Nagano T. (2011). Fluorescent probes for sensing and imaging. *Nat Methods*. **8**, p642-645.

Wang L, Chen S, Zhang M, Li N, Chen Y, Su W, Liu Y, Lu D, Li S, Yang Y, Li Z, Stupack D, Qu P, Hu H, Xiang R. (2012). Legumain: a biomarker for diagnosis and prognosis of human ovarian cancer. *J Cell Biochem*. **113**, p2679-2686.

Zhen Y, Chunlei G, Wenzhi S, Shuangtao Z, Na L, Rongrong W, Xiaohe L, Haiying N, Dehong L, Shan J, Xiaoyue T, Rong X. (2015). Clinicopathologic significance of legumain overexpression in cancer: a systematic review and meta-analysis. *Sci Rep.* **5,** p16599.

# Chapter 4 New colour reagents for Amino group detection and use in SPPS

## 4.1 Abstract

During the solid phase peptide synthesis (SPPS), it is essential to monitor the completion of the Fmoc cleavage and the coupling reaction. Some drawbacks with classical methods for amino group detection, notably unsatisfactory results with secondary amino acids and complex procedures have provided the motivation to develop a new colour test here as a simple, sensitive and efficient method for visual detection of the resin beads. Three compounds (HZ20, HZ22 and HZ24) with different colours were synthesised and evaluated. The new compounds were each based on highly coloured aminoanthraquinones. The data presented here shows that these reagents are capable of detecting free amino groups on resin beads used for SPPS. In addition to reaction monitoring, for one of these reagents, it was shown that on-bead labelling can be performed, leading to recovery of a labelled peptide after cleavage, suitable for characterisation. HPLC methods were developed for separation of labelled structurally related compounds.

## 4.2 Introduction

Solid phase peptide synthesis (SPPS), pioneered by Merrifield, is largely used in construction of chemical libraries, particularly in medicinal chemistry (Merrifield, 1963). SPPS has many advantages over traditional synthesis such as all reagents can be simply washed away each step, overall quicker time for synthesis, convenient work-up and the synthetic intermediates do not have to be isolated (ref). Fmoc-SPPS is the universally applied method of choice for SPPS, mainly due to the low cost of commercially available Fmoc amino acids and

continuing improvements in Fmoc solid-phase technology (Behrendt, White, & Offer 2016). Fmoc-protected amino acids are increasingly used in automated technologies to synthesise medicinally useful peptides including chemically engineered peptides (Mäde, Els-Heindl S, & Beck-Sickinger AG, 2014). However, the efficiency of SPPS is often limited by the low level of completeness of amino acid coupling steps. Efficiency of coupling is especially important in the application of combinatorial methods to the synthesis of peptide based drug susbtances on solid-phase (Gordon *et al*., 1994). In this case, the development of a more reliable and sensitive visual colourimetric assay to detect free amines on solid support is essential.

To date, several colourimetric assays are available for detection of the amino acid coupling in SPPS. The ninhydrin-based Kaiser test (Kaiser *et al*., 1970) and a later modification (Sarin *et al*., 1981), and use of TNBS (2,4,6 trinitrobenzenesulphonic acid; (Hancock and Battersby, 1976) are two of the most common colourimetric tests. The ninhydrin based tests are not very sensitive to sensitive to aromatic amines, nor are they able to detect secondary amines such as proline. TNBS is not effective for sterically hindered amines. An alternative is 4-N,N'-dimethylaminoazobenzene-4'-isothiocyanate (DABITC) which is able to detect primary and secondary amines and has been used for detection HPLC detection of side-chain-labelled lysines in peptides (Nair *et al*., 1994) and N-terminal sequencing of peptides (Chang, 1981). However, the visual colour of the treated resin is yellow to orange which cannot be desirable because the resin will become a similar colour during successive rounds of the SPPS process. The MGI (malachite green isothiocyanate) method is wasteful and time-consuming and needs 1 hour reaction time and 4 mg of resin. The so-called DMT (dimethoxytrityl) and NPIT (nitrophenylisothiocyanate-*O*-trityl) tests rely on UV-measurements. More recently, the use of a p-nitrophenylester of

Disperse Red 1 (known as NF31) has been reported as a more sensitive method but requires a reacting condition of 70°C (Madder *et al.,* 1999; Steven *et al.,* 2007). The latter, because it contains a diazo-group, cannot be used under reducing conditions. The shortcomings of all the above methods encouraged this work to develop a new colourimetric assay for SPPS.

This chapter reports three new reagents with different colours (blue, red, and purple) for monitoring coupling step of SPPS were synthesized and evaluated. They are all rapid (within 2 min), sensitive and reactive at room temperature. Furthermore, these methods are applicable to both sterically hindered primary and secondary amines. These new colour reagents have very low toxicity and are safe to handle during SPPS; dry, they are stable stored in the solid state at 4°C for more than 12 months.

## 4.3 Results and discussion

Three colour test reagents HZ20, HZ22 and HZ24 (blue, red and purple respectively) were developed for SPPS and their syntheses, properties and some applications are described in the following sections. The chromophores were aminoanthraquinones with varying numbers of additional hydroxy groups that enhance the colur of the compound (the visible absorption maxima being shifted to longer wavelength). The design of the new chemical tools for amine detection and peptide coupling reaction monitoring on-resin was based upon creating new O-pentafluorophenyl active esters of anthraquinone-spacer carboxylic acids (AQ-spacer-COOPfp). Reaction of on-resin amino groups with these reagents was expected to colour the beads unless all amino groups had been fully acylated during couplings. Removal of a sample of beads after a coupling step allowed treatment with the given anthraquinone-pentafluorophenolate and a positive colour on visual inspection indicated that the reaction had not gone to completion due to capping of residual amino groups in the beads.

## 4.3.1 Synthesis of AQ-Gly-methyl (HZ18)

Reaction of leucoquinizarin with amines is a well-known reaction to produce either 1-substituted or 1,4-disubstituted anthraquinones (Greenhalgh and Hughes, 1968), Zee-Cheng and Cheng,1978; Zee-Cheng *et al*., 1979; Murdock *et al*., 1979).

Leucoquinizarin and glycine-methylester hydrochloride were mixed and dissolved in DMF, followed by the addition of $K_2CO_3$ as the base (**Scheme 39)**. The reaction mixture was heated on a steam bath for 1 hour and then aerated for another 1 hour. The reaction solution was extracted with chloroform and water. The extraction process was very difficult as both aqueous and organic layers

were darkly coloured. The organic layers were combined and dried with anhydrous sodium sulphate. After filtration and evaporation, the solid compound HZ18 was collected and purified by column chromatography using the solvent system chloroform to ethyl acetate 9:1. The appropriate fractions containing the major product were combined and collected.
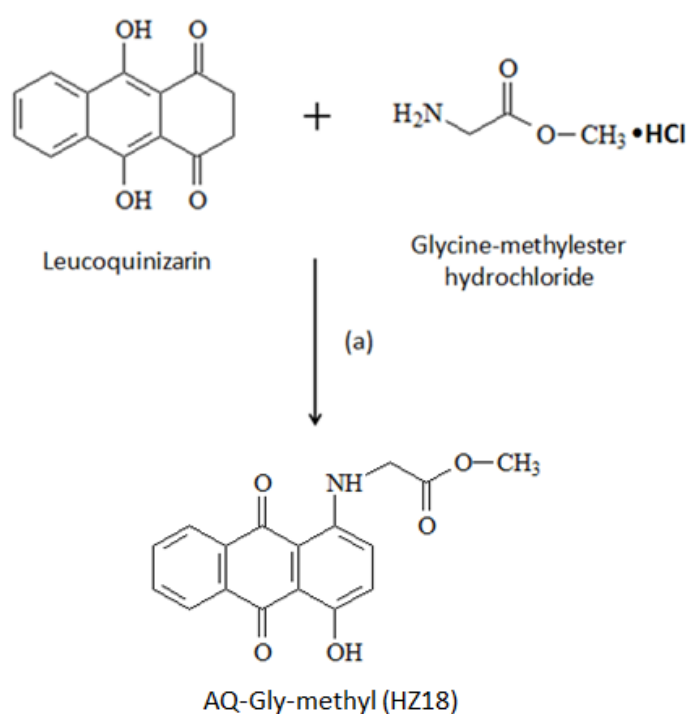

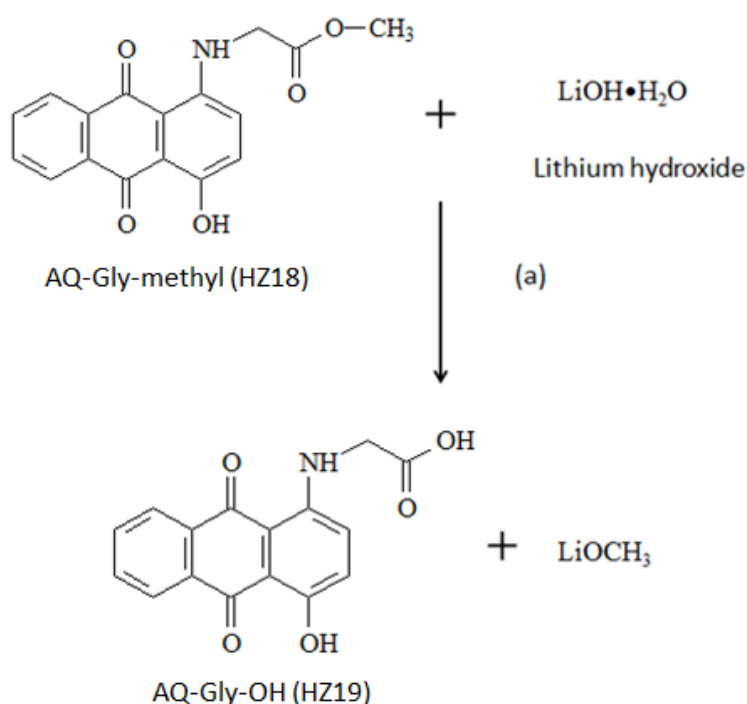
Reagents and Conditions: (a) $K_2CO_3$ in DMF

**Scheme 39.** Outline of HZ18 synthesis

The synthesis required conditions that allow the formation of the mono-amination product in order to prevent reaction at the 1-, and 4-positions of the leucoqunizarin ring. The TLC of the reaction mixture showed traces of the blue bis-aminated byproduct but the target compound was the major product unless reaction times were extended. The structure of HZ18 was confirmed by its $^1H$ nmr spectrum (in $CDCl_3$) which showed, for example, the expected pattern of signals for the AA'BB' system at δ 8.41-8.39 (1H, d, H-8); 8.36-8.33 (1H, d, H-5) and 7.85-7.81 (1H, m, H-7); 7.80-7.75 (1H, m, H-6). The methyl ester protons were assigned to a three-proton singlet at 3.86 ppm and the

anthraquinone NH proton was a clear one-proton triplet at 10.49 ppm. The 4-hydroxy group proton was shifted to higher ppm as a result of chelation to the C-10 carbonyl group of the quinone. Remaining protons were all assigned. The product ester HZ18 formed the source of the required carboxylic acid (HZ19) by hydrolysis of the methyl ester.

## 4.3.2 Synthesis of AQ-Gly-OH (HZ19)

In order to introduce the required acid group into the new anthraquinone-glycine conjugate colour test reagent, the methyl ester had to be hydrolysed. AQ-Gly-methyl (HZ18) and lithium hydroxide (LiOH•H$_2$O) were dissolved in aqueous methanol (**Scheme 40**). The mixture was stirred for 1.5 hours and then extracted by chloroform and water. All the organic layers were combined and evaporated to dryness. The dry crude product HZ19, clean on TLC was considered ready for the next reaction (conversion to the OPfp active ester) without further purification.



Reagents and Conditions: (a) aqueous methanol

**Scheme 40.** Outline of HZ19 synthesis

### 4.3.3 Synthesis of AQ-Gly-OPFP (HZ20)

The SPPS colour test reagent HZ20 was synthesised by mixing the glycine conjugate HZ19, DCC and pentafluorophenol (PFP) together in ethyl acetate (**Scheme 41**). The reaction was completed in 2 hours by checking the TLC. Silica gel chromatography was performed for the purification of HZ20 running with a solvent mixture of chloroform to ethyl acetate 7:1. The chromtographically homogeneous final product was collected by evaporation and drying under vacuum.



AQ-Gly-OH (HZ19)

PFP

(a)

AQ-Gly-OPFP (HZ20)
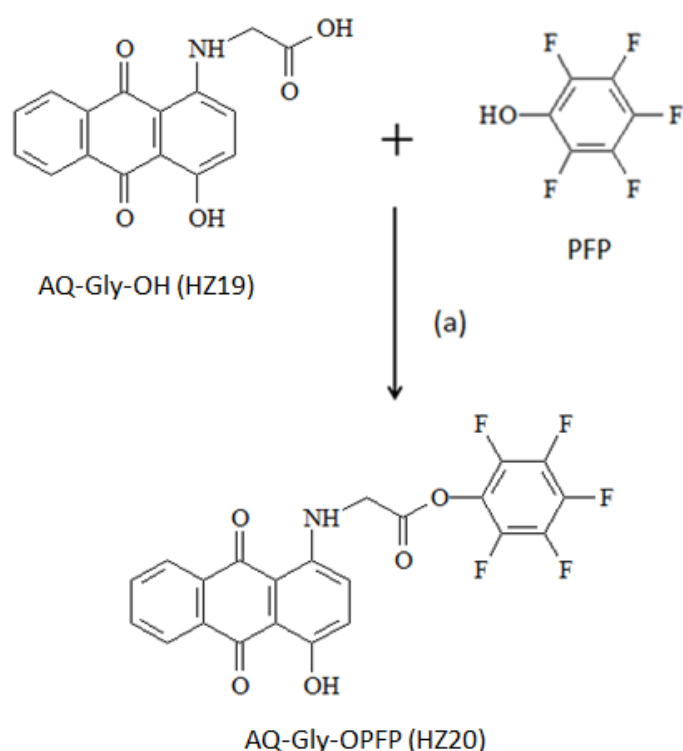
Reagents and Conditions: (a) DCC, DMAP in ethyl acetate

**Scheme 41.** Outline of HZ20 synthesis

The structure of pentafluorophenolate HZ20 was confirmed by its ^{1}H NMR spectrum (in CDCl$_3$) that included two one-proton singlets at 13.46 and 10.52 ppm for the 4-OH and NH protons, respectively. In addition to the assignment of all aromatic protons, the methylene group protons of the glycine residue were assigned to a distinct two-proton singlet at 4.61 ppm. In the proton decoupled and ^{13}C decoupled, ^{19}F nmr spectrum of HZ20 the three environments for the

fluorine signals of the ortho, meta and para fluorine atoms were recorded at -152.4; -156.8 and -161.5, respectively.

### 4.3.3.1 Colour test with HZ20

H-Leu-2-ClTrt resin was first used for the colour test. A small amount of the commercially available resin (Novabiochem) was transferred into an SPPS reaction vessel. Dichloromethane was poured into the vessel to swell the resin beads for 1 hour. Dichloromethane was drained off by use of a vacuum pump and the resin was washed with DMF. A few beads were transferred into a small sample bottle. HZ20 in DMF (1 mmol, 200 μl) and about a drop of DIPEA were added to the bottle. After 2 minutes, the purple solution was pipetted out and the beads were washed with DMF. The beads became purple in colour and under the microscope the beads were captured in the image shown in **Figure 64**.
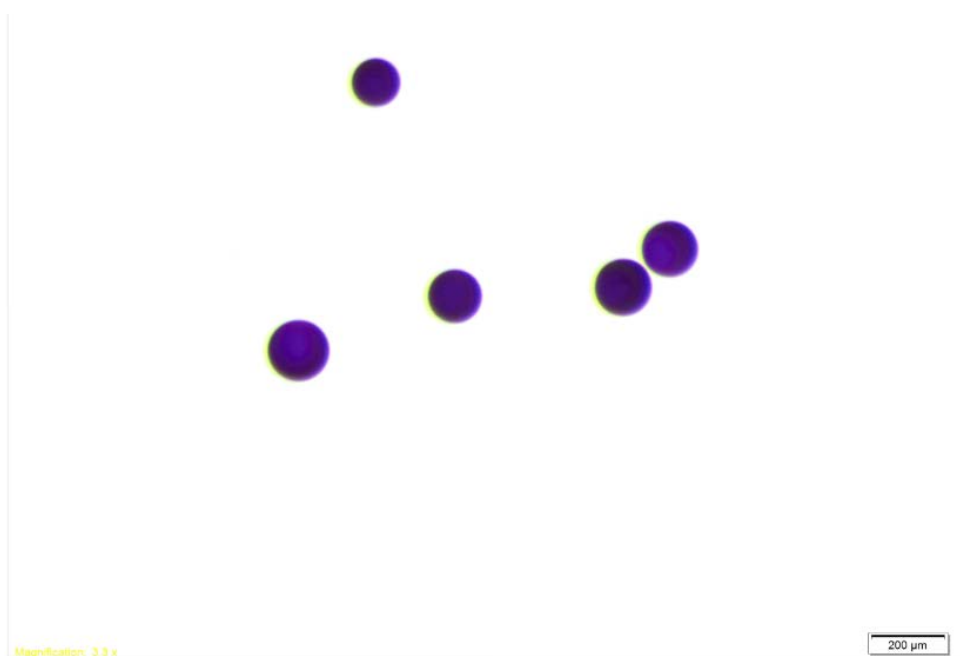


**Figure 64**. Resin beads coloured by HZ20

The resin beads clearly had become strongly coloured through reaction between

the pentafluorophenolate active ester of HZ20 and the free amino groups on the surface of the native beads. The coloured reagent was clearly chemically attached to the beads since it the colour persisted when repeatedly washed with solvent.

### 4.3.4 Synthesis of AQ-Ahx-OH (HZ21)

For the synthesis of the second pentafluorophenolate colour test reagent HZ22, the starting material 1-chloroanthraquinone was reacted with 6-aminohexanoic acid in DMSO on the 100ºC water bath **(Scheme 42)**. The reaction was confirmed by TLC, showing the formation of a new major product spot of anthraquinone-acid HZ21, and the solution was cooled to room temperature. The purification of HZ21 used the silica gel chromatography with the solvent system of dichloromethane and methanol (9:1). The product fractions containing the new product were combined, dried and collected for further reaction and characterisation.
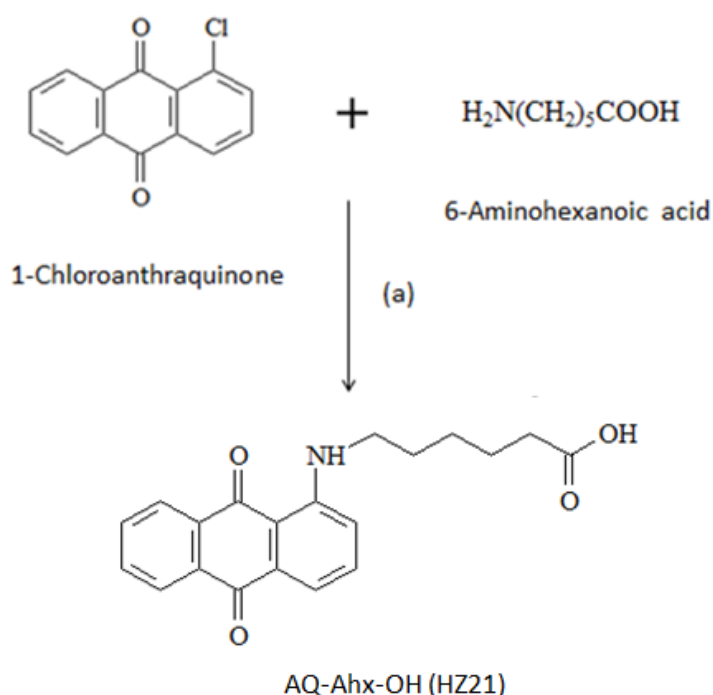


Reagents and Conditions: (a) DMSO, 100ºC water bath

**Scheme 42.** Outline of HZ21 synthesis

The structure of the anthraquinone aminohexanoic acid conjugate HZ21 was confirmed by its $^1$H NMR spectrum (in CDCl$_3$), which showed, for example, a one-proton triplet (AqNH) at 9.77 ppm and a two proton multiplet at 3.40-3.36 ppm for the adjacent methylene group protons. The Anthraquinone H-2 proton was a doublet at 7.09 ppm. The methylene group protons adjacent to the ester carbonyl group were assigned to a two-proton triplet at 2.46-2.43 ppm. All other protons could be assigned with the exception of the carboxylic acid proton which was deemed to have undergone proton exchange broadening. However, the presence of the carboxylic acid group was confirmed by identification of a third carbonyl quaternary carbon atom in the proton decoupled $^{13}$C NMR spectrum at 178.4 ppm, in addition to the C-9 and C-10 quinone carbonyl carbons at 185.05 and 183.85 ppm respectively. The anthraquinone acid HZ21 was then ready for esterification with pentafluorophenol to afford the target reagent HZ22.

### 4.3.5 Synthesis of AQ-Ahx-OPFP (HZ22)

The second SPPS colour test compound HZ22 was synthesised by the reaction of HZ21 and pentafluorophenol in dichloromethane, by using DCC and DMAP as the coupling reagents **(Scheme 43)**. The final product was purified by column chromatography using the solvent system dichloromethane to ethyl acetate 9:1. The purified solid compound was collected by precipitation in hexane.
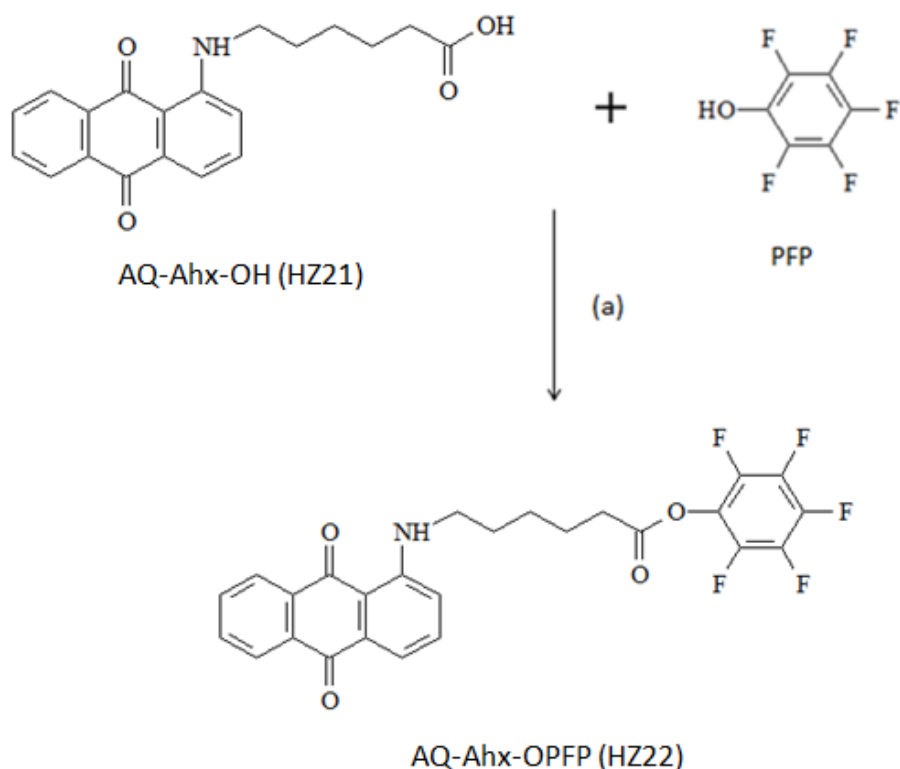
Reagents and Conditions: (a) DCC & DMAP in Dichloromethane

**Scheme 43.** Outline of HZ22 synthesis

The structure of the pentafluorophenolate HZ22 was confirmed by its nanoelectrospray ESI (+) spectrum that showed a strong signal at m/z 504 corresponding to $(M + H)^+$; M 503 Da.

The structure was also confirmed by its $^1H$ NMR spectrum, which showed signals for example at 9.79 ppm (one-proton triplet AqNH) and a two proton multiplet at 3.42-3.37 ppm for the adjacent methylene group protons. The anthraquinone H-2 proton was a doublet at 7.08 ppm. Adjacent to the ester carbonyl group, the methylene group protons were assigned to a two-proton triplet at 2.77-2.73. The remaining methylene group signals for the hexyl spacer in HZ22 were all assigned together with the AA'BB' system for H5, H8 and H6, H7 and remaining aromatic protons. Furthermore, in the proton decoupled and $^{13}C$ decoupled, $^{19}F$ NMR spectrum of HZ22 the three environments for the fluorine signals of the ortho, meta and para fluorine atoms were recorded at

-152.8; -158.1 and -162.2, respectively.

**4.3.5.1 Colour test with HZ22**

A small amount of Fmoc-Ala-Wang resin was allowed to swell in dichloromethane. The resin beads were washed by DMF. A few beads were transferred to a small sample bottle which contained the solution of HZ22 dissolved in DMF (1 mmol, 200 µl). One drop of DIPEA was added to the reaction. After 2 minutes, the red solution was pipetted out and the beads in the bottle were washed with DMF. The beads had no red colour by visual observation, indicative of there being no residual free amine groups on the Fmoc resin and confirming that there was no red colouration as a result of any possible staining or physical absorption of the reagent into the resin matrix.

The Fmoc-Ala-Wang resin was N-terminal deprotected by using standard conditions of 20% piperidine in DMF. The resin beads were then washed by DMF 3 times. The colour test by HZ22 showed that all beads turned red as shown in **Figure 65**. The beads were also observed under the microscope as shown in **Figure 66.**
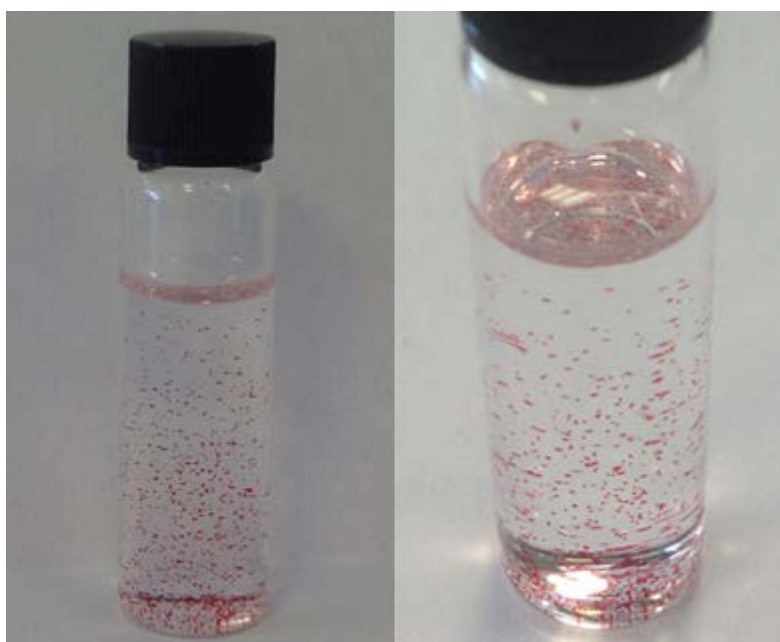


**Figure 65.** Resin beads coloured by HZ22 in the sample bottle

**Figure 66.** Resin beads coloured by HZ22

### 4.3.6 Synthesis of AQ-[4-Hydroxyl]-Ahx-OH (HZ23)

Preparation of a third candidate colour test pentafluorophenolate was carried out to create an analogue of HZ22 which had an additional hydroxyl group in the 4-position of the anthraquinone chromophore. The procedure was analogous to that used for the synthesis of the 1-amino-4-hydroxy analogue, HZ20, to afford a mono aminated product.

Leuoquinizarin was reacted with 6-aminohexanoic acid by the addition of $K_2CO_3$ in DMF on the $100^0C$ water bath **(Scheme 44)**. The reaction solution was cooled to RT and aerated for 1 hour. The crude product AQ-[4-Hydroxyl]-Ahx-OH (HZ23) was purified by column chromatography using the solvent system dichloromethane to methanol 10:1. The resulting acid then required esterification with pentafluorophenol to afford the third candidate test reagent (HZ24).
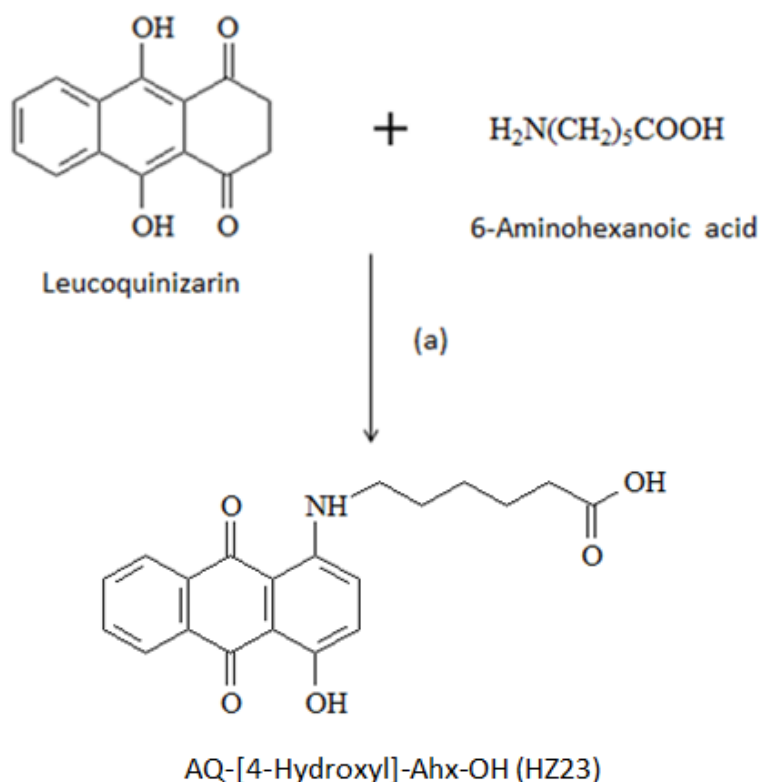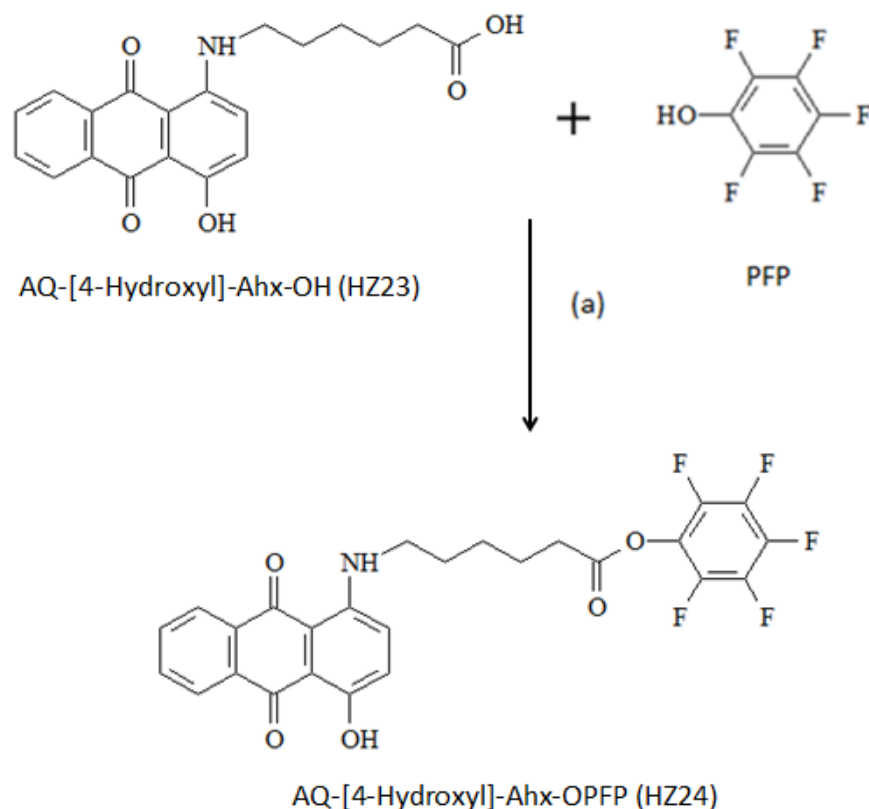
Reagents and Conditions: (a) $K_2CO_3$ in DMF

**Scheme 44.** Outline of HZ23 synthesis

### 4.3.7 Synthesis of AQ-[4-Hydroxyl]-Ahx-OPFP (HZ24)

The synthesis of the third SPPS colour test reagent HZ24 was completed by the coupling reaction of AQ-[4-Hydroxyl]-Ahx-OH (HZ23) and pentafluorophenol by the addition of DCC and DMAP. The reaction mixture was dissolved in dichloromethane **(Scheme 45)**. Purification of the final target compound AQ-[4-Hydroxyl]-Ahx-OPFP (HZ24) was performed by silica gel chromatography. The column was eluted by a solvent mixture of dichloromethane and ethyl acetate. Hexane was then used to precipitate the purified solid product.

AQ-[4-Hydroxyl]-Ahx-OH (HZ23)

PFP

(a)

AQ-[4-Hydroxyl]-Ahx-OPFP (HZ24)

Reagents and Conditions: (a) DCC & DMAP in Dichloromethane

**Scheme 45.** Outline of HZ24 synthesis

The structure of HZ24 was confirmed by its $^1$H NMR spectrum (CDCl$_3$), which showed signals for example, the singlet at 13.76 ppm for the strongly de-shielded 4-hydroxy group proton, chelated to the quinone carbonyl, and a one proton triplet at 10.37 ppm for the amino group proton. The anthraquinone H-2 and H-3 protons were assigned as one-proton multiplets at 7.25 and 7.23 respectively. Methylene group signals adjacent to the anthraquinone and to the ester carbonyl appeared at 3.48-3.43 and 2.77-2.73 ppm respectively. Furthermore, in the proton decoupled and $^{13}$C decoupled, $^{19}$F NMR spectrum of HZ24, the three environments for the fluorine signals of the ortho, meta and para fluorine atoms were recorded at -152.7; -158.01 and -162.30, respectively.

### 4.3.7.1 Colour test using HZ24

**Figure 67** shows the photograph of chlorotrityl resin beads with free amino groups and coloured by AQ-[4,Hydroxyl]-Ahx-OPFP (HZ24). The beads were all a dark purple colour. For comparison, samples of the resin beads coloured separately by the three new test reagents HZ20, HZ22 and HZ24 were mixed to obtain the photograph shown in **Figure 68**.
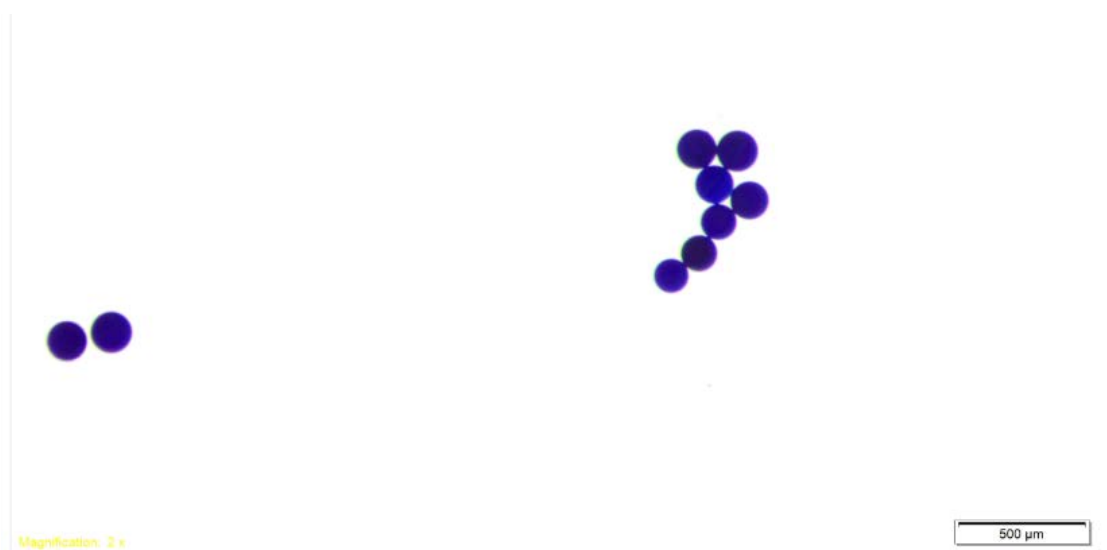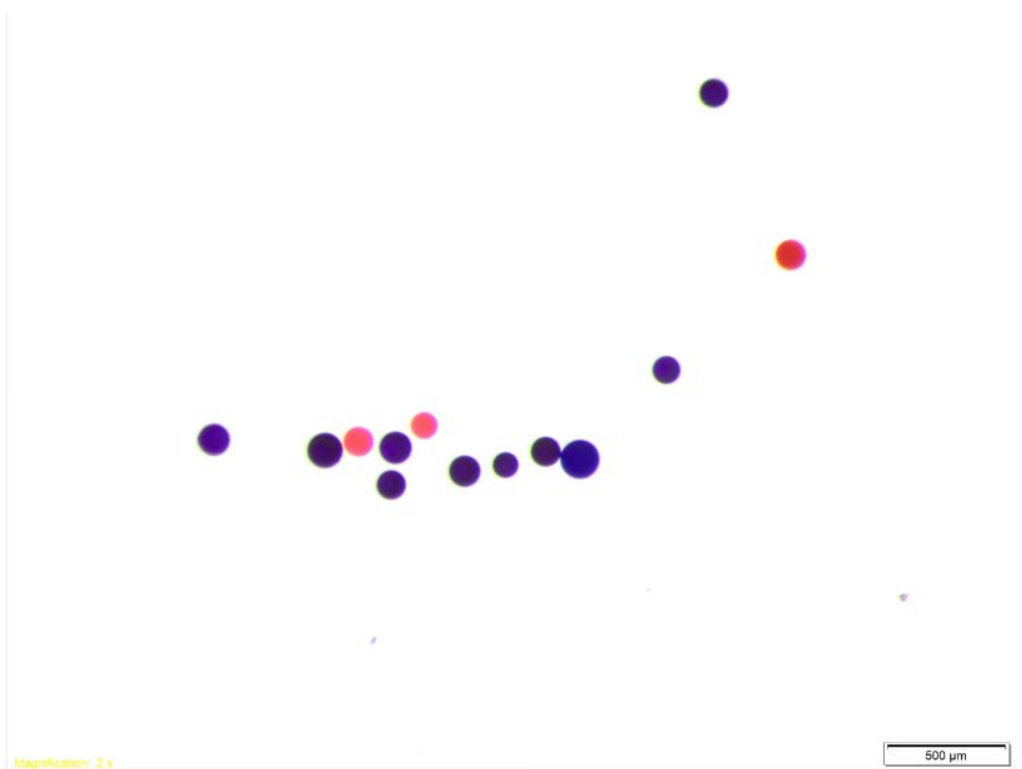


**Figure 67.** Resin beads coloured by HZ24

**Figure 68.** Mixture of resin beads coloured by HZ20, HZ22 & HZ24

### 4.3.8 HPLC analysis of HZ22 labelled peptides

It was recognised that the newly synthesised colour reagents can have wider applications than just monitoring the coupling reaction of SPPS. It was envisaged the reagents could be used to label deprotected peptides on resin and then perhaps be cleaved from the resin to afford N-labelled peptides suitable for peptide characterisation. There are several methods reported for the characterisation of N-labelled peptides and the most common ones rely on analysis of their Fmoc derivatives since these are the ones that emerge from SPPS methods. Methods have relied on UV properties of the Fmoc group and have been combined with mass spectrometric characterisation for both free and resin-bound amino acid and peptides. Use of combined HPLC-tandem mass spectrometry after derivatisation with Fmoc chloride is a recent example (Ziegler and Abel 2014). In this project, it was reasoned that, for example, the red reagent AQ-Ahx-OPFP (HZ22) is able to label peptides which will be further

analysed by HPLC, provided an HPLC method could be developed.

**Figure 69** shows the chemical structure of an HZ22 labelled pentapeptide which was synthesised to investigate the potential for HZ22 labelling at the N-terminus followed by further characterisation by HPLC. The peptide sequence was chosen because it was relevant to the work described in Chapter one of this thesis. The sequence contained a gly-nva cleavage site for MMP-9. The pentapeptide was synthesied by standard SPPS methods. AQ-Ahx-OPFP (HZ22) was reacted with the free amine group of the pentapeptide on resin by using only the DIPEA catalyst in DMF. The resulting labelled product, AQ-Ahx-Pro-Ala-Gly-Nva-Pro-OH (HZ60) was cleaved from the resin by TFA treatment. **Figure 70** illustrates the overall planned synthesis of HZ60.
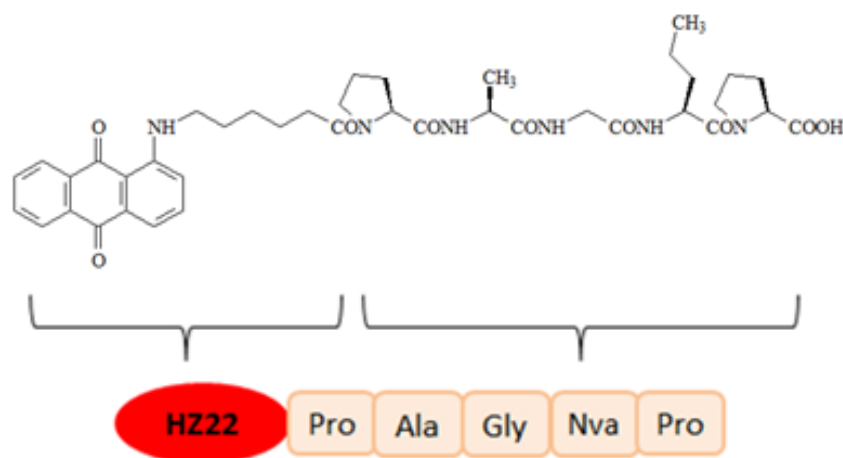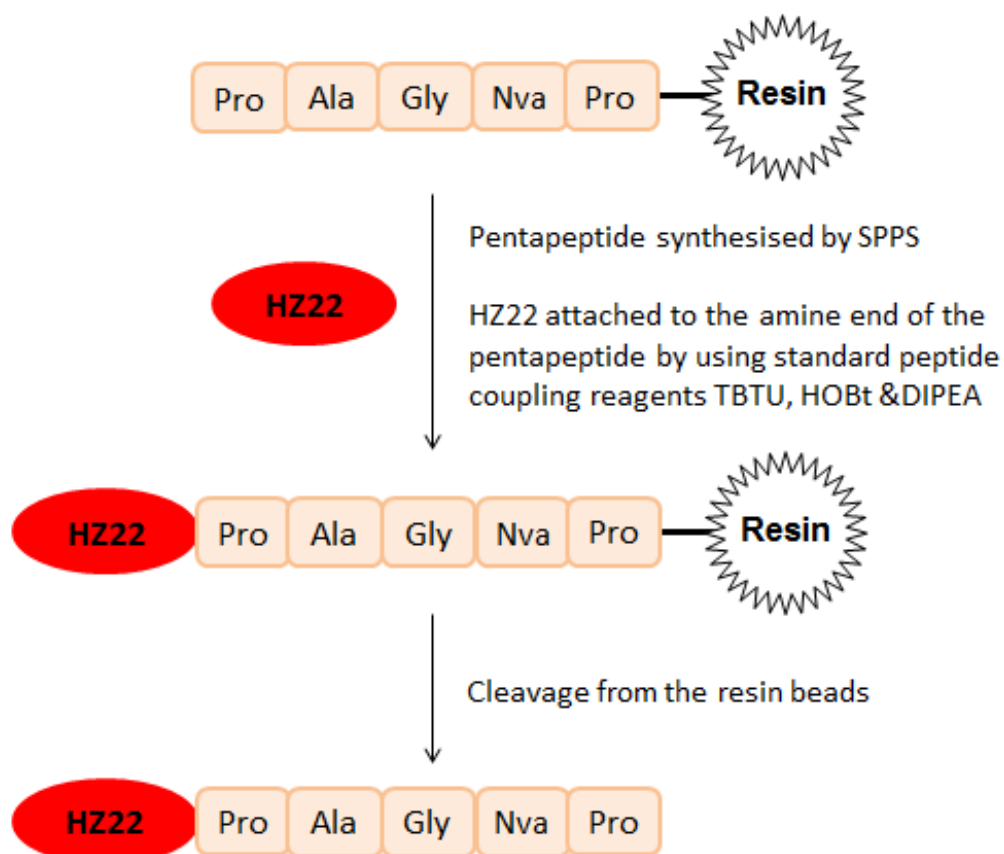


**Figure 69.** The chemical structure of HZ60

**Figure 70.** Synthesis route for N-labelled pentapeptide HZ60

The N-labelled pentapeptide, AQ-Ahx-Pro-Ala-Gly-Nva-Pro-OH (HZ60) was successfully characterised by nanoelectrospray negative ionisation mass spectrometry **(Figure 71)**. A signal at m/z 757 [M – 1]⁻, (100%) corresponded to a molecular mass of 758 Da.
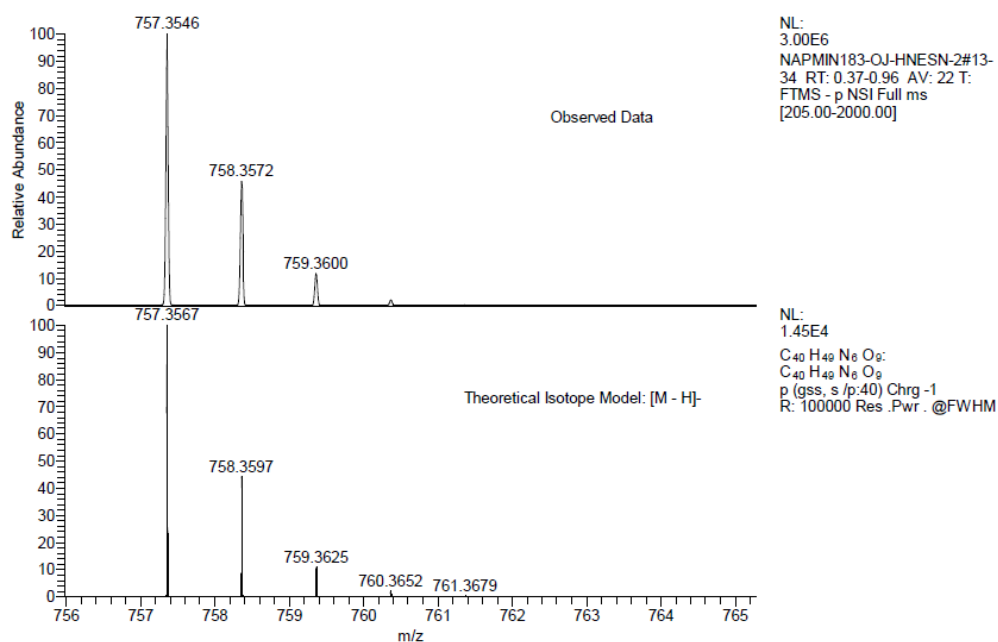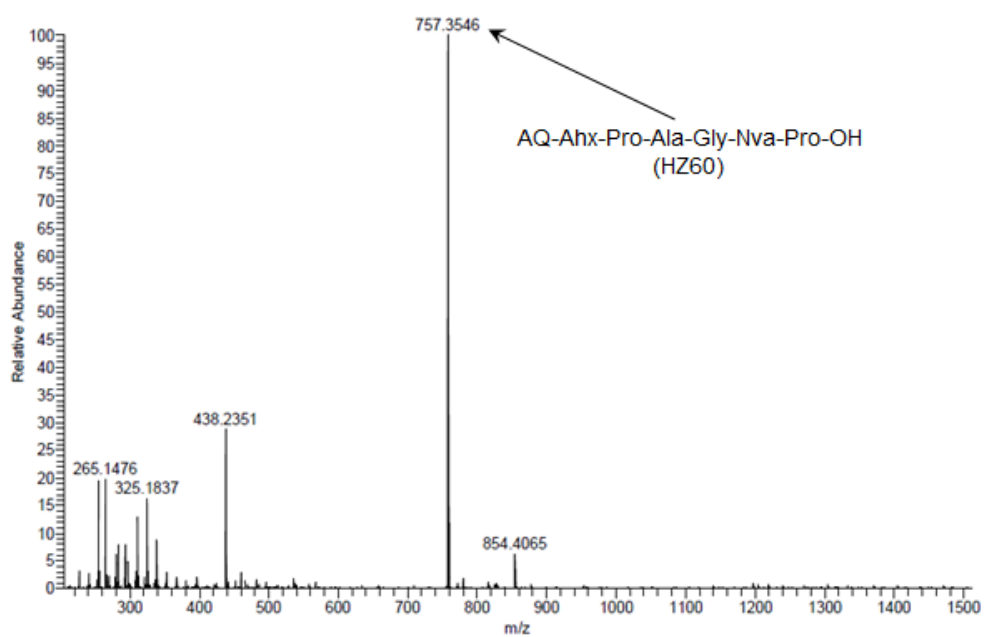
**Figure 71.** The ESI (-) Mass spectrum of AQ-Ahx-Pro-Ala-Gly-Nva-Pro-OH (HZ60)

The anthraquinone-pentapeptide conjugate HZ60 was shown to be accessible to characterisation by negative ion electrospray MS, affording a strong signal (100% R.A. and base peak), together with good agreement between the theoretical isotope pattern and the observed ions for M-1.

## 4.3.8.1 Further examples of N-labelled members of the series

Another two compounds AQ-Ahx-Pro-Ala-Gly-OH (HZ106) and AQ-Ahx-Pro-OH (HZ107) were synthesised by same SPPS method as AQ-Ahx-Pro-Ala-Gly-Nva-Pro-OH (HZ60) starting with the appropriate amino acid loaded resin. The chemical structures are shown in **Figures 72 and 73.** These compounds were prepared for an HPLC study to explore the feasibilty of deriving a simple, reliable method for separating closely structurally related series of labelled peptides.
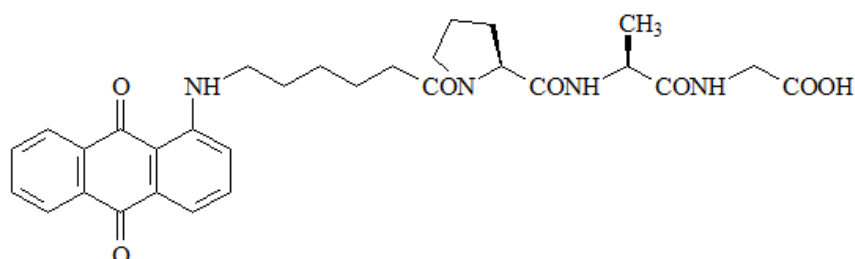


**Figure 72.** Chemical structure of HZ22 N-labelled prolylalanine HZ106
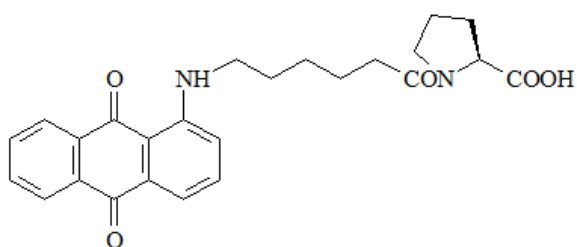


**Figure 73.** Chemical structure of HZ22 N-labelled proline HZ107

## 4.3.8.2 HPLC/UV analysis of HZ22 N-labelled amino acids and peptides

HPLC was performed using a WATERS e2695 Alliance HPLC instrument and WATERS 2489 UV/VIS detector (Edinburgh Napier University). Mobile phase A consisted of 100% Acetonitrile, 0.1% TFA and mobile phase B of 100% HPLC water, 0.08% TFA, pH 2.00 (±0.05). A reverse phase column (Agilent Zorbax

Extend C18, 5 µm, 4.6 mm x 50 mm) was used with gradients developed over a 15 min period. Mobile phase A was changed from 40% to 42% over 5 minutes and isocratic hold at 42% A for 5 column volume time, then re-equilibration at initial conditions for 10 column volume time. Samples were injected onto the column in volumes of 10 µl with a flow rate of 1 ml/min and a column temperature of 40 ºC. The absorbance in the UV was recorded at wavelength 505 nm.

Stock solutions of compound (1 mg/ml) were prepared in 100% DMSO. The compound solutions were then diluted further in 50% acetonitrile in $dH_2O$ to the concentration of 100 µM.

HPLC analysis of anthraquinone-pentapeptide conjugate AQ-$(CH_2)_5$-Pro-Ala-Gly-Nva-Pro-OH (HZ60) was conducted and the retention time was recorded. **Figure 74** shows the HPLC chromatogram of the compound.
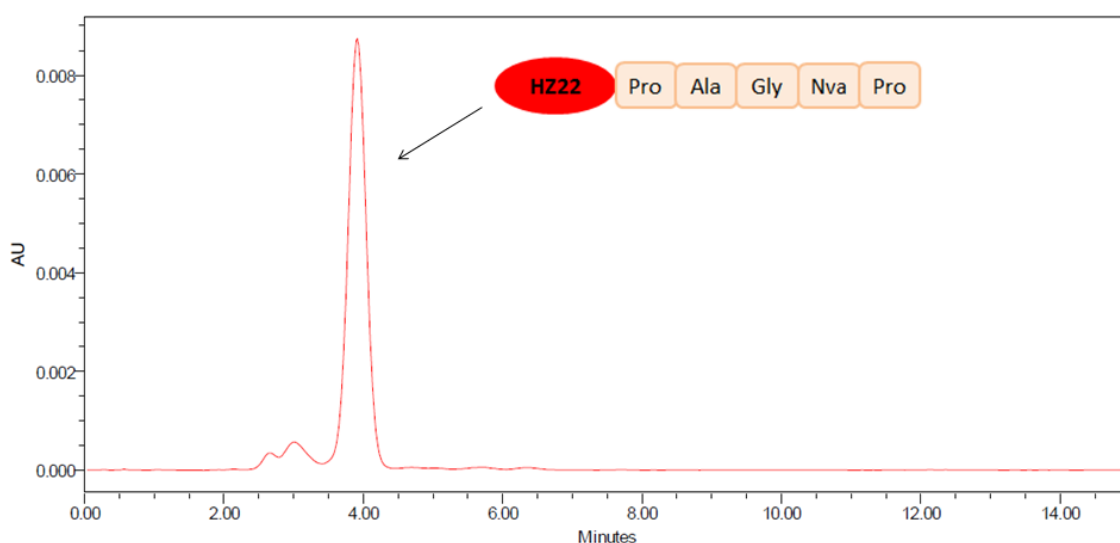


**Figure 74.** HPLC chromatogram of 100 µM HZ60 (pentapeptide), Retention time: 3.92 min

The HPLC chromatogram of AQ-$(CH_2)_5$-Pro-Ala-Gly-OH (HZ106) was shown in

**Figure 75.** There is a single peak in the chromatogam which indicated the high purity of the compound. The retention time is different from HZ60 above under the same column conditions. **Figure 76** shows a chromatogam of the HPLC analysis of 'red'-labelled proline: AQ-(CH$_2$)$_5$-Pro-OH (HZ107).
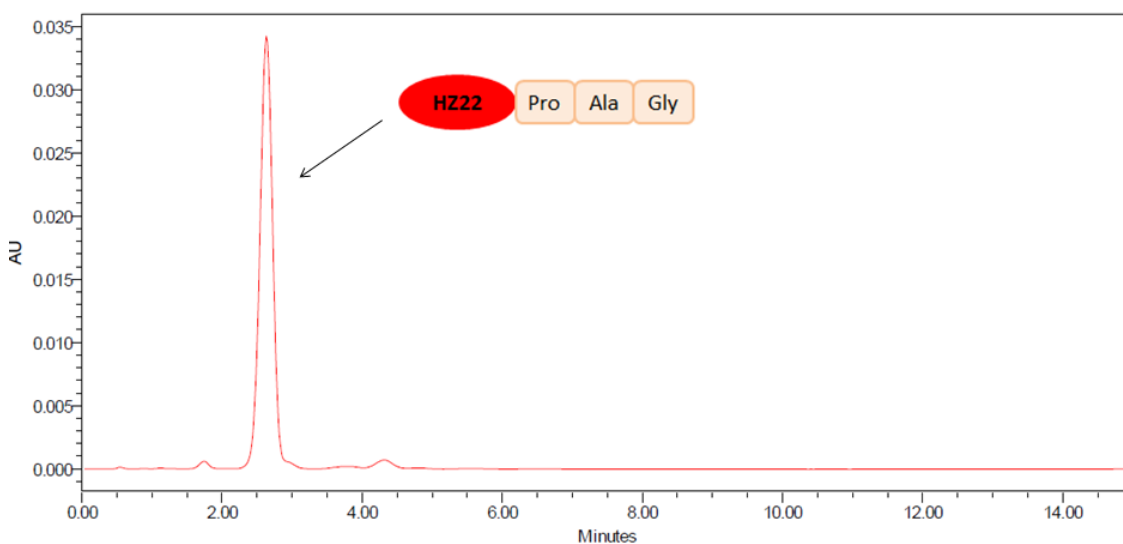


**Figure 75.** HPLC chromatogram of 100 μM HZ106 (tripeptide), Retention time: 2.62 min
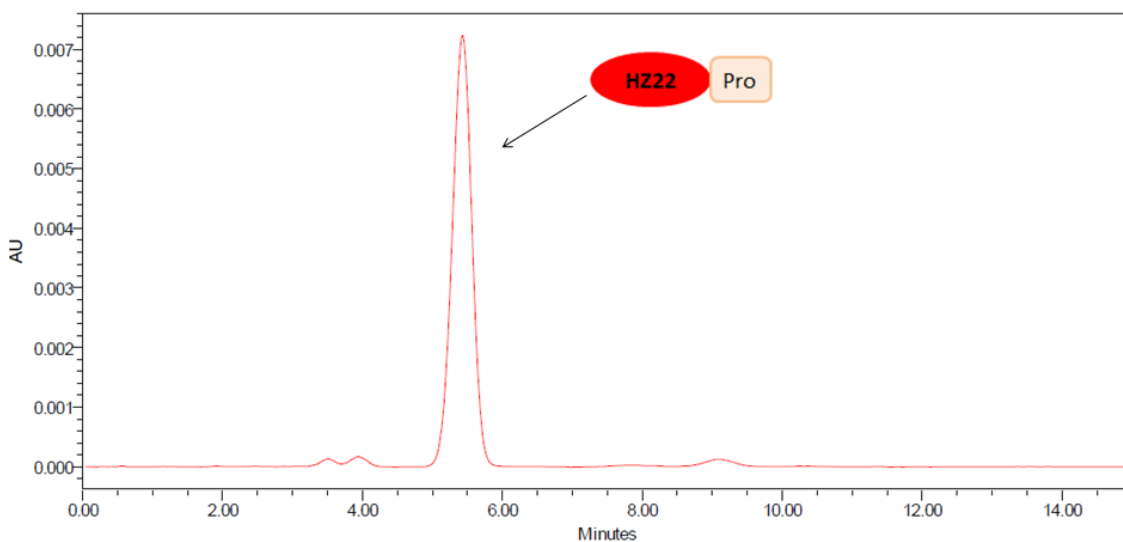


**Figure 76.** HPLC chromatogram of 100 μM HZ107 (proline conjugate), Retention time: 5.5 min

A mixture of the three N-labelled compounds: pentapeptide AQ-(CH$_2$)$_5$-Pro-Ala-Gly-Nva-Pro-OH (HZ60), tripeptide

AQ-(CH$_2$)$_5$-Pro-Ala-Gly-OH (HZ106) and single amino acid AQ-(CH$_2$)$_5$-Pro-OH (HZ107) was further analysed by HPLC as shown in **Figure 77.**
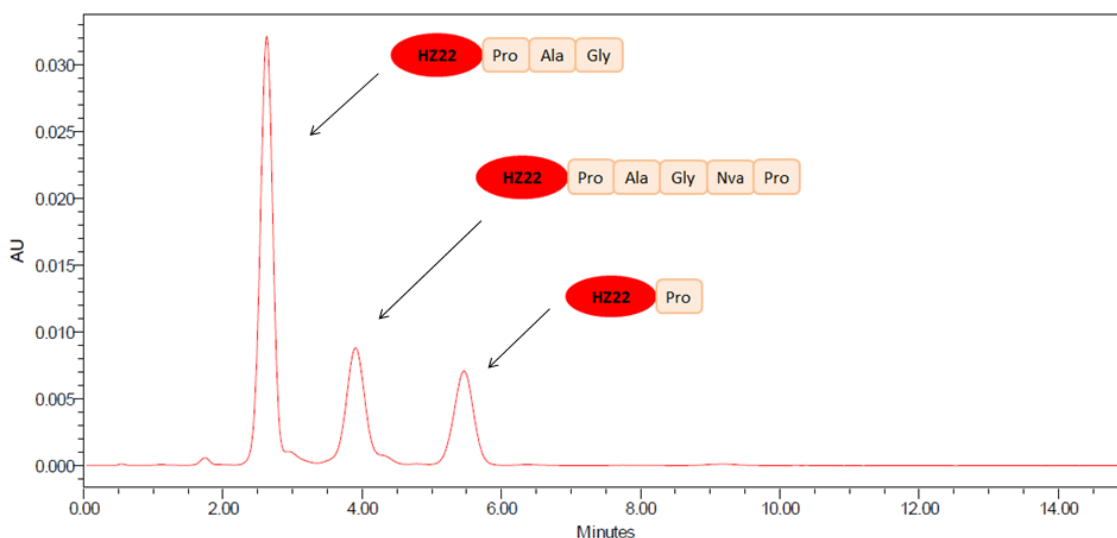


**Figure 77.** HPLC chromatogram of the mixture of 100μM HZ60, 100μM HZ106 and 100μM HZ107

The data presented in **Figure 77** shows that the HZ22 labelled proline amino acid conjugate (HZ107), the tripeptide (HZ106) and pentapeptide conjugates (HZ60) were separated with satisfactory base line resolution.

This indicates that it is likely to be feasible to separate and identify components in a reaction mixture if, for example, a larger peptide such as the pentapeptide HZ60 is subjected to cleavage by action of a protease such as MMP-9.

**4.4 Conclusion**

The newly synthesised compounds HZ20, HZ22 and HZ24 were considered as useful colour test reagents to monitor coupling reactions involving free amines during SPPS. The red labelling agent HZ22 was used to demonstrate its versatility for labelling amines on resin and for isolation of N-labelled peptides to create derivatives that are helpful for characterising the peptide. A simple, time-efficient HPLC method using uv/visible detection was developed for separation of examples of closely related amino acids and peptides. The pattern of behaviour shown by HZ22 would be expected to occur in a similar manner for the other two reagents HZ20 and HZ24. In future work, it would be instructive to try to use e.g. HZ22 in reactions to label amino groups in natural peptides for biological process investigations. Furthermore, it is of interest to extend the characterisation to a combined HPLC-MS method, given the ease of ionisation of the carboxylic acid group of the pentapeptide HZ60 in negative ion electrospray ionisation mass spectrometry.

## 4.5 Structure library
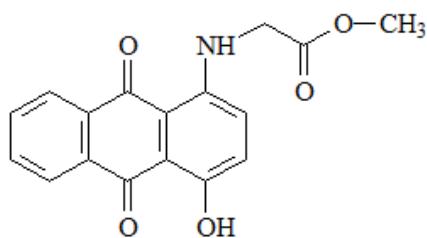


(4-Hydroxy-9,10-dioxo-9,10-dihydro-anthracen-1-ylamino)-acetic acid methyl ester

**AQ-Gly-methyl (HZ18)**
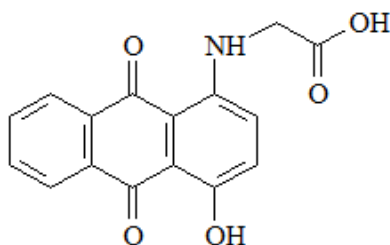


(4-Hydroxy-9,10-dioxo-9,10-dihydro-anthracen-1-ylamino)-acetic acid

**AQ-Gly-OH (HZ19)**
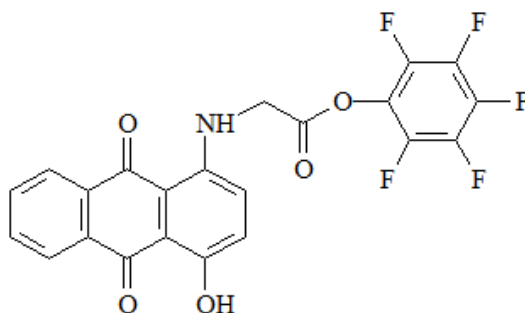


(4-Hydroxy-9,10-dioxo-9,10-dihydro-anthracen-1-ylamino)-acetic acid pentafluorophenyl ester

**AQ-Gly-OPFP (HZ20)**
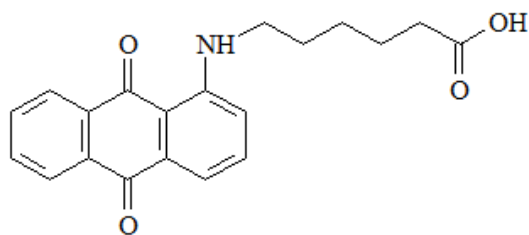
6-(9,10-Dioxo-9,10-dihydro-anthracen-1-ylamino)-hexanoic
acid

**AQ-Ahx-OH (HZ21)**
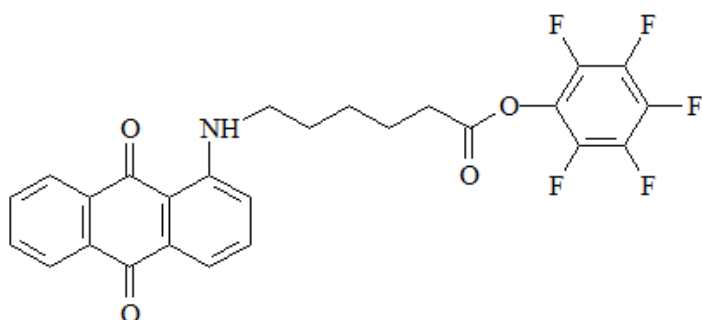
6-(9,10-Dioxo-9,10-dihydro-anthracen-1-ylamino)-hexanoic acid pentafluorophenyl
ester

**AQ-Ahx-OPFP (HZ22)**
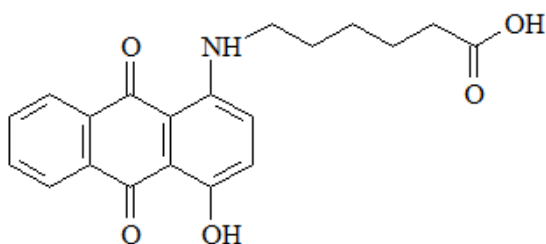
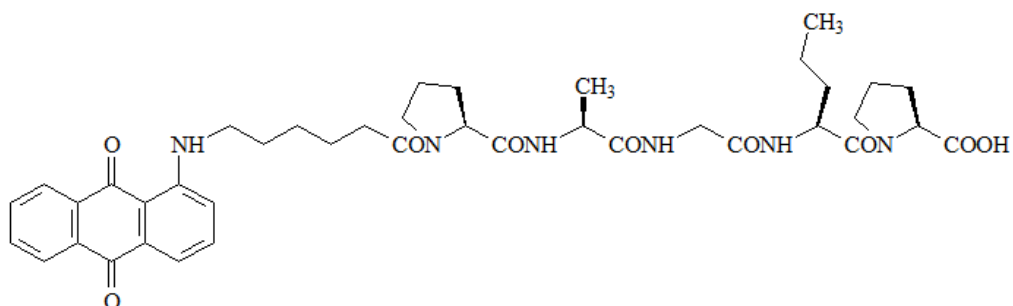6-(4-Hydroxy-9,10-dioxo-9,10-dihydro-anthracen-1-ylamino)-hexanoic acid

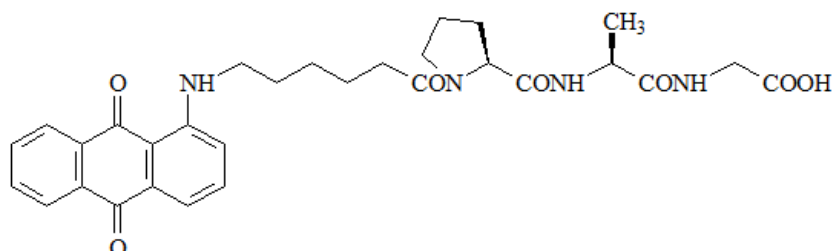**AQ-[4, Hydroxyl]-Ahx-OH (HZ23)**
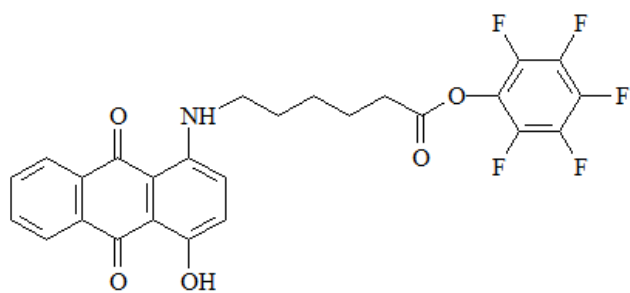
6-(4-Hydroxy-9,10-dioxo-9,10-dihydro-anthracen-1-ylamino)-hexanoic acid pentafluorophenyl ester
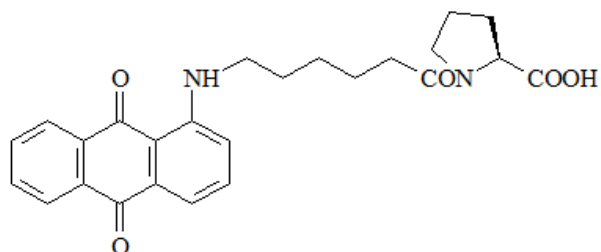
**AQ-[4, Hydroxyl]-Ahx-OPFP (HZ24)**



**AQ-Ahx-Pro-Ala-Gly-Nva-Pro-OH (HZ60)**



**AQ-Ahx-Pro-Ala-Gly-OH (HZ106)**



**AQ-Ahx-Pro-OH (HZ107)**

## 4.6 Experimental

### 4.6.1 Synthesis of AQ-Gly-methyl (HZ18)

HZ18 was prepared from the reaction of Leucoquinizarin (1 g, 4.13 mmol) with glycine-methylester-hydrochloride (2.07 g, 16.5 mmol) and potassium carbonate (2.05 g, 14.9 mmol) in DMF (30 ml) on the boiling water bath for 1 h. TLC of the crude product (Rf 0.54) used the solvent system, toluene-ethyl acetate 4:1. The foregoing reaction mixture was aerated for 1 h and then extracted with chloroform-water. All the organic extracts were combined, dried with anhydrous sodium sulphate, filtered and evaporated to dryness. The compound was purified by column chromatography using the eluting system, chloroform-ethyl acetate 9:1. The product (purple) was dried under vacuum. Yield: 579 mg, 45%.

$^1$H NMR spectrum (CDCl$_3$, 400 MHz) δ: 3.86 (3H, s, H-14); 4.21 (2H, s, H-12); 7.08 (1H, d, H-2); 7.31 (1H, d, H-3); 7.80-7.75 (1H, m, H-6); 7.85-7.81 (1H, m, H-7); 8.36-8.33 (1H, d, H-5); 8.41-8.39 (1H, d, H-8); 10.49 (1H, s, NH); 13.52 (1H, s, OH).

$^{13}$C NMR spectrum (CDCl$_3$, 100.6 MHz, 25°C) δ: 11.7 ; 52.6 ; 110.0 ; 114.1 ; 123.3 ; 126.4 ; 127.0 ; 128.7 ; 132.7 ; 132.8 ; 134.3 ; 135.2 ; 146.1 ; 156.8 ; 170.0 ; 183.0 ; 187.8 ppm.

### 4.6.2 Synthesis of AQ-Gly-OH (HZ19)

AQ-Gly-methyl HZ18 (100 mg, 0.32 mmol) and LiOH·H$_2$O (44 mg, 0.32 mmol) were dissolved in 40ml of aqueous methanol (3:1) and reacted at RT for 1.5 h. TLC (Rf 0.15) was checked using the solvent system, chloroform-methanol 6:1. The reaction solution was extracted with chloroform, acetic acid and water. All the organic layers were combined, dried with anhydrous sodium sulphate, filtered and evaporated to dryness. The product (purple) was collected with a

yield of 88.8 mg, 93%. The product was considered sufficiently pure for further use without further purification.

### 4.6.3 Synthesis of AQ-Gly-OPFP (HZ20)

AQ-Gly-OPFP HZ20 was prepared from the reaction of AQ-Gly-OH HZ19 (85 mg, 0.29 mmol), DCC (65 mg, 0.32 mmol) and PFP (58 mg, 0.32 mmol) in ethyl acetate (30 ml) for 3 h. TLC of the crude product (Rf 0.93) used the solvent system, dichloromethane-ethyl acetate 5:1. Column chromatography was performed for the purification of HZ20 by using the solvent system, dichloromethane-ethyl acetate 7:1. The product (purple) solution was filtered and evaporated to dryness. Yield: 56 mg, 42%.

<u>$^1$H NMR spectrum (CDCl$_3$, 400 MHz) δ</u>: 4.61 (2H, s, H-12); 7.14 (1H, d, H-2); 7.38 (1H, d, H-3); 7.80-7.77 (1H, m, H-7); 7.86-7.81 (1H, m, H-7); 8.37-8.35 (1H, d, H-5); 8.40-8.38 (1H, d, H-8); 10.52 (1H, s, NH); 13.46 (1H, s, OH).

<u>$^{13}$C NMR spectrum (CDCl$_3$, 100.6 MHz, 25°C) δ</u>: 25.0 ; 29.7 ; 34.0 ; 44.2 ; 114.3 ; 122.6 ; 126.5 ; 127.1 ; 128.8 ; 133.2 ; 134.4 ; 135.0 ; 145.5 ; 157.0 ; 183.7 ; 187.9 ppm.

<u>$^{19}$F NMR spectrum (CDCl$_3$) δ</u>: -152.4; -156.8 and -161.5

### 4.6.4 Synthesis of AQ-Ahx-OH (HZ21)

1-Chloroanthaquinone (1 g, 4.12 mmol) and 6-aminohexanoic acid (2.16 g, 16.5 mmol) were dissolved in 40 ml of DMSO and refluxed for 1 h. TLC of the crude product (Rf 0.57) used the solvent system, dichloromethane-methanol 9:1. The reaction solution was cooled to RT for extraction with chloroform. The crude product was purified by column chromatography using the same solvent system as TLC The product solution was evaporated to dryness. Diethyl ether (30 ml)

was slowly added to the product and the mixture was refrigerated for 1 h after which gave the chromatographically pure dark red product precipitate. Yield: 352 mg, 25%.

^{1}H NMR spectrum (CDCl$_3$, 400 MHz) δ: 1.63-1.55 (2H, m, H-14); 1.79-1.74 (2H, m, H-15); 1.87-1.81 (2H, m, H-13); 2.46-2.43 (2H, t, H-16); 3.40-3.36 (2H, m, H-12); 7.09 (1H, d, H-4); 7.29 (1H, d, H-4); 7.63-7.57 (1H, m, H-3); 7.75-7.71 (1H, m, H-6); 7.81-7.77 (1H, m, H-7); 8.29-8.25 (1H, d, H-5); 8.32-8.30 (1H, d, H-8); 9.77 (1H, s, NH).

^{13}C NMR spectrum (CDCl$_3$, 100.6 MHz, 25°C) δ: 24.4 ; 26.6 ; 28.8 ; 33.7 ; 42.7 ; 112.9 ; 115.7 ; 117.8 ; 126.7 ; 132.9 ; 133.1 ; 134.0 ; 134.7 ; 135.1 ; 135.3 ; 151.8 ; 178.4 ; 183.9 ; 185.1 ppm.

## 4.6.5 Synthesis of AQ-Ahx-OPFP (HZ22)

AQ-Ahx-OPFP HZ22 was prepared from the reaction of AQ-Ahx-OH HZ21 (300 mg, 0.89 mmol), DCC (202 mg, 0.98 mmol), DMAP (120 mg, 0.98 mmol), and PFP (180 mg, 0.98 mmol) in dichloromethane for 4 h. TLC of the crude product (Rf 0.94) used the solvent system, dichloromethane-ethyl acetate 9:1. Column chromatography was performed for the purification of crude HZ22 by using the eluting system, dichloromethane-ethyl acetate 8:1. The red product fractions were combined, filtered and evaporated to dryness. Yield (precipitation from hexane): 346 mg, 77.3%.

^{1}H NMR spectrum (CDCl$_3$, 400 MHz) δ: 1.70-1.63 (2H, m, H-14); 1.87-1.83 (2H, m, H-15); 1.95-1.89 (2H, m, H-13); 2.77-2.73 (2H, t, H-16); 3.42-3.37 (2H, m, H-12); 7.08 (1H, d, H-2); 7.58-7.547(1H, m, H-4); 7.63-7.60 (1H, m, H-3); 7.78-7.74 (1H, m, H-6); 7.80 (1H, m, H-7); 8.27-8.25 (1H, d, H-5); 8.30-8.28 (1H,

d, H-8); 9.79; (1H, s, NH).

$^{13}$C NMR spectrum (CDCl$_3$, 100.6 MHz, 25°C) δ: 24.5 ; 26.5 ; 28.7 ; 33.2 ; 42.6 ; 113.0 ; 115.7 ; 117.7 ; 126.6 ; 126.7 ; 132.9 ; 133.0 ; 133.9 ; 134.7 ; 135.0 ; 135.3 ; 139.1 ; 139.9 ; 140.7 ; 142.3 ; 151.7 ; 169.3 ; 183.8 ; 185.1 ppm.

$^{19}$F NMR spectrum (CDCl$_3$) δ: -152.8; -158.1 and -162.2

ESMS (+): 504 m/z 100% (M+H)$^+$

### 4.6.6 Synthesis of AQ-[4-Hydroxyl]-Ahx-OH (HZ23)

Leucoquinzarin (1 g, 4.1 mmol) was reacted with 6-aminohe`xanoic acid (2.2 g, 16.7 mmol) by the addition of K$_2$CO$_3$ (2.05 g, 14.9 mmol) in DMF on the 100$^o$C water bath. The TLC was checked in the solvent system chloroform: methanol (9:1): R$_f$ 0.65. After 1.5 hours the reaction had mostly completed. The round bottomed flask was cooled to RT and the reaction mixture was aerated for 1 h. The mixture was then filtered to get rid of solid impurity. The column chromatography was performed for the product purification. Solvent system dichloromethane to methanol 10:1 was used. The appropriate fractions were combined and collected. Yield: 900 mg, 62%.

### 4.6.7 Synthesis of AQ-[4-Hydroxyl]-Ahx-OPFP (HZ24)

AQ-[4-Hydroxyl]-Ahx-OH HZ23 (50 mg, 0.14 mmol) was dissolved in dichloromethane by the addition of the reagents PFP (28 mg, 0.15 mmol), DCC (32 mg, 0.15mmol) and DMAP (18.3 mg, 0.15 mmol). After 2 h, the TLC (chloroform to ethyl acetate 9:1, R$_f$ 0.9) showed the reaction has completed. The crude product was purified by column chromatography using the solvent system dichloromethane to ethyl acetate 15:1. The appropriate fractions were combined, filtered and evaporated to dryness. The solid HZ24 compound was precipitated

in Hexane. Yield: 38 mg, 52%

$^1$H NMR spectrum (CDCl$_3$, 400 MHz) δ: 1.69-1.63 (2H, m, H-14); 1.88-1.83 (2H, m, H-15); 1.97-1.90 (2H, m, H-13); 2.77-2.73 (2H, t, H-16); 3.48-3.43 (2H, m, H-12); 7.23 (1H, m, H-3); 7.25 (1H, m, H-2); 7.74-7.73 (1H, m, H-7); 7.78-7.76 (1H, m, H-6); 7.86-7.80 (2H, d, H-5 and H-8); 8.36-8.34 (1H, d, H-8); 10.37 (1H, s, NH); 13.76 (1H, s, OH).

$^{13}$C NMR spectrum (CDCl$_3$, 100.6 MHz, 25°C) δ: 24.4 ; 26.4 ; 29.1 ; 33.2 ; 42.6 ; 108.5 ; 113.7 ; 123.9 ; 126.4 ; 126.6 ; 129.0 ; 132.5 ; 132.7 ; 134.2 ; 147.6 ; 156.8 ; 169.3 ; 182.2 ; 187.5 ppm.

$^{19}$F NMR spectrum (CDCl$_3$) δ: -152.7; -158.01 and -162.30

**4.6.8 Synthesis of AQ-(CH$_2$)$_5$-Pro-Ala-Gly-Nva-Pro-OH (HZ60)**

The H-Pro-2-ClTrt resin (500 mg, 0.6 mmol/g) was used for the SPPS of AQ-(CH$_2$)$_5$-Pro-Ala-Gly-Nva-Pro-OH (HZ60). The pentapeptide (H-Pro-Ala-Gly-Nva-Pro-reisin) was synthesized on resin using the same method as Fmoc-Pro-Ala-Gly-Leu-Ala-Ala-OH (HZ31). The red reagent HZ22 (151 mg, 0.3 mmol) in DMF (8 ml) was added to the SPPS reaction vessel containing the bound, deprotected pentapeptide and shaken for 1.5 h. The red solution was drained off by the aid of a vacuum pump and another portion of HZ22 (151 mg, 0.3 mmol) in DMF (8 ml) was added to the vessel. The final target compound AQ-(CH$_2$)$_5$-Pro-Ala-Gly-Nva-Pro-OH (HZ60) was cleaved off the resin by 1% TFA in dichloromethane (30 ml in total). The solution was dried and the solid HZ60 was collected in diethyl ether (50 ml). The crude HZ60 was purified by thick layer silica gel chromatography using the solvent mixture of dichloromethane and methanol (9:1). The title compound was recovered from the silica in a chromatographically homogeneous form. Yield: 52 mg, 23 %.

ESMS (-): 757 m/z (100%) (M-H)⁻

HPLC Retention time: 3.92 min

### 4.6.9 Synthesis of AQ-(CH$_2$)$_5$-Pro-Ala-Gly-OH (HZ106)

The H-Gly-2-ClTrt resin (100 mg, 1.1 mmol/g) was used for the SPPS of AQ-(CH$_2$)$_5$-Pro-Ala-Gly-OH (HZ106). The tripeptide (H-Pro-Ala-Gly-reisin) was synthesized using the same method as Fmoc-Pro-Ala-Gly-Leu-Ala-Ala-OH (HZ31). The red reagent HZ22 (55 mg, 0.11 mmol) was dissolved in DMF (5 ml) first and then added to the SPPS reaction flask. After 1 h, the solution was drained off, and other portion of HZ22 (55 mg, 0.11 mmol) was dded to the reaction. The SPPS vessel was shaken for another 1 h. The final comound AQ-(CH$_2$)$_5$-Pro-Ala-Gly-OH (HZ106) was cleaved by 2% TFA in dichloromethane (20 ml in total). The solution was dried (Na$_2$SO$_4$, anhydrous) and the solid was collected in diethyl ether (30 ml). Yield: 20 mg, 32 %

ESMS (-): 561 m/z (100%) (M-H)⁻

HPLC Retention time: 2.62 min

### 4.6.10 Synthesis of AQ-(CH$_2$)$_5$-Pro-OH (HZ107)

The H-Pro-2-ClTrt resin (100 mg, 0.6 mmol/g) was used for the synthesis of AQ-(CH$_2$)$_5$-Pro-OH (HZ107). The resin was transferred into a SPPS reaction vessel, added with dichloromethane (10 ml) for swelling the beads and shaken at RT, 650 rpm for 1.5 h. Dichloromethane was drained off and the red reagent HZ22 (50 mg, 0.1 mmol) in DMF was added to the vessel. The vessel was shaken for 1.5 h. The product AQ-(CH$_2$)$_5$-Pro-OH (HZ107) was cleaved off the resin by 2% TFA in dichloromethane (15 ml in total). The solution was dried and the solid was collected under diethyl ether (20 ml). Yield: 11 mg, 42 %.

ESMS (-): 433 m/z (100%) (M-H)⁻; HPLC Retention time: 5.5 min

## 4.7 References

Behrendt R, White P, Offer J. (2016). Advances in Fmoc solid‑phase peptide synthesis. *Journal of Peptide Science*. **22**(1), p4–27.

Gordon EM, Barrett RW, Dower WJ, Fodor SP, Gallop MA. (1994). Applications of combinatorial technologies to drug discovery. 2. Combinatorial organic synthesis, library screening strategies, and future directions. *J Med Chem*. **37**(10), p1385-1401.

Greenhalgh CW, Hughes N, (1968). The reaction of leucoquinizarins with alkylenediamines  *J. Chem Soc.* p1284-1291.

Hancock WS, Battersby JE. (1976). A new micro-test for the detection of incomplete coupling reactions in solid-phase peptide synthesis using 2,4,6-trinitrobenzenesulphonic acid. *Anal Biochem*. **71**(1), p260-264.

Chang JY. (1981). N-terminal sequence analysis of polypeptide at the picomole level. *Biochem J*. **199**, p557–564.

Kaiser E, Colescott RL, Bossinger CD, Cook PI. (1970). Color test for detection of free terminal amino groups in the solid-phase synthesis of peptides. *Anal Biochem*. **34**(2), p595-598.

Madder A, Farcy N, Hosten NGC, Muynck HD, Clercq PJD, Barry J, Davis PA. (1999). A Novel Sensitive Colorimetric Assay for Visual Detection of Solid-Phase Bound Amines. *Eur. J. Org. Chem.* **1**, p2787-2791.

Mäde V, Els-Heindl S, Beck-Sickinger AG. (2014). Automated solid-phase peptide synthesis to obtain therapeutic peptides. *Beilstein J Org Chem*. **10**, p1197-1212.

Merrifield RB. (1963). Solid phase peptide synthesis. I. The synthesis of a tetrapeptide. *J. Am. Chem. Soc. 85*(14), p2149.

Murdock KC, Child RG, Fabio PF, Angier RB, Wallace RE, Durr FE, Citarella RV. (1979). Antitumor agents. 1.1,4-Bis[(aminoalkyl)amino]-9,10-anthracenediones. *J Med Chem*. **22**(9). p1024-1030.

Nair PP, Kessie G, Patnaik R, Guidry C. (1994). Isolation and HPLC of N-epsilon-lithocholyl lysine as its fluorescamine and dimethylaminoazobenzene isothiocyanate derivatives. *Steroids*. **59**(3), p212-216.

Sarin VK, Kent, SBH, Tam, JP, Merrifield R.B. (1981) Quantitative monitoring of solid-phase peptide synthesis by the ninhydrin reaction. *Anal Biochem*. **117**(1), p147-157.

Steven E, Van der Plas SE, De Clercq PJ, Madder, A. (2007). Fast and easy detection of aromatic amines on solid support. *Tetrahedron Letters.* **48**, p2587-2589.

Zee-Cheng RK, Cheng CC. (1978). Antineoplastic agents. Structure-activity relationship study of bis(substituted aminoalkylamino)anthraquinones. *J Med Chem*. **21**(3), p291-4.

Zee-Cheng RK, Podrebarac EG, Menon CS, Cheng CC. (1979). Structural modification study of bis(substituted aminoalkylamino)anthraquinones. An evaluation of the relationship of the [2-[(2-hydroxyethyl)amino]ethyl]amino side chain with antineoplastic activity. *J Med Chem*. **22**(5), p501-505.

Ziegler J, Abel S. (2014) Analysis of amino acids by HPLC/electrospray negative ion tandem mass spectrometry using 9-fluorenylmethoxycarbonyl chloride (Fmoc-Cl) derivatization. *Amino Acids*. **46**(12), p2799-2808.